THE SPATIAL CONTROL OF RAP1 VIA EPAC PROTEINS

By

Chang Liu

A THESIS

Presented to the Department of Cell & Developmental Biology
And the Oregon Health & Science University
School of Medicine
In partial fulfillment of the requirements for the degree of
Doctor of Philosophy

April 2010

School of Medicine
Oregon Health & Science University

CERTIFICATE OF APPROVAL

This is to certify that the Ph.D. thesis of

Chang Liu

has been approved

Mentor/Advisor: Philip J.S. Stork, M.D.

Committee Chair: Peter S. Rotwein, M.D.

Member: Melissa H. Wong, Ph.D.

Member: David L. Farrens, Ph.D.

Member: Ujwal Shinde, Ph.D.

TABLE OF CONTENTS

LIST OF CHAPTERS

CHAPTER ONE

Spatial Regulation of Small GTPases of the Ras Superfamily

CHAPTER TWO

Ras Is Required for the cAMP-dependent Activation of Rap1 via Epac2

CHAPTER THREE

The Interaction of Epac1 and Ran Promotes Rap1 Activation at the Nuclear Envelope

CHAPTER FOUR

Summary and Future Directions

APPENDICES

LIST OF FIGURES AND TABLES

CHAPTER ONE

CHAPTER TWO

CHAPTER THREE

CHAPTER FOUR

APPENDICES

LIST OF ABBREVIATIONS

2OMe	8-(4-chloro-phenylthio)-2'-O-methyl-cyclic adenosine-3’, 5’-cyclic monophosphate
Ab	Antibody
BFA	Brefeldin A
Bp	Base pair
BSA	Bovine serum albumin
C terminal	Carboxy-terminal
Ca^{2+}	Calcium ion
CaM	Calmodulin
cAMP	Cyclic adenosine monophosphate
CCD	Conserved domain database
CDC25-HD	CDC25 homology domain
cDNA	Complementary deoxyribonucleic acid
cNBD	Cyclic nucleotide binding domain
DAG	Diacylglycerol
DH-PH	Dbl homology-pleckstrin homology
DMSO	Dimethylsulfoxide
DNA-PK	DNA-dependent protein kinase
EGF	Epidermal growth factor
EGF	Epidermal growth factor
EM	Electronic microscopy
Epac	Exchange proteins directly activated by cAMP

ER	Endoplasmic reticulum
ERK	Extracellular signal-regulated kinase
F/H	Forskolin, IBMX and H89
FTase	Farnesyltransferase
GAP	GTPase- activating protein
GDF	GDI displacement factor
GDI	GDP-dissociation inhibitor
GFP	Green fluorescent protein
GGTase I	Geranylgeranyltransferase I
GLP-1	Glucagon-like peptide 1
GST	Glutathione S-transferase
GTP/GDP	Guanosine triphosphate/diphosphate
GTPase	Guanosine triphosphatases
IBMX	3-isobutyl-1-methylxanthine
IP	Immunoprecipitation
IPTG	Isopropyl-β-D-thiogalactopyranoside
ISO	Isoproterenol
Kb	Kilo bases
kDa	Kilodalton
MβCD	5-methyl-β-cyclodextrin
MAPK	Mitogen-activated protein kinase
MARCKS	Myristoylated alanine-rich C-kinase substrate
MDCK cells	Madin-Darby canine kidney cells
MEF	Mouse embryonic fibroblast

Min	Minutes
N terminal	Amino terminal
NCBI	National center for biotechnology information
NE	Nuclear envelope
NGF	Nerve growth factor
NMT	N-myristoyltransferase
NPC	Nuclear pore complex
Oligo	Oligonucleotide
P loop	Phosphate-binding loop
PAT	Palmitoyl acyltransferase
PBS	Phosphate buffered saline
PCR	Polymerase chain reaction
PDGF	Platelet-derived growth factor
PIP2	Phosphatidylinositol-4,5-bisphosphate
PKA	Protein kinase A
PKD	Protein kinase D
PM	Plasma membrane
PMSF	Phenylmethanesulfonyl fluoride
RA	Ras association domain
RalGDS	Ral guanine nucleotide dissociation stimulator
RanBP2	Ran binding protein 2
RanGAP	Ran GTPase-activating protein
RBD	Ras binding domain
RCC1	Regulator of chromosome condensation 1

REM	Ras exchange motif
RGL	RalGDS-like protein
Rin	Ras interaction/interference
RT-PCR	Reverse transcriptase polymerase chain reaction
sAPPα	Soluble form of amyloid precursor protein
SDS-PAGE	Sodium dodecyl sulfate polyacrylamide gel electrophoresis
Sec	Seconds
shRNA	Short hairpin RNA
siRNA	Small inhibitory RNA
Sos	Son of Sevenless
TBS	Tris buffered saline
TGF-βR	Transfoming growth factor-β receptor
UBQ	Ubiquitin homologs

ACKNOWLEDGMENT

I would like to thank my mentor Dr. Philip Stork who brought me into the wonderful world of cell signaling. He is passionate about science, and his instincts and experiences guided me to important discoveries. I spent one of the happiest times of my life in his lab, where I was always encouraged and supported, and was always free to think and imagine. I am also a fan of his artistic expression, which has become a strong influence on my illustration of scientific ideas. Dr. Stork also shaped my career path in the future where I will have the opportunity to pursue my interests in both basic and clinical research.

It is my great honor to work with all the present and past members of the Stork lab. I am especially grateful for Drs. Maho Takahashi and Yanping Li. Their unrelenting support and immense contribution make my thesis possible. Their experimental expertise and dedication to science set excellent examples for me to follow. I am also indebted to Drs. Zhiping Wang and Tara Dillon. They taught me basic techniques, and their work opened up new directions and was the origin of my research projects. My special thanks go to Chris Fenner, Srilatha Tavisala, Brian Hunter, Kirstin Labudda, Linda Wang, Drs. Michael Pelligrino, Quentin Low, Yutaro Obara, Viji Pokala, and Snigdha Mishra. They will always be part of my fondest memories of the Stork Lab.

It took a village to raise a graduate student. I would like to thank the members of my thesis committee and other faculty members at OHSU, who made my academic experience as wonderful as it possibly can be. Dr. Peter Rotwein, as the founder of my favorite journal club, deeply influenced the way I evaluate the scientific literature. Dr. Melissa Wong, with her expertise in teaching and mouse models, primed me for future adventures into the world *in vivo*. Dr. David Farrens and Dr. Ujwal Shinde helped me

harness the power of biophysics and bioinformatics to address fundamental questions in biochemistry. My rotation with Dr. Wenbiao Chen and Dr. Buddy Ulman during my first year at OHSU also helped me acquire important techniques and experiences with different model systems. Dr. Mike Forte reviewed both of my manuscripts and provided invaluable advices. Dr. Gary Thomas enthusiastically recommended me for Vertex Scholarship. And of course, Dr. Hua Lu saw the potential in me six years ago and I sincerely thank him for inviting me on board.

For technical expertise that was vital to my thesis project, I thank Dr. Stefanie Kaech, who helped build the advanced imaging facilities at OHSU and trained me to catch the spectacular moment of a living cell. I also thank Dr. Larry David and members in his lab, John Klimek and Debra McMillen, for their expertise in mass spectrometry.

I owe thanks to my many friends and classmates at OHSU for going through all the tough exams and frustrations with me, and growing up together with me. I am thankful to the Department of Cell and Developmental Biology for continuous support and excellent service from the faculty and staff. I am also proud to be a Vertex Scholar and acknowledge the funding from the Vertex Pharmaceutical for my fifth academic year.

I have been showered in love from my parents, Huawu Liu and Naihui Ye. So far away from home, I have not been able to give them a real hug in return. They worked very hard, sent me to the best school and helped me make the right choices. What I am investigating in the lab may be very abstract to them, yet they inspired me, with their wisdom and life experiences, that I should always discard the fears and carry on. I also thank the other members of my big family in China who love me very much and are always with me no matter where I am. Regrettably, my loving grandmother, Suqing Yang,

passed away during the writing of this thesis. She always took pride in my academic success and I sincerely dedicate my work to her.

Finally, I want to thank my wife, Shuang Song, who fills my life with her love, care and humor. We supported each other throughout our graduate educations, endured the longest distance and time apart, and found our way to balance science and family. We share so many dreams about the future and we will continue to explore the world together.

ABSTRACT

Rap1 is a small GTPase of the Ras superfamily, playing important roles in the regulation of many cellular processes, including proliferation, differentiation and adhesion. The activation of Rap1 occurs through exchange of GDP for GTP under the catalysis of a variety of guanine nucleotide exchange factors (GEFs). Our lab previously revealed that different GEFs can dictate different modes of Rap1 activation, which are coupled to downstream pathways differently. My thesis focused on two GEFs for Rap1, exchange proteins directly activated by cAMP (Epac1 and Epac2), and tested the hypothesis that Rap1 activation and signaling can be spatially regulated through targeting of these GEFs to different compartments of the cell.

While both Epac1 and Epac2 can be directly activated by cAMP through relief of auto-inhibition, the distinct Ras association (RA) domains in Epac1 and Epac2 confer them specific subcellular locations via interaction with Ran and Ras, respectively. Epac2 has a classical RA domain that binds to GTP-loaded Ras with high affinity. Disruption of this interaction reduces Epac2-dependent Rap1 activation, and increased level of Ras-GTP enhances the activation. Ras-GTP does not help relieve the auto-inhibition of Epac2, or activate Epac2 allosterically. Instead, Ras-GTP promotes the compartmentalization of Epac2 at the plasma membrane (PM), where it has better access to its substrate Rap1. This is mimicked by targeting Epac2 to the PM through an engineered CAAX motif to its C terminus. Thus Epac2 is fully activated only when cAMP opens its conformation and when it is properly targeted to the PM via Ras-GTP. In PC12 cells, expression of exogenous Epac2, or induction of endogenous Epac2 by NGF,

allows synergistic activation of ERKs by cAMP and Ras, which is correlated to increased neurite outgrowth.

In a proteomic survey, we discovered that Epac1 interacts with several components of the nuclear pore complex (NPC), with Ran and Ran binding protein 2 (RanBP2) being the most abundant. Epac1 can be immunoprecipitated with Ran and RanBP2 from the cell lysates. Purified Ran and Epac1 also interact *in vitro* in a GTP-dependent manner. Consistently, Epac1 co-localizes with the NPC by confocal live imaging. The Ran-Epac1 interaction is dependent on a previously uncharacterized RA domain of Epac1 (referred to as RA1). An Epac1 mutant with the original RA1 domain replaced by the RA domain of Epac2, named Epac1RA2, loses the association with Ran and displays reduced localization at the NPC. As compared to the wild type Epac1, Epac1RA2 activates Rap1 poorly which is restored to a higher level by overexpressing GTP-loaded Ras. Alternatively, Epac1RA2 can be further enriched at the NPC by fusion to a GTP-loaded Ran, and the chimerical protein activates Rap1 more efficiently. Using a GFP-tagged Ras binding domain from RalGDS (GFP-RBD_{RalGDS}) as reporter for Rap1-GTP *in vivo*, the Epac1-dependent activation of Rap1 can be observed at the nuclear envelope.

In conclusion, Epac proteins are compartmentalized at the PM and NPC via interactions with Ras and Ran, respectively. The proper localizations of these two GEFs are necessary for efficient activation of different pools of Rap1 by cAMP.

Chapter 1

Spatial Regulation of Small GTPases of the Ras superfamily

"Signal transduction efficiency adheres to the classic real-estate mantra: location, location, location." – Anonymous

1.1 INTRODUCTION

Guanosine triphosphatases (GTPases or G proteins) play important roles in transducing diverse extracellular stimuli to various cellular responses (Hall, 1990; Neves et al., 2002). They are diverse group of molecules comprising the alpha subunits of the heterotrimeric GTPases, monomeric small GTPases of the Ras superfamily, and up to 50 other GTPases (Colicelli, 2004). The Ras superfamily is founded based on the homology to the Ras oncogene proteins (Wennerberg et al., 2005). The spatial regulation of the small GTPases of this superfamily will be the focus of this chapter.

1.2 SMALL GTPASES OF THE RAS SUPERFAMILY

The over 150 members of the Ras superfamily can be grouped into five major families based on sequence homology and functional similarities: Ras, Rho, Rab, Arf and Ran (Wennerberg et al., 2005). Figure 1.1 shows an alignment of selected members of the human Ras superfamily organized in the form of a phylogenetic tree. The members of each family are clustered together based upon higher levels of sequence homology within each family. The five families of small GTPases, namely Ras, Rho, Rab, Arf and Ran, regulate distinct yet sometimes overlapping cellular functions. The Ras sarcoma (Ras) family members play important roles in the regulation of cellular differentiation and proliferation. Chapter 2 will focus on two members from this family, H-Ras and Rap1. The Ras homologous (Rho) family members regulate cell shape, the cytoskeleton and cell migration. The Ras-like proteins in the brain (Rab) and the ADP-ribosylation factor (Arf) family proteins are involved in vesicle-associated processes, including vesicle formation, transport and exocytosis. The Ras-like nuclear (Ran) protein is the only molecule of its branch and participates in the nuclear transport, assembly of nuclear envelope and spindle

formation. The relationship between Ran and Rap1, two members from two different families, will be closely examined in Chapter 3.

For small GTPases that have not been intensively studied, their classification into the above five branches is based solely on sequence homology. For some well-characterized proteins, newly discovered functions may expand their roles to overlap with those of the other families. One such example is Rap1 which was initially identified to mediate growth inhibition or interfere with Ras signaling (Kitayama et al., 1989). It was later found to activate ERKs through the direct interaction with B-Raf and promote differentiation of PC12 cells (Vossler et al., 1997; York et al., 1998). Recently, Rap1 was reported to play important roles in insulin secretion (Shibasaki et al., 2007), and its isoform Rap2 participates in the regulation of nuclear transport (Huston et al., 2008). Thus, Rap isoforms seem to overlap functionally with proteins of the Rab and Ran families, although the detailed mechanisms underlying these processes remain unclear.

The G domains (corresponding to residues 5-166 of Ras) of representative members from each of the above five families, including H-Ras, Rac2, Rab28, Ran and Arf6, are largely conserved based on the structural comparison of these domains (Figure 1.2A & B). One of the most important common features of the G domains is the presence of switch I and II regions, and the guanosine triphosphate/diphosphate (GTP or GDP) clamped between them (Figure 1.2A, in gray). Another common motif is the N terminal phosphate-binding loop (P loop), consisting of a glycine-rich sequence followed by a conserved lysine, which interacts with the phosphate groups of the nucleotide and the Magnesium ion (Saraste et al., 1990).

The high affinity and specificity of guanine nucleotides for the small GTPases requires three important elements established from studies of individual members. First, the β phosphate of GDP or GTP allows these two nucleotides to interact with the P loop of Ras at affinities 10^6-fold higher than that between GMP and the P loop (Rensland et al., 1995). Second, the high affinity of small GTPases for the nucleotides also requires Mg^{2+} coordination and the lysine of the P loop (Hall and Self, 1986; Renault et al., 2001). Third, the relative orientation of the phosphate and base binding regions dictates selective binding for GTP/GDP, but not polyphosphate alone or ATP/ADP (Rensland et al., 1995).

Small G proteins function as GTP/GDP-dependent molecular switches to turn on and off downstream signaling pathways. When small GTPases are loaded with GTP, they assume an active conformation, which allows them to interact with specific effectors. These interactions may engage different parts of the surface of the G domains, but the switch I and II regions are always, at least partially, involved in the interface (Vetter and Wittinghofer, 2001). When small G proteins are GDP-loaded, they switch to an inactive conformation and are incapable of effector binding.

1.3 GUANINE NUCLEOTIDE EXCHANGE FACTORS

Small GTPases are cycling between their GTP and GDP-bound states in the cell. The bound GTP can be hydrolyzed to GDP due to the triphosphatase activity, and the GDP is subsequently released in exchange for GTP which is in substantial excess in the intracellular environment. The intrinsic rates of these two processes are very slow, and the nucleotide exchange and GTP hydrolysis are catalyzed and accelerated by guanine nucleotide exchange factors (GEFs) and GTPase-activating proteins (GAPs), respectively. Thus, GEFs switch on small GTPases by driving them into their active conformations and

GAPs switch them off by driving them into their inactive conformations. While both GEFs and GAPs are important regulators of GTPases, this chapter will focus on the GEFs only, as the GEFs are an integral part of this dissertation.

GEFs are predominantly proteins with multiple domains, allowing nucleotide exchange and autoinhibition through intra-molecular interactions as well as providing spatio-temporal controls through mechanisms such as protein interactions, ligand binding and post-translational modifications. A number of GEF families selectively activates their cognate family of small G proteins to ensure signaling specificity (Bos et al., 2007). The catalytic mechanisms of GEFs for each family of the Ras superfamily will be introduced in this section, and the catalytic domain unique to each family will also be used later in a bioinformatic search for GEFs that are capable of relaying signals from one type of small GTPase to another (Section 1.6). While the catalytic domains are responsible for facilitating the exchange reaction of small GTPases, the spatial regulation of GEFs is usually mediated by domains other than the catalytic domain, which will be the focus of Section 1.6 and 1.7.

1.3.1 Ras GEFs

At least 50 GEFs regulate the activation of Ras family GTPases, and they have similar catalytic regions that contain a CDC25 homology domain (CDC25-HD) in close relationship to a Ras exchange motif (REM). The working mechanisms for these GEFs are further discussed below in the case of Sos and Epac2.

Ras and Sos. The crystal structure of human H-Ras in complex with the catalytic region of the Son of Sevenless (Sos), one of its many GEFs, was reported in 1998 (Boriack-Sjodin et al., 1998). The release of the bound nucleotide from Ras is facilitated

by Sos in two ways. First, the insertion of a helical hairpin structure from the CDC25-HD domain of Sos displaces the Switch I region of Ras and opens up the nucleotide-binding site (Figure 1.3A). Second, side chains from the hairpin and from the distorted Switch II region of Ras alter the chemical environment of the binding sites for the terminal phosphate groups of the nucleotide and the magnesium ion, which favors a nucleotide-free intermediate state. The REM domain is indispensible for the exchange activity and functions to orientate and stabilize the helical hairpin of the catalytic domain (Figure 1.3A). As the binding sites for the base and the ribose of GTP or GDP are not occluded by Sos, the Ras-Sos complex allows both nucleotide release and rebinding. The structure of Ras-Sos revealed a mechanism for the activation of Ras, which could be common for all members of the Ras family. This mechanism is different from existing models for EF-Tu, a small G protein in *E*scherichia *coli* (Kawashima et al., 1996), Arf (Cherfils et al., 1998) and Ran (Renault et al., 1998).

Subsequent structural and functional studies demonstrated complicated regulatory mechanisms for Sos mediated catalysis. First, an additional and highly conserved binding site for Ras-GTP is present distally to the catalytic site. Binding of Ras-GTP to this distal site stabilizes the catalytic site of Sos allosterically and increases the rate of nucleotide release from Ras by about five fold (Boykevisch et al., 2006; Freedman et al., 2006; Margarit et al., 2003). Second, Sos also contains a Dbl homology-pleckstrin homology (DH-PH) unit which occludes the allosteric binding site for Ras-GTP, thus gating the reciprocal and allosteric activation of Sos by Ras-GTP (Sondermann et al., 2004). Third, when the allosteric Ras is tethered to lipid vesicles *in vitro*, the Sos catalytic unit is up to 500-fold more active than when the allosteric Ras is in solution. Sos construct with the

intact N terminal DH-PH unite also responds to the membrane concentration of phosphatidylinositol-4,5-bisphosphate (PIP2), which facilitates the release of autoinhibition from the N terminus (Gureasko et al., 2008). The wealth of knowledge about the Sos mediated Ras activation indicates that multiple levels of regulations might exist for a single exchanger to ensure precise control of its activity.

Rap1 and Epac. Exchange proteins directly activated by cAMP (Epacs; Epac1 and Epac2) are GEFs that activate Rap GTPases. The crystal structures of Epac2 in auto-inhibited (Rehmann et al., 2006) and active (Rehmann et al., 2008) states have been solved recently, and provided useful information on the regulation of this protein. Given their sequence homology, the structure of Epac1 is predicted to be similar to Epac2. Epac2 contains an N-terminal regulatory region consisting of two cAMP binding (CNB-A and B) domains and between them a DEP (Dishevelled, Egl-10, and Pleckstrin) domain, and a C-terminal catalytic region consisting of a REM domain, Ras association (RA) domain and a CDC25-HD domain. The two regions are linked by a switchboard like structure. In the absence of cAMP, the ionic interactions between the regulatory and catalytic regions occlude the access of Rap to the catalytic site and lock Epac2 in an auto-inhibited state. The relief of auto-inhibition in Epac2 is initiated by the binding of cAMP to the CNB-B domain, which triggers a conformational change that moves the regulatory region away from the catalytic core and clears the steric hindrance for the access of Rap proteins. The active state is reinforced by interaction among cAMP, the CNB-B domain, and the REM domain. Within the catalytic region, despite being interrupted by the RA domain, the spatial relationship between the REM and CDC25-HD domains of Epac2 resembles that of Sos (Freedman et al., 2006), and the helical hairpin within the CDC25-

HD of Epac2 is similarly stabilized by the REM domain through hydrophobic interactions. In the structure of the active Epac2 in complex with Rap1 (Rehmann et al., 2008), the helical hairpin pries open the Switch I and II of Rap1 and lowers its affinity for the guanine nucleotides (Figure 1.3B). Unlike the catalytic domain of Sos, which undergoes conformational change upon interaction with the allosteric Ras, the conformation of the Epac2 CDC25-HD remains unchanged in the active state (Gloerich and Bos, 2010), suggesting activation of Epac2 by relief of auto-inhibition instead of allosterism. The role of the RA domains of Epac2 and Epac1 will be closely examined in Chapter 2 and 3, respectively.

1.3.2 Rho GEFs

GEFs for the Rho family GTPases consist of 69 distinct members, all related to a transforming gene from diffuse B-cell-lymphoma (Dbl) cells (Rossman et al., 2005). The catalytic regions of these Rho GEFs contain a DH domain that catalyzes the exchange of nucleotides, and an adjacent PH domain that regulates GEF activity through binding phosphoinositides or allosteric mechanisms. Our understanding of the catalysis of the DH domain was shaped by the crystal structure of the DH-PH unit from Tiam1 in complex with its substrate Rac1 (Worthylake et al., 2000). An auto-inhibitory interaction is likely to be present between the DH and PH domains, as remarkable changes were observed by comparing the GTPase-free structure of the DH-PH unit from Sos with the PH-DH unit from the active Tiam1 in complex with Rac1 (Soisson et al., 1998; Worthylake et al., 2000). In the active state, this PH domain does not contact Rac1, and the DH domain contacts the nucleotide-free Rac1 with opened Switch I and II regions. Similar to the catalytic mechanism of Sos, Tiam1 interferes with the binding of magnesium ion to Rac1.

However, unlike Sos, Tiam1 does not directly interfere with the binding of α- or β-phosphate group of the guanine nucleotide. Instead, Tiam1 promotes the release of bound nucleotide by interfering with the binding of the nucleotide sugar.

1.3.3 Arf GEFs

The Arf GEFs comprise 15 proteins in the human genome, and they belong to five subfamilies with a common Sec7 domain that catalyzes the exchange activity (Casanova, 2007). From the first structure of the Sec7 domain of the human Arf exchanger Arno (Cherfils et al., 1998; Mossessova et al., 1998), the Sec7 domain assumes an elongated, all-helical conformation, with a distinctive and highly conserved hydrophobic groove. This groove and an adjacent conserved loop serve as the putative Arf-interacting surface. The structure of the Sec7 domain of Arno in complex with Arf was subsequently solved. Arno inserts residues, including a highly conserved “glutamic finger”, into the nucleotide-binding site of Arf, expelling the nucleotide sterically and electrostatically (Goldberg, 1998). In addition to the Sec7 domain, a variety of additional domains are present in different Arf exchangers to regulate the subcellular localization of these GEFs and to integrate upstream signals.

1.3.4 Rab GEFs

At least 61 members belong to the Rab family, the largest branch of the Ras superfamily (Zerial and McBride, 2001). Unlike the Ras, Rho and Arf families, each being activated by easily identifiable GEF domains, CDC25-HD, DH-PH and Sec7 respectively, GEFs that activate specific Rab proteins show limited sequence homology or functional overlap (Carney et al., 2006). The best studied Rab GEFs are the Vps9 domain-containing proteins (Carney et al., 2006).

Vps9 domain-containing proteins. Rabex-5, Rin1-3 and several other GEFs contain the conserved Vps9 domain and activate the Rab5, Rab21 and Rab22 that have overlapping subcellular distributions and functions (Carney et al., 2006; Delprato and Lambright, 2007; Pereira-Leal and Seabra, 2001). The crystal structure of Rabex-5 in complex with Rab21 revealed that the overall mode of interaction between Vps9 domain and Rab21 resembles that between Sec7 and Arf. Both GEF domains contact the switch regions of their cognate substrates through a hydrophobic groove between anti-parallel helices. In both cases, the Switch I region of the GTPase is in an open, nucleotide-accessible conformation, with the positively charged P loop lysine stabilized by either the "glutamic finger" from Sec7 domain or the "aspartic finger" from Vps9 domain (Delprato and Lambright, 2007).

1.3.5 Ran GEFs

Ran is included in the discussion here as a single member family as treated previously in the literature (Wennerberg et al., 2005), although other classifications might exist. Ran is activated exclusively in the nucleus by its principle GEF called regulator of chromosome condensation (RCC1). The unique crystal structure of RCC1 resembles a "seven-bladed propeller", each blade consisting of 51-68 residues forming a four-stranded antiparallel β-sheet (Renault et al., 1998). Further mutational analysis identified at least seven residues that are crucial for the exchange reaction, and these residues are all located on the same side of the propeller (Renault et al., 1998), thus defining a putative Ran-binding side, while the opposite side of the propeller being the chromatin-interacting region.

The structure of RCC1 in complex with Ran confirmed this hypothesis (Renault et al., 2001). RCC1 also features a β wedge, a small prominently protruding β sheet in blade

3 (residue 146-153), at its interface with Ran. It wedges between residues of switch II and the P loop, and was envisioned as the major determinant of the structural changes that loosen the nucleotide binding. Interestingly, due to the presence of a sulfate ion in the P loop of Ran in this structure, the phosphate binding region of the nucleotide binding site is perturbed only marginally, thus mimicking a nucleotide-containing (instead of nucleotide-free) intermediate of the multi-step exchange reaction. This is different from many other GEF-GTPase complexes, where the collapse of the P loop is more pronounced. Why this particular intermediate state seemed to be more favored during the crystallization is unknown. However, it has been shown that the GEF activity of RCC1 is coupled to its binding to the chromatin (Nemergut et al., 2001). It is possible that the structure of RCC1-Ran complex would be modulated in the presence of chromatin.

Recently, RanBP10 (Schulze et al., 2008) and Importin-β (Lonhienne et al., 2009) are reported to exhibit exchange activities toward Ran. As neither of these novel exchangers for Ran have the propeller motif, they might drive the Ran activation through different mechanisms.

1.4 SPATIAL REGULATION OF SMALL GTPASES: AN OVERVIEW

Cell signaling mediated by small GTPases is tightly regulated in time and space. The temporal component of this regulation is largely determined by the timing of the GTP/GDP cycle of a small GTPase. How fast the GEF of a small GTPase start to work in response to stimulation could dictate when the small GTPase becomes loaded with GTP. The timing of GEF inactivation and GAP activation will dictate how long the small GTPase stays in the GTP-loaded active form. For example, Rap1 can be activated via Epac2 after isoproterenol treatment within 1 minute and the Rap1-GTP levels quickly

diminishes after 5 minutes (see Chapter 2). As discussed previously, a GTPase is only active and capable of interaction with its effectors when loaded with GTP. Thus, the timing of GTP loading and hydrolysis will dictate the onset and termination of the signals emanating from a particular GTPase, and the frequency and duration of its GTP/GDP cycle could be coupled to different cellular outcomes. Because the loading and hydrolysis of GTP are directly catalyzed by GEF and GAP respectively, a small GTPases could be considered as a precise molecular timer with an “ON” button controlled by GEFs and an “OFF” button controlled by GAPs.

Distinct from the temporal control, the spatial regulation of GTPases is necessary for the organization of signaling pathways within a compartmentalized cell. Several important properties of small GTPases and their GEFs contribute to this regulation. First, small GTPases are commonly modified by covalently linked lipid groups, which target them to different subcellular locations. Second, one small GTPase can interact with the GEF of another small GTPase through Ras association domains present in many GEFs, or other domains discussed below. These domains allow proper localization of GEFs and the coupling of two different small GTPases. Third, the localization of GEFs can also be controlled through their interaction with proteins other than small GTPases, post-translational modifications and binding of second messengers. These mechanisms for spatial control of small GTPases will be reviewed in the next three sections, followed by a discussion of the physiological importance of these regulations.

1.5 MEMBRANE TARGETING OF SMALL GTPASES

As described before, small GTPases are substrates for GEFs. The membrane targeting of small GTPases generally necessitates the membrane targeting of their cognate GEFs to

allow efficient exchange reactions to happen. This general mechanism will be illustrated by the examples of Epac2 and Epac1 in Chapter 2 and 3 respectively, and this section will briefly review the membrane targeting of small GTPases before the localization of GEFs are discussed in Sections 1.6 and 1.7.

1.5.1 Lipid modifications of small GTPases

Most small GTPases of the Ras superfamily are lipid modified through prenylation and/or fatty acylation, and only rare examples, such as with Ran, Rit and Rin, lack such modifications. The covalently attached lipophilic moieties facilitate the targeting of small GTPases to various intracellular membranes, where the small GTPases serve as anchors to recruit their downstream effectors.

Prenylation. This type of posttranslational reaction links a farnesyl (15-carbon) or a geranylgeranyl (20-carbon) group through thioether bond to one or more cysteine residues at or near the C terminus of a small GTPase (Resh, 2006b). Almost all of the prenylated small GTPases contain a CAAX motif at the C terminus, which means a cysteine followed by two consecutive aliphatic amino acids and then any amino acid at the C terminal position. Depending on whether the last amino acid is a leucine or not, the cysteine within the CAAX motif is geranylgeranylated by geranylgeranyltransferase I (GGTase I) and farnesylated by farnesyltransferase (FTase) respectively, followed by cleavage of the AAX sequence (Sebti, 2005). Most members of the Ras and Rho families satisfy the above rule, but the rule is not without exceptions. For example, RhoB and K-Ras can both be either farnesylated or geranylgeranlyated in cells, especially depending on whether the FTase is blocked in the case of K-Ras (Armstrong et al., 1995; Lerner et al., 1997; Rowell et al., 1997). Although the 15-carbon and 20-carbon isoprenoids may

interact with the lipid membrane differently, it is still yet to be clarified whether farnesyl and geranylgeranyl modifications target proteins to distinct compartments in the cell. Double geranylgeranylation occurs almost solely on Rab family members which usually contain motifs, such as "CC, CXC or $CC(X)_{n=1-3}$" at the C terminus. The reaction is catalyzed by GGTase II, and requires that the Rab protein first be complexed with Rab escort protein (Resh, 2006b).

Fatty acylation. N-myristoylation and palmitoylation are two major forms of fatty acylations for small GTPases, and they involve the covalent attachment of myristate (14-carbon) and palmitate (16-carbon) to proteins, respectively. These two modifications are not mutually exclusive, and can also be combined with different types of prenylation. N-myristoylation is catalyzed by N-myristoyltransferase (NMT) (Farazi et al., 2001), and occurs at the glycine residue within a MGXXXS/T motif during protein synthesis (Maurer-Stroh et al., 2002). In contrast to the prenylation of most members of the Ras family, N-myristoylation is a conserved feature of all Arf proteins, and it is proposed to regulate the activation and stable membrane association of Arf GTPases (D'Souza-Schorey and Chavrier, 2006; Liu et al., 2009). Palmitoylation attaches palmitate or other long-chain fatty acids through thioester bonds to one or more cysteine residues under the catalysis of palmitoyl acyltransferases (PATs) (Resh, 2006b). No consensus sequence has been identified for this type of modification (Resh, 2006a). Palmitoylation can be dynamically reversed by depalmitoylation, depending on the strength of local PATs and palmitoyl thioesterases. For example, H-Ras is palmitoylated at the Golgi and targeted to the plasma membrane, and then it is internalized to the Golgi after depalmitoylation (Goodwin et al., 2005; Rocks et al., 2005). The regulated cycles of palmitoylation and

depalmitoylation maintain different pools of H-Ras signaling from distinct subcellular locations (Chiu et al., 2002).

While prenylation and fatty acylation are the major covalent modifications for small GTPases, additional post-translational modifications have been discovered, and they are important in specifying the subcellular localization of certain small GTPases. For example, the Arf-like protein Arl3p is not myristoylated, but acetylated at the N-terminus, and this modification is required for its targeting to the trans-Golgi network via an interaction with an integral membrane protein (Behnia et al., 2004; Setty et al., 2004).

1.5.2 The two-signal hypothesis

While myristoylation and prenylation are irreversible modifications, neither alone provides sufficient hydrophobicity to anchor proteins stably to a lipid bilayer (Peitzsch and McLaughlin, 1993; Resh, 2006b; Silvius and l'Heureux, 1994). They are commonly supplemented with one of the following mechanisms as a “second signal” to confer tighter membrane binding. The irreversible lipid modifications and the variety of additional signals, including the net charges and palmitoylations etc., are summarized in Figure 1.4 for representative members of the Ras superfamily.

Polybasic motif. Many small GTPases of the Ras and Rho families, such as K-Ras and CDC42, require a cluster of positively charged amino acids (polybasic motif) at their C termini in addition to their prenylation for PM localization and function (Heo et al., 2006; Michaelson et al., 2001; Teruel and Meyer, 2000). Arf proteins similarly use a “myristate + polybasic motif” mechanism for membrane localization (Heo et al., 2006). The polybasic motif and the lipid modifications have a synergistic effect on the targeting of a GTPase to the negatively charged membrane domains (Ghomashchi et al., 1995).

The phosphatidylserine and PI(4,5)P2, with one and four negative charges respectively, have been indicated as the physiological binding partners for the polybasic motifs at the PM (Cadwallader et al., 1994; Ghomashchi et al., 1995; McLaughlin and Murray, 2005). Recently, PI(3,4,5)P3 was also shown to be important for membrane targeting of small GTPases containing the polybasic motif, as depletion of both PI(4,5)P2 and PI(3,4,5)P3 is required to dissociate such proteins from the PM (Heo et al., 2006). The levels of phosphoinositides are dynamically regulated locally through the action of kinases and phosphatases in specific membrane domains (McLaughlin and Murray, 2005; Simonsen et al., 2001), which might allow dynamic and flexible distribution of small GTPases with polybasic motifs.

Palmitoylation. As introduced previously, palmitoylation is a type of fatty acylation and is characteristically reversible. Among the best studied Ras isoforms, while K-Ras use the strategy of “farnesyl + polybasic motif” to achieve stable membrane localization, H-Ras and N-Ras are well-known examples modified by farnesyl + palmitate. Prenylated H-Ras that lacks palmitoylation can induce cell transformation, but only at a lower efficiency compared to wild type H-Ras that is dually modified (Hancock et al., 1989; Hancock et al., 1990). On the other hand, prenylation of palmitoylated H-Ras could be replaced by artificially engineered polybasic motif, and the mutant H-Ras can function well as a transforming protein (Booden et al., 1999), suggesting that the “two signals” can be any combination with or without prenylation. Importantly, it is not only palmitoylation *per se* but also depalmitoylation that together confer the proper distribution of H-Ras. This is supported by the experiment showing that a Ras protein linked to a fatty acid through a noncleavable thioether bond associates with nearly all

internal membranes (Rocks et al., 2005). This is also consistent with the “kinetic bilayer trapping” hypothesis, which postulates that the localization of the PAT determines the final localization of palmitoylated proteins (Shahinian and Silvius, 1995).

Apparent exceptions to the two-signal hypothesis can be found in Figure 1.4, including many Rab family members, whose two geranylgeranyl groups at the C terminus seem to provide enough hydrophobicity for stable anchorage to the membrane. Their C terminal tails are usually neutral in charge, with or without cysteines for additional palmitoylations. Additional examples are Rit and Rin, which have tails rich for positively charged residues but lack covalent lipid modifications.

1.5.3 Switches for membrane association/dissociation

The targeting of small GTPases to the membrane is dynamically regulated and reversible association and dissociation could be achieved through a variety of molecular switches. The cycle of palmitoylation and depalmitoylation discussed in section **1.5.2** provides not only a “second signal” but also a switch to regulate the localization of small GTPases such as H-Ras. Additional switches that control the interaction between small GTPases and lipid membranes are described as follow.

Myristoyl switch. Myristoyl switch regulates the binding of Arf GTPases to the membrane (Behnia and Munro, 2005). As the myristoylation of Arf GTPases binds promiscuously to membranes and is not sufficient for specific targeting, the specificity of their localization is dictated by where they become GTP-loaded which is coupled to the myristoyl switch. When Arf is GDP bound, an N-terminal amphipathic helix is masked inside a hydrophobic pocket on the core of the GTPase (Pasqualato et al., 2002). As a consequence, the N-myristol group can only interact with the membrane rapidly and

reversibly. The GTP loading of Arf induces a conformational change not only in the switch 1 and 2 regions but also in the interswitch loop which moves to displace the N-terminal amphipathic helix out of the hydrophobic pocket (Goldberg, 1998; Robert et al., 2004). Arf-GTP then can bind tightly to membranes through the hydrophobic residues of the amphipathic helix and the myristoyl anchor, and start to recruit its effectors at the correct location.

GDP-dissociation inhibitors (GDIs). GDIs utilize their hydrophobic pockets to sequester lipid moieties of Rho and Rab GTPases (Resh, 2006b). Using the Rab GTPases as an example, GDP-bound Rab proteins form a complex with GDIs, which release the GTPases from the membrane (An et al., 2003). The reverse process employs a set of membrane proteins, called GDI displacement factors (GDFs), which catalyzes the dissociation of Rab from its GDI so that the dual geranylgeranyl groups of the Rab GTPase are exposed and ready for insertion into the target membrane (Pfeffer and Aivazian, 2004; Seabra and Wasmeier, 2004).

Ca^{2+}/calmodulin (Ca/CaM) switch. The Ca/CaM switch was first shown to regulate a type of natively unstructured proteins called myristoylated alanine-rich C-kinase substrate (MARCKS), which can be anchored to the membrane through its N-terminal myristate and a conserved basic cluster domain in the middle of the molecule (McLaughlin and Murray, 2005). When the cytoplasmic [Ca^{2+}] increases, Ca/CaM can bind to the basic cluster with high affinity, thus reverses its charge from positive to negative and repels the MARCKS from the membrane. Both K-Ras and Rap1A have polybasic regions at their C-termini, and the Ca/CaM switch was also shown to regulate the reversible dissociation of K-Ras and Rap1A, but not H-Ras, from the membrane.

Similar to the working mechanism of GDI, the prenyl modification of K-Ras is part of the motif interacting with Ca/CaM. Different from GDI, the C terminal tails of K-Ras and Rap1A are sufficient to bind to Ca/CaM, suggesting an interaction independent of the GTP/GDP loading status of the small GTPases themselves. After dissociation from the membrane, K-Ras and Rap1A reversibly translocate between the PM and the Golgi/early endosome in cultured hippocampal neurons, the mechanism of which remains unknown (Fivaz and Meyer, 2005).

Electrostatic switch. In addition to the Ca/CaM switch, an alternative mechanism was discovered to regulate the dissociation of K-Ras from the membrane. An evolutionarily conserved serine within the polybasic region of the K-Ras tail (Ser181) can be phosphorylated in a protein kinase C dependent manner. The phosphorylation of this single residue suffices to weaken the interaction between the polybasic region and the membrane and trigger the dissociation of K-Ras from the membrane (Bivona et al., 2006). Upon dissociation, K-Ras translocates to the mitochondria where it induces apoptosis. The Ca/CaM switch and PKC-dependent electrostatic switch might be mutually exclusive in the regulation of K-Ras, because phosphorylation of a single serine in a polybasic region can dramatically decrease the Ca/CaM binding by 200-fold (McIlroy et al., 1991). The differential utilization of the two switches might also be dependent on cell-type and stimulation, as the studies on the Ca/CaM switch and the electrostatic switch used hippocampal neurons stimulated by glutamate, and MDCK cells stimulated by bryostatin-1, respectively (Bivona et al., 2006; Fivaz and Meyer, 2005).

In addition to K-Ras, the electrostatic switch might be repeatedly used in small GTPases with polybasic tails. Using the Prosite database for patterns in a protein

sequence, the last 25 amino acids at the C termini of representative members of the Ras family were analyzed, and known targets and predicted sites of phosphorylation by protein kinase A (PKA) and PKC were illustrated in Figure 1.4. Whether all of these possible phosphorylation sites serve as electrostatic switches to regulate a synchronized dissociation of a variety of small GTPases from the membrane in response to PKA and PKC activation is yet to be systematically examined.

1.5.4 Localization of small GTPases to macrodomains and microdomains

Given the variety of lipid modifications of small GTPases and their additional properties including the presence or absence of polybasic tails and electrostatic switches, it is possible that the different combinations of features collectively function as “zip codes” that target small GTPases to different membranous regions. It is important to correlate these different “zip codes” with the specific subcellular locations, such as the plasma membrane (PM), nuclear envelope (NE), mitochondria and different stages of endosomes. This chapter tentatively names these subcellular locations that can be distinguished under the light microscope as macrodomains in contrast to the microdomains that are better appreciated with the electronic microscopy (EM) or other advanced techniques. As most small GTPases are translated and processed at the endoplasmic reticulum (ER) and Golgi complex, it is possible that these are locations where the distributions of small GTPases can greatly overlap. It is important to mention here that the aforementioned “zip code” is not only an intrinsic property of a small GTPase, but can also undergo changes under different physiological contexts. For example, the presence of a PKC-dependent electrostatic switch in the c terminal end of K-Ras allows K-Ras to shuffle between the plasma membrane and the mitochondria (Bivona et al., 2006). Specifically, the

phosphorylation of serine 181 of K-Ras upon PKC activation allows translocation of K-Ras to the mitochondria where oncogenic K-Ras can promote cell apoptosis (Bivona et al., 2006).

Macrodomains. The subcellular localization of Ras isoforms has been studied extensively and is used as an example here to illustrate how proteins with similar spectrum of binding effectors achieve different localizations based on the features of their C termini. Despite having the same farnesyl group, H-Ras and N-Ras are distributed throughout the exocytic pathway, and mutation of their palmitoylation sites results in their accumulation at the ER and Golgi (Apolloni et al., 2000; Choy et al., 1999). In contrast, K-Ras bypasses the Golgi and reaches the PM probably through a non-exocytic pathway, and its trafficking is not inhibited by brefeldin A (BFA) or dominant-negative Arf proteins (Hancock, 2003). This could be explained by a diffusion of the K-Ras, guided by its polybasic C terminus, down an electrostatic gradient to the negatively charged area of PM (Roy et al., 2000). Alternatively, the trafficking of K-Ras could be a microtubule dependent process, and taxol treatment has been reported to mislocalize K-Ras to structures resembling late endosomes (Thissen et al., 1997).

While the PM has long been the focus of most studies investigating the localization of Ras family members, the outer membrane of the nuclear envelope (NE) might also serve as a location for active signaling mediated by small GTPases. Both previous report (Bivona et al., 2004) and Chapter 3 of this dissertation make the observation that fluorescent protein tagged Rap1B is localized not only throughout the exocytic pathway, but also at the NE. Importantly, Rap1B can be dynamically activated at the NE by its exchanger Epac1, which is anchored at the nuclear pore (see Chapter 3). The localization

of Rap1B at the NE might be dependent on its polybasic tail, as its isoform Rap2B, which has the same geranylgeranyl modification but lacks the polybasic tail, is completely excluded from the NE. The extremely high levels of negatively charged PIP2 at the NE (Larijani and Poccia, 2009) might also contribute to the enrichment of Rap1B at this location. However, it remains to be examined to what extent it could be generalized that geranylgeranyl and polybasic motif allows localization of a small GTPase to the NE. A recent study surveyed the subcellular location of 125 fluorescent protein tagged members of the Ras superfamily (Heo et al., 2006). Although the authors of that study primarily focused on the PM, from the representative images shown, it can be appreciated that Rap1B as well as multiple other members of the Ras superfamily are present on the NE. These members include R-Ras, Rheb, RalA/B and Rap1A of the Ras family, RhoA/C/D/F/G, Rho7, Rif, Rac2/3 and CDC42H of the Rho family, Rab6C, Rab8A/B, Rab18, Rab22B, and Rab23 of the Rab family. Since the imaging conditions in this study might be optimized for the PM instead of the NE, it is possible that this list of small GTPases localized on the NE might be an underestimation. Although most of these small GTPases possess both the geranylgeranyl group and the polybasic motif as expected, it should be noted that exceptions exist, for example Rheb and R-Ras, which are present on the NE, have only 2 and 3 positively charged residues, respectively, while M-Ras, which has both the geranylgeranyl group and a strongly polybasic motif, was not observed on the NE (Ohba et al., 2000).

Microdomains. Small GTPases are postulated to cluster at membrane microdomains to achieve high-fidelity signaling (Harding and Hancock, 2008; Kenworthy, 2007; Tian et al., 2007). Because these microdomains, including the lipid

rafts, are not directly visible under the light microscope (<100nm), alternative strategies such as FRET and EM plus statistical analysis were used to characterize the likelihood of the clustering of small GTPases (Abankwa et al., 2008; Parton and Hancock, 2004), which indirectly defines the membranous domains at a scale beyond direct measurement.

The rationale for the FRET based analysis is that nondimerizing FRET pairs (CFP/YFP or RFP/GFP) could be linked to different small GTPases or their minimal sequences that are subjected to lipid modifications and the tendency of these pairs to cluster at the membrane of living cells could be described by plotting the FRET efficiency against the acceptor density. The clustering of the FRET pairs should be attributed to the partitioning of different lipid components into microdomains, as the clustering can be abolished by 5-methyl-β-cyclodextrin (MβCD) treatment, which disrupts lipid rafts and caveolae by depletion of cholesterol. Initial studies suggest that acylated but not prenylated fluorescent proteins cluster in lipid rafts (Zacharias et al., 2002). A recent study utilized a much more elaborate set of FRET probes as markers for distinct nanodomains to describe the lateral segregation and orientation of H-Ras (Abankwa et al., 2008). This study demonstrated that in addition to the lipid modifications, certain basic residues in helix α4 or the hypervariable region are also critical for the interaction between H-Ras and the plasma membrane.

The segregation of Ras proteins in discrete microdomains have also been examined using EM and spatial analysis (Prior et al., 2001; Prior et al., 2003). This approach relies on the generation of two dimensional (2D) sheets of PM from cultured cells expressing Ras proteins, which are immediately fixed with glutaraldehyde and labeled with immunogold. The EM images are converted into a set of (x,y) coordinates that describes

the 2D array of gold particles, which can be analyzed in a unbiased and quantitative manner using spatial statistics, and whether the particles cluster and the radius of clusters can be determined (Parton and Hancock, 2004). The EM-based spatial analysis revealed that H-Ras clusters in the lipid raft in a cholesterol-dependent manner and the constitutively active H-Ras resides in the nonraft microdomains. On the other hand, K-Ras is also clustered but in a cholesterol-independent manner. Moreover, wild type and constitutively active K-Ras show identical clustering, which can be dramatically reduced if the farnesyl group is replaced by a geranylgeranyl group (Prior et al., 2003). These data suggest that the plasma membrane comprises a heterogeneous mosaic of microdomains, and different Ras proteins are segregated spatially and can also dynamically redistribute to different domains.

It should be noted that the FRET and EM based analyses only measure the clustering of Ras proteins without direct visualization of the “microdomains” *per se*. However, these approaches do reveal important information on the distance between clustered Ras proteins, which should be in an estimated range of 10-100nm. It will be important to expand the study to other small GTPases because of the emerging data in recent years supporting the coupling of different small GTPases at the membranous domains as discussed in the following section.

1.6 GEFS AND CASCADES OF SMALL GTPASES

Having discussed the membrane targeting of small GTPases themselves, the next question is how the localization of GEFs can be coordinated with the localization of their substrates in order to maximize the efficiency of the exchange reaction. It is now known that a GEF can not only stimulate GTP-loading of its substrate GTPases, but also interact

with upstream, regulatory small GTPases. This section will focus on this phenomenon which serves as an important strategy for the spatial regulation of GEFs as well as the coupling of different small GTPases together in interconnected cascades. The mechanisms of the spatial regulation of Epac2 (Chapter 2) and Epac1 (Chapter 1) are also analogous to this general strategy.

1.6.1 Cascades of small GTPases and Ras/Rap interacting domains

Although many well known effectors for small GTPases such as Ras and Rap are kinases, it is also quite common that a GEF for one small GTPase can also be a *bona fide* effector of another small GTPase. This mode of signaling might serve two purposes. First, the selective interaction with the upstream small GTPase ensures proper localization of the GEF and efficient activation of the next small GTPase. Second, this arrangement may allow modulation of the strength and specificity of particular signaling pathways. This is theoretically analogous to a canonical kinase cascade as illustrated in Figure 1.5.

In most of the cascades mentioned above, the small GTPases that initiate the cascades are isoforms of Ras and Rap, and they interact with the GEFs via domains such as Ras association (RA) domain, Ras binding domain (RBD) or Protein kinase C conserved region 1 (C1). RA domain and RBD are conserved domain families of the ubiquitin homologs (UBQ) superfamily (Larsen and Wang, 2002). They are structurally similar to ubiquitin and are present in one or two copies in signaling molecules that bind to the switch I and switch II regions of Ras and/or Rap in a GTP dependent manner. Examples for RA domain and RBD containing proteins are RalGDS (Huang et al., 1998) and Raf-1 (Nassar et al., 1995) respectively. Using Reverse Position-Specific BLAST (RPS-BLAST), a BLAST algorithm more sensitive for the identification of conserved

domains in proteins, 54 proteins with RA domain and 9 proteins with RBD can be retrieved from the human reference sequences. C1 domains are usually rich in cysteines and can bind to zinc, phorbol esters, diacylglycerol (DAG), or Ras/Rap (Mott et al., 1996). Examples for C1 containing proteins that interact with Ras/Rap include Raf-1 and B-Raf (Hu et al., 1995; Okada et al., 1999). Distinct from the RA domain or RBD, the interaction between Ras and the Raf-C1 domain is independent of the GTP bound state, and is enhanced by the farnesylation of Ras (Williams et al., 2000). The presence of both RBD and C1 domains in Raf proteins may allow diverse modes of regulation of Raf proteins by Ras. Using RPS-BLAST, 106 proteins with C1 domain can be retrieved from the human reference sequences.

1.6.2 Bioinformatic search for GEFs capable of Ras/Rap association

Having discussed the protein domains that can interact with Ras and/or Rap, it would be interesting to assemble a comprehensive list of proteins that feature both Ras/Rap binding domains and catalytic domains for a certain family of small GTPases. Theoretically, the proteins in this list would be able to couple different small GTPases into cascades and contribute to the spatial regulation of the small GTPases involved. One traditional approach to assemble such a list is to summarize isolated reports of such proteins from the literature empirically. However, in addition to this approach, we can also utilize the existing database of conserved protein domains to identify the group of proteins that can simultaneously satisfy the above two criteria, namely the presence of a Ras/Rap binding domain and the presence of a catalytic domain for a certain family of small GTPases. As will be discussed later, the latter approach did identify quite a comprehensive list of GEFs, most of which have been confirmed recently in the literature to be capable of Ras/Rap

binding and activating of another small GTPases. Although the search result does not appear to be novel in light of the current literature, the comprehensive result was achieved independent of detailed knowledge of those GEFs identified, and it provided a clear frame work for me to organize these GEFs into distinct categories: GEFs that can mediate coupling of small GTPases within the Ras family and GEFs that can mediate coupling of small GTPases between different small GTPases families. It is reasonable to argue that were this approach taken 5-10 years earlier, it would actually be of certain predicative value to identify GEFs capable of coupling different small GTPases into cascades.

Based on the rationale described above, I performed a bioinformatic search using the Conserved Domain Database (CDD) of National Center for Biotechnology Information (NCBI) (Marchler-Bauer et al., 2009). The general approach is illustrated in Figure 1.6A and explained below.

For the first step, all human proteins related to the UBQ superfamily by RPS-BLAST to include all possible proteins with domains similar to the RA domain and RBD. It is necessary to use the UBQ superfamily rather than a combination of RA domain and RBD, because the latter two families do not include atypical RA domains such as the Epac2 RA domain (Li et al., 2006; Liu et al., 2008), which is instead annotated generally as a member of the UBQ superfamily. Using this approach, all human proteins containing the RasGEF domain, RhoGEF domain, Vps9 domain or Sec7 domain were also identified. Seventeen proteins were found at the intersection of the UBQ related and RasGEF related proteins, two at the intersection of the UBQ related and RhoGEF related proteins, three at the intersection of the UBQ related and Vps9 related proteins. No protein was identified

at the intersection of UBQ related and Sec7 related proteins. For C1 related proteins, despite its considerable overlap with RasGEF and RhoGEF containing proteins, only one type of protein (Vav proteins) were reported to interact with Rap (Arthur et al., 2004). In contrast, all other C1 containing proteins identified in this search (e.g. RasGRP) interact with DAG (Mitin et al., 2005). In the following sections, the GEFs capable of coupling different small GTPases will be discussed in detail.

Theoretically, it is possible that a small GTPase other than Ras and Rap can also promote activation of a second small GTPase via its GEF that is capable of binding to the first GTPase. However, binding domains specific for non-Ras/Rap small GTPases are not as well defined as the RA domains and RBDs. I examined one of the binding partners for the small GTPase RalA/B, RalBP1. This protein has a putative Ral interaction site, which is widely used in pulldown assays to identify activated Ral *in vitro* (Tian et al., 2002). However, no domain family has been built around this domain, and the structural determinants of Ral binding are yet to be fully understood. Interestingly, Ral-RalBP1 interaction does bridge Ral to the inhibition of Rho pathways, as RalBP1 has a conserved RhoGAP domain as well (Jullien-Flores et al., 1995). At the end of this section, I will also discuss an unexpected interaction between Ran and a putative RA domain in Epac1, which couples Ran to efficient Rap1 activation.

1.6.3 Signaling cascades within the Ras family

Several GEFs for small GTPases of the Ras family can bind to Ras and/or Rap, thus linking different small GTPases within the Ras family (e.g. PDZ-GEF2 and Epac2), or mediating amplification of the activation of a small GTPase itself (e.g. PDZ-GEF1 and Sos) (Figure 1.7 and 1.9).

RapGEF2 (PDZ-GEF1). RapGEF2 is better known as RA-GEF or PDZ-GEF1, and is closely related to the Epac proteins (de Rooij et al., 1999) (Figure 1.7A). It was initially identified through a yeast two-hybrid screen and was the first GEF of the Ras family found to have a RA domain (Liao et al., 1999). PDZ-GEF1 not only catalyzes exchange activity of Rap1 and Rap2, but also binds to these Rap proteins in a GTP-dependent manner via its RA domain (de Rooij et al., 1999; Liao et al., 1999; Rebhun et al., 2000), suggesting a positive feedback loop. No Ras binding was detected for PDZ-GEF1, and in this sense, RA domain should be expanded to a broader concept meaning "Ras/Rap Association" domain. PDZ-GEF1 also has a PDZ domain, which will be discussed later in section 1.7.2.

RapGEF6 (PDZ-GEF2). RapGEF6 is better known as RA-GEF2 or PDZ-GEF2, and among its 6 isoforms, isoforms 1-5 contain intact RasGEF domains. PDZ-GEF2 has very similar domain structure as PDZ-GEF1 (Figure 1.7B), and like PDZ-GEF1, PDZ-GEF2 stimulates GTP/GDP exchange of both Rap1 and Rap2 (Kuiperij et al., 2003). However, the RA domain of PDZ-GEF2 binds to and colocalizes with M-Ras, but not other Ras family GTPases including H-Ras, N-Ras, Rap1A, Rap2A, R-Ras, RalA, Rin, Rit and Rheb (Gao et al., 2001). Although M-Ras does not enhance the exchange activity of PDZ-GEF2 *in vitro*, M-Ras does enhance PDZ-GEF2 mediated activation of coexpressed Rap1A at the plasma membrane (Gao et al., 2001). Thus, the RA domain of PDZ-GEF2 allows it to be properly targeted to M-Ras at the plasma membrane and activate its substrate efficiently. The physiological significance of the cascade from M-Ras to Rap is unclear.

Phospholipase C, epsilon 1 (PLCε). PLCε (Figure 1.7C) is a bifunctional enzyme that can hydrolyze phosphatidylinositol 4,5-bisphosphate (PIP2) and promote the activation of Rap1 (Jin et al., 2001). Whether PLCε activates Ras is still a matter of debate (Jin et al., 2001; Lopez et al., 2001). The RA domain of PLCε binds to GTP-bound H-Ras, K-Ras, and N-Ras, but interacts poorly with Rap1A, Rap1B, Rap2A and Rap2B (Bunney et al., 2006). The preference of PLCε RA domain for Ras to Rap can be partly explained by the charge reversal of a glutamate at position 31 in Ras to lysine in Rap. The positively charged lysine at this position would disrupt the favorable interaction with K2173 within the PLCε RA domain (Bunney et al., 2006). Consistent with the binding data, Ras can potentiate PLCε-mediated production of inositol phosphate, while Rap isoforms exhibit only modest effect (Kelley et al., 2001; Kelley et al., 2004; Song et al., 2002). PLCε also translocates to the plasma membrane in cells expressing constitutively active H-Ras or treated with EGF, and the overexpression of PLCε can significantly augment EGF triggered activation of Rap1A (Jin et al., 2001; Song et al., 2001). Despite the poor interaction between PLCε and Rap2B, PLCε was shown to be activated downstream of the beta adrenergic receptor-Epac1 signaling via Rap2B, based on studies using an inactivate mutant Rap2B-N17 (Evellin et al., 2002; Schmidt et al., 2001; vom Dorp et al., 2004). It would be important to examine whether depletion of endogenous Rap2B can uncouple cAMP signals and the activation of PLCε.

RapGEF4 (Epac2). Unlike the PDZ-GEFs and PLCε introduced previously, RapGEF4 (Figure 1.7D), also known as Epac2, is activated by cAMP as discussed in Section 1.3.1. Epac2 has an RA domain that binds to H-Ras, K-Ras, and N-Ras, but not M-Ras, R-Ras, Rap1A, Rap2B, RalA, Rheb, Rin or Rit (Li et al., 2006). The interaction

between Epac2 and H-Ras has an affinity comparable to those of other classical Ras effectors such as B-Raf and Raf-1, and requires an intact RA domain of Epac2, which is readily accessible in the absence of cAMP (Liu et al., 2008). Expression of a constitutively active mutant of H-Ras and activation of endogenous Ras significantly enhance the Rap1 activation by Epac2, whereas an Epac2 mutant with a K684E mutation within the RA domain is incapable of Ras binding and activates Rap1 poorly. Importantly this mutant can fully activate Rap1 when targeted to the membrane through an engineered CAAX motif at its C terminus, suggesting that the interaction between Ras and Epac2 causes compartmentalization of Epac2 to the plasma membrane where it has better access to Rap1 (Liu et al., 2008). Alternative strategies for membrane translocation of Epac2 independent of Ras have been proposed, including membrane association via the first cAMP-binding domain of Epac2 and the interaction between Epac2 and neuroligin (Niimura et al., 2009; Woolfrey et al., 2009). The necessity and sufficiency of the first cAMP-binding domain in the membrane localization of Epac2 is a somewhat unexpected observation, and no N-terminal lipid modification such as myristoylation or other mechanism has been revealed to explain this phenomenon. Neuroligins are neuronal cell adhesion molecules that interact with beta-neurexins and form intercellular junctions. The cytoplasmic C-termini of neuroligins bind to one of the three PDZ domains of PSD-95, which also interacts with NMDA2 receptors and potassium channels through the other two PDZ domains (Irie et al., 1997). Thus, Epac2 could be part of a huge complex at the postsynaptic densities, and whether it interacts with neuroligins directly has not been shown. The different models of targeting Epac2 to the membrane might reflect differences in the experimental systems used these studies. It is also likely that multiple interactions coexist to ensure stable association of Epac2 with the membrane, although

Ras-Epac2 association seems to be the only direct link that is regulated by specific physiological cues.

Ral GEFs. The GEFs for Ral proteins (RalA and RalB) include Ral guanine nucleotide dissociation stimulator (RalGDS) and RalGDS-like proteins (RGL) (Figure 1.7E&F). RalGDS was found to interact with R-Ras, H-Ras, K-Ras, Rap1 and Rap2 through an yeast two-hybrid screen, and the interaction requires the RBD at its C terminus (Hofer et al., 1994; Nancy et al., 1999; Spaargaren and Bischoff, 1994). Although RalGDS interacts with multiple small GTPases, it is only activated robustly by H-Ras (Urano et al., 1996). If H-Ras activates RalGDS by recruiting it to the membrane, it is difficult to explain why Rap proteins, which interact with RalGDS at a higher affinity than Ras *in vitro* (Herrmann et al., 1996; Nassar et al., 1996; Shirouzu et al., 1998; Wohlgemuth et al., 2005), can not activate RalGDS very well *in vivo*. One explanation is that H-Ras functions more than an anchor for RalGDS. This is supported by the observation that the activation of RalGDS by Ras can be achieved independently of its RBD (Linnemann et al., 2002). In this study, the authors identified a point mutation within the RBD of RalGDS that abrogated the Ras binding, and when the mutant was artificially targeted to the membrane, it can still be activated by Ras in a manner dependent on the switch II region (Linnemann et al., 2002). Interestingly, the PI3K-dependent kinase 1 (PDK1), which is downstream of the EGF stimulated Ras activation, can induce RalGDS activation by relieving the auto-inhibitory effect of its N-terminus on the catalytic domain by a kinase-independent mechanism (Tian et al., 2002). Together, these data shed light on the complicated relationship between Ras, Rap and RalGDS. Ras is sufficient to activate RalGDS probably because it can target RalGDS to the membrane

as well as relieve the autoinhibition of RalGDS via PI3K and PDK1. While Rap can provide a better anchor than Ras for the membrane targeting of RalGDS because of the much higher affinity between Rap and RalGDS, it is not sufficient to activate RalGDS probably because it is not a strong activator of PI3K, thus can not relieve the autoinhibition of RalGDS via PDK1. Since Ras and Rap are often concurrently activated by growth factors such as EGF and PDGF (Zwartkruis et al., 1998), it is possible that the two small GTPases can cooperate to activate RalGDS synergistically, with Rap providing a better anchor at the membrane and Ras relieving the autoinhibition via PI3K and PDK1. Moreover, the C-termini of RalA/B are more similar to Rap1A/B, both being rich in positively charged residues and being attached to geranylgeranyl groups (Figure 1.4), thus Rap1A/B may bring RalGDS closer to the vicinity of RalA/B. It would be interesting to determine whether the activation of RalGDS can be reduced in Rap deficient cells either by RNA interference or dominant negative mutants of Rap.

RGL1, another exchanger for Ral with 69% amino acid similarity with RalGDS, also interacts with Ras in a yeast two-hybrid system (Kikuchi et al., 1994). Products of the other two RGL genes (RGL2 and 3) also possess conserved RA domains at their C-termini, suggesting a shared mechanism of regulation by Ras. All three RGLs can bind to Rap as well and are potential Rap effectors (Peterson et al., 1996; Wolthuis et al., 1996; Xu et al., 2007). Interestingly, RGL2 can be phosphorylated by PKA at a residue within its RA domain, which reduces the interaction between RGL2 and Ras (Ferro et al., 2008). This provides a possible mechanism for the termination of the interaction between Ras and the RA domain of RGL2, and it is worth investigating whether interactions between

Ras/Rap and other RA domains could be terminated by phosphorylation of residues at the binding interface.

Sos and RapGEF5 (Repac). These two proteins do not have RA domain or RBD, and were not retrieved by the bioinformatic search for mediators of small GTPase signaling cascades. However, they are still regulated by Ras or similar small GTPases and will be discussed briefly below.

Sos, the Ras exchanger mentioned previously in section 1.3.1, requires binding of a GTP-loaded Ras to its allosteric site to achieve full activation (Boykevisch et al., 2006; Margarit et al., 2003). This interaction also serves as mechanism to recruit Sos to the membrane (Gureasko et al., 2008). In this case, Sos functions as an amplifier for the activation of Ras itself instead of coupling signaling cascade from one small GTPase to another.

Repac, also called RapGEF5 or MR-GEF (Figure 1.7G), exhibits close sequence similarity to Epac proteins, but lacks a cAMP binding domain. It is a constitutive activator of both Rap1 and Rap2 (de Rooij et al., 2000), and contains a nuclear localization signal (NLS), which might be responsible for its presence in the nuclei when transfected in HeLa cells (Ichiba et al., 1999). However, it is unclear where the endogenous Repac is localized and whether the NLS is important for its activity toward Rap. Although Repac contains a region resembling the classical RA domains, it does not meet the criteria set for RA domains at the NCBI database for Conserved Domains. However, this region from Repac does interact with GTP-loaded M-Ras (Rebhun et al., 2000), which may localize it to the plasma membrane (Heo et al., 2006). Interestingly, when Rap1A was overexpressed, a constitutively active M-Ras(71L) mutant inhibited the

ability of Repac to activate Rap1A in a dose-dependent manner (Rebhun et al., 2000). The authors hypothesize that M-Ras is a negative regulator of Rap1 either by subcellular sequestration of Repac or by inhibition through interaction with the putative RA domain (Rebhun et al., 2000). However, it would be important to rule out that the observation was due to simultaneous overexpression of all three different proteins in their experimental system, and it is yet unknown whether M-Ras could promote activation of endogenous Rap1 via Repac.

1.6.4 Signaling from Ras family to the Rho family

Small GTPases of different families can also be coupled to form a cascade. This section discusses the coupling of members of the Ras family, Ras and Rap1, to Rac of the Rho family.

Tiam1 (Figure 1.8A), a specific exchanger for Rac, was the first protein found to link Ras activation to Rac activation (Lambert et al., 2002). Ras-GTP interacts with the Ras-binding domain (RBD) of Tiam1 and stimulates its GEF activity toward Rac. The endogenous Tiam1 is required for the Ras-mediated activation of Rac, which is significantly impaired in Tiam1 null cells (Lambert et al., 2002). Alternatively, Rac can also be activated by Ras via Sos and PI3K (Nimnual et al., 1998; Scita et al., 1999; Scita et al., 2000). The Ras-Tiam1-Rac cascade is physiologically relevant based on the following observations. One, Tiam1-deficient mice are resistant to Ras-induced skin tumors (Malliri et al., 2002). Two, the dominant-negative Rac can block Ras-mediated transformation of rodent fibroblasts (Khosravi-Far et al., 1995; Qiu et al., 1995). Three, interference of endogenous Ras by siRNA or dominant-negative Ras can block the Tiam1-mediated Rac activation and the migration of Schwann cells treated with

neurotrophin-3 (Yamauchi et al., 2005). The mechanism by which Ras triggers Tiam1-mediated Rac activation is unclear. It is possible that Ras facilitates the translocation of Tiam1 to the plasma membrane or Ras directly activates the intrinsic catalytic activity of Tiam1 (Lambert et al., 2002).

The signaling cascade from Rap1 to Rac has also been reported (Arthur et al., 2004; Maillet et al., 2003; Zaldua et al., 2007). Rac was initially found to be activated downstream of the cAMP/Epac1/Rap1 pathway to regulate a soluble form of amyloid precursor protein (sAPPα) (Maillet et al., 2003). Rac also functions downstream of Rap1 to promote cell spreading, and the mechanism involves recruitment of Tiam to the edge of spreading cells via its DH-PH domains instead of RBD (Arthur et al., 2004). This suggests that the potential connections between small GTPases (e.g. Ras and Rap1) and their downstream exchangers (e.g. Tiam) could be much more diverse than would be predicted with interactions mediated by RA/RBD alone. In addition to cell spreading, the sequential activation of Rap1 and Rac has been shown to play important roles in the platelet-derived growth factor (PDGF)-induced formation of leading edge structures and cell movement (Takahashi et al., 2008), as well as atrial natriuretic peptide (ANP)-induced protection of pulmonary endothelial barrier (Birukova et al., 2010; Birukova et al., 2008), although the specific role of Tiam1 in coupling Rap1 and Rac in these models was not vigorously tested.

Since both Ras and Rap1 can interact with Tiam1 and promote Rac activation, one unresolved issue is the extent of selectivity in terms of the differential Ras or Rap1 binding for Tiam1. It is also important to know which cascade, Ras/Tiam1/Rac or Rap1/Tiam1/Rac, is predominant and in which cellular processes. Adding to the

complexity of the issue is the recent discovery that Tiam2 (Figure 1.8B), also called STEF, can interact with Rap1 much better than Tiam1 (Zaldua et al., 2007), which raises the possibility of Tiam2 being the major Rap1 effector to mediate the activation of Rac.

In addition to Tiam1 and Tiam2, another Rac exchanger, Vav2 (Figure 1.8F), has been shown to couple Rap1 to Rac (Arthur et al., 2004). The Rap1-Vav2 interaction can be detected *in vitro* and *in vivo* and requires the DH-PH domains of Vav2, which suggests that Vav2 functions similarly as Tiam1 and directly mediates the signaling from Rap1 to Rac. However, an alternative model was also reported, where Rap1 affects Vav2 indirectly via PI3K (Fukuyama et al., 2005).

Despite the many studies linking Ras/Rap1 to Rac as discussed above, it is yet to be investigated whether Ras/Rap1 is coupled to specific Rac isoforms (Rac1, Rac2 and Rac3), which exhibit different subcellular localizations and function in different cellular processes (ten Klooster and Hordijk, 2007). It would also be interesting to evaluate the proximity of Ras/Rap1 to different Rac proteins at microdomains of the lipid membrane, given that the C termini and lipid modifications of certain pair of small GTPases are more similar than those of other pairs.

1.6.5 Signaling from Ras family to the Rab family

One addition group of proteins identified in the bioinformatic search for exchangers that mediate the crosstalk from Ras family to the Rab family are Ras interaction/interference (Rin) proteins, including Rin1, Rin2 and Rin3 (Figure 1.8C, D&E). All three proteins contain a RA domain and a Vps9p domain which catalyzes the activation of Rab5 and Vps21p-like proteins.

Rin1 was initially discovered as a molecule that interferes with the Ras function in the yeast. Its interaction with H-Ras is GTP-dependent and requires an intact “effector domain”, and it is targeted to the plasma membrane where Ras is located (Han and Colicelli, 1995). As a downstream effector for Ras, Rin1 is unique in that it inhibits cellular transformation by activated mutant Ras, while other Ras effectors commonly enhances transformation (Wang et al., 2002). Ras binds to Rin1 via its RA domain at its C-terminus (Han et al., 1997), and the affinity (Kd, 22nM) approximates that observed for Raf1 and Ras interaction (Wang et al., 2002). Interestingly, the Ras-Rin1 interaction is regulated by the interaction between Rin1 and the scaffolding protein 14-3-3, which occurs upon phosphorylation of serine 351 of Rin1 by protein kinase D (PKD) (Wang et al., 2002). Mutation of serine 351 to alanine abolishes the binding of this mutant to 14-3-3, and allows the mutant to shift to the plasma membrane to block Ras-mediated transformation more efficiently.

Besides the capability of Ras binding, the role of Rin1 as a mediator of the cascade from Ras to Rab proteins is also dictated by the presence of a functional, Vps9p-like catalytic domain, which was first discovered to interact with a GDP-bound Rab5A mutant in a yeast-two hybridization (Tall et al., 2001). Rin1 stimulates the guanine nucleotide exchange of Rab5, Rab5A-dependent endosomes fusion, and EGF receptor-mediated endocytosis. Importantly, the effect of Rin1 on all these three processes is potentiated by activated Ras (Tall et al., 2001). Although the authors stated that Ras directly enhances the exchange activity of Rin1 toward Rab5 *in vitro*, the rate of guanine nucleotide exchange stimulated by Rin1 does not appear to be dramatically increased in the presence of Ras-GTP. It would be important to test directly whether the positive effect of RasGTP

on the above mentioned three processes is due to proper localization of Rin1 to the plasma membrane where Ras is localized.

Rin1 also regulates signaling downstream of insulin receptor. Rin1 is recruited to the insulin receptor upon tyrosine phosphorylation of the receptor itself, and enhances insulin-receptor mediated endocytosis (Hunker et al., 2006). However, a truncated Rin1 lacking the C-terminal GEF and RA domains, but not the truncation lacking the N-terminal SH2 domain and proline-rich domains, can also stimulate endocytosis, suggesting that Ras and its interaction with the RA domain of Rin1 might play a less important role in this process.

In addition to the regulation of the trafficking and signaling of EGFR and insulin receptor, Rin1 participates in the TGF-β receptor (TGF-βR) signaling, which could be modulated by Ras independent of its interaction with the RA domain of Rin1 (Hu et al., 2008). Rin1 promotes TGF-βR signaling through enhanced endocytosis, and TGF-βR activation in turn reduces Rin1 expression through induction of a transcription repressor called snail. The dynamic balance can be disturbed by constitutive Ras signaling, which stabilizes snail at the protein level, resulting in strong silencing of Rin1 and reduction in Rab5-mediated trafficking of TGF-βR (Hu et al., 2008).

Similar to Rin1, Rin2 connects Ras to Rab5 and plays an important role in the endocytosis of E-cadherin in Madin-Darby canine kidney (MDCK) cells induced by hepatocyte growth factor (Kimura et al., 2006). Rin3 has the similar domain structure as Rin1 and Rin2, thus might use the same strategy to couple Ras to Rab5.

1.6.6 Signaling from Ran to the Ras family

The coupling of Ran to Rap1 of the Ras family via Epac1 will be briefly introduced here and then described in detail in Chapter 3.

Ran is a small GTPase that is activated in the nucleus and inactivated upon exiting the nuclear pore. This gradient of Ran-GTP and Ran-GDP across the nuclear envelope plays an important role in the nuclear transport, and is established by the compartmentalization of RCC within the nucleus and binding of RanGAP to RanBP2 at the cytoplasmic side of the nuclear pore complex. In addition to the interaction with RanGAP, RanBP2 also has four binding domains for GTP bound Ran that were thought to bring Ran close to RanGAP so as to facilitate the inactivation of Ran by RanGAP. Interestingly, Ran, RanBP2 and several other components of the NPC were found to interact with Epac1 by a proteomic survey for the binding partners for Epac1. The Ran-Epac1 interaction is direct and GTP-dependent, suggesting that Epac1 is a *bona fide* Ran effector. Epac1 has a region between its REM domain and catalytic domain that bears resemblance to the RA domain of Epac2, but Epac1 does not bind to Ras and this region did not satisfy the criteria for the UBQ superfamily. This putative RA domain of Epac1 is required, though not sufficient, for Epac1 binding to Ran. Importantly, this Ran-binding region of Epac1 contributes to the localization of Epac1 to the NPC and Epac1-dependent activation of Rap1 on the nuclear envelope. The regulatory region of Epac1 also seems to contribute to the association of Epac1 with the NPC but in a Ran-independent fashion. The above results provide the first evidence of a connection of Ran to another small GTPase of the Ras superfamily. Since Ran exhibits different patterns of localization

throughout the cell cycle, it might dynamically regulate the spatial organization of Epac1-dependent Rap1 activation at multiple stages of the cell cycle.

1.6.7 A network of small GTPases linked together by GEFs

As summarized in Figure 1.9, the cascades of small GTPases mediated by different GEFs can be organized into a network. Although it has been difficult to study the collective behavior of such a heterogeneous group of small GTPases across four different families, this network model allows us to make some assumptions worthy of further investigation. First, Ras proteins sit at the top of a hierarchy of small GTPases. Ras proteins are rapidly activated by various extracellular stimuli and their effectors include a wide spectrum of GEFs for other small GTPases. There is currently no example of a cascade from non-Ras small GTPases to Ras proteins, further supporting role of Ras proteins as "commander-in-chief" among small GTPases. Second, multiple GEFs couple Ras-GTP to Rap1 activation. In fact, five out of the six RAPGEFs (RAPGEF1-6) have RA domains or putative RA domains, and they either promote Rap1 activation downstream of Ras activation (e.g. PDZ-GEF2 and Epac2), or function as an amplifier of the activation of Rap1 itself. These observations support the idea that Rap1 possibly augments and sustain signals emanating from Ras. Third, both Ras and Rap1 may converge on either Ral or Rac, forming more complex relationships among these small GTPases instead of simple linear relationships. The relative contribution of Ras and Rap1 to the activation of Ral and Rac and how the reaction rate of each cascade affects the kinetics of the whole network have yet to be elucidated. Fourth, while we have significant amount of knowledge on the signaling of Ras, Rap1, Ral and Rac on the PM, few studies so far looked at the signaling of small

GTPases at the NE. The coupling of Ran and Rap1 by Epac1 at the NE do suggest that signaling network of small GTPases may exist on the NE as well.

1.7 ADDITIONAL MECHANISMS FOR SPATIAL REGULATION OF RAPGEFS

Given the topic of the thesis on the spatial regulation of Rap1, this section will focus on examples of GEFs for Rap GTPases whose localizations are controlled by mechanisms other than RA domain mediated protein interaction.

1.7.1. RAPGEF1 (C3G) and adaptor proteins

Out of the six known RAPGEFs, C3G is the only one that does not have a RA or putative RA domain (Figure 1.10A). The proper localization of C3G is also crucial for its ability to activate Rap, and it provides an example of how adaptor proteins and post-translational modifications regulate targeting and activity of a GEF.

The activation of C3G requires adaptor proteins that recruit C3G to various docking proteins on the membrane. The adaptor proteins for C3G include Crk, Crk like proteins (CrkL) and Crk-associated substrate (Cas) (Kirsch et al., 1998; Knudsen et al., 1994; Smit et al., 1996). Crk and CrkL belong to the adaptor-type Src homology (SH)2-containing molecules, and they also contain SH3 domains, which bind to the proline-rich sequences of C3G (Tanaka et al., 1994). Unlike many other SH3-binding proteins which interact with SH3 domains of multiple proteins, C3G has four proline-rich sequences in the center region of the protein, and these sequences are capable of binding individually to the SH3 domain of Crk, supporting the idea that C3G plays a specific role in Crk signaling pathways (Knudsen et al., 1994). The third adaptor molecule, Cas, was found to interact with C3G in a two-hybrid screen (Kirsch et al., 1998) and it binds to C3G via its

SH3 domain both *in vitro* and *in vivo*. The interaction involves a proline-rich Cas-binding site located N-terminal to the Crk binding motifs characterized previously.

Instead of directly targeting C3G to the lipid membrane, CrK and CrKL couple C3G to a variety of docking proteins at the membrane where C3G functions to activate Rap. Examples of these docking proteins include platelet-derived growth factor alpha (PDGFα) receptor (Yokote et al., 1998), Cas-L (Crk-associated substrate-related protein) (Ohashi et al., 1998), Cbl (Schmitt and Stork, 2002; Uemura and Griffin, 1999), Gab1 (Sakkab et al., 2000), Shp2/Gab2/TrkA complex (Wu et al., 2001), and Dab1 (Ballif et al., 2004). The common mechanism for these docking proteins involves tyrosine-phosphorylation by upstream signals and direct interaction with the SH2 domains of Crk or CrkL. The wide selection of docking proteins may allow targeting of C3G to specific compartments within the cell in response to different extracellular stimuli.

1.7.2. PDZ domains of PDZ-GEF1 and PDZ-GEF2

In addition to its interaction with Rap, PDZ-GEF1 also binds to synaptic scaffolding molecule (S-SCAM) through heterodimerization of PDZ domains. In rat brain, this interaction localizes PDZ-GEF1 to the synaptic areas of the cerebellum (Ohtsuka et al., 1999). In PC12 cells, PDZ-GEF1 and S-SCAM form a complex with ankyrin repeat-rich membrane spanning protein (ARMS) and TrkA receptor in a NGF-dependent manner at the late endosomes, and promote sustained Erk activation and neurite outgrowth (Hisata et al., 2007). PDZ-GEF1 was also reported to associate with beta-catenin through S-SCAM at cellular junctions (Kawajiri et al., 2000).

The PDZ-GEF2, which also features a PDZ domain, plays an important role in the maturation of adherens junctions and cell mighration selectively via Rap1A (Dube et al.,

2008; Severson et al., 2009). During the process of cell migration, PDZ-GEF2 interacts with junctional adhesion molecule-A (JAM-A) and AF6 through PDZ-mediated binding, which increases the local levels of Rap1A-GTP and beta1 integrin (Severson et al., 2009). As mentioned previously, PDZ-GEF2 also possesses a RA domain that interacts with M-Ras. The relationship between the PDZ and RA domains in the spatial regulation of PDZ-GEF2-mediated Rap1 activation is yet to be clarified.

1.7.3. Direct spatial regulation of Epac1 by cAMP

Epac1 has a similar domain structure as Epac2 (Figure 1.10B). GFP-tagged Epac1 was previously reported by our lab to colocalize with immunofluorescent-labeled endogenous NPC (Wang et al., 2006), and this is confirmed by our recent proteomic survey, in which flag-Epac1 coimmunoprecipitates with multiple components of the NPC. The localization of Epac1 at the NPC is very stable and it remains unchanged upon stimulation with an Epac1-specific cAMP analog (see Chapter 3). However, cAMP seems to regulate a pool of Epac1 in the cytoplasm and promote their translocation to the PM (Ponsioen et al., 2009). The membrane translocation of Epac1 allows Rap1 activation at the PM which contributes to enhanced cell adhesion. This phenomenon is especially pronounced in cells expressing high levels of GFP-Epac1 based on images shown in the original study and our own observation. The cAMP-dependent translocation of Epac1 from the cytoplasm to the PM is reversible and requires the DEP domain of Epac1. However, no binding partner at the PM has been identified for Epac1, and this translocation is likely to be mediated by the direct interaction between the DEP domain and the inner side of PM.

It is possible that Epac1 promote Rap1 activation both at the PM and the NE. However, since Epac1 is predominantly enriched at the NPC, NE might be the primary

site of Epac1 dependent Rap1 activation. The latter is supported by previous study using cell fractionation (Wang et al., 2006). In this study, the Epac1-specific cAMP analog activates Rap1 only in the nuclear fraction but not the membrane fraction (including the PM), where cAMP activates Rap1 via C3G in a PKA dpendent manner.

1.7.4. Regulation of RasGRP2 and RasGRP3 by DAG and Calcium

RasGRP2 and RasGRP3, also known as CalDAG-GEFI and CalDAG-GEFIII (Figure 1.10C&D), are unique GEFs that are capable of activating both Ras and Rap (Mitin et al., 2005; Springett et al., 2004). Other members of this group of proteins, RasGRP1 and RasGRP4, activate Ras only. All RasGRPs contain a C-terminal catalytic region, consisting of a REM domain and a CDC25 domain with GEF activity, and an N-terminal regulatory region, consisting of two EF-hand motifs in tandem for calcium binding and a C1 domain for interaction with diacylglycerol (DAG).

The interaction between DAG and the C1 domain of RasGRP3, as well as RasGRP1 and RasGRP4, is the primary mechanism for the membrane targeting and activation of these RasGRPs (Ebinu et al., 1998; Kawasaki et al., 1998a; Lorenzo et al., 2001; Tognon et al., 1998). In contrast, RasGRP2 exhibits low affinity towards DAG and its subcellular localization is highly dependent on actin dynamics (Caloca et al., 2004). Upon induction of F-actin by cytoskeletal regulators such as Vav, Vav2, Dbl and Rac1 leads to translocation of RasGRP2 from the cytosol to membrane ruffles where its interaction with F-actin promotes compartmentalized activation of Rap1. Interestingly, a longer isoform of RasGRP2 was reported to have extra signal sequences at the N-terminus for myristoylation and palmitoylation, and these lipid modifications lead to constitutive membrane association of this isoform (Clyde-Smith et al., 2000).

The EF-hand motifs of RasGRPs serve as sensors for calcium ions but cause distinct responses in different contexts. While calcium ionophore was reported to activate Rap1A via RasGRP2 and H-Ras and R-Ras via RasGRP1 (Kawasaki et al., 1998b), it can also inhibit the exchange activity of RasGRP2 towards N-Ras (Clyde-Smith et al., 2000). The effects of Calcium and DAG on RasGRP2 appears to be additive (Kawasaki et al., 1998b), thus RasGRP2 and probably other RasGRPs, can serve as coincidence detectors for Calcium and DAG signals.

1.8 PHYSIOLOGICAL SIGNIFICANCE OF THE SPATIAL REGULATION OF RAP PROTEINS IN MOUSE MODELS

1.8.1 The reality

Most studies on the spatial regulation of small GTPases and their GEFs were carried out by comparing wild type and mutated proteins in cell culture systems. The endpoints of these studies usually involve measurements of changes in certain cellular processes, e.g. endocytosis (Tall et al., 2001), neurite outgrowth (Liu et al., 2008), cell adhesion (Ponsioen et al., 2009), etc. These systems allow convenient correlation of protein interactions, subcellular localizations and cellular phenotypes. However, they fall short on addressing the relevance of the spatial control of cell signaling in physiological processes *in vivo*. To attempt to close this gap in our knowledge, at least two stages of work on genetic animal models will be useful. First, characterize the phenotype of an animal null for a small GTPase or a GEF. Second, characterize the phenotype of an animal with knocked-in alleles encoding mutated proteins with normal enzyme activity but defective localization. A similar strategy has been applied, for example, in a study investigating the requirement of Ras-PI3K (p110α) interaction in growth factor signaling

and Ras-driven tumorigenesis *in vivo* (Der and Van Dyke, 2007; Gupta et al., 2007). However, in the field of signaling of small GTPases and their GEFs, such studies have not been carried out, and possible hurdles should be anticipated, e.g. the redundancy of similar small GTPases and GEFs that might easily compensate subtle phenotypes.

Based on the current literature on mouse models with genetic depletion of small GTPases or GEFs, can we correlate the phenotypes to the known mechanisms of spatial control of these signaling molecules? For certain phenotypes and cellular processes, we can tentatively correlate protein localization to biological function when the subcellular location of a particular protein matches the location where the physiological process occurs. However, whether the molecular connections shown *in vitro* are actually happening *in vivo* will need further investigation. The following sections will focus on genetic mouse models lacking certain Rap GTPases or GEFs for Rap. These mouse models have defects in processes such as cell adhesion, angiogenesis and exocytosis, all of which clearly involve signaling events at the PM. Thus they serve as general examples *in vivo* for Rap signaling at the PM, although it remains unknown how the theory of microdomains and the activation of Rap at other subcellular locations fit into the physiology of a whole animal.

1.8.2 Cell adhesion

Several lines of evidences support a physiological role of Rap1A and Rap1B in cell adhesion. In one study, the primary hematopoietic cells from spleen or thymus of $Rap1A^{-/-}$ mice exhibit diminished adhesion on ICAM and fibronectin. The phenotype is relatively mild and the authors attributed it to the functional complementation by Rap1B (Duchniewicz et al., 2006). However, in another study from Quilliam's group,

backcrossing into C57BL/6J mice led to death of some Rap1A$^{-/-}$ embryos (Li et al., 2007). The authors further showed decreased adhesion and increased haptotaxis in the isolated Rap1A$^{-/-}$ macrophages. Rap1B is the dominant isoform in B cells, and in one study, B cells from Rap1B$^{-/-}$ mice displayed reduced adhesion to stromal cell line, while their proliferation and BCR-mediated activation of ERK1/2, p38 MAPKs and AKT are intact (Chu et al., 2008). Rap1B is also abundant in platelets and can be rapidly activated upon stimulation. Accordingly, in another study, Rap1B$^{-/-}$ mice exhibit a prolonged bleeding time due to decreased activation of integrin αIIbβIII and defective aggregation of platelets (Chrzanowska-Wodnicka et al., 2005). Mice null for Rap2a or Rap2B are not available and whether they affect cell adhesion *in vivo* is unclear.

The genetic ablations of several GEFs for Rap also cause defective cell adhesion in mice. First, C3G null mice die before E7.5, and Cre-mediated ablation of C3G in MEFs causes impaired cell adhesion and accelerated migration, which can be complemented by Rap1 activation (Ohba et al., 2001). Second, PDZ-GEF2 as well as its upstream M-Ras are involved in TNFα-stimulated and Rap1-mediated integrin activation in splenocytes (Yoshikawa et al., 2007), and this exemplified a crucial role of the cascade from M-Ras to Rap1 via PDZ-GEF2 (see Figure 1.9) in adhesion *in vivo*. Third, CalDAG-GEFI is expressed preferentially in the brain and blood, and platelets from CalDAG-GEFI$^{-/-}$ mice are severely compromised in integrin-dependent aggregation (Crittenden et al., 2004).

1.8.3 Angiogenesis

Angiogenesis is a more complicated trait than cell adhesion, and it could involve multiple aspects of the endothelial cell functions including proliferation, adhesion and migration.

Rap1 and some of its GEFs have been shown to play important roles in this dynamic process.

While Rap1B$^{-/-}$ mice have defective platelets as mentioned before (Chrzanowska-Wodnicka et al., 2005), the authors also reported 85% embryonic and perinatal lethality of the Rap1B-null mice. Moreover, at least 40% of the Rap1B$^{-/-}$ embryos had abdominal, cranial and hepatic bleedings and died in utero between E13.5 and E18.5. This indicates that at least during certain stage of embryonic development, Rap1B has critical and non-redundant roles. The finding also raises the question of whether the bleeding in the embryo could be explained by defective platelets at all. A new study from the same group demonstrated that Rap1B$^{-/-}$ mice are actually defective in angiogenesis (Chrzanowska-Wodnicka et al., 2008). The authors attributed the phenotype to impaired signaling downstream of VEGF and bFGF in the Rap1B null mice, as the activation of p38 and ERKs are reduced and the endothelial cells show decreased proliferation and migration. Similarly, angiogenesis and neovascularization are also impaired in Rap1A$^{-/-}$ mice, and the activation of p38 and ERKs in response to FGF2 is reduced as well (Carmona et al., 2009; Yan et al., 2008). It is likely that Rap1A and Rap1B cooperate in the regulation of angiogenesis and endothelial cell functions, and it would be of great value to test whether double knockout of Rap1A and Rap1B will result in more severe phenotypes. Interestingly, genetic ablation of B-Raf, a common effector for Ras and Rap1, also leads to embryonic lethality in mice as a result of endothelial apoptosis and defective placenta (Galabova-Kovacs et al., 2006; Wojnowski et al., 1997). Perhaps the signals from both Rap1A and Rap1B impinge on B-Raf in the endothelial cells, thus the ablation of the latter compromise the vascular development to a greater extent than the ablation of either

Rap1A or Rap1B alone. Because effective Rap1-B-Raf signaling to ERKs occurs preferably at the PM (Wang et al., 2006), these *in vivo* data also suggest an important role for Rap1 signaling at the PM in angiogenesis.

Disruption of several GEFs for Rap proteins also lead to defective vasculature in mice. While a previous line of C3G$^{-/-}$ mice died before E7.5 (Ohba et al., 2001), another line of C3G$^{-/-}$ mice reported recently died around E11.5 (Voss et al., 2003). In this new study, the authors observed embryonic hemorrhage due to severe vascular defects. Different than the models surrounding the endothelial cell functions established with Rap1A or Rap1B null mice, the authors stated that the vascular defects in the C3G$^{-/-}$ mice is caused by abnormal vascular myogenesis and compromised vascular supporting cells. Thus, endothelial cells might not be the only target regulated by Rap signaling during angiogenesis. Mice null for another Rap exchanger, PDZ-GEFI, also exhibit defects in angiogenesis (Wei et al., 2007). PDZ-GEFI starts to express at E8.5 in wild-type mice and continues thereafter. The embryos of PDZ-GEFI$^{-/-}$ mice become grossly abnormal around the time of PDZ-GEFI expression and die by E9.5 with severe abnormality of yolk sac blood vessels. The embryos proper also show defects in the formation of major blood vessels (Wei et al., 2007). These data together support non-redundant roles for C3G and PDZ-GEFI in angiogenesis during early embryonic development.

1.8.4 Exocytosis

The limited evidence for the involvement of Rap1 signaling in exocytosis *in vivo* mostly came from works on mice lacking the Rap GEF Epac2. cAMP can potentiate the high glucose (16.7mM) induced exocytosis of insulin granules over time, with a first phase of prompt, marked and transient increase and second phase of moderate and sustained

increase. Knockout of Epac2 significantly diminishes the cAMP-dependent potentiation of the first phase of insulin release, but not the second phase (Shibasaki et al., 2007). The authors went on to show, using an insulin secreting cell line, that cAMP can activate Rap1 through Epac2 and knockdown of Rap1 reduces insulin secretion from these cells (Shibasaki et al., 2007). Whether the aforementioned $Rap1A^{-/-}$ or $Rap1B^{-/-}$ mice have defect in insulin secretion has not been examined, and if they do, the results would confirm the role of Epac2/Rap1 pathway in β cell function *in vivo*.

It is worth noticing that the initial observation of compromised exocytosis of insulin granules in $Epac2^{-/-}$ β cells was made by total internal reflection fluorescence (TIRF) imaging using Venus (enhanced yellow fluorescent protein) tagged insulin. The actual phenotype in the whole animals turns out to be very subtle. The $Epac2^{-/-}$ mice are not apparently diabetic. When challenged with oral glucose, the levels of serum insulin and blood glucose are not significantly different between wild type and $Epac2^{-/-}$ mice (Zhang et al., 2009). It is unknown whether backcrossing can achieve a more clearcut phenotype. However, the authors stated that Epac2 serves as a direct target for antidiabetic sulfonylurea drugs, which increase serum insulin and lower blood glucose in wild type mice but not in $Epac2^{-/-}$ mice. Although the authors did not rule out the possibility that sulfonylurea drugs activate Epac2 indirectly via elevation of endogenous cAMP, the study did shed light on the regulatory role of Epac2 in insulin secretion *in vivo*.

Epac2 is also abundantly expressed in the brain (Kawasaki et al., 1998a), so it is possible that Epac2/Rap1 signaling could analogously regulate the exocytosis of neurotransmitter granules from neuronal axons. Given the role of Epac2 in neurite out

growth (Liu et al., 2008) and synapse remodeling (Woolfrey et al., 2009), it would be of great importance to examine the brain development and function in the Epac2$^{-/-}$ mice.

1.9 CONCLUDING REMARKS AND RELEVANCE OF THIS DISERTATION

In summary, this chapter reviewed how small GTPases of the Ras superfamily are activated, and how these events are spatially organized and become interconnected. The proper localization of small GTPases and their GEFs not only enhances the efficiency of the exchange activities, but also serves as an important mechanism to modulate the specificity of signaling pathways.

The data presented in the following two chapters will provide additional examples for many of the regulatory mechanisms discussed in this Chapter. First, all three small GTPases related to my work, including Rap1, Ras and Ran, are compartmentalized in the cell through lipid modifications of Rap1 and Ras, and through interaction with a scaffolding protein in the case of Ran. Secondly, the coupling of Ras to Rap1 via Epac2 at the plasma membrane and the coupling of Ran to Rap1 via Epac1 at the nuclear envelope illustrate how GEFs can link different small GTPases into local cascades through protein interactions. Thirdly, the Ras-Epac2 interaction and Ran-Epac1 interaction at two locations also allow spatial control of distinct pools of Rap1 downstream of the same second messenger, cAMP. Fourth, the catalytic domains of Epac proteins responsible for the exchange reaction and their RA domains responsible for their localizations function independently of each other. However, the proper localizations of Epac proteins are required for the exchange reactions to occur efficiently *in vivo* because the Epac proteins need to be co-compartmentalized with their substrates, Rap1.

Before moving on to the experimental data, it would also be important to explain how the thesis projects were initiated and why they are important. The concept of the spatial regulation of different pools of Rap1 in the cell was first introduced in a publication by our lab in 2006 (Wang et al., 2006). This study established that Epac1, which exhibits a perinuclear distribution, activates a pool of Rap1 that is not couple to the activation of extracellular signal-regulated kinases (ERKs). However, when targeted to the plasma membrane through an engineered CAAX motif, Epac1-CAAX can activate a pool of Rap1 that is coupled to the activation of EKRs. In the same year, Epac2 was reported to have a RA domain and can be recruited to the PM by Ras (Li et al., 2006), but the role of Ras in Epac2 dependent Rap1 activation and the downstream effect were not clear. Since Epac2 can be targeted to the PM via Ras binding, my thesis project initially set out to test the hypothesis that Epac2 is a Ras effector and can activate the PM pool of Rap1 that is coupled to ERK activation. This hypothesis turns out to be correct and in addition we discovered that Ras and cAMP regulate Epac2 in parallel and both signals are required for efficient Rap1 activation via Epac2. Another gap in our knowledge at the same time was the lack of understanding about the detailed mechanism for the perinulcear localization of Epac1. A clear biochemical basis for this localization would not only confirm the microscopic observation, but also shed light on the signaling property of Epac1. Therefore, my thesis project also focused on the molecular basis for Epac1 localization. Using unbiased proteomic survey, I discovered that Epac1 is in association with components of the nuclear pore complex. Furthermore, a direct interaction between Epac1 and Ran was revealed, which turns out to be essential for the localization of and Rap1 activation by Epac1.

The direct impact of my work is the clarification, at the molecular level, of the differential regulations of Rap1 by Epac1 and Epac2 at two different locations within the cell. These findings provided direct support for the emerging theory of spatial regulation of different pools of Rap1 within the cell downstream of the same second messenger cAMP. The initial characterization of the Ras-Epac2 complex and the Ran-Epac1-RanBP2 complex, including their biochemical properties and roles in Rap1 activation, make important steps towards a better understanding the functional aspects of the signaling events related to these complexes in the future. Although my thesis links the Epac2-Rap1 signaling at the PM to ERK activation and neurite growth, the direct physiological significance of Epac1-Rap1 signaling at the NE is still lacking at this point. There is also a gap between the new knowledge about the abovementioned molecular complexes and their eventual physiological roles in whole organisms. For Epac2, further examination of the neurobehavioral changes of the Epac2$^{-/-}$ mice is likely to resolve the ultimate question of whether the Epac2-Rap1 pathway plays a critical role in neuronal differentiation and function. For Epac1, we need to reconcile its perinuclear localization to the role of Epac1 in cell adhesion established previously. Moreover, given the connection of Epac1 with the NPC, it would be important to investigate how the Epac1 dependent Rap1 activation on the NE regulates nucleus-related processes such as nuclear transport and the assembly and remodeling of the NE itself, which would be of vast significance to the normal cell physiology.

Figure 1.1 Phylogenetic tree of representative members from the Ras superfamily.

Sixty one reference sequences of representative members of the Ras superfamily in human were aligned using CLUSTALW at http://workbench.sdsc.edu. Major multiple alignment parameters: Weight matrix: Gonnet series, Gap open penalty: 10 (0-100), Gap extension penalty: 0.2. The result of the alignment is displayed in the form of a rooted phylogenetic tree to show the clustering of these small GTPases into five distinctive families. The members of the Ras, Rho, Arf, Ran and Rab families are shown in red, purple, blue, orange and green respectively.

Figure 1.1

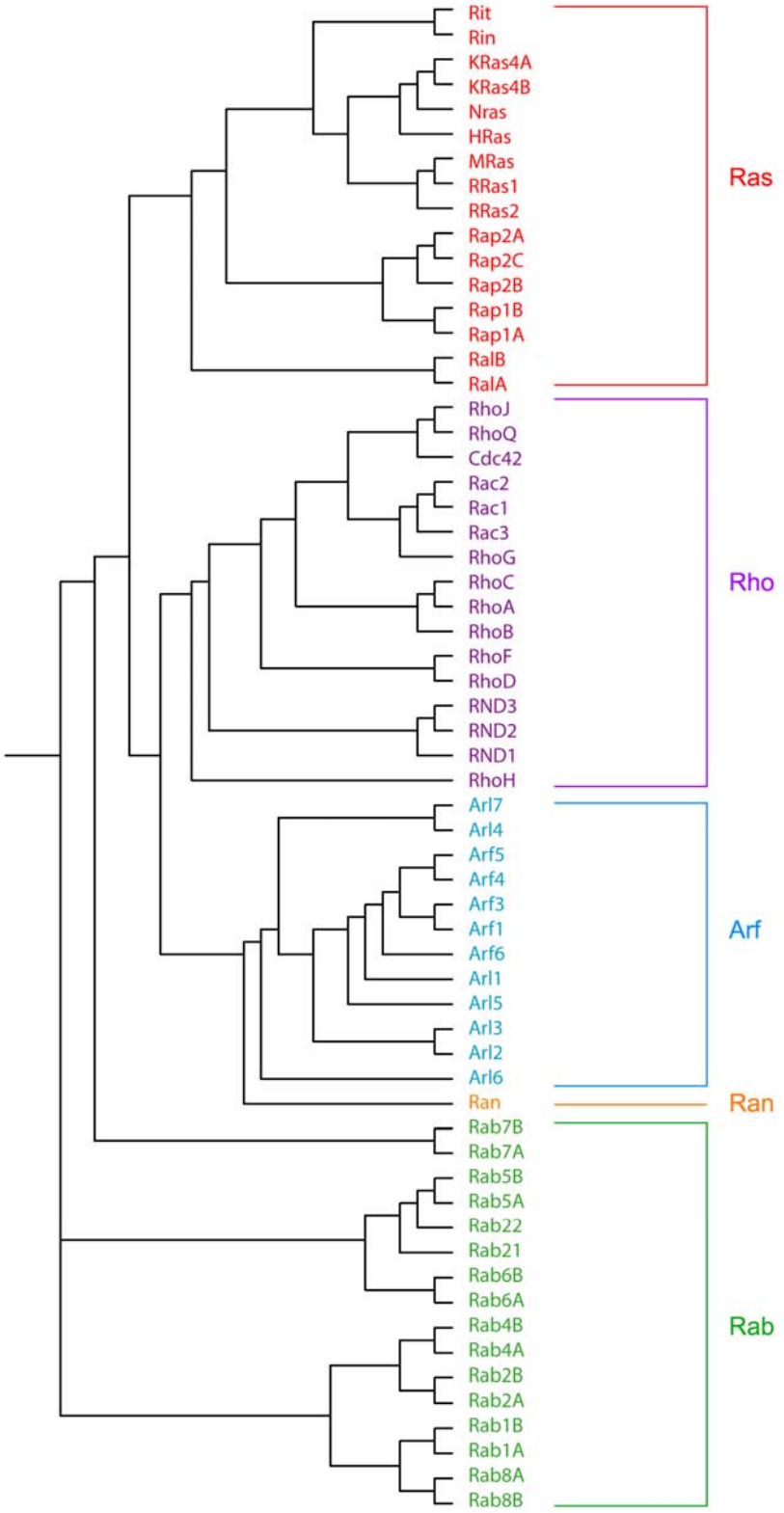
Rit
Rin
KRas4A
KRas4B
Nras
HRas
MRas
RRas1
RRas2
Rap2A
Rap2C
Rap2B
Rap1B
Rap1A
RalB
RalA
Ras
RhoJ
RhoQ
Cdc42
Rac2
Rac1
Rac3
RhoG
RhoC
RhoA
RhoB
RhoF
RhoD
RND3
RND2
RND1
RhoH
Rho
Arl7
Arl4
Arf5
Arf4
Arf3
Arf1
Arf6
Arl1
Arl5
Arl3
Arl2
Arl6
Arf
Ran
Ran
Rab7B
Rab7A
Rab5B
Rab5A
Rab22
Rab21
Rab6B
Rab6A
Rab4B
Rab4A
Rab2B
Rab2A
Rab1B
Rab1A
Rab8A
Rab8B
Rab

Figure 1.2 Structure of small GTPases of the Ras superfamily and GTP/GDP cycling of small GTPases.

(A) Structure of H-Ras-GTP. The surface contour of GppNHp, a non-hydrolysable GTP analogue, is in gray, H-Ras in red. Switch I region (corresponding to amino acids 32-38) and swith II region (corresponding to amino acids 59-67) are also indicated. a.a. amino acid.

(B) Superimposition of the structures of representative members of the Ras, Rho, Arf, Ran and Rab family. GTP-loaded Ras, Rac2, Arf6, Ran and Rab are shown in red, yellow, blue, green and pink, respectively. The orientation of Ras (red) was kept the same as in A. The guanine nucleotides are omitted.

(C) Schematic of GTP/GDP cycling of small GTPases. GTP bound small GTPase (active form) and GDP bound small GTPase (inactive form) are cycling under the catalysis of guanine nucleotide exchange factor (GEF) and GTPase activating protein (GAP). When in the active form, a small GTPase can interact with its effectors and carry out its function.

Figure 1.2

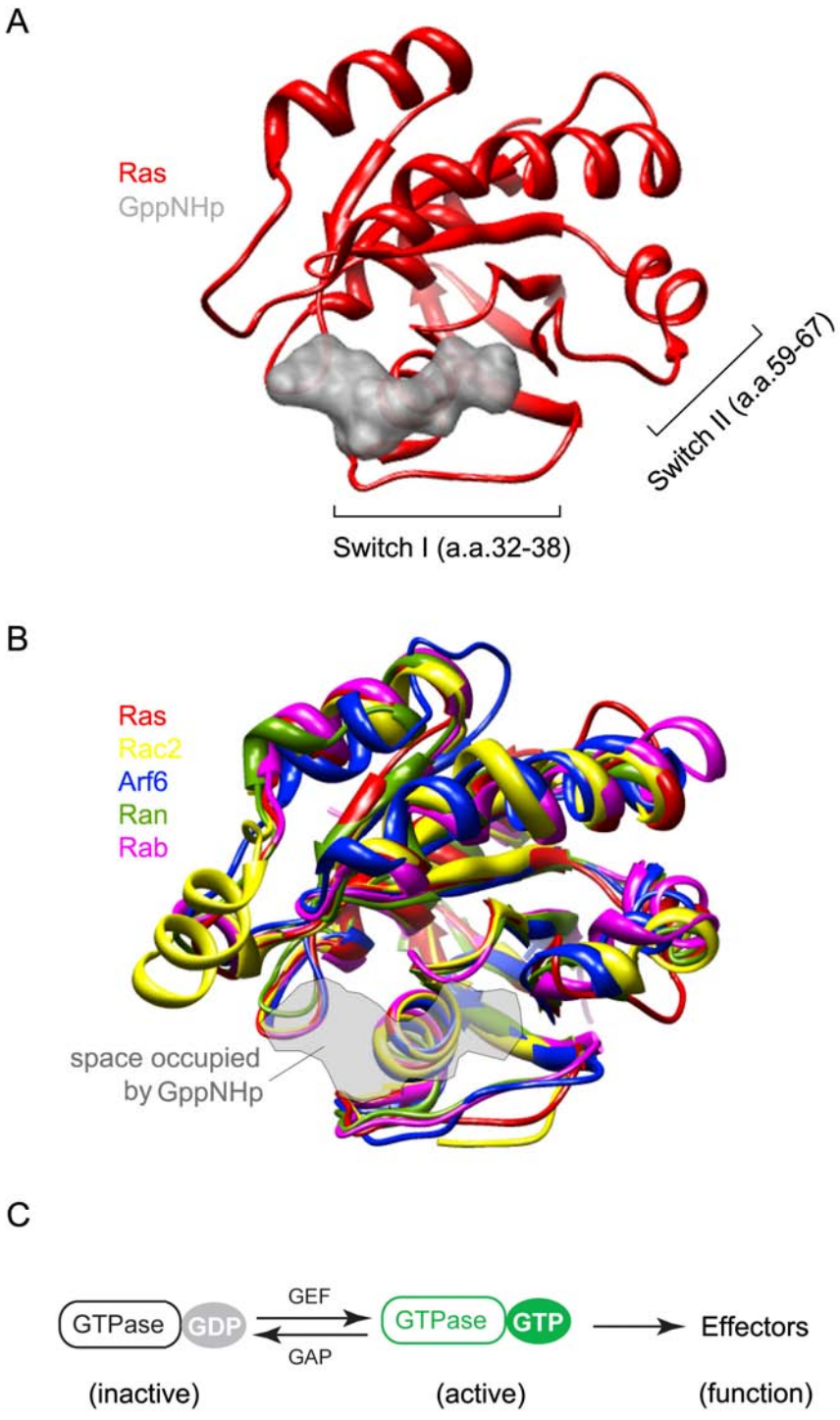
A
Ras
GppNHp
Switch II (a.a.59-67)
Switch I (a.a.32-38)
B
Ras
Rac2
Arf6
Ran
Rab
space occupied
by GppNHp
C
GTPase
GDP
GEF
GAP
GTPase
GTP
Effectors
(inactive)
(active)
(function)

Figure 1.3 Comparison of the Ras-Sos complex and Rap1-Epac2 complex.

(A) Ras in complex with the catalytic domain of Sos (PDB code: 1BKD). Ras is colored in red, catalytic domain of Sos in gray. The hairpin structure within the CDC25-HD of Sos is highlighted in black. HP, hairpin. REM, Ras exchange motif. CDC25-HD, CDC25-homology domain. Switch I and II regions are also labeled in the shown structures.

(B) Rap1 in complex with the catalytic region of Epac2, based on the structure encoded as 3CF6. Rap1 is colored in blue, the catalytic region of Epac2 in green. The hairpin structure within the CDC25-HD of Epac2 is highlighted in dark green.

(C) Comparison of the conformations of Ras on and off the catalytic site of Sos. Ras bound to Sos (the intermediate state) is colored in red, with the same orientation as presented in (A). Ras off Sos and in its GTP-loaded conformation is in purple. A dramatic shift of the Switch I region (arrow) can be observed accompanied by other minor changes.

Figure 1.3

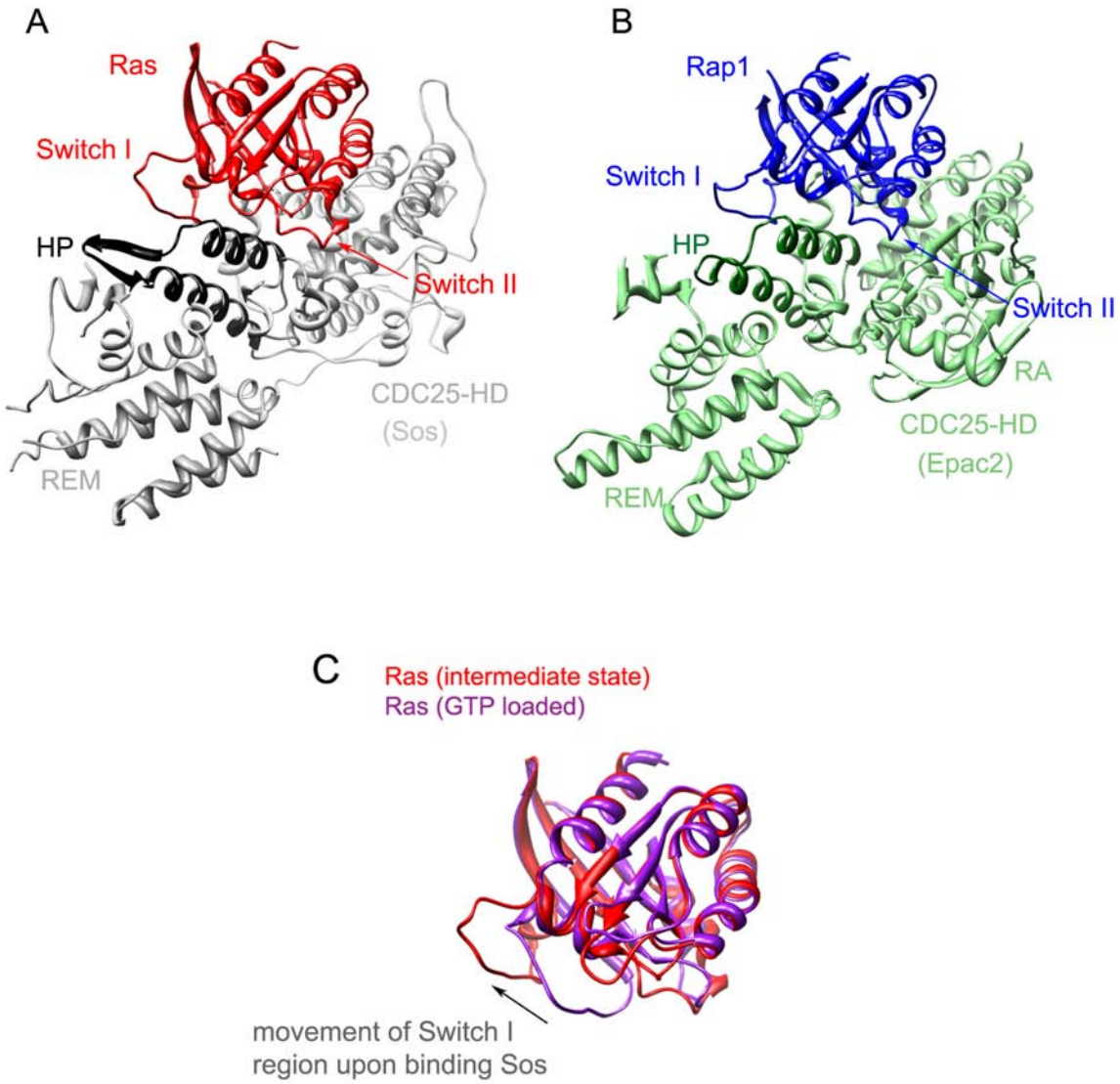
A
Ras
Switch I
HP
Switch II
CDC25-HD
(Sos)
REM
B
Rap1
Switch I
HP
Switch II
RA
CDC25-HD
(Epac2)
REM
C
Ras (intermediate state)
Ras (GTP loaded)
movement of Switch I
region upon binding Sos

Figure 1.4 Properties of the C-terminal ends of representative members from the Ras superfamily.

The last 25 amino acids of the C-termini of 61 representative members of the Ras superfamily were characterized in the following categories. (1) Lipid groups attached to the CAAX box, including geranylgeranyl (indicated as filled squares in lime), farnesyl (filled blocks in light orange) and myristate (filled squares in light blue). (2) Net charge as the sum of the positive and negative charges of the residues among the 25 amino acids counted for each small GTPase. The net charges form a continuous spectrum and are indicated as filled squares colored according to the spectrum scale bar at the lower right corner. The exact numbers of net charges are shown within the squares. (3) Reversible post-translational modifications including palmitoylation (squares labeled with “P”) and phosphorylation mediated by protein kinase A (PKA) (squares labeled with “A”) and protein kinase C (PKC) (squares labeled with “C”). Most of the palmitoylation sites have been confirmed. The PKA/PKC sites are predicted based on their consensus motifs, and the filled squares indicate sites that have been confirmed in the literature or by our own unpublished data. The members of the Ras, Rho, Arf, Ran and Rab families are shown in red, purple, blue, orange and green respectively.

Figure 1.4

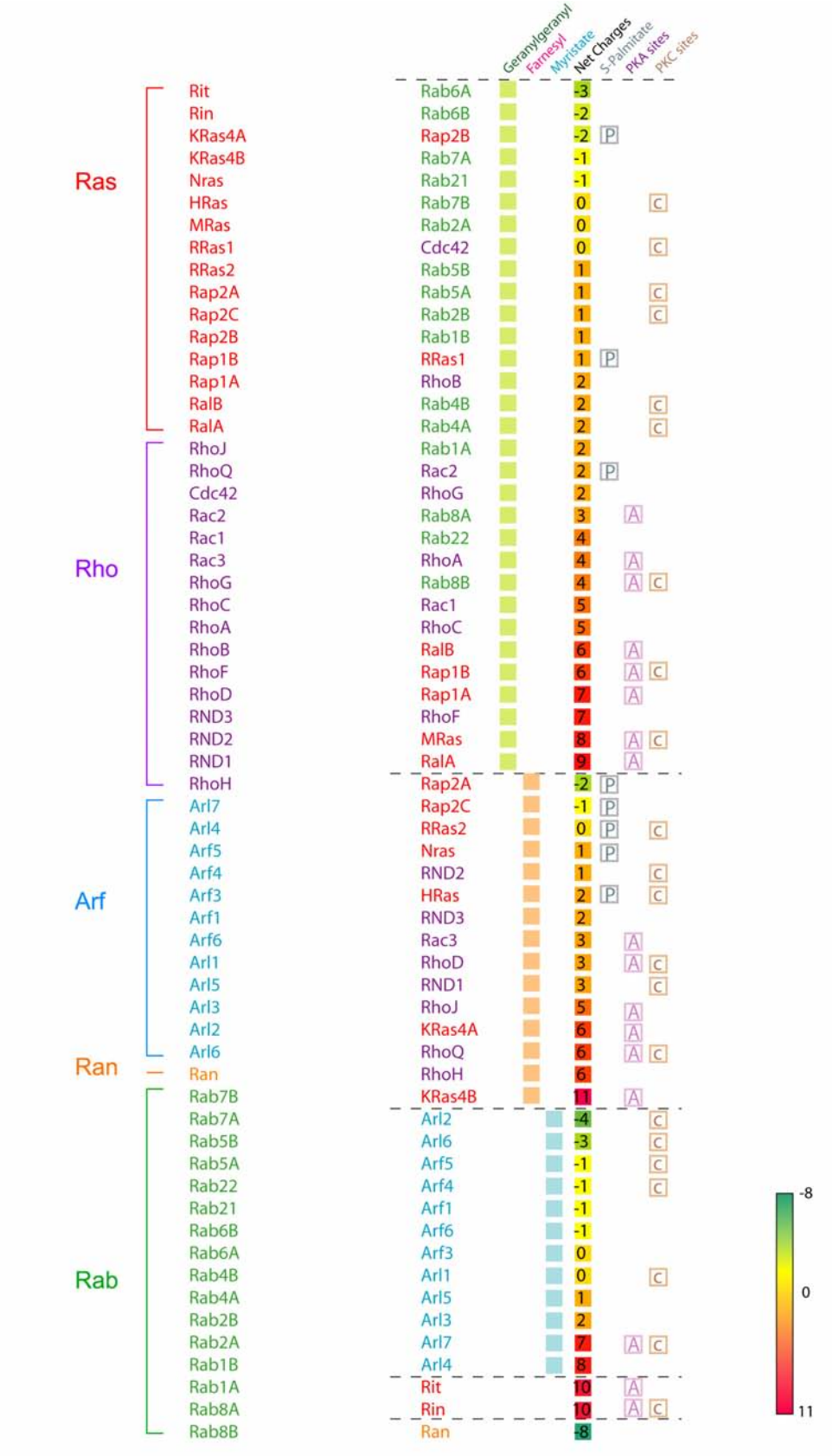
Geranylgeranyl
Farnesyl
Myristate
Net Charges
S-Palmitate
PKA sites
PKC sites
Ras
Rho
Arf
Ran
Rab
Rit
Rin
KRas4A
KRas4B
Nras
HRas
MRas
RRas1
RRas2
Rap2A
Rap2C
Rap2B
Rap1B
Rap1A
RalB
RalA
RhoJ
RhoQ
Cdc42
Rac2
Rac1
Rac3
RhoG
RhoC
RhoA
RhoB
RhoF
RhoD
RND3
RND2
RND1
RhoH
Arl7
Arl4
Arf5
Arf4
Arf3
Arf1
Arf6
Arl1
Arl5
Arl3
Arl2
Arl6
Ran
Rab7B
Rab7A
Rab5B
Rab5A
Rab22
Rab21
Rab6B
Rab6A
Rab4B
Rab4A
Rab2B
Rab2A
Rab1B
Rab1A
Rab8A
Rab8B
Rab6A -3
Rab6B -2
Rap2B -2 P
Rab7A -1
Rab21 -1
Rab7B 0 C
Rab2A 0
Cdc42 0 C
Rab5B 1
Rab5A 1 C
Rab2B 1 C
Rab1B 1
RRas1 1 P
RhoB 2
Rab4B 2 C
Rab4A 2 C
Rab1A 2
Rac2 2 P
RhoG 2
Rab8A 3 A
Rab22 4
RhoA 4 A
Rab8B 4 A C
Rac1 5
RhoC 5
RalB 6 A
Rap1B 6 A C
Rap1A 7 A
RhoF 7
MRas 8 A C
RalA 9 A
Rap2A -2 P
Rap2C -1 P
RRas2 0 P C
Nras 1 P
RND2 1 C
HRas 2 P C
RND3 2
Rac3 3 A
RhoD 3 A C
RND1 3 C
RhoJ 5 A
KRas4A 6 A
RhoQ 6 A C
RhoH 6
KRas4B 11 A
Arl2 -4 C
Arl6 -3 C
Arf5 -1 C
Arf4 -1 C
Arf1 -1
Arf6 -1
Arf3 0
Arl1 0 C
Arl5 1
Arl3 2
Arl7 7 A C
Arl4 8
Rit 10 A
Rin 10 A C
Ran -8
-8
0
11

Figure 1.5 Comparison of a cascade of kinases and a cascade of small GTPases.

(A) Schematic of a cascade formed by kinase 1, 2 and 3. Kinase 2 is the substrate of kinase 1, and kinase 3 is the substrate of kinase 2. When kinase 1 is activated by an upstream signal, the signal could propagate down through the cascade of kinases to generate amplified and specific outcomes. For simplicity, additional mechanisms that facilitate the signal transduction are not shown, for example, scaffolding proteins that bring together these kinases spatially. Phosphotases can potentially weaken the signaling at each kinase within the cascade as shown. Activated kinases are shown in pink attached to phosphate groups (filled circles with “P”).

(B) Schematic of a cascade formed by small GTPase A, B and C. The guanine nucleotide exchange factor (GEF) for small GTPase B is the effector of small GTPase A, and the GEF for small GTPase C is the effector of small GTPase B. When small GTPase A is activated by an upstream signal, the signal could propagate down through the cascade of small GTPases to generate amplified and specific outcomes. Being the effector of the upstream small GTPase, the GEF for the downstream small GTPase could be properly compartmentalized with its cognate small GTPase or be activated allosterically. For simplicity, additional mechanisms that facilitate the signal transduction are not shown. GTPase activating proteins (GAPs) can potentially weaken the signaling at each small GTPase within the cascade as shown. Activated small GTPases are shown in green loaded with GTP.

Figure 1.5

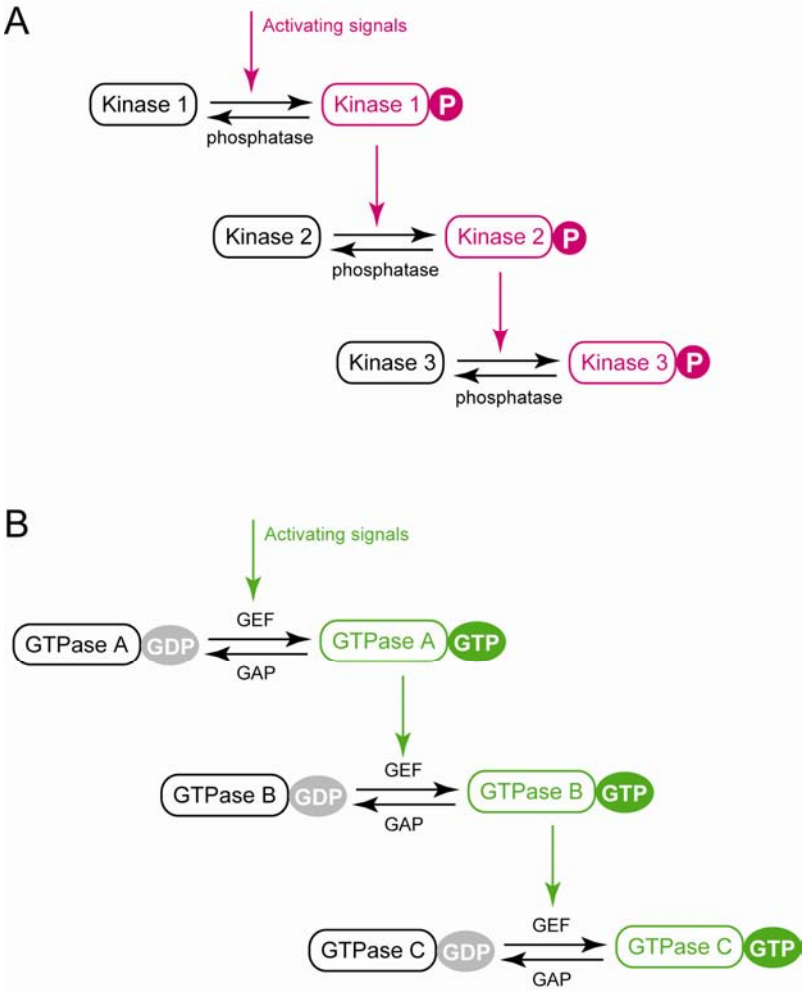
A
Activating signals
Kinase 1
Kinase 1
P
phosphatase
Kinase 2
Kinase 2
P
phosphatase
Kinase 3
Kinase 3
P
phosphatase
B
Activating signals
GEF
GTPase A
GDP
GTPase A
GTP
GAP
GEF
GTPase B
GDP
GTPase B
GTP
GAP
GEF
GTPase C
GDP
GTPase C
GTP
GAP

Figure 1.6 Bioinformatic search for GEFs capable of Ras/Rap binding.

(A) Human proteins related to the Ubiquitin homologs (yellow), RasGEF (green), RhoGEF (purple), Vps9 (blue) and Sec7 (pink) superfamilies were identified using Reverse Position-Specific BLAST (RPS-BLAST). The numbers of proteins within each superfamily and at the overlaps are shown in round brackets. The numbers of protein isoforms are shown in square brackets. Asterisk indicates the reference sequence number of a predicted protein similar to RAPGEF2, partial.

(B) Nomenclatures of human proteins/genes identified in the above bioinformatic search. The official symbol, full name, Gene ID and other names for each protein identified are shown.

Figure 1.6

A

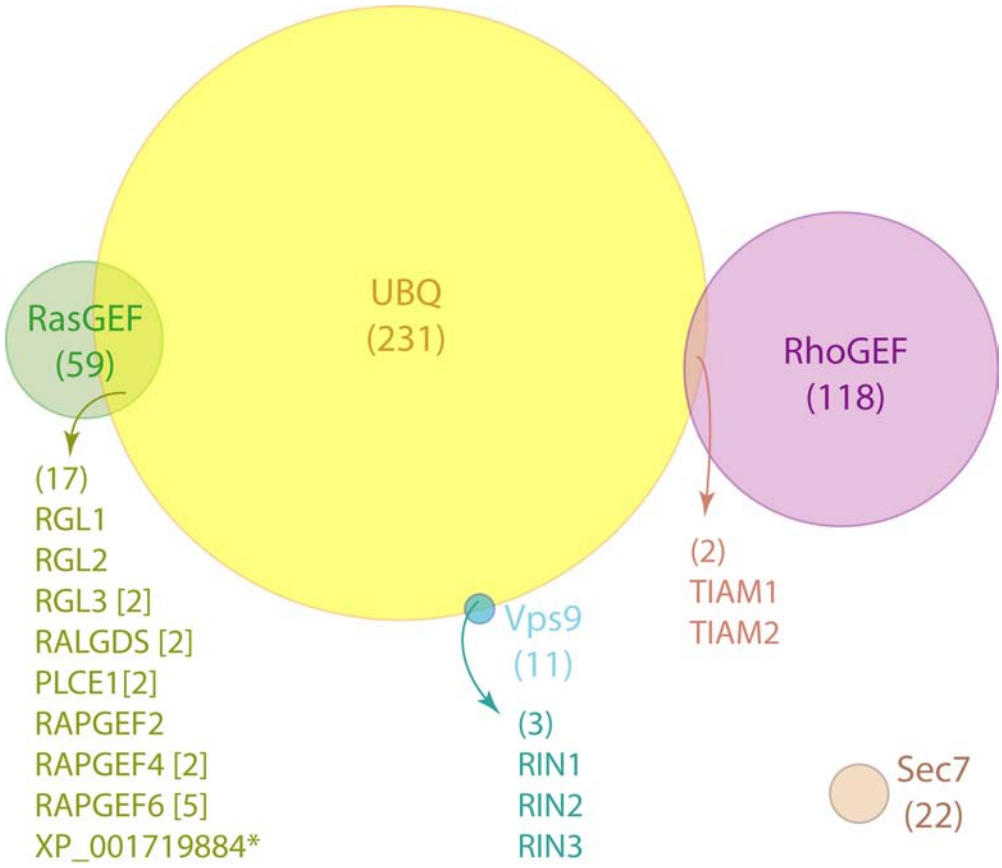
RasGEF
(59)
UBQ
(231)
RhoGEF
(118)
(17)
RGL1
RGL2
RGL3 [2]
RALGDS [2]
PLCE1[2]
RAPGEF2
RAPGEF4 [2]
RAPGEF6 [5]
XP_001719884*
Vps9
(11)
(3)
RIN1
RIN2
RIN3
(2)
TIAM1
TIAM2
Sec7
(22)

Figure 1.6 (continued)

B

Official symbol	Official full name	GeneID	Also known as
RGL1	Ral guanine nucleotide dissociation stimulator-like 1	23179	RGL; KIAA0959
RGL2	Ral guanine nucleotide dissociation stimulator-like 2	5863	KE1.5; RAB2L; HKE1.5
RGL3	Ral guanine nucleotide dissociation stimulator-like 3	57139	FLJ00153; FLJ32585; FLJ44275; MGC126805; MGC138163
RALGDS	Ral guanine nucleotide dissociation stimulator	5900	RGF; RGDS; RalGEF; FLJ20922
PLCE1	Phospholipase C, epsilon 1	51196	PLCE; PPLC; NPHS3; FLJ23659; KIAA1516; MGC167842
RAPGEF2	Rap guanine nucleotide exchange factor (GEF) 2	9693	RA-GEF; NRAPGEP; PDZGEF1; Rap-GEP; CNrasGEF; PDZ-GEF1
RAPGEF4	Rap guanine nucleotide exchange factor (GEF) 4	11069	CGEF2; EPAC2; Nbla00496; CAMP-GEFII
RAPGEF6	Rap guanine nucleotide exchange factor (GEF) 6	51735	RAGEF2; PDZGEF2; KIA001LB; PDZ-GEF2; RA-GEF-2; DKFZp667N084; DKFZp686I15116
RIN1	Ras and Rab interactor 1	9610	n/a
RIN2	Ras and Rab interactor 2	54453	MACS; RASSF4
RIN3	Ras and Rab interactor 3	79890	FLJ11700; FLJ22439; DKFZp762H1613
TIAM1	T-cell lymphoma invasion and metastasis 1	7074	FLJ36302
TIAM2	T-cell lymphoma invasion and metastasis 2	26230	STEF; FLJ41865

Figure 1.7 Domain structures of representative guanine nucleotide exchange factors (GEFs) that mediate signaling cascades within the Ras family.

(A-G) Graphical summary of the conserved domains of the GEFs as indicated (graphics are directly derived from the NCBI Conserved Domains Database). See text for details.

(H) Nomenclature of RAPGEF5 illustrated in (G). The official symbol, full name, Gene ID and other names are shown.

Figure 1.7

A. RAPGEF2

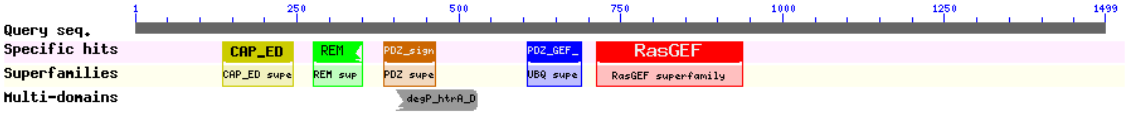

B. RAPGEF6, isoform 1

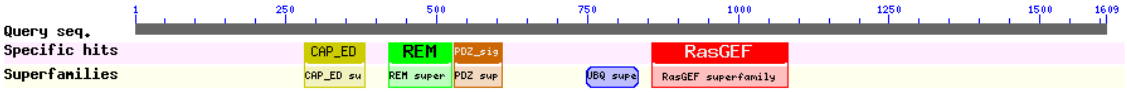

C. PLCE1, isoform 1

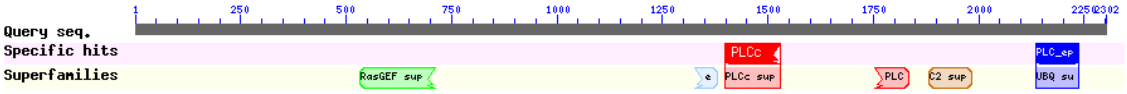

D. RAPGEF4 (Epac2), isoform a

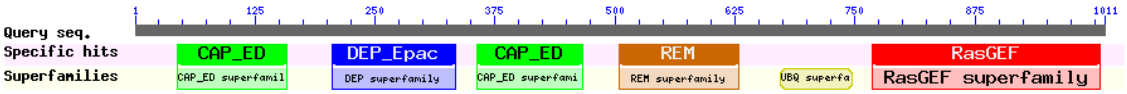

E. RALGDS, isoform 1

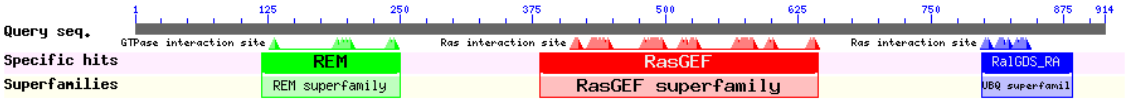

F. RGL1

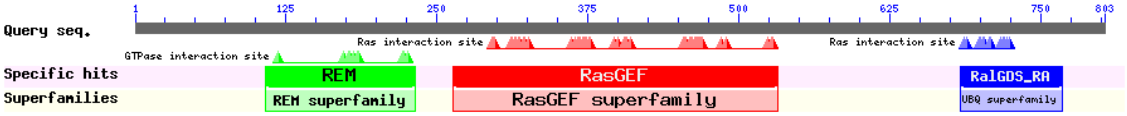

G. RAPGEF5

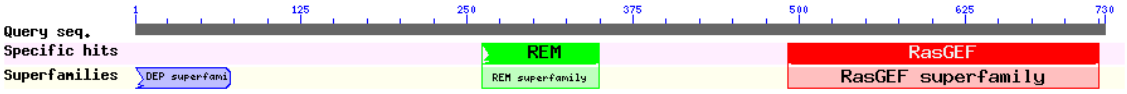

H.

Official symbol	Official full name	GeneID	Also known as
RAPGEF5	Rap guanine nucleotide exchange factor (GEF) 5	9771	GFR; REPAC; MR-GEF; KIAA0277

Figure 1.8 Domain structures of major GEFs that mediate signaling cascades from the Ras family to the Rho or Rab family.

(A-F) Graphical summary of the conserved domains of the GEFs as indicated (graphics are directly derived from the NCBI Conserved Domains Database). See text for details.

(G) Nomenclature of Vav2 illustrated in (F). The official symbol, full name, Gene ID and other names are shown.

Figure 1.8

A. TIAM1

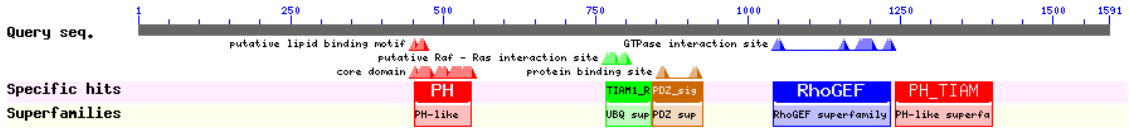

B. TIAM2, isoform a

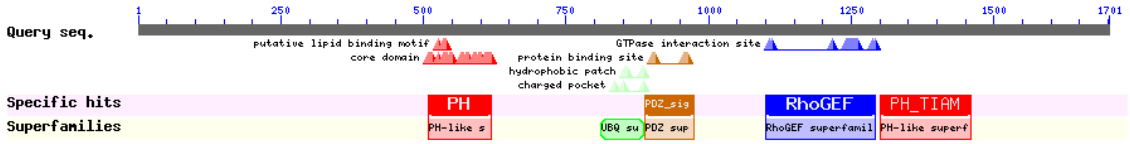

C. RIN1

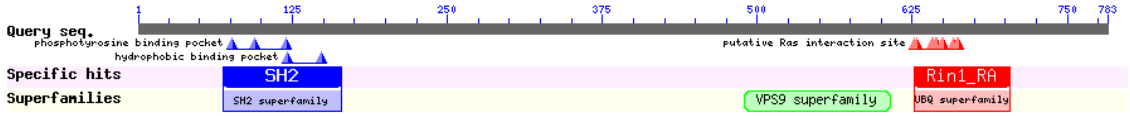

D. RIN2

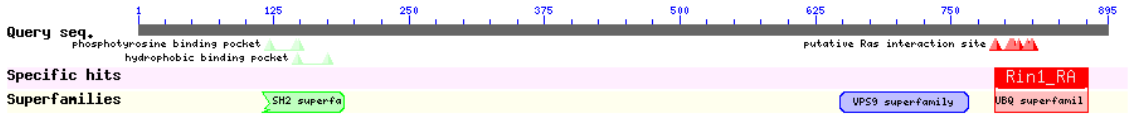

E. RIN3

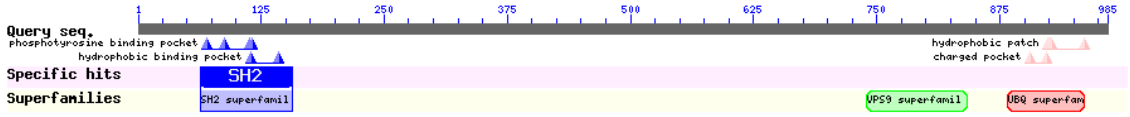

F. VAV2, isoform 1

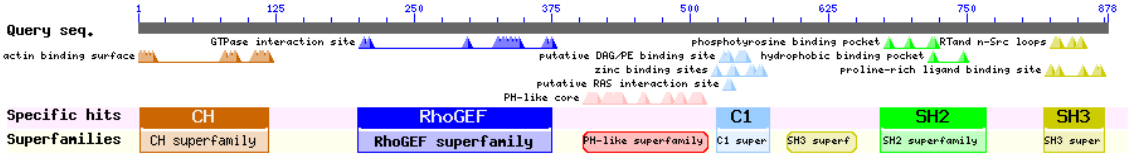

G.

Official symbol	Official full name	GeneID	Also known as
VAV2	Vav 2 guanine nucleotide exchange factor	7410	n/a

Figure 1.9 Network of small GTPases of the Ras superfamily.

Cascades of small GTPases of the Ras superfamily reviewed in Chapter 1 can be organized into a network as shown. Different Ras genes, including N-Ras, K-Ras, H-Ras and M-Ras can be coupled to Rap1 (and/or Rap2, not shown) through PLCε, Epac2 or PDZ-GEF2. Additional signals required for full activation of these GEFs, e.g. cAMP for Epac2, are not shown. The signals flow unidirectionally, always from Ras to Rap1. Ran plays an important role in Epac1 dependent Rap1 activation at the nuclear envelope. Ras can activate Ral via RalGDS and RGL. Rap1 has strong affinity towards these GEFs for Ral, but its role in Ral activation has not been clarified (indicated as dotted line). Both Ras and Rap1 can activate Rac of the Rho family via GEFs such as Tiam1, Tiam2 and Vav2. Ras is also coupled to Rab5 activation via Rin1. Self-amplifications of Ras-GTP and Rap1-GTP are mediated by Sos and PDZ-GEF1 respectively.

Figure 1.9

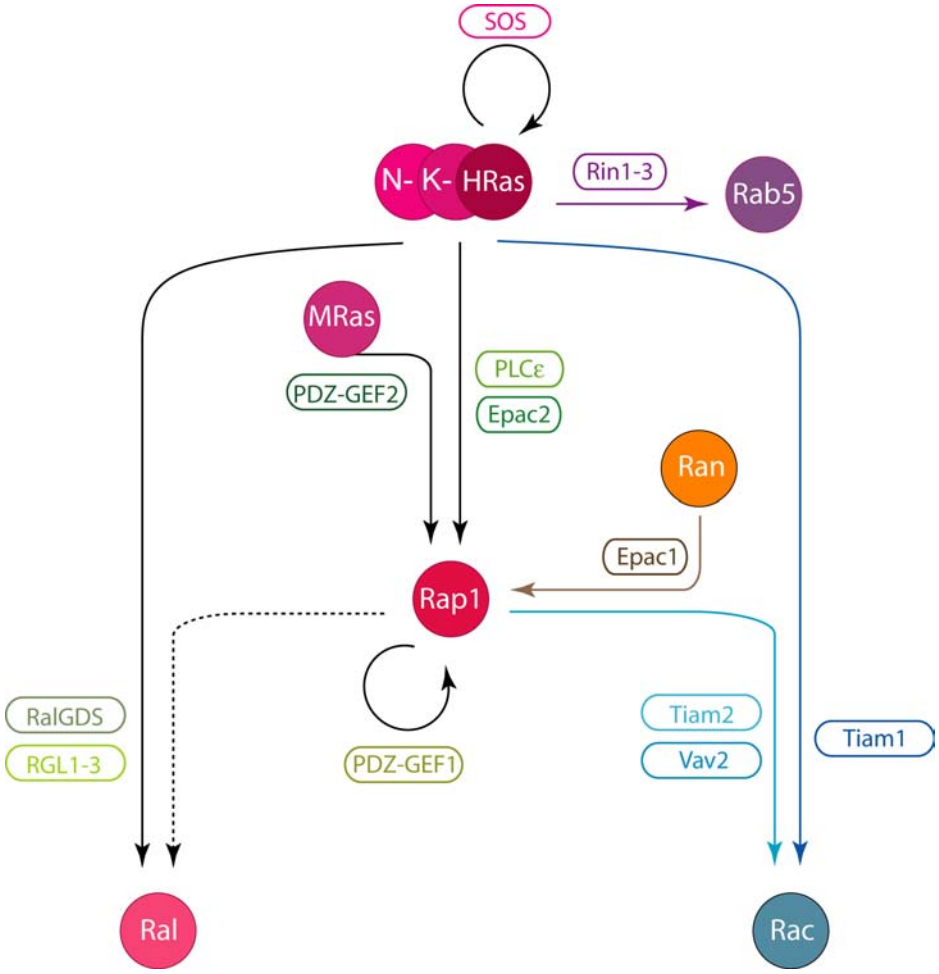
SOS
N- K- HRas
Rin1-3
Rab5
MRas
PDZ-GEF2
PLCε
Epac2
Ran
Epac1
Rap1
PDZ-GEF1
RalGDS
RGL1-3
Tiam2
Vav2
Tiam1
Ral
Rac

Figure 1.10 Domain structures of additional GEFs for Rap proteins discussed in section 1.7.

(A-D) Graphical summary of the conserved domains of the GEFs discussed in section 1.7 as indicated (graphics are directly derived from the NCBI Conserved Domains Database). See text for details.

(E) Nomenclatures of GEFs illustrated in (A and B). The official symbol, full name, Gene ID and other names for each protein identified are shown.

Figure 1.10

A. RAPGEF1 (C3G), isoform a

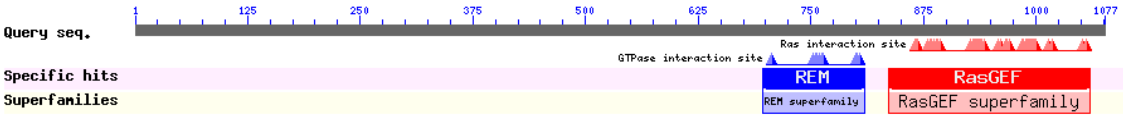

B. RAPGEF3 (Epac1), isoform a

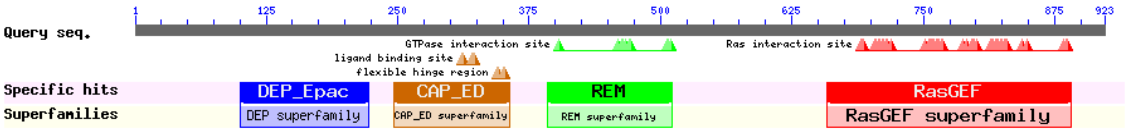

C. RASGRP2 (CalDAG-GEFI)

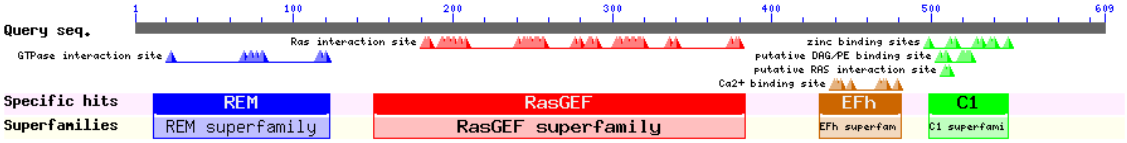

D. RASGRP3 (CalDAG-GEFIII), isoform 1

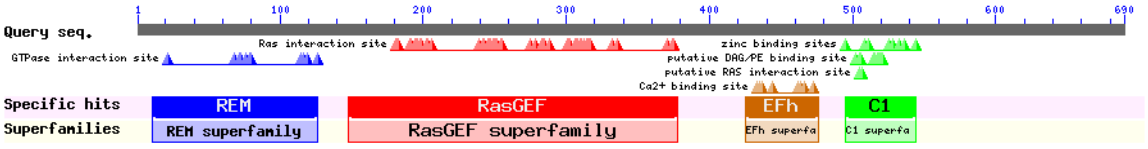

E.

Official symbol	Official full name	GeneID	Also known as
RAPGEF1	Rap guanine nucleotide exchange factor (GEF) 1	2889	C3G; GRF2; DKFZp781P1719
RAPGEF3	Rap guanine nucleotide exchange factor (GEF) 1	10411	EPAC; EPAC1; bcm910; HSU79275; MGC21410; CAMP-GEFI
RASGRP2	Ras guanyl releasing protein 2 (calcium and DAG regulated)	10235	CDC25L; CALDAG-GEFI
RASGRP3	Ras guanyl releasing protein 3 (calcium and DAG regulated)	25780	GRP3; KIAA0846

Chapter 2

Ras Is Required for the cAMP-dependent Activation of Rap1 via Epac2

Chang Liu[1,2], Maho Takahashi[1,3], Yanping Li[1], Shuang Song[4],

Tara J. Dillon[1], Ujwal Shinde[5], & Philip J. S. Stork[1,2*]

[1]Vollum Institute, [2]Department of Cell and Developmental Biology, Oregon Health & Science University, Portland, Oregon 97201, USA, [3]Tumor Endocrinology Project, National Cancer Center Research Institute, Tokyo 104-0045, Japan, [4]Vision Science, School of Optometry, University of California, Berkeley, CA 94701, USA, [5]Department of Biochemistry, Oregon Health & Science University, Portland, Oregon 97201, USA.

*Corresponding author. Mailing address: *Vollum Institute, Oregon Health & Science University, 3181 SW Sam Jackson Park Road, Portland, OR 97239.*

Tel: 503-494-5494. Fax: 503-494-4976. E-mail: stork@ohsu.edu

Published, in part, in the Molecular and Cellular Biology. 2008 Dec; 28(23):7109-25.

I gratefully acknowledge the contribution of Dr. Maho Takahashi to Figure 2.6F, 2.7F&G and the construction of multiple plasmids, Dr. Yanping Li to Figure 2.4C-E, Dr. Shuang Song to Figure 2.5G&H, and Dr. Ujwal Shinde to Figure 2.2B.

2.1 ABSTRACT

Exchange proteins activated by cAMP 2 (Epac2) is a guanine nucleotide exchange factor (GEF) for Rap1, a small G protein involved in many cellular functions including cell adhesion, differentiation and exocytosis. Epac2 interacts with Ras-GTP via a Ras association (RA) domain. Previous studies have suggested that the RA domain was dispensable for Epac2 function. Here we show for the first time that Ras and cAMP regulate Epac2 function in a parallel fashion, and the Ras-Epac2 interaction is required for the cAMP-dependent activation of endogenous Rap1 by Epac2. The mechanism for this requirement is not allosteric activation of Epac2 by Ras, but the compartmentalization of Epac2 on the Ras-containing membranes. A computational modeling is consistent with this compartmentalization being a function of both the level of Ras activation and the affinity between Ras and Epac2. In PC12 cells, a well-established model for sympathetic neurons, the Epac2 signaling is coupled to activation of mitogen-activated protein (MAP) kinases and contributes to neurite outgrowth. Taken together, Epac2 is not only a cAMP sensor but also a *bona fide* Ras effector. Coincident detection of both cAMP and Ras signals is essential for Epac2 to activate Rap1 in a temporally and spatially controlled manner.

2.2 INTRODUCTION

Rap1 is a small GTPase involved in the regulation of multiple cellular functions such as adhesion, differentiation and exocytosis. Like all small G proteins, Rap1 cycles between a GTP-loaded active state and a GDP-loaded inactive state, which is mediated via the opposing actions of G protein activation proteins (GAPs) that promote hydrolysis of bound GTP to GDP, and guanine nucleotide exchange factors (GEFs) that catalyze the exchange of bound GDP for GTP.

Exchange proteins activated by cAMP (Epac1 and Epac2) are unique Rap1 GEFs that link cAMP elevation to Rap1 activation (de Rooij et al., 1998). This is achieved via the direct binding of cAMP to the Epac protein itself, thereby defining a novel cAMP signaling pathway that is independent of protein kinase A (PKA). Both Epac1 and Epac2 contain a catalytic region and a regulatory region. The catalytic region consists of a CDC25 homology domain that catalyzes Rap1 activation, a REM domain, and a Ras association (RA) domain that lies in between. The regulatory region consists of one or two cAMP binding domains (cNBDs) and a DEP (dishevelled, Egl-10 and pleckstrin homology) domain. Under resting conditions, Epac proteins are inactive due to the inhibitory interaction between the regulatory and catalytic regions. The binding of cAMP to the cNBD relieves the intramolecular inhibition by exposing the catalytic site to Rap1 (Rehmann et al., 2008; Rehmann et al., 2006; Rehmann et al., 2003a; Rehmann et al., 2003b). Previous studies have been largely focused on the mechanism of cAMP regulation of Epacs. Whether other molecular interactions play a role in Epac regulation is unknown.

A number of features of Epac2 distinguish it from Epac1, which suggest distinctive regulatory mechanisms for Epac2. While Epac1 is expressed ubiquitously, Epac2 is highly enriched in neuronal tissues (Kawasaki et al., 1998a). Moreover, Epac1 is localized to the perinuclear mitochondria through a specific N-terminal sequence (Qiao et al., 2002), or interaction with specific AKAPs (Dodge-Kafka et al., 2005), while Epac2 is largely cytosolic. Importantly, although both proteins contain potential RA domains, only Epac2 interacts with Ras-GTP (Li et al., 2006). In these studies, Quilliam and colleagues have demonstrated the ability of Ras-GTP to recruit Epac2 to the plasma membrane (Li et al., 2006). However, the necessity of the RA domain for the Epac2-mediated Rap1 activation has not been firmly established. Our study shows that Ras-Epac2 interaction is required for Epac2 activity, suggesting that Epac2 is a *bona fide* Ras effector as well as a cAMP sensor, thereby acting as a coincidence detector for signals emanating from Ras and cAMP.

Several models could explain the mechanism for the regulation of Epac2 by Ras-GTP. First, Ras-GTP could facilitate the cAMP-mediated relief of autoinhibition. Second, Ras-GTP could enhance the enzymatic activity of Epac2 by inducing allosteric changes within the catalytic domain through its interaction with the RA domain. This model is analogous to the model of allosteric activation of Sos by Ras-GTP (Margarit et al., 2003). A third model considers the compartmentalization of Epac2. As both Ras and Rap1 are lipid modified at their carboxy-termini and tethered to the lipid membrane, the interaction between Ras and Epac2 may greatly increase the Epac2 concentration at the membrane, therefore accelerating the rate of Rap1 activation. We examined each of the three models and demonstrate here that Ras regulates Epac2 function independently of cAMP, and that

enrichment of Epac2 on the membrane through Ras binding is crucial for Epac2-mediated Rap1 activation.

It is possible that this Ras-dependent mode of activation could favor the activation of selective targets of Rap1. As we have shown recently, relocation of Epac1 from the perinuclear region to the plasma membrane allows Rap1 activation to be coupled to the phosphorylation of extracellular signal-regulated kinases (ERKs) (Wang et al., 2006). While this relocation of Epac1 was artificially achieved, we hypothesized that the Ras-dependent membrane recruitment of Epac2 could also activate Rap1 on Ras-containing membranes to trigger ERK activation. Our results show that Epac2 potentiates ERK activation induced by Ras activation and cAMP elevation and this pathway contributes to neurite outgrowth in PC12 cells as a model of sympathetic neurons.

2.3 MATERALS AND METHODS

Reagents.

The following antibodies were used for western blot or immunoprecipitation. Anti-Rap1 A/B and unconjugated and agarose-coupled anti-flag (M2) were from Sigma-Aldrich (St. Louis, MO). Anti-phospho-ERK (threonine 202 and tyrosine 204) was from Cell Signaling Technology (Beverly, MA). Anti-Epac2 (rabbit) and GFP anti-serum (rabbit) were from Abcam (Cambridge, MA). Anti-Ras (RAS10) was from Upstate Biotechnology. Anti-HA was from Covance (Princeton, NJ). Anti-ERK2, anti-H-Ras and anti-GST were from Santa Cruz biotechnology Inc. (Santa Cruz, CA). Secondary antibodies against mouse and rabbit IgGs were from GE healthcare. Forskolin, 3-isobutyl-1-methylxanthine (IBMX), 8-Br-cAMP and H89 were from Calbiochem (Riverside, CA). Epidermal growth factor (EGF), Isoproterenol (ISO), GTP, GTPγS, Glutathione peptide and Glutathione-Agarose bead were from Sigma-Aldrich (St. Louis, MO). Nerve growth factor (NGF) was from Axxora (San Diego, CA). 3'-(N-Methyl-anthraniloyl)-2'-deoxy-guanosine-5'-diphosphate, Triethylammonium salt (Mant-dGDP) was from Jena Bioscience (Jena, Germany).

Plasmids.

Mouse Epac2 was subcloned downstream of GFP in pEGFP-C1 vector (Clontech, Mountain View, CA) between *Pst*I site and blunted *Not*I/*Sma*I fusion site, or downstream of flag in pcDNA3 vector (Invitrogen) between *EcoR*I and *Not*I. The K684E and R667E mutations were introduced into flag-Epac2 with QuickChange site-directed mutagenesis kit from Stratagene (La Jolla, CA) according to the manufacturer's instructions. Epac2-684E was also subcloned downstream of GFP. GFP-Epac2Δ430 and GFP-Epac2Δ430-

684E were generated by deletion of the sequences corresponding to the 430 amino acids at the amino-terminus from the parent plasmids using available *EcoR*I and *Sal*I sites, filling in with T4 polymerase and self-ligation. Human H-RasV12 and H-RasN17 were subcloned into mCherry-C1 vector (Clontech) using available *EcoR*I and *Apa*I sites. For the mCherry-RasV12-SAAX construct, the C186S mutation was introduced by PCR through the antisense primer, and then the mutant was subcloned back to the mCherry-C1 vector using available *EcoR*I and *Xba*I sites. Flag-Epac2-CAAX and flag-Epac2-684E-CAAX mutants were created by inserting annealed double-strand oligonucleotides corresponding to the carboxy-terminal 24 amino acids of human H-Ras containing the H-CAAX motif (amino acids 166 to 189 of H-Ras) into flag-Epac2 and flag-Epac2 684E, respectively. HA-Soscat comprising the catalytic domain of the Ras exchanger Sos was a gift of Dafna Bar-Sagi, NYU School of Medicine. HA-Epac2 was a gift of Lawrence Quilliam, Indiana University. Epac1 was a gift of Johannes Bos, Utrecht University.

Cell culture conditions and treatments.

COS and HEK293 cells were cultured in DMEM plus 10% fetal calf serum, penicillin-streptomycin and L-glutamine at 37°C and 5% CO_2. PC12 cells were kindly provided by Pat Casey (Duke University) and cultured in DMEM with 10% horse serum and 5% fetal calf serum plus penicillin, streptomycin and L-glutamine at 37°C and 5% CO_2. To generate stable cell populations, HEK293 cells were transfected with GFP-Epac2 and selected using 0.5 mg/ml G418 (Invitrogen, Carlsbad, CA) for 4 weeks. Cells were starved in serum-free medium for 16hr prior to treatments. Cells were treated with 5 μM Forskolin and 50 μM IBMX for 15 min unless otherwise indicated. H89 was used at 10 μM and was added 15 min prior to Forskolin treatment. EGF and NGF were used at 10

ng/ml and 50 ng/ml, respectively, unless otherwise indicated. 8-Br-cAMP was used at 100 μM for times indicated. Transient transfections were performed using Lipofectamine 2000 according to the manufacturer's instructions. The control vectors, pcDNA3, pEGFP-C1 or mCherry-C1 was included in each set of transfections to assure that each plate received the same amount of transfected DNA.

RNA interference.

The RNA interference targets within Epac2 was identified and validated by testing three double-stranded RNA oligoribonucleotides from Ambion Inc. (Austin, TX). The most effective target site which corresponds to the positions 1144 to 1162 of mouse Epac2 (NM_019688) and positions 1238 to 1256 of rat Epac2 (XM_001060956) was chosen. The sequences used for Rap1A efficiently eliminate rat Rap1A, the major isoforms of Rap1 in PC12 cells (Hisata et al., 2007). The Epac2, Rap1A, and scrambled pairs of oligonucleotides were synthesized by Integrated DNA technologies Inc. (Coralville, IA), annealed and cloned into the pTER vector (van de Wetering et al., 2003) using available *Bgl*II and *Hind*III sites. The sequences of the oligonucleotides used for Epac2, Rap1A and scrambled shRNA were as follow. Epac2: 5'-ATTATTAGATCTGGATCCGTGAATGTAGTCATTCAAGAGATGACTACATTCACGGATCCTTTTTGGAAAAAGCTTATTATT-3'; Rap1A: 5'-ATTATTAGATCTCAGAATTTAGCAAGACAGTGGTGTTCAAGAGACACCACTGTCTTGCTAAATTCTGTTTTTGGAAAAAGCTTATTATT-3'; Scrambled: 5'-AATAATAAGCTTTTTCCAAAAAGCGCGCTTTGTAGGATTCGTCTCTTGAACGAATCCTACAAAGCGCGCAGATCTAATAAT-3'.

Western blotting, immunoprecipitation and GST pulldown.

Western blotting and immunoprecipitation were performed as described previously (Wang et al., 2006). For GST pull down, 10 μg GST-RasV12 loaded with GTPγS and 20 μl of 25% agarose beads were incubated with amounts of cell lysates indicated at 4°C for 3 hr followed by three washes. The proteins were eluted from the beads via 2x Laemmli buffer and applied to 7.5-12% SDS-PAGE gels.

Rap1 activation assay.

Active GTP-bound Rap1 was assayed using GST tagged RBD of RalGDS (gift of J.L. Bos, Utrecht University, Utrecht, Netherlands) in an *in vitro* pull down assay as previously described (Franke et al., 1997). Active GTP-bound Ras was assayed using a Ras activation assay kit (Upstate Biotechnology) as per the manufacturer's instructions.

RT-PCR.

Total RNAs were extracted from PC12 cells, treated as indicated or left untreated, using TRIzol® from Invitrogen as per manufacturer's instruction. Equal amounts of total RNA were used for first-strand cDNA synthesis with oligo-dT and Superscript II reverse transcriptase (Invitrogen), and the cDNA obtained was used as a template for PCR. The Epac2 primers: Sense: 5'-CATTACCACGCACAGCCTTC-3', Antisense: 5'-TTGTACTCCTTGCAGTGAGC-3' generated an 881bp fragment corresponding to 1620-2500 of the Epac2 cDNA. Protein gene product 9.5/ubiquitin carboxyl-terminal hydrolase (PGP9.5) was used as an internal control (Li et al., 2003). The PGP primers (gift of B. Habecker, Oregon Health & Science University, Portland, OR, USA): Sense: 5'-TAATGTGGACGGCCACCTCT-3', Antisense: 5'-GCTCGCGCTCAGTGAATTCT-3'

generated a 109bp fragment corresponding to 531-639 of the PGP9.5 cDNA. Amplification of Epac2 cDNA was analyzed at 28 and 30 cycles, both of which yielded similar results.

Cell fractionation.

Cell fractionation was performed as previously described (Wang et al., 2006). Briefly, cells were scraped in ice-cold hypotonic buffer (10 mM KCl, 1.5 mM $MgCl_2$, 1 mM Na-EDTA, 1 mM DTT, 1 μM leupeptin, 10 μg/ml soybean trypsin inhibitor, 0.1 μM aprotinin, 1 mM sodium orthovanadate, 1 mM β-glycerophosphate and 10 mM Tris-HCl, pH 7.4). Cells were homogenized with 50 strokes in a Dounce-type homogenizer. Lysates were then spun at 800g for 5 min at 4°C to pellet the nuclear fraction and to isolate the supernatant. The supernatant was transferred to a new tube and spun at 20,000g for 30 min at 4°C to pellet the membrane fraction (M), which was washed twice in the above hypotonic buffer and then resuspended in 50 μl lysis buffer. The remaining supernatant (400μl) represented the cytosolic fraction (C). 40% (20μl) and 5% (20μl) of the total volumes of the M and C fractions were supplemented with 6x Laemmli buffer and loaded on the gel for western blot, and from the percentages of the total input and densities of the western blot bands, the percentage of membrane recruitment could be estimated. Presence of endogenous Ras and β-actin was also examined as markers for membrane and cytosol respectively.

Protein expression and purification.

Human H-RasV12 (referred to as RasV12) and bovine Rap1B (referred to as Rap1) were subcloned into pGEX-4T3 vector downstream of the GST tag between *EcoR*I and fused *Xba*I/*Sma*I sites. The construct was transformed into the bacterial strain BL21 (DE3)

from Invitrogen and kept as a glycerol stock. 100ml of standard LB medium was inoculated and grown overnight at 37°C as a pre-culture, which was used to inoculate 2L medium and rocked at 37°C until reaching an OD_{600} of 0.8. Protein expression was induced by IPTG to a final concentration of 100 μM, and the culture was grown at 37°C for 10 hr with 200 rpm. The cells were harvested and frozen at -80°C overnight. The pellets were then resuspended in ice-cold PBS supplemented with 5 mM DTT, 5 mM EDTA and protease inhibitors, and lysed with French press at 15,000psi for 3 cycles. The debris was removed from the lysates by centrifuge and the supernatants were incubated with 2 ml of 50% glutathione-agarose for 3 hr at 4°C. The beads were washed for three times with 10 ml PBS. For GST-Rap1, the fusion protein was eluted with 10 mM glutathione (50 mM Tris-HCl, pH 8) followed by dialysis to remove glutathione. For RasV12, the GST tag was cleaved by incubation with thrombin (Sigma-Aldrich) followed by elution. Epac2Δ430 and Epac2Δ430-684E were subcloned into pGEX-4T3 vector (GE healthcare) downstream of the GST tag using available *EcoR*I and *Not*I sites. The transfection and expression process was similar to RasV12 except that the cells were induced and rocked at 25°C for 15 hr. The purification was similar to what was described previously for Epac1 (Rehmann, 2006), except that the cells were lysed with French press instead of sonication. The concentrations of the purified proteins were determined by both BCA assay (Bio-Rad protein assay reagent) and absorbance at 280nm (A_{280}), and the values generated by the two methods agreed with each other.

Nucleotide exchange assay.

We used mant-dGDP for the exchange assay to avoid artifacts caused by isomerization of the fluorescent label (Guo et al., 2005). RasV12 and GST-Rap1 were loaded with GTPγS

and mant-dGDP, respectively in loading buffer (50 mM Tris-HCl, pH 7.5, 50 mM NaCl, 5 mM EDTA, 5 mM DTT, 5% glycerol) with 10 times molar excess of the respective nucleotides, and the free nucleotides were removed by gel filtration using NAP-5 column (GE Healthcare) equilibrated in exchange buffer (50 mM Tris-HCl, pH 7.5, 50 mM NaCl, 5 mM MgCl2, 5 mM DTT, and 5% glycerol). The exchange assays were performed similarly as described previously (Freedman et al., 2006; Margarit et al., 2003; Rehmann, 2006). Briefly, dissociation rates were measured on a Photon Technologies (PTI) spectrophotometer with a DeltaRam excitation source. Fluorescence was excited at 360 nm, and emission was monitored at 435 nm. In a quartz cuvette, 100 nM Rap1-mant-dGDP was mixed with the exchange buffer supplemented with 100 μM GTP and incubated at 25°C in a final volume of 250 μl. When indicated, reactions were supplemented with 1 μM Epac2Δ430 or Epac2Δ430-684E, and/or 1 μM RasV12-GTPγS. Dissociation was measured for 1000s. The data were fitted to a single-exponential function ($Y=A_0+A_1e^{-kt}$), and the decay due to photobleaching was minimal and ignored. After fitting, the raw data for each reaction were normalized independently between 0 and 1 by using the formula $Y_{\text{normalized}}= (Y_{\text{raw}}-A_0)/(M-A_0)$, where A_0 represents the offset value from the exponential fit and M is the initial, maximum fluorescence.

Fluorescence microscopy.

COS cells were cultured in 12-well plate and transfected with the GFP- or mCherry-tagged plasmids as indicated. The cells were imaged after 24 hr alive at room temperature. Wide field microscopy images were obtained with a Leica DMIRE2 inverted fluorescence microscope. The TIFF images were acquired with MagnaFIRE 2.1software and processed using Adobe Photoshop. Intensity profiling data is provided along the

indicated line across the cell using Scion Image (Scion Corp., Frederick, MD) and plotted using Prism 3 (GraphPad Software, La Jolla, CA).

Neurite outgrowth assay.

PC12 cells were grown on poly-D-lysine-coated plates (Sigma-Aldrich) and serum-starved for 16 hr prior to treatment with EGF (50 ng/ml), or Forskolin (0.5 μM), and pretreatment with H89 (10 μM), which was added 15 min prior to Forskolin treatment. After 24 hr, the cells were examined microscopically for evidence of neurite outgrowth(Obara et al., 2004). Processes greater than two cell body lengths were scored as neurites. Representative photomicrographs are shown of more than 200 cells examined for each condition, in five independent experiments. For experiments utilizing transfection, a vector expressing GFP was cotransfected as a reporter for transfected cells and morphological assessment was restricted to GFP-positive cells. For pretreatment experiments using NGF, NGF (50ng/ml) was applied for 8 hr and washed out prior to subsequent treatment with EGF (50 ng/ml) and/or Forskolin (0.5μM) plus H89 (10μM).

Data processing and statistics.

The densities of the bands from western blot or RT-PCR were quantified using Scion Image (Scion Corp., Frederick, MD). The densities of the bands of interest were adjusted according to the input or loading controls. All the experiments were repeated at least three times and data from multiple data sets were normalized within the scale of 0-100% and analyzed using Prism 3 (GraphPad Software, La Jolla, CA). Unpaired *t* tests were performed between two groups of data as indicated and $p<0.05$ was regarded as statistically significant.

2.4 RESULTS

2.4.1 Epac2 interacts with Ras-GTP in a cAMP-independent manner.

In the GTP-loaded active state, Ras binds the classical effectors like B-Raf and C-Raf via their Ras binding domain (RBD). Epac2, but not Epac1, was also reported to interact with Ras-GTP (Li et al., 2006). To estimate the strength of the Ras-Epac2 binding, the binding profiles of Epac2 and B-Raf toward Ras were compared *in vitro*. We expressed flag-tagged Epac2, B-Raf and Epac1 in COS cells and performed GST pull down assays using increasing amounts of lysates in the presence of purified GST-RasV12 (a constitutively active Ras mutant) that was loaded with GTPγS. Epac1 interacted poorly with GST-RasV12, whereas both Epac2 and B-Raf bound to RasV12 at much higher and comparable levels (Figure 2.1A). When transfected into mammalian cells, RasV12 became stably GTP-loaded under basal conditions (data not shown) and associated with flag-Epac2 in the absence of extracellular stimuli (Figure 2.1B). Ras effectors interact with Ras mainly through the effector loop of Ras and specific mutations along the effector loop can selectively interfere with a subset of effectors. For example, RasV12-40C interacts poorly with B-Raf and C-Raf but interacts normally with PI3 kinase (White et al., 1995). In contrast, 37G interacts poorly with C-Raf but interacts well with another Ras effector, RalGDS (McFall et al., 2001). As shown in Figure 2.1B, Epac2 associated with RasV12 at levels similar to that seen with RasV12-37G, whereas its interaction with RasV12-40C was almost completely lost (Figure 2.1B). Therefore, the Ras-Epac2 interaction requires an intact effector loop, as shown by Quilliam and colleagues (Li et al., 2006).

cAMP is a well-studied regulator of Epac2, and was reported to be necessary for the interaction between Ras and Epac2 in cells (Li et al., 2006). However, treatment with 8-Br-cAMP, an analog of cAMP that is capable of activating Epac2 (data not shown), neither enhanced nor inhibited the binding of Epac2 and RasV12 *in vitro* (Figure 2.1C & D), suggesting that the conformational change of the regulatory region triggered by cAMP was not required for Ras binding. Importantly, the cAMP-independent nature of the Ras-Epac2 interaction is consistent with the crystal structure of Epac2 in its auto-inhibited state, in which its RA domain is well exposed in the solvent and free of steric hindrance from its regulatory region (Rehmann et al., 2006).

To examine whether the Ras-Epac2 interaction could be induced by physiological stimuli, flag-Ras was expressed in Hek293 cell lines stably transfected with GFP-Epac2. Low levels of interaction between Epac2 and Ras were detected under basal condition, which was significantly enhanced upon EGF stimulation (Figure 2.1E). Next, we used epifluorescent microscopy to investigate the distribution of Epac2 in the presence of either RasV12 or RasN17, an inactive mutant of Ras that is constitutively in the GDP-bound state. When transfected alone, mCherry-RasV12 and mCherry-RasN17 were both detected at the plasma membrane, while GFP-Epac2 was not seen at the plasma membrane (Figure 2.1F). When cotransfected with mCherry-RasV12, GFP-Epac2 colocalized with RasV12 at the plasma membrane. In contrast, when cotransfected with mCherry-RasN17, GFP-Epac2 remained largely in the cytosol (Figure 2.1F). In summary, Epac2 binds to the effector loop of Ras-GTP in a cAMP-independent manner, and this interaction recruits Epac2 to the plasma membrane.

2.4.2 Identification of Epac2 mutants with loss of Ras binding.

The Epac2 RA domain is located between the REM domain and CDC25 domain. Therefore, it is possible that deletion of the RA domain may affect the interaction between REM and CDC25 domains as well as the overall structure of Epac2. Indeed, an Epac2 deletion mutant lacking the entire RA domain appeared to be unstable when expressed in COS cells (data not shown). Therefore, to further our understanding of Epac2 and Ras interaction, we looked for specific point mutations within the Epac2 RA domain that could disrupt the Ras-Epac2 interaction without affecting the overall structure of the Epac2 protein.

Comparison of the sequences of RA domains from Epac2 and Epac1 revealed two positively charged residues in Epac2, K684 and R667 that are conserved across species in Epac2 but are replaced by glutamate and glutamine respectively in Epac1 (see blue boxes in Figure 2.2A). To predict the role of these residues in RA domain function, we modeled the interaction between Epac2 and Ras-GTP, taking advantage of the existing structure of Epac2 (Rehmann et al., 2006), as well as the structure of the complex of C-Raf-RBD and Rap1, which has served as a structural model for RBD and Ras interaction (Nassar et al., 1995) (Figure 2.2B). A high degree of similarity between the RA domain of Epac2 and the RBD of C-Raf was observed. Importantly, the position of the side chain of K684 of Epac2 partially overlapped with that of R89 of C-Raf RBD. R89 of C-Raf has previously been identified as a critical residue for Ras interaction (Block et al., 1996; Fabian et al., 1994) (Figure 2.2B). Therefore, we predict that mutation of K684 could similarly abolish the Ras-Epac2 interaction. The above model also highlighted the lack of steric restriction from the regulatory region of Epac2 on the Ras-Epac2 interaction.

As predicted by the sequence alignment and structural modeling, mutation of K684 to glutamate (Epac2-684E) dramatically decreased the Epac2 and Ras binding as measured by GST pull down (Figure 2.2C), and the dissociation constant (Kd) increased from 189.8±9.6 nM to 2898±369.4 nM. The loss of the association of this mutant with Ras-GTP was also demonstrated by immunoprecipitation in cells cotransfected with RasV12 and either wild type Epac2 or Epac2-684E (Figure 2.2D). Mutant Epac2-667E was also included in this experiment, but the loss of Ras binding for this mutant was less pronounced than that for Epac2-684E. Because Ras-Epac2 interaction recruits Epac2 to the plasma membrane (Figure 2.1F), we asked if this effect was reduced when examining the RA domain mutant. We demonstrated that compared to wild type Epac2, the amount of the RA domain mutant within the membrane fraction in the presence of RasV12 was reduced (Figure 2.2E). Taken together, the mutational analysis indicates that an intact RA domain is required for Ras-Epac2 interaction, and that the 684E mutant can be used to investigate how loss of Ras binding affects Epac2 function.

2.4.3 Effect of Ras binding on Rap1 activation via Epac2.

In general, Ras effectors are selective Ras-GTP binding proteins whose functions are modified by that association (Repasky et al., 2004). To examine whether the interaction of Epac2 with Ras modulated Epac2 function, we examined Epac2-dependent activation of Rap1. Previous studies have suggested that RA domain is dispensable for Epac2 function, and that Ras binding to Epac2 does not change its overall ability to activate Rap1 (Li et al., 2006). However, those studies examined transfected Rap1, which was basally activated by cotransfected Epac2 in the absence of cAMP. To avoid any potential pitfall of Rap1 overexpression, we focused on activation of endogenous Rap1 by Epac2.

To elevate intracellular cAMP levels, we used a combination of Forskolin (an adenylyl cyclase activator) and IBMX (a phosphodiesterase inhibitor). To eliminate cAMP-dependent activation of PKA, we pretreated the cells with H89 (a PKA inhibitor). As shown in Figure 2.3A, this cocktail (referred throughout the text as F/H) modestly activated endogenous Rap1 following transfection of wild type Epac2 but not Epac2-684E (Figure 2.3A). Similar results were seen with isoproterenol (Figure 2.3B). That the RA domain mutant exhibited diminished activity in response to cAMP was surprising since the mutation is distant from the catalytic core of Epac2 and is not expected to have any influence on its catalytic activity. Thus, the interaction between Epac2 and Ras appears to be necessary for efficient activation of Rap1 by Epac2 following cAMP elevation. However, F/H is a poor activator of Ras in these cells (data not shown). Therefore, the different activities of Epac2 versus Epac2-684E may reflect their abilities to associate with low levels of basally active Ras.

We next examined whether increased level of Ras-GTP can potentiate the Rap1 activation by Epac2. Indeed, RasV12 dramatically augmented the Epac2-mediated Rap1 activation triggered by cAMP, while Rap1 activation by Epac2-684E was slightly enhanced by RasV12, probably due to residual Ras binding of the mutant (Figure 2.3C). Furthermore, RasV12 boosted the cAMP-triggered Rap1 activation at all time points examined (Figure 2.3D). This enhancement was specific for Epac2 but not Epac1 (Figure 2.3E). Son of Sevenless (Sos) is a well-studied Ras exchanger whose catalytic domain shows constitutive and specific activity toward Ras (Gureasko et al., 2008). When cotransfected into cells, the catalytic domain of Sos (Soscat) also dramatically enhanced

the ability of Epac2 to activate Rap1 (Figure 2.3F), demonstrating the ability of endogenous Ras-GTP to couple Epac2 to Rap1 activation.

2.4.4 Mechanism of Ras-dependent Epac2 activation.

cAMP binding to the cNBD within the regulatory region of Epac2 has been proposed to reorient the regulatory region away from the catalytic domain allowing access of Rap1 to the catalytic site (Rehmann et al., 2008; Rehmann et al., 2006; Rehmann et al., 2003a). To understand the mechanism for the requirement of Ras-GTP in Epac2-mediated Rap1 activation, we first tested whether Ras-Epac2 interaction facilitated this action of cAMP. Deletion of the regulatory region of Epac2, including both cNBDs and the DEP domain, produced a constitutively active truncation (Epac2Δ430) whose function was no longer regulated by cAMP. Epac2Δ430 activated Rap1 in a dose-dependent manner when expressed in COS cells. In contrast, the Epac2Δ430 mutant containing the additional K684E mutation (Epac2Δ430-684E) exhibited significantly reduced ability to activate Rap1 (Figure 2.4A). This suggests that an intact RA domain is still required for Rap1 activation by the catalytic region even in the absence of intramolecular inhibition. Importantly, the Epac2Δ430-mediated Rap1 activation could be further enhanced by RasV12, which was ineffective in enhancing Epac2Δ430-684E activity (Figure 2.4B). Together, these results indicate that Ras-mediated regulation of Epac2 is independent of the mechanism by which cAMP activates Epac2.

To test the possibility of allosteric activation of Epac2 by Ras-GTP, we examined the kinetics of nucleotide exchange *in vitro* using purified proteins (Figure 2.4C). The rate of nucleotide release from Rap1 in the presence of Epac2Δ430 ($5\pm0.2x10^{-3}s^{-1}$for 1 μM exchange factor) is comparable to the rate in the presence of Epac2Δ430-684E

($5\pm0.7x10^{-3}s^{-1}$ for 1 μM exchange factor), and is significantly higher than the intrinsic rate of nucleotide release by isolated Rap1 ($0.3x10^{-3}s^{-1}$; Figure 2.4D). These data confirm that the Epac2-684E mutant is fully functional and the loss of Rap1 activation by this RA mutant in cell-based Rap1 activation assays cannot be explained by the loss of its intrinsic catalytic activity (see Figure 2.3A and 4A). In addition, in the presence of saturating concentrations of RasV12 preloaded with GTPγS, the rate of nucleotide release from Rap1 catalyzed by Epac2Δ430 was not accelerated (Figure 2.4E). These results suggest that Ras does not enhance Epac2-mediated Rap1 activation *in vitro*, despite activating it within cells.

One possible explanation for these findings is that the compartmentalization of Ras and Rap1 is critical for the Ras-dependent Rap1 activation by Epac2 in intact cells. To test this hypothesis, we first performed structural modeling to visualize the Ras-Epac2Δ430-Rap1 ternary complex in the context of the plasma membrane. The ternary complex was assembled based on the crystal structures of Epac2 in complex with Rap1 and a cAMP analog (Rehmann et al., 2008), and the complex of Rap1-C-Raf RBD (for detailed methods see section on Structural modeling, Supplemental information). From this model (Figure 2.5A) we observed that Ras, Rap1 and the RA and cdc25 domains of Epac2 were aligned on a single plane parallel to the membrane plane. Importantly, the carboxy-terminal ends of both Ras and Rap1 were oriented toward the plasma membrane in this model. This is a necessary constraint, since both Ras and Rap1 are lipid modified at the carboxy-terminals and tethered to the lipid membrane.

Based on this structural model, it is possible that Ras-mediated membrane recruitment may play a crucial role in Rap1 activation by Epac2. We predict that tethering

Epac2 to the membrane may mimic the effect of Ras-Epac2 binding. To address this possibility, we targeted Epac2 to the membrane by introducing a CAAX motif at its carboxy-terminal end. This increased the amount of Epac2 that could be recovered from membrane fractions (Figure 2.5B) and dramatically enhanced the ability of Epac2 to activate Rap1 (Figure 2.5C). Importantly, membrane targeting rescued the defect of Epac2-684E (Figure 2.5C), and occluded the enhancing effect of RasV12 on Epac2-mediated Rap1 activation (Figure 2.5D). Next, we tested whether sequestration of Epac2 in the cytosol could prevent it from activating Rap1. We achieved this by cotransfection of RasV12-SAAX, which was constitutively GTP loaded but mislocalized in the cytosol due to the loss of lipid modification (data not shown). RasV12-SAAX dramatically reduced Epac2-mediated Rap1 activation in response to cAMP (Figure 2.5E), suggesting that RasV12-SAAX was acting as an interfering mutant. This finding further supports the role of endogenous Ras-GTP in Epac2 mediated activation of Rap1. We next validated the above membrane-recruitment model *in vitro* by incubating purified Epac2Δ430 and membrane fractions from cells expressing RasV12 or control cells, and RasV12 significantly enhanced the activation of endogenous Rap1 within the membrane fraction by Epac2Δ430 (Figure 2.5F).

We propose that compartmentalization of Epac2 by Ras-GTP increases the concentration of Epac2 in the sub-membrane space, thus greatly enhancing the subsequent interaction between Epac2 and Rap1. This was demonstrated by using computational simulation (Figure 2.5G). In the absence of active recruitment of Epac2 to the membrane, the rate of Rap1 activation is very slow and solely dependent on the expression level of Epac2 (see section on Computational modeling, Supplemental

information, for details). However, active membrane recruitment by Ras binding provided an additional level of regulation, which could dramatically accelerate the reaction rate even in the presence of small increase of membrane recruitment (Figure 2.5G).

In this model, membrane recruitment of Epac2 is influenced by two factors: the level of Ras activation and the affinity of Epac2 toward Ras-GTP. As demonstrated in Figure 2.5H, rate of Epac2-mediated Rap1 activation is predicted to be very sensitive to initial changes in Ras-GTP levels and reaches a plateau at higher Ras-GTP levels. This may explain the apparent dependence of Epac2 activation on interaction with low levels of Ras-GTP that may be present in cells stimulated with cAMP alone (see Figure 2.3A). The model also explains the decreased level of Rap1 activation by Epac2-684E by showing that it can be fully accounted for as a result of decreased Ras association (Figure 2.5H). Taken together, Ras association converts Epac2 into an efficient, membrane-based Rap1 activator, and this recruitment is required for Epac2 function.

2.4.5 Epac2-mediated Rap1 activation at the membrane is coupled to ERK activation and neurite outgrowth.

We have recently shown that activation of Rap1 at the plasma membrane is coupled to ERK activation via B-Raf (Wang et al., 2006). Therefore, we tested whether recruitment of Epac2 to the plasma membrane by Ras could also couple Rap1 to ERK activation in B-Raf-expressing cells. PC12 cells express abundant levels of B-Raf, and Rap1 activation of B-Raf/ERKs in these cells has been well documented (Hisata et al., 2007; Limpert et al., 2007; York et al., 1998). However, these cells express low levels of Epac1 or Epac2 and have shown little PKA-independent activation of Rap1(Wang et al., 2006).

Accordingly, F/H treatment triggered little activation of ERKs, even in the presence of EGF (Figure 2.6A & B). However, upon expression of Epac2, F/H and EGF were able to synergistically and robustly activate ERKs in a PKA-independent manner (Figure 2.6A & B). Importantly, Rap1A contributed to the robust ERK activation by F/H and EGF in the presence of Epac2, as knockdown of Rap1A with shRNA (Figure 2.6C) significantly reduced this effect (Figure 2.6D). The modest ERK activation via Epac2 triggered F/H alone was enhanced when Epac2 was targeted to the membrane via the CAAX motif, and was absent in cells expressing the Epac2-684E mutant (Figure 2.6E). Moreover, the enhanced activity of Epac2-CAAX no longer required Ras binding, as similar levels of ERK activation were seen with the Epac2-684E-CAAX mutant (Figure 2.6E).

Augmented ERK signaling has been associated with neurite outgrowth in PC12 cells (Boykevisch et al., 2006; Hisata et al., 2007; Kao et al., 2001). To provide a physiological correlation for the Epac2 mediated augmentation of ERK signaling, we measured neurite outgrowth in PC12 cells with or without exogenous Epac2. In the presence of overexpressed Epac2, EGF and F/H induced neurite outgrowth in about 10% and 40% of the transfected cells respectively. However, the combination of EGF and F/H had a synergistic action, promoting neurite outgrowth in 80% of the transfected cells (Figure 2.6F). These data correlated with the pattern of ERK activations observed with these treatments (Figure 2.6A & B). Interestingly, in the absence of transfected Epac2, the combination of EGF and F/H also synergistically induced neurite outgrowth in about 40% of the cells (Figure 2.6F). This may reflect the presence of endogenous Epac2 in these cells (see below). The ability of F/H to induce neurite outgrowth to a level greater than EGF alone may depend on a low level of basal Ras activation in PC12 cells.

Moreover, the inability of EGF to promote neurite outgrowth is consistent with the inability of EGF to stimulate cAMP levels.

The levels of neurite outgrowth via Epac2 mutants also correlated with the levels of ERK activation (Figure 2.6E). Unlike Epac2, Epac2-684E did not enhance neurite outgrowth above levels seen in cells transfected with GFP alone, suggesting that the action of Epac2 required an intact RA domain (Figure 2.6E). Targeting Epac2 to the plasma membrane via the CAAX motif resulted in equally high levels of neurite outgrowth by F/H in the presence or absence of EGF. This suggests that the EGF potentiated the F/H effect primarily through recruitment of Epac2 to the membrane. Taken together, these data suggest that Epac2 activation at the membrane is coupled to ERK activation and neurite outgrowth.

2.4.6 Endogenous Epac2 is increased by NGF and contributes to ERK activation and neurite outgrowth.

Epac2 is enriched in the neuronal tissues (Kawasaki et al., 1998a). Therefore, we hypothesized that NGF induced differentiation of PC12 cells might be accompanied by increased expression of Epac2. Indeed, although basal levels of Epac2 mRNA and protein were detected using RT-PCR and western blot respectively, both were significantly enhanced after 8 hrs of NGF pretreatment (Figure 2.7A and B). Therefore, we could increase endogenous levels of Epac2 by brief pretreatment with NGF and examine the role of Epac2 in neurite outgrowth without elevating Epac2 levels by transfection. Importantly, the 8 hr NGF pretreatment dramatically augmented the synergism between EGF and F/H on the activation of endogenous ERKs (Figure 2.7C). Pretreatment with NGF can also enhance the basal level of Ras-GTP. This may account for the ability of

F/H to induce significant higher levels of ERK activation following NGF pretreatment, compared to F/H treatment alone in the absence of NGF pretreatment (Figure 2.7C). Interestingly, EGF was also capable of inducing a modest increase in Epac2 expression (Figure 2.7A and B).

The enhanced ERK activation was significantly diminished in cells expressing shRNA targeting Epac2, but not scrambled shRNA (Figure 2.7E). The efficacy of shRNA knock down of Epac2 is shown in Figure 2.7D. Knockdown of Epac2 by shRNA also inhibited neurite outgrowth (Figure 2.7F & G). In the presence of Epac2 shRNA (but not scrambled shRNA or GFP control) the level of neurite outgrowth triggered by EGF and F/H was reduced from 40% to 20% (Figure 2.7G), suggesting that the basal level of Epac2 mediates synergistic effect of EGF and F/H on neurite outgrowth in PC12 cells. Importantly, short-term NGF pretreatment itself did not trigger neurite outgrowth by itself if NGF was washed out after 8 hr. However, this pretreatment had an enhancing effect on the outcome of subsequent treatment with F/H alone or F/H plus EGF (Fig 7F & G). This priming effect was largely dependent on the expression of Epac2, as the enhancement was blocked by Epac2 shRNA but not scrambled shRNA (Figure 2.7F & G). Taken together, endogenous Epac2, either basal or induced by NGF, integrates signals from cAMP and Ras and contributes to ERK activation and neurite outgrowth in PC12 cells.

2.5 DISCUSSION

Recently, Quilliam and colleagues showed that Ras recruits Epac2 to the plasma membrane. Here we extend their model by demonstrating that this recruitment is essential for the maximal action of Epac2 as a Rap1 exchanger. The classical definition of Ras effectors requires that effector binding be dependent on the GTP-bound state of Ras and that binding modifies the effector's function (Mitin et al., 2005). Epac2 has met this definition and is a *bona fide* Ras effector. While Epac proteins need cAMP to relieve their auto-inhibition, our study shows for the first time that Epac2 also requires the interaction with Ras-GTP via the RA domain for its ability to activate Rap1 efficiently. This is based on a number of findings. (1) A specific mutation that disrupts the association of Epac2 with Ras-GTP diminishes the Epac2-dependent activation of Rap1 without affecting intrinsic exchange activity or cAMP-mediated regulation of Epac2. (2) Interference with endogenous Ras using the mutant RasV12-SAAX that cannot associate with the membrane blocks cAMP-dependent activation of Epac2. (3) Activation of endogenous Ras by a Ras-specific exchanger, as well as expression of a constitutively active Ras mutant, enhances Epac2 dependent activation of Rap1. These data provide strong support for the necessity of Ras interaction for Epac2 function.

Thus, Epac2 is both a cAMP sensor and a novel Ras effector that couples coincident cAMP elevation and Ras activation to the activation of Rap1. This Rap1 activation is significantly higher than that seen following stimulation via either Ras or cAMP alone. While the cross-talk between the cAMP and Ras signaling pathways has been shown to occur at multiple levels (Dumaz and Marais, 2005; Stork and Schmitt,

2002), Epac2 provides a unique example of a single molecule integrating the two pathways through the independent actions of discrete domains.

Regarding the mechanism for Ras-dependent regulation of Epac2, Ras neither facilitates the relief of Epac2 auto-inhibition, nor induces allosteric changes to activate the Epac2 catalytic domain. Instead, Ras recruits Epac2 to the membrane, dramatically increases its local concentration and accelerates the rate of Rap1 activation. This action may be similar to what was recently proposed for Ras activation of Sos. However, in that model, both membrane recruitment and allosteric modulation of Sos by Ras contributed to Sos activation (Boykevisch et al., 2006) (Gureasko et al., 2008). As supported by the structural modeling and our experimental data, cAMP binding to the cNBD and the interaction between Ras and RA domain are two independent events, which allows the relief of auto-inhibition and membrane localization of Epac2 to be independently regulated by cAMP and Ras respectively.

The requirement of Ras in the Epac2-dependent activation of Rap1 has many potential consequences for cell signaling. Temporally, Rap1 activated by Epac2 would accompany both cAMP elevation and Ras activation. Spatially, Epac2 mediated Rap1 activation would be restricted to Ras-containing membranes. Rap1 signaling from Ras-containing membranes has previously been shown to couple to ERKs through the Raf isoform B-Raf (Wang et al., 2006). This may reflect the properties of B-Raf itself, as the Raf family of kinases has been shown to be much more efficient at coupling to ERKs from the plasma membranes as compared to intracellular locales (Harding et al., 2005). The participation of Rap1 in Ras-dependent activation of ERKs may also provide amplification, since many Rap1 molecules can be activated following the recruitment of a

single Epac2 molecule to Ras. Moreover, the inactivation of Rap1 by Rap1-selective GAPs may be slower than that of Ras (Sasagawa et al., 2005; Stork, 2005), permitting Rap1 activation to be sustained. Distinct Ras isoforms are selectively activated in different subcellular compartments, resulting in that activation of distinct intracellular signaling pathways (Hancock, 2003). Epac2 has been reported to interact with all Ras isoforms via its RA domain (Li et al., 2006). Therefore, it is possible that recruitment of Epac2, and resultant Rap1 activation, differentially modulates the signals emanating from each of these Ras isoforms.

Neurite outgrowth of PC12 cells has been a well-studied physiological reporter for neuronal differentiation that accompanies activation of the ERK pathway, with increased activation of ERK correlating with the extension of neuritic processes (Boykevisch et al., 2006; Hisata et al., 2007; Sasagawa et al., 2005; York et al., 1998). Importantly, transient activation of ERKs by EGF is not capable of triggering neurite outgrowth in the absence of additional signals. Using PC12 cells, we show that the inclusion of Epac2/Rap1 signaling to that of EGF can enhance EGF-dependent signaling to ERKs and together can induce robust neurite outgrowth. Of course, the Epac2-mediated Rap1 activation is also likely to regulate other actions of Rap1 that occur at or near the plasma membrane including exocytosis (Holz et al., 2006; Ozaki et al., 2000) and cell adhesion (Bos, 2005; Bos et al., 2001).

Indirect activation of Rit by Epac has also been reported to mediate PACAP triggered p38 phosphorylation and neurite outgrowth in the related PC6 cells (Shi et al., 2006) and ERK activation in other cell types (Lein et al., 2007; Rudolph et al., 2007). These reports and our findings together reveal the complexity of Epac signaling upstream

of MAP kinase cascades. It may be that Rap1 and Rit, working through ERKs and p38, act in concert to promote neurite outgrowth in these cells. Rap1 activation of p38 has been reported (Huang et al., 2004; Sawada et al., 2001) and it is possible that this is mediated by the coupling of Rap1 to Rit activation. Since Epac is not the direct GEF for Rit (Shi et al., 2006), it will be important to identify the Rit exchanger and to determine whether there is direct interaction between Rap1 and this exchanger that might mediate the coupling between these two small G proteins. Conversely, the possibility that Rit itself can bind to the RA domain of Epac and potentiate its actions remains to be tested.

Epac2 is a neuronal-expressed isoform of the Epac family of exchangers. It is possible that Epac2 is involved in neuronal functions such as neuronal differentiation and synaptic plasticity that can be potentiated by both Ras-dependent and cAMP-dependent signals (Je et al., 2006; Waltereit and Weller, 2003). Because Ras can be activated via multiple signals, including intracellular calcium (Krapivinsky et al., 2003), Epac2 might also function as a coincidence detector for cAMP and calcium. In pancreatic beta cells, exocytosis of insulin stimulated by cAMP has a PKA-independent component that requires Epac2 (Kashima et al., 2001). It will be important to determine whether Ras-dependent recruitment of Epac2 by glucose, growth factors or hormones potentiates this action, as well as other PKA-independent actions of cAMP.

We propose that Epac2 levels will also be induced by NGF in neuronal cells. The Epac2 promoter contains cAMP-responsive element (CRE) sites (Impey et al., 2004; Zhang et al., 2005) that are well established targets of NGF signaling (Riccio et al., 1997). The induction of Epac2 by NGF may serve to enhance signaling through Rap1 as part of a positive feedback loop to potentiate neurite outgrowth following its initiation. It is also

possible that NGF also induces post-translational modifications of Epac2 to further enhance its function. We do not believe that the induction of Epac2 by NGF is unique to NGF, but its induction by EGF does not by itself contribute to neurite outgrowth in the absence of additional stimulators of cAMP. However, it does provide a mechanism by which EGF and cAMP can act together to promote neurite outgrowth.

In summary, we show that Epac2 is a novel Ras effector that can act as a coincidence detector for Ras and cAMP. The mechanism by which Epac2 permits Ras to activate Rap1 may be shared by other GEFs that contain functional RA domains (Rodriguez-Viciana et al., 2004). Therefore, activation of small G proteins by recruitment of their cognate GEFs to the plasma membrane via RA domains may be a fundamental mechanism to couple distinct G proteins to each other.

2.6 ACKLOWLEDGMENTS

The authors thank David Farrens, Satinder Singh, Peter Rotwein, Mike Forte, and Zhiping Wang for scientific discussion and Quentin Low, Mark DeWitt, Jon Fay, and Srilatha Tavisala for technical assistance. This work was funded by NIH NCI grant number CA72971. We would also like to thank Dafna Bar-Sagi, NYU School of Medicine, Lawrence Quilliam, Indiana University, Johannes Bos, Utrecht University, and Daniel Altschuler, University of Pittsburgh, for generous sharing of reagents.

Figure 2.1 Epac2 interacts with Ras-GTP independently of cAMP.

(A) Epac2 and B-Raf, but not Epac1, bind to Ras-GTP. COS cells were transfected with flag-Epac1, Epac2, or B-Raf, as indicated, and increasing amount of lysates were incubated with purified GST-RasV12 loaded with GTPγS, followed by GST-pull down and western blot. Upper panel shows data from three experiments (mean ± s.e.) and curve fitting. Lower panel shows a representative result from one experiment. Input and protein levels recovered after pull down are shown for Epac2 (top), B-Raf (middle), and Epac1 (bottom).

(B) Epac2 interacts with Ras at its effector loop. Flag-Epac2 was cotransfected along with either HA-RasV12 or its effector loop mutants (37G or 40C) into COS cells followed by immunoprecipitation (IP) using anti-HA antibody and western blot (top). The expression levels of flag-Epac2 (middle) and HA-Ras V12 and mutants (bottom) are shown.

(C) Ras-Epac2 interaction is not enhanced by the cAMP analog 8-Br-cAMP *in vitro*. Purified GST-RasV12 loaded with GTPγS was incubated with cell lysates containing flag-Epac2 in the presence or absence of 8-Br-cAMP, followed by GST-pull down. Left panel: western blot using flag Ab (top) and GST antibody (bottom). Right panel shows the quantification of three experiments (mean ± s.e.).

(D) Time course of Ras-Epac2 binding is not affected by 8-Br-cAMP. Purified GST-RasV12 loaded with GTPγS was incubated with cell lysates containing flag-Epac2. 8-Br-cAMP or vehicle was added to the incubation after 30 min. GST-pull down was performed at the time points indicated.

(E) Ras-Epac2 association was induced by EGF treatment. Flag-Ras was transiently expressed in Hek293 cells stably transfected with GFP-Epac2 or in wild type cells as indicated, and IP was performed with anti-GFP antibody after EGF (+) or mock (-) treatment, followed by western blot. The amounts of flag-Ras and GFP-Epac2 recovered within the IP and the expression of transfected proteins were shown.

(F) Epac2 and Ras-GTP colocalized on the plasma membrane. Upper row: GFP-Epac2 (left), mCherry-RasV12 (middle), and mCherry-RasN17 (right) were transfected into COS cells respectively and imaged using epifluorescent microscopy. Middle row: GFP-Epac2 (left) and mCherry-RasV12 (middle) were cotransfected into COS cells. The merged fluorescent images are shown in the right panel. Lower row: GFP-Epac2 (left) and mCherry-RasN17 (middle) were cotransfected. The merged images are shown in the right panel. For both the middle and the bottom row, the far right panel shows intensity profiles across the cell at the white line indicated in the right panel. The broken lines denote the position of the plasma membranes.

Figure 2.1

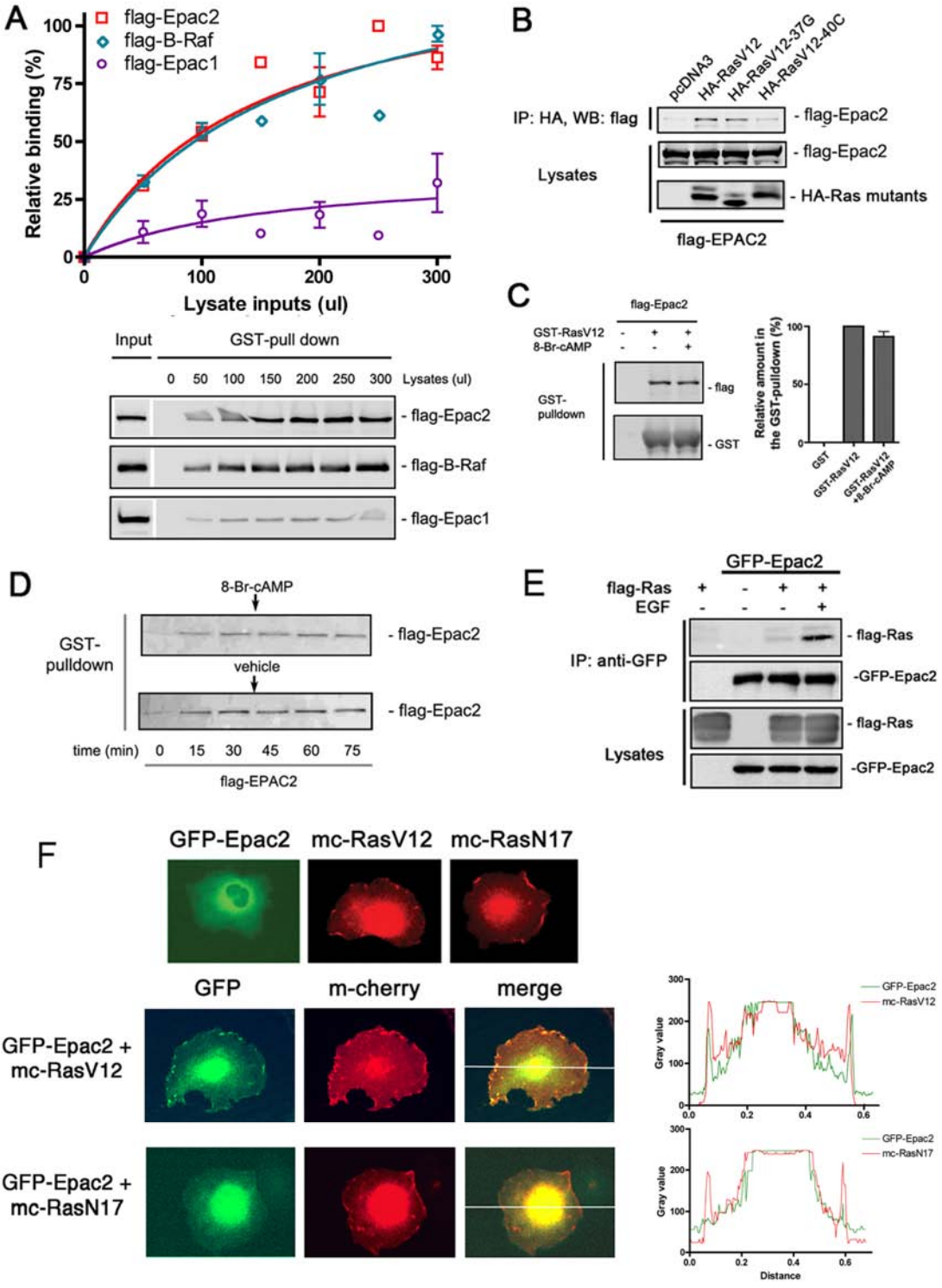
A
flag-Epac2
flag-B-Raf
flag-Epac1
Relative binding (%)
Lysate inputs (ul)
Input
GST-pull down
Lysates (ul)
- flag-Epac2
- flag-B-Raf
- flag-Epac1
B
pcDNA3
HA-RasV12
HA-RasV12-37G
HA-RasV12-40C
IP: HA, WB: flag
- flag-Epac2
Lysates
- flag-Epac2
- HA-Ras mutants
flag-EPAC2
C
flag-Epac2
GST-RasV12
8-Br-cAMP
GST-pulldown
- flag
- GST
Relative amount in the GST-pulldown (%)
GST
GST-RasV12
GST-RasV12 +8-Br-cAMP
D
8-Br-cAMP
GST-pulldown
- flag-Epac2
vehicle
- flag-Epac2
time (min)
flag-EPAC2
E
GFP-Epac2
flag-Ras
EGF
IP: anti-GFP
- flag-Ras
-GFP-Epac2
Lysates
- flag-Ras
-GFP-Epac2
F
GFP-Epac2
mc-RasV12
mc-RasN17
GFP
m-cherry
merge
GFP-Epac2 + mc-RasV12
GFP-Epac2 + mc-RasN17
Gray value
Distance

Figure 2.2 Disruption of Ras-Epac2 interaction by a single point mutation within the RA domain.

(A) Sequence alignment of the RA domains from Epac1 and Epac2, as well as the Ras binding domain from B-Raf (BRAF-RBD) and C-Raf (CRAF-RBD). The residues within Epac2 that were targeted for mutational analysis are highlighted.

(B) Structural modeling demonstrating the position of K684 at the Ras-Epac2 binding interface. The crystal structure of Rap1 in a complex with CRAF-RBD was used as template, and the structures of Ras and Epac2 were superimposed onto Rap1 and CRAF-RBD, respectively, using the program Chimera (UCSF). Left panel shows an overview of the predicted Ras-Epac2 complex; right panel shows a close-up of the binding interface. The side chains of K684 (Epac2) and R89 (C-Raf) are highlighted as red and green sticks, respectively (see arrows).

(C) Epac2-684E was incapable of Ras binding. Increasing amounts of flag-Epac2 WT, or Epac2-684E were incubated with GTPγS-loaded GST-RasV12, flowed by GST-pull down and western blot. The concentration of flag-proteins was quantified by comparing to purified protein standards. The graph shows data from three experiments (mean ± s.e.) with curve fitting. The right panel shows the amounts of Epac proteins within the pull down in the presence or absence of GST-RasV12, as well as the input levels of all proteins.

(D) Ras association with wild type Epac2 and Epac2 mutants. Flag-Epac2 WT and mutant (Epac2-667E or Epac2-684E) were cotransfected with HA-RasV12 into COS cells and IP was performed using anti-HA agarose antibody, followed by western blot.

The first two rows show the levels of Epac2 proteins and HA-RasV12 within the IP. The third and forth rows show levels of transfected proteins within the lysates.

(E) The recruitment of Epac2-684E to the membrane is reduced when compared to that of WT Epac2. Flag-Epac2 WT or -684E were cotransfected with mCherry (mc)-RasV12 into COS cells followed by cell fractionation. The membrane fraction (M) and the cytosolic fraction (C) were isolated and examined by western blot using flag Ab (top). Both transfected RasV12 (mc-RasV12, middle) and endogenous Ras (bottom) were also monitored as markers for the membrane fraction using Ras antibody. The percentages of Epac2 WT and Epac2-684E that were recruited to the membrane were calculated as described in the Methods, and right panel summarizes data from three experiments (mean ± s.e.).

Figure 2.2

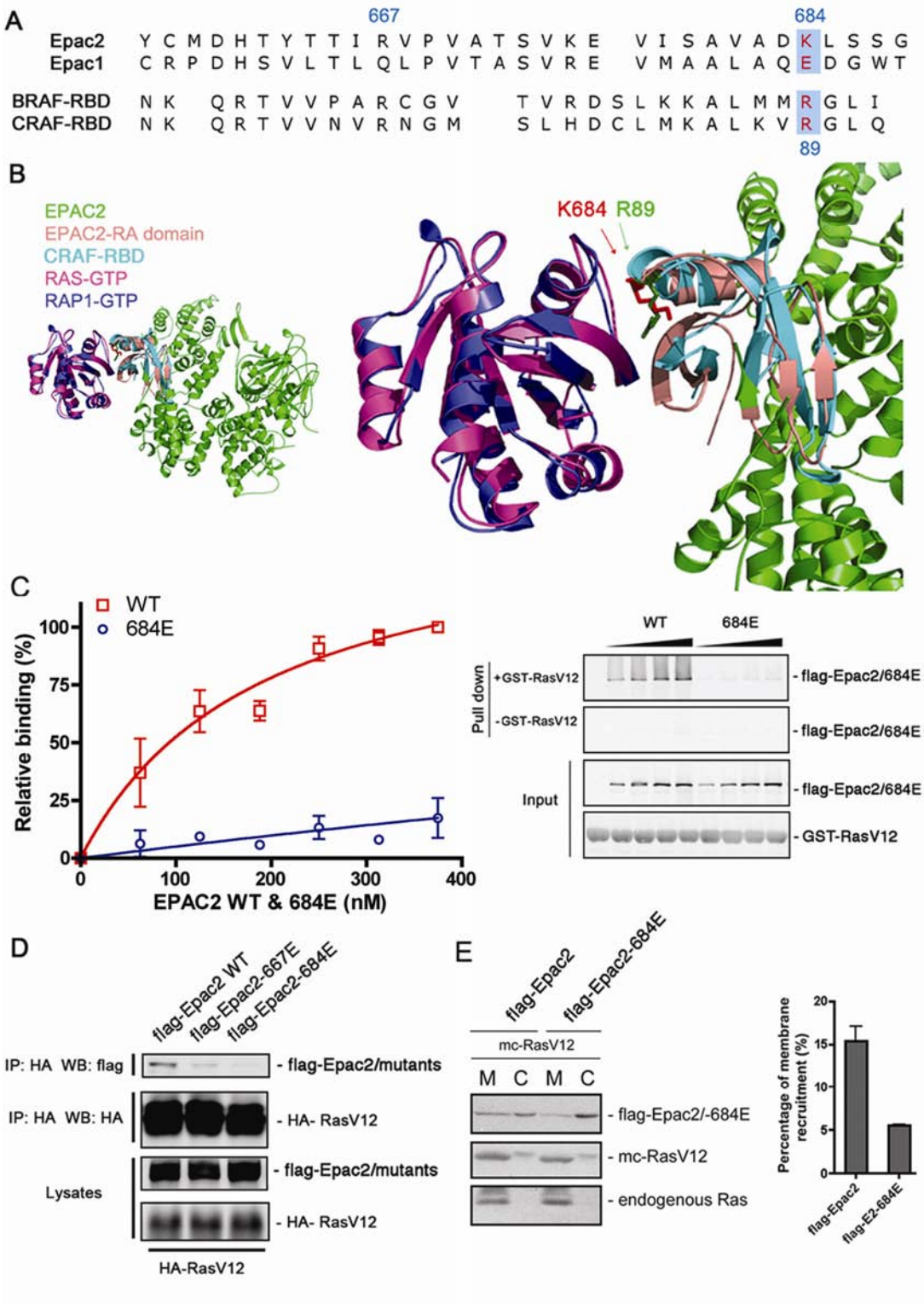
A
667
684
Epac2 Y C M D H T Y T T I R V P V A T S V K E V I S A V A D K L S S G
Epac1 C R P D H S V L T L Q L P V T A S V R E V M A A L A Q E D G W T
BRAF-RBD N K Q R T V V P A R C G V T V R D S L K K A L M M R G L I
CRAF-RBD N K Q R T V V N V R N G M S L H D C L M K A L K V R G L Q
89
B
EPAC2
EPAC2-RA domain
CRAF-RBD
RAS-GTP
RAP1-GTP
K684 R89
C
WT
684E
Relative binding (%)
EPAC2 WT & 684E (nM)
WT
684E
Pull down
+GST-RasV12
-GST-RasV12
Input
- flag-Epac2/684E
- GST-RasV12
D
flag-Epac2 WT
flag-Epac2-667E
flag-Epac2-684E
IP: HA WB: flag
IP: HA WB: HA
Lysates
- flag-Epac2/mutants
- HA- RasV12
HA-RasV12
E
flag-Epac2
flag-Epac2-684E
mc-RasV12
M C M C
- flag-Epac2/-684E
- mc-RasV12
- endogenous Ras
Percentage of membrane recruitment (%)
flag-Epac2
flag-E2-684E

Figure 2.3 Ras-Epac2 interaction is required for efficient Rap1 activation by Epac2.

(A) Time course of activation of endogenous Rap1 triggered by F/H (H89, Forskolin and IBMX) in cells expressing Epac2 WT and Epac2-684E. COS cells were transfected with pcDNA3, flag-Epac2 or flag-Epac2-684E for 24hr. Serum-starved cells were treated with F/H for the times indicated and harvested. Rap1 activation assay was performed using GST-RalGDS-RBD, followed by western blot for endogenous Rap1. Left panel shows quantification of data from three independent experiments (mean ± s.e.). Right panel shows representative gels from one experiment. In this and all the following Rap1 activation assays, Rap1 activation and Rap1 protein levels are shown in the top two rows, respectively, and the levels of transfected proteins are shown in bottom rows. At least three independents experiments were performed.

(B) Time course of activation of endogenous Rap1 triggered by isoproterenol (ISO) in cells expressing Epac2 WT and Epac2-684E. COS cells were transfected with pcDNA3, flag-Epac2 or flag-Epac2-684E for 24hr. Serum-starved cells were treated with ISO for the times indicated, harvested and subjected to Rap1 activation assay. Left panel shows quantification of data from three independent experiments (mean ± s.e.); right panel shows representative gels from one experiment.

(C) Co-expression of RasV12 enhances Rap1 activation by Epac2. COS cells were transfected with mCherry (mc)-RasV12, flag-Epac2, or both, as indicated, and treated with F/H (+) for 15 min or left untreated (-). The lysates were subjected to Rap1 activation assay. Epac2-684E was included for comparison.

(D) Time course of RasV12 enhanced Rap1 activation by Epac2. COS cells were transfected as in (C) and treated with F/H for the indicated times and lysates subjected to Rap1 activation assay.

(E) RasV12 dependent enhancement of Rap1 activation is specific for Epac2 but not Epac1. Flag-Epac1 or Epac2 was transfected alone or together with mc-RasV12 (V12). After F/H treatment for 10 min, cells were harvested for Rap1 activation assay.

(F) Specific activation of endogenous Ras enhances Epac2-mediated Rap1 activation. COS cells were transfected with HA-tagged catalytic domain of Sos (Soscat) and/or HA-Epac2 as indicated, treated with F/H for ten min or left untreated (Untr.). Lysates were subjected to Rap1 activation assay. Left panel shows representative gels from one experiment. Right panel shows quantification of data from three experiments (mean ± s.e.).

Figure 2.3

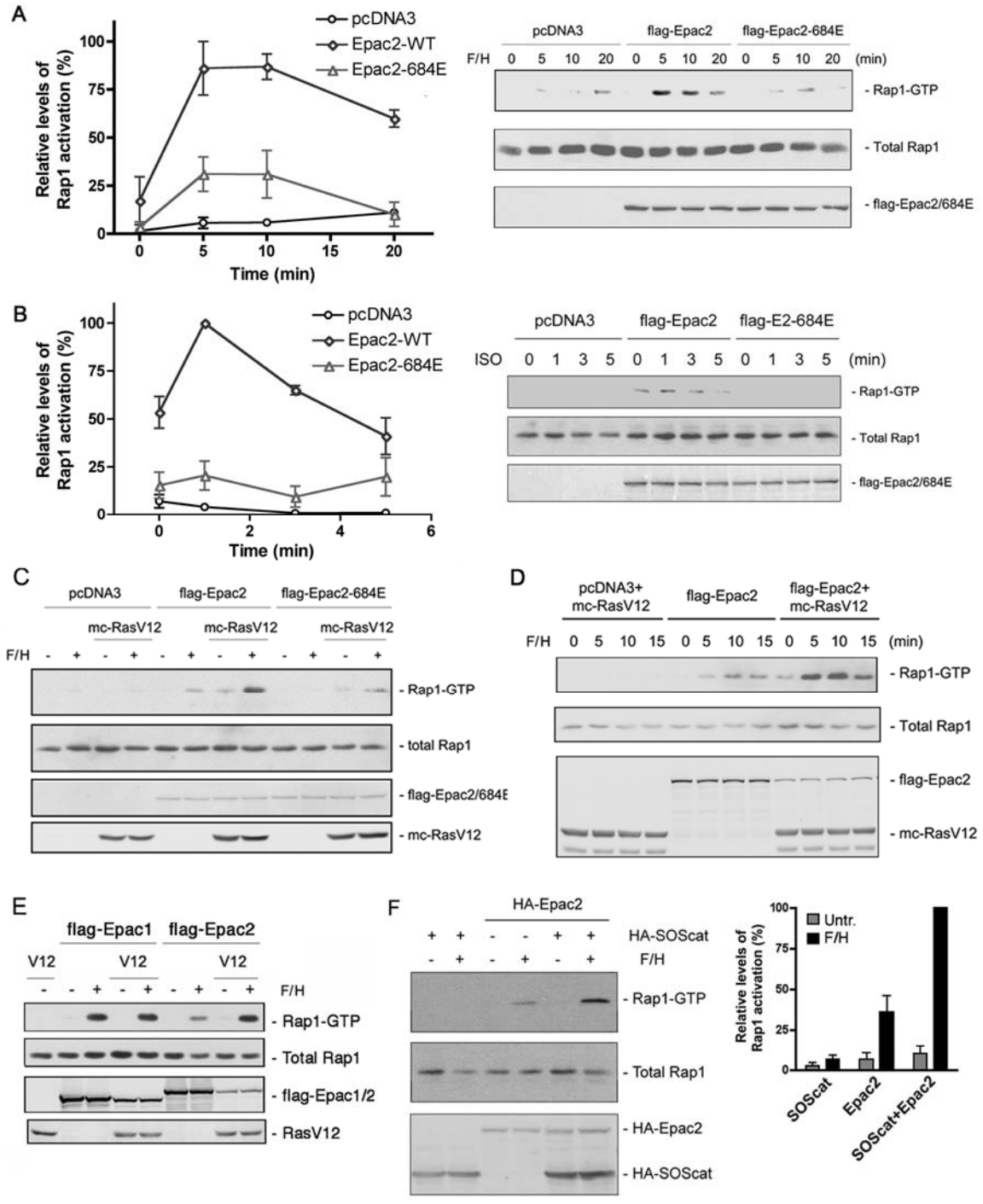
A
pcDNA3
Epac2-WT
Epac2-684E
Relative levels of Rap1 activation (%)
Time (min)
pcDNA3
flag-Epac2
flag-Epac2-684E
F/H
(min)
- Rap1-GTP
- Total Rap1
- flag-Epac2/684E
B
pcDNA3
Epac2-WT
Epac2-684E
Relative levels of Rap1 activation (%)
Time (min)
pcDNA3
flag-Epac2
flag-E2-684E
ISO
(min)
- Rap1-GTP
- Total Rap1
- flag-Epac2/684E
C
pcDNA3
flag-Epac2
flag-Epac2-684E
mc-RasV12
F/H
- Rap1-GTP
- total Rap1
- flag-Epac2/684E
- mc-RasV12
D
pcDNA3+ mc-RasV12
flag-Epac2
flag-Epac2+ mc-RasV12
F/H
(min)
- Rap1-GTP
- Total Rap1
- flag-Epac2
- mc-RasV12
E
flag-Epac1
flag-Epac2
V12
F/H
- Rap1-GTP
- Total Rap1
- flag-Epac1/2
- RasV12
F
HA-Epac2
HA-SOScat
F/H
- Rap1-GTP
- Total Rap1
- HA-Epac2
- HA-SOScat
Untr.
F/H
Relative levels of Rap1 activation (%)
SOScat
Epac2
SOScat+Epac2

Figure 2.4 Ras-GTP potentiates the Rap1 activation by the catalytic region of Epac2 *in vivo* but not *in vitro*.

(A) Comparison of Rap1 activation by Epac2Δ430 and Epac2Δ430-684E. Increasing amounts of Epac2Δ430 or Epac2Δ430-684E were expressed in COS cells and lysates subjected to Rap1 activation assay. Left panel shows linear regression of data from one representative experiment. Levels of Rap1 activation were plotted against the expression levels of constructs as indicated. Right panel shows representative gels from one experiment. Three independent experiments were performed. AU, artificial unit.

(B) RasV12 enhancement of Rap1 activation by Epac2Δ430 requires an intact RA domain. GFP-Epac2Δ430 and Epac2Δ430-684E were transfected alone or cotransfected with mCherry (mc)-RasV12 and lysates subjected to Rap1 activation assay. Left panel shows the quantification of data from three experiments (mean ± s.e.); right panel displays gels from one representative experiment.

(C) Coomassie staining of purified Epac2Δ430, Epac2Δ430-684E, GST-Rap1 and RasV12. Protein markers are shown on the left.

(D) Both Epac2Δ430 and Epac2Δ430-684E catalyzed nucleotide exchange reaction on Rap1 at identical rates *in vitro*. Upper panel shows the comparison of intrinsic (red) exchange reaction and that catalyzed by Epac2Δ430 (cyan) or Epac2Δ430-684E (pink). Rap1-mant-dGDP (100 nM) was incubated in buffer containing 100 μM unlabeled GTP in the absence or presence of 1 μM of Epac2Δ430 or Epac2Δ430-684E. Dissociation of mant-dGDP was monitored by the decrease of fluorescence emission at 435 nm over time. Bottom panel, reaction rates were fitted to single exponentials and 3-6 independent measurements for each condition were pooled in the bar graph (mean ± s.e.).

(E) RasV12 does not enhance the exchange activity of Epac2Δ430 *in vitro*. Upper panel, comparison of intrinsic (red) exchange reaction and that catalyzed by Epac2Δ430 in the presence (orange) or absence (cyan) of Ras-GTP. Rap1-mant-dGDP (100 nM) was incubated in buffer containing 100 μM unlabeled GTP in the absence or presence of 1 μM of Epac2Δ430 alone or in addition to GTPγS-loaded RasV12. Dissociation of mant-dGDP was monitored. Bottom panel, reaction rates were fitted to single exponentials, and 3 independent measurements were summarized in the bar graph (mean ± s.e.).

Figure 2.4

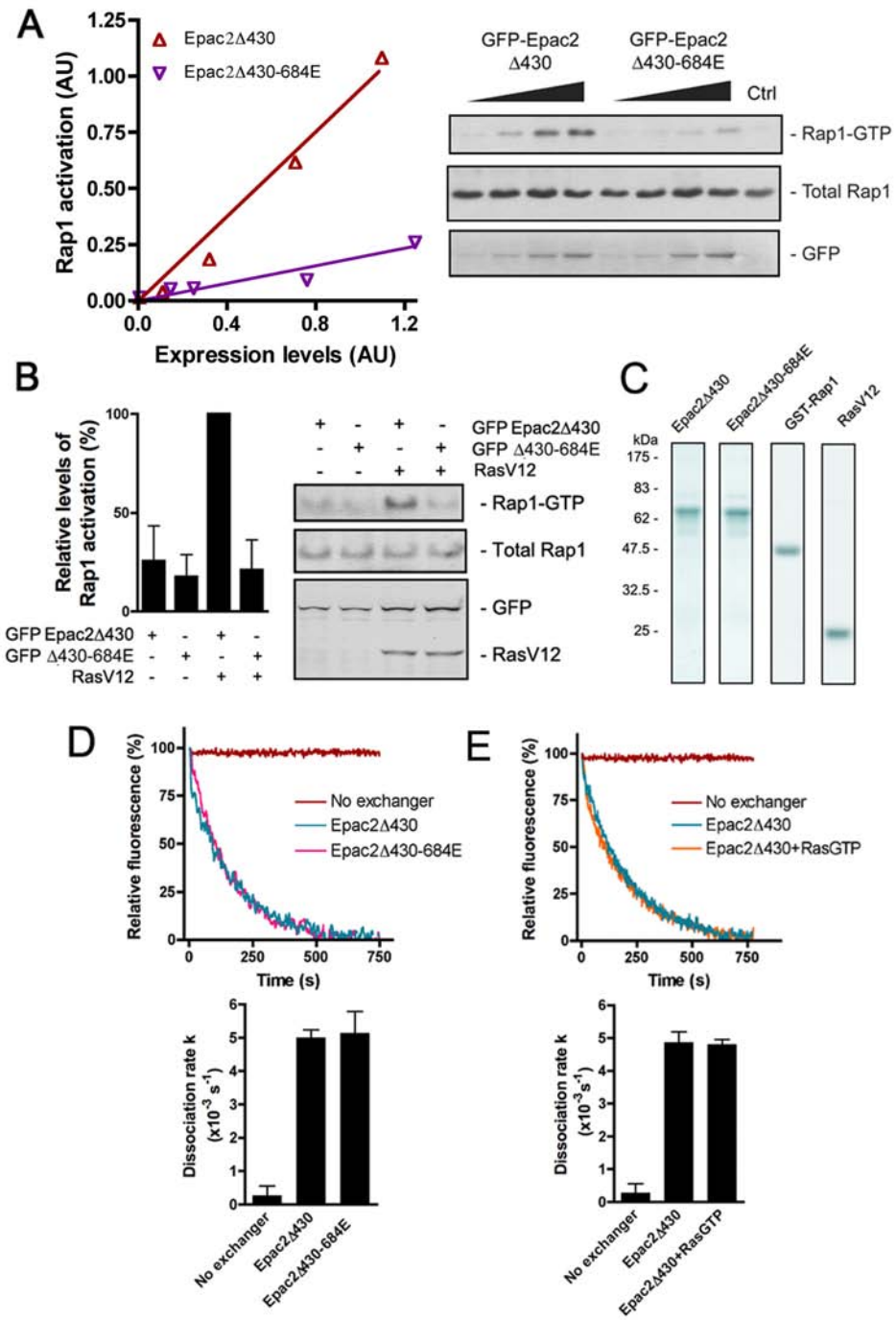
A
Epac2Δ430
Epac2Δ430-684E
Rap1 activation (AU)
Expression levels (AU)
GFP-Epac2 Δ430
GFP-Epac2 Δ430-684E
Ctrl
- Rap1-GTP
- Total Rap1
- GFP
B
Relative levels of Rap1 activation (%)
GFP Epac2Δ430
GFP Δ430-684E
RasV12
- Rap1-GTP
- Total Rap1
- GFP
- RasV12
C
Epac2Δ430
Epac2Δ430-684E
GST-Rap1
RasV12
kDa
175
83
62
47.5
32.5
25
D
Relative fluorescence (%)
No exchanger
Epac2Δ430
Epac2Δ430-684E
Time (s)
Dissociation rate k (x10-3 s-1)
No exchanger
Epac2Δ430
Epac2Δ430-684E
E
Relative fluorescence (%)
No exchanger
Epac2Δ430
Epac2Δ430+RasGTP
Time (s)
Dissociation rate k (x10-3 s-1)
No exchanger
Epac2Δ430
Epac2Δ430+RasGTP

Figure 2.5 Mechanism of Ras facilitated Rap1 activation by Epac2.

(A) Structural modeling of the Ras-Epac2-Rap1 ternary complex in relation to the plane of lipid membrane. The ternary complex demonstrates that Rap1 engages the CDC25-homology domain of Epac2 to the left; the RA domain of Epac2 interacts with Ras to the right. The carboxy-terminal ends of Rap1 and Ras point towards the membrane plane. This accommodates the lipid modifications of both proteins that tether both carboxy-terminal ends to the membrane. Additional details are provided in the section on Structural modeling, Supplemental information.

(B) Additon of the H-Ras CAAX motif increased the amounts of Epac2 and Epac2-684E localized to the membrane. Flag-tagged Epac2, Epac2-CAAX, Epac2-684E (E2-684E) and Epac2-684E-CAAX (E2-684E-CAAX) were transfected into COS cells for 24 hr and cell fractionation was performed. The membrane fraction (M) and cytosolic fraction (C) were subjected to western blot. Representative gels from one experiment are shown. Upper row shows flag-proteins within the two fractions. Middle and lower rows are endogenous Ras and β-actin as markers for membrane and cytosol, respectively.

(C) Anchoring Epac2 to the plasma membrane by the CAAX motif from H-Ras results in enhanced level of Rap1 activation and rescues the defect of Epac2-684E (E2-684E). COS cells were transfected with Epac2, Epac2-CAAX, Epac2-684E, and Epac2-684E-CAAX, as indicated, starved, and treated with F/H or left untreated. Lysates were subjected to Rap1 activation assay. Upper panel shows representative gels from one experiment. The bottom panel shows quantification of three experiments (mean ± s.e.).

(D) Membrane targeting of Epac2 (Epac2-CAAX) occluded the effect of RasV12 on Epac2-mediated Rap1 activation. mCherry RasV12 was co-transfected with Epac2,

Epac2-CAAX, Epac2-684E, or Epac2-684E-CAAX into COS cells, as indicated, starved, and treated with F/H for 10 min or left untreated. Lysates were subjected to Rap1 activation assay. Upper panels show representative gels from one experiment. The bottom panel shows quantification of three experiments (mean ± s.e.).

(E) Sequestration of Epac2 in the cytosol by RasV12-SAAX prevents Epac2 from activating endogenous Rap1. COS cells were transfected with flag-Epac2 and/or Ras-SAAX, as indicated and starved cells were treated with F/H for 10 min or left untreated, followed by Rap1 activation assay. The upper panel shows gels from one representative experiment. The bottom panel shows quantification of three experiments (mean ± s.e.).

(F) Purified Epac2Δ430 activates Rap1 within membrane preps containing RasV12 *in vitro*. Increasing amounts of Epac2Δ430 were incubated with membrane fractions isolated from COS cells that were transfected with pcDNA3, mCherry-RasN17 (RasN17) or mCherry-RasV12 (RasV12) in 100μl of exchange buffer and the presence of 100 μM GTP for 15 min at room temperature. The membrane fractions were recovered by centrifuge and endogenous Rap1 activity within the membranes was assayed. The upper panel shows a representative result from one experiment. The bottom panel shows quantification of three experiments (mean ± s.e.).

(G-H) Computational model of Epac2-mediated Rap1 activation. For details, see the section on Computational modeling, Supplemental information. (G) The relative rate of Rap1 activation is shown as a function of the relative intracellular concentration of Epac2 (ranging from 0 to 1) and the percentage of its membrane recruitment (from 0 to 100%). (H) The relative rate of Rap1 activation is shown as a function of the relative levels of Ras activation (varying from 0 to 1) and the affinity between Ras and Epac2 or its

mutants. The upper, middle and lower surfaces represent high, intermediate, and low affinities of Epac2/Ras interactions, respectively.

Figure 2.5

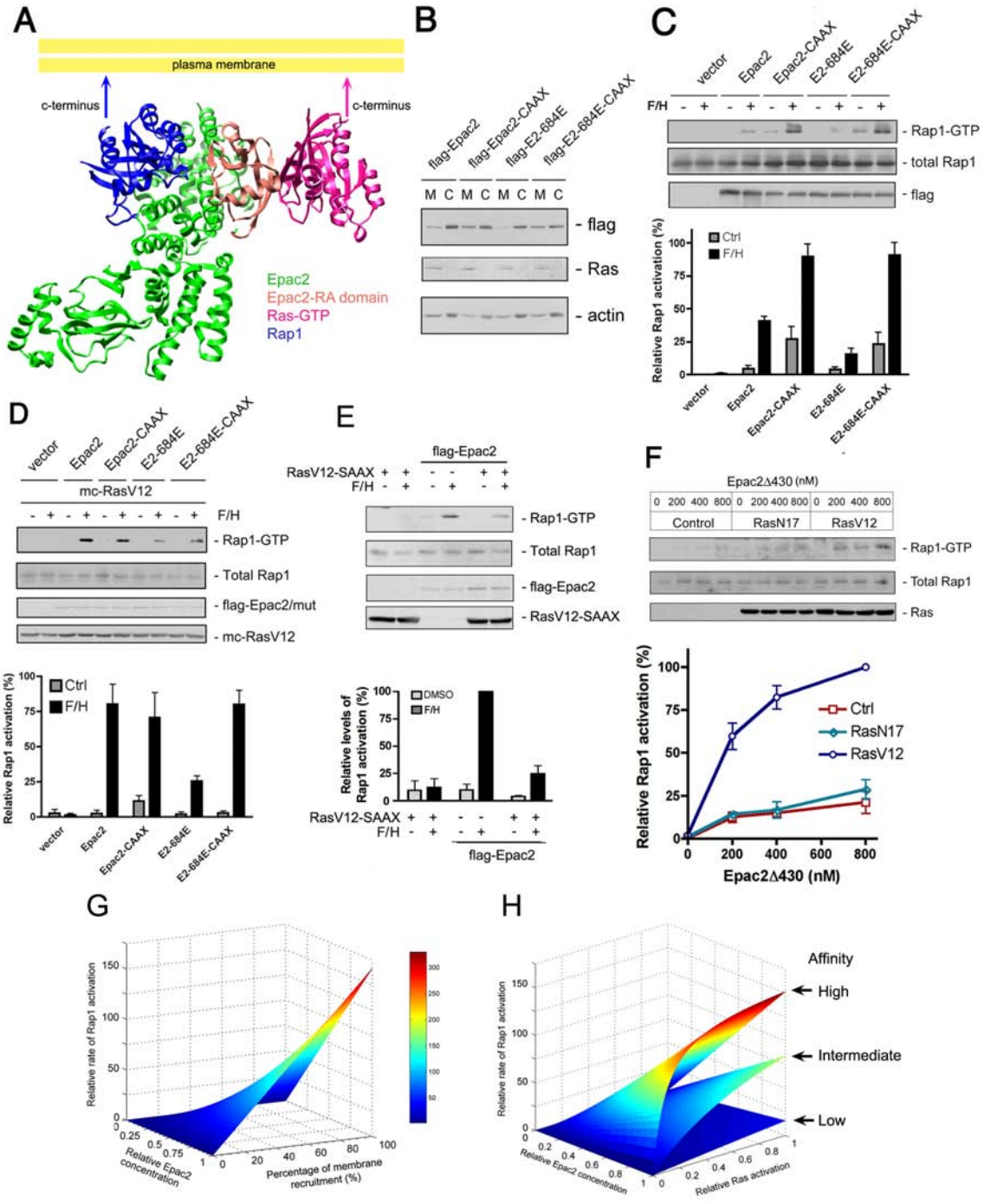
A
plasma membrane
c-terminus
c-terminus
Epac2
Epac2-RA domain
Ras-GTP
Rap1
B
flag-Epac2
flag-Epac2-CAAX
flag-E2-684E
flag-E2-684E-CAAX
M C M C M C M C
- flag
- Ras
- actin
C
vector
Epac2
Epac2-CAAX
E2-684E
E2-684E-CAAX
F/H
- Rap1-GTP
- total Rap1
- flag
Relative Rap1 activation (%)
Ctrl
F/H
D
mc-RasV12
F/H
- Rap1-GTP
- Total Rap1
- flag-Epac2/mut
- mc-RasV12
Relative Rap1 activation (%)
E
flag-Epac2
RasV12-SAAX
F/H
- Rap1-GTP
- Total Rap1
- flag-Epac2
- RasV12-SAAX
Relative levels of Rap1 activation (%)
DMSO
F/H
F
Epac2Δ430 (nM)
Control
RasN17
RasV12
- Rap1-GTP
- Total Rap1
- Ras
Relative Rap1 activation (%)
Ctrl
RasN17
RasV12
Epac2Δ430 (nM)
G
Relative rate of Rap1 activation
Relative Epac2 concentration
Percentage of membrane recruitment (%)
H
Affinity
High
Intermediate
Low
Relative rate of Rap1 activation
Relative Epac2 concentration
Relative Ras activation

Figure 2.6 Enhancement of ERK activation and neurite outgrowth by Epac2.

(A) Expression of Epac2 enhances the activation of ERKs by EGF and F/H. PC12 cells were transfected with vector (pcDNA3) or flag-ERK2, and treated for 15 minutes with F/H, EGF, EGF plus F/H, or left untreated. For this and all subsequent ERK activation assays, the levels of phosphorylated flag-ERK2 are shown using a phospho-ERK antibody following flag IP (first row). Total levels of transfected flag-ERK2 (second row) and flag-Epac2 (third row) are also shown.

(B) Expression of Epac2 enhances the activation of ERKs by EGF and F/H. PC12 cells were transfected with flag-ERK2 along with GFP or Epac2, and treated with EGF or EGF plus F/H. Representative gels from one experiment are shown on the left. Right panel shows quantification of data from three independent experiments (mean ± s.e.).

(C) Rap1A shRNA reduces the expression of cotransfected Rap1A. PC12 cells were cotransfected with flag-Rap1A (rat) and flag-ERK2 cDNA with either Rap1A shRNA or scrambled control (scrm.) for 24 hrs followed by flag IP. Left panel shows levels of flag-Rap1A (upper row) and flag-ERK2 as transfection control (lower row) by western blot. Right panel: quantification of data from three independent experiments (mean ± s.e.).

(D) Rap1A knockdown blocks ERK activation via Epac2 triggered by EGF plus F/H. PC12 cells were cotransfected with flag-Epac2 and flag-ERK2 along with scrambled shRNA (scrm.) or Rap1A shRNA, and treated as indicated. The upper panel shows quantification of data from three experiments, and the lower panel shows representative gels from one experiment.

(E) Membrane targeting of Epac2 overcomes mutation within RA domain. PC12 cells were transfected with flag-ERK2 along with Epac2 (E2) wild type or mutants as indicated, and treated with F/H. ERK activation assay was performed and the upper panel shows gels from a representative experiment. Bottom panel: quantification of data from three independent experiments (mean ± s.e.).

(F) Expression of Epac2 increases neurite outgrowth induced by EGF and F/H. Left panel: PC12 cells were transfected with GFP and either vector, Epac2, Epac2-684E (E2-684E), or Epac2-CAAX and treated with EGF and/or F/H as indicated. 24hr later, neurite outgrowth was assessed under epifluorescent microscopy. Right panel: representative photomicrographs are shown. Left panel: quantification of data from five independent experiments (mean ± s.e.). Bar in the lower left panel represents 20 μM.

Figure 2.6

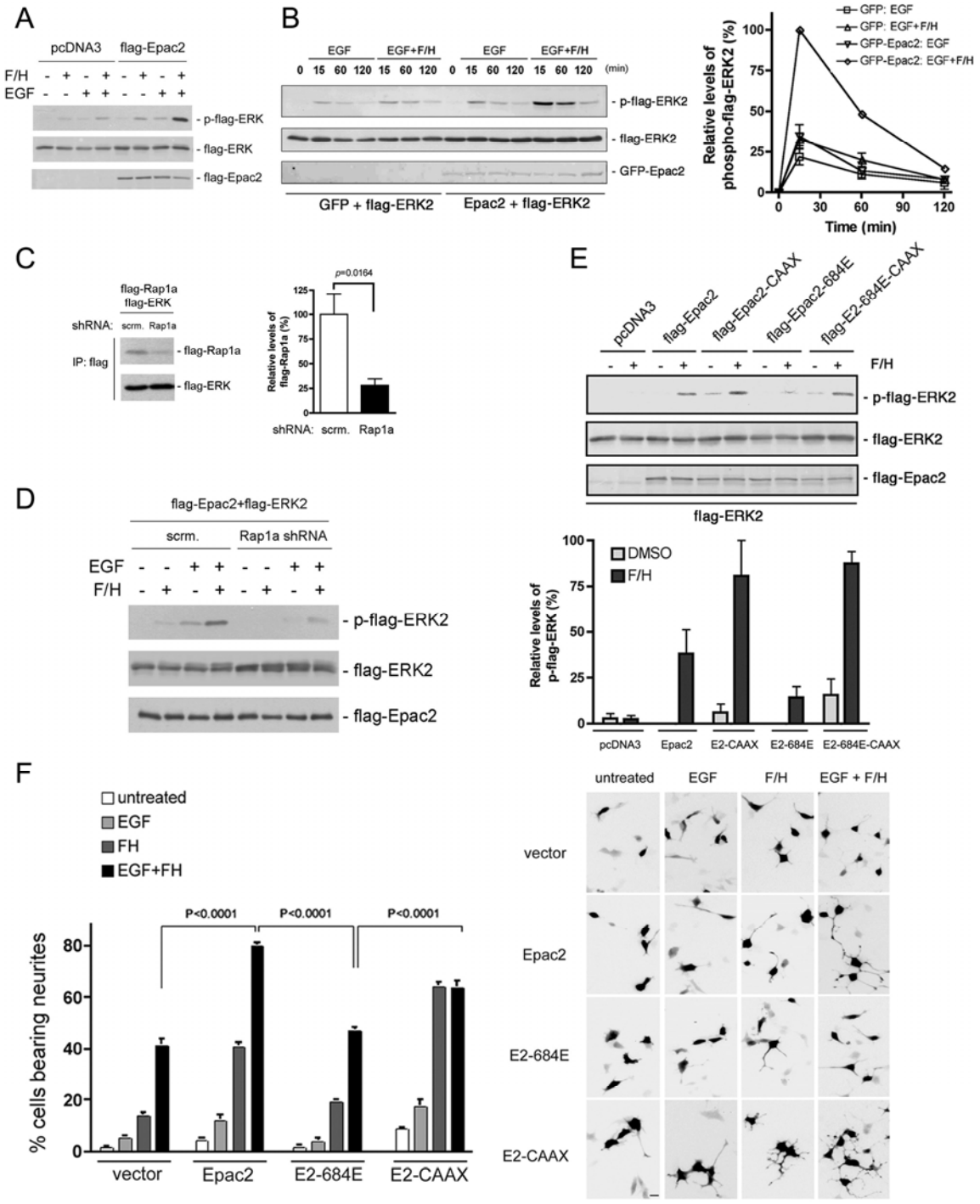
A
pcDNA3
flag-Epac2
F/H
EGF
- p-flag-ERK
- flag-ERK
- flag-Epac2
B
EGF
EGF+F/H
0 15 60 120 15 60 120 0 15 60 120 15 60 120 (min)
- p-flag-ERK2
- flag-ERK2
- GFP-Epac2
GFP + flag-ERK2
Epac2 + flag-ERK2
GFP: EGF
GFP: EGF+F/H
GFP-Epac2: EGF
GFP-Epac2: EGF+F/H
Relative levels of phospho-flag-ERK2 (%)
Time (min)
C
flag-Rap1a
flag-ERK
shRNA: scrm. Rap1a
IP: flag
- flag-Rap1a
- flag-ERK
p=0.0164
Relative levels of flag-Rap1a (%)
shRNA: scrm. Rap1a
D
flag-Epac2+flag-ERK2
scrm.
Rap1a shRNA
EGF
F/H
- p-flag-ERK2
- flag-ERK2
- flag-Epac2
E
pcDNA3
flag-Epac2
flag-Epac2-CAAX
flag-Epac2-684E
flag-E2-684E-CAAX
F/H
- p-flag-ERK2
- flag-ERK2
- flag-Epac2
flag-ERK2
DMSO
F/H
Relative levels of p-flag-ERK (%)
pcDNA3
Epac2
E2-CAAX
E2-684E
E2-684E-CAAX
F
untreated
EGF
FH
EGF+FH
P<0.0001
P<0.0001
P<0.0001
% cells bearing neurites
vector
Epac2
E2-684E
E2-CAAX
untreated
EGF
F/H
EGF + F/H
vector
Epac2
E2-684E
E2-CAAX

Figure 2.7 Endogenous Epac2 is increased by NGF and contributes to ERK activation and neurite outgrowth.

(A) Epac2 mRNA is increased by NGF or EGF treatment. PC12 cells were treated with NGF or EGF (50 ng/ml) for 8 hrs, or left untreated. Total RNAs extracted from the cells were subjected to reverse transcription and PCR (RT-PCR) for Epac2 (upper row). PGP (lower row) was used as a control. Lower panel shows quantification of data from five experiments (mean ± s.e.).

(B) Epac2 protein is increased by NGF or EGF treatment. PC12 cells were treated with NGF or EGF for 8 hrs or left untreated. Total cell lysates were subjected to western blot. Upper panel: western blot showing endogenous Epac2 protein (upper row). ERK2 was used as the loading control (lower row). Bottom panel: quantification of data from four experiments (mean ± s.e.).

(C) NGF pretreatment enhances the activation of ERKs by EGF plus F/H. PC12 cells were pretreated with NGF for 8 hr or left without pretreatment, and subsequently treated with EGF and/or F/H as indicated. Top panel: average of data from three independent experiments. Bottom panel: the levels of phosphorylation of endogenous ERKs and total levels of ERKs are shown.

(D) Epac2 shRNA reduces the expression of cotransfected Epac2. PC12 cells were cotransfected with flag-Epac2 and flag-ERK2 cDNA with either Epac2 shRNA or scrambled control for 24 hrs followed by flag IP. Left panel shows levels of flag-Epac2 (upper row) and flag-ERK2 as transfection control (lower row) by western blot. Right panel: quantification of data from three independent experiments (mean ± s.e.).

(E) Knockdown of endogenous Epac2 by shRNA decreases the activation of ERKs by EGF plus F/H after NGF pretreatment. PC12 cells were cotransfected with flag-ERK2 along with scrambled shRNA (scrm.) or Epac2 shRNA, and treated as indicated. Upper panel shows gels from one representative ERK activation assay. Lower panel shows quantification of data from three independent experiments (mean ± s.e.).

(F) Epac2 knockdown decreases neurite outgrowth induced by F/H after NGF pretreatment. PC12 cells were transfected with GFP, scrambled shRNA, or shRNA for Epac2. Cells were pretreated with NGF for 8hr, and subsequently treated with F/H. 24hr later, neurite outgrowth was assessed under epifluorescent microscopy. Top panel: representative photomicrographs are shown. Bottom panel: The percentage of cells bearing neurites is shown with standard error (s.e.) from at least three independent experiments.

(G) Epac2 knockdown decreases neurite outgrowth induced by treatment with EGF plus F/H in the presence or absence of NGF pretreatment. PC12 cells were transfected with GFP, scrambled shRNA, or shRNA for Epac2. Cells were pretreated with NGF for 8hr or left without pretreatment, and subsequently treated with EGF and F/H. 24hr later, neurite outgrowth was assessed under epifluorescent microscopy. Right panel: representative photomicrographs are shown. Bar in the lower left photomicrograph represents 20 μM. Left panel: The percentage of cells bearing neurites is shown with standard error (s.e.) from five independent experiments.

Figure 2.7

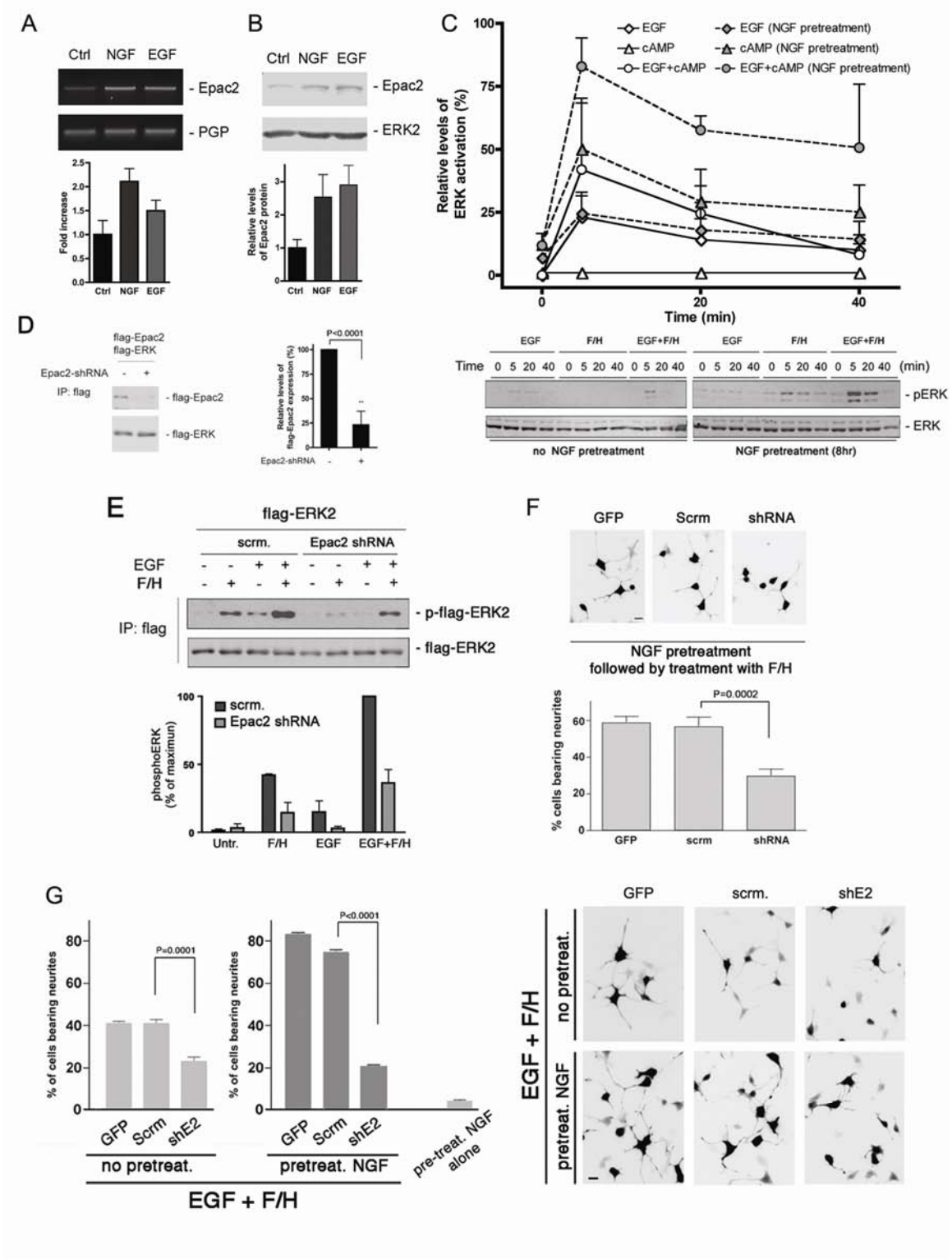
A
Ctrl NGF EGF
- Epac2
- PGP
Fold increase
B
Ctrl NGF EGF
- Epac2
- ERK2
Relative levels of Epac2 protein
C
EGF
cAMP
EGF+cAMP
EGF (NGF pretreatment)
cAMP (NGF pretreatment)
EGF+cAMP (NGF pretreatment)
Relative levels of ERK activation (%)
Time (min)
EGF F/H EGF+F/H EGF F/H EGF+F/H
Time 0 5 20 40 0 5 20 40 0 5 20 40 0 5 20 40 0 5 20 40 0 5 20 40 (min)
- pERK
- ERK
no NGF pretreatment
NGF pretreatment (8hr)
D
flag-Epac2
flag-ERK
Epac2-shRNA
IP: flag
- flag-Epac2
- flag-ERK
P<0.0001
Relative levels of flag-Epac2 expression (%)
E
flag-ERK2
scrm.
Epac2 shRNA
EGF
F/H
IP: flag
- p-flag-ERK2
- flag-ERK2
scrm.
Epac2 shRNA
phosphoERK (% of maximun)
Untr.
F/H
EGF
EGF+F/H
F
GFP
Scrm
shRNA
NGF pretreatment followed by treatment with F/H
P=0.0002
% cells bearing neurites
G
P=0.0001
P<0.0001
% of cells bearing neurites
GFP
Scrm
shE2
no pretreat.
pretreat. NGF
pre-treat. NGF alone
EGF + F/H
GFP
scrm.
shE2
EGF + F/H
no pretreat.
pretreat. NGF

Chapter 3

The Interaction of Epac1 and Ran Promotes Rap1 Activation at the Nuclear Envelope

Chang Liu[1,2], Maho Takahashi[1], Yanping Li[1],

Tara J. Dillon[1], Stefanie Kaech Petrie[3], & Philip J. S. Stork[1,2*]

[1]Vollum Institute, [2]Department of Cell and Developmental Biology, Oregon Health & Science University, Portland, Oregon 97239, USA, [3]Jungers Center, Oregon Health & Science University, Portland, Oregon 97239, USA.

*Corresponding author. Mailing address: *Vollum Institute, Oregon Health & Science University, 3181 SW Sam Jackson Park Road, Portland, OR 97239.*

Tel: 503-494-5494. Fax: 503-494-4976. E-mail: stork@ohsu.edu

In final review, Molecular and Cellular Biology, March 2010.

I gratefully acknowledge the contribution of Dr. Maho Takahashi to Figure 3.2A-C and the construction of multiple plasmids, and Dr. Yanping Li to Figure 3.1B-D and 3.8B. For the part of this project using mass spectrometry, the extracted peptides were sent to the Proteomics Shared Resource at OHSU and the analysis was performed by John Klimek and Debra McMillen.

3.1 ABSTRACT

Epac1 (Exchange protein directly activated by cAMP) couples intracellular cAMP to the activation of Rap1, a Ras family GTPase that regulates cell adhesion, proliferation and differentiation. Using mass spectrometry, we identified the small G protein Ran and the Ran binding protein 2 (RanBP2) as potential binding partners of Epac1. Ran is a small G protein best known for its role in nuclear transport and can be found at the nuclear pore through its interaction with RanBP2. Here, we demonstrate that Ran-GTP and Epac1 interact with each other *in vivo* and *in vitro*. This binding requires a previously uncharacterized Ras association (RA) domain in Epac1. Surprisingly, the interaction of Epac1 with Ran is necessary for the efficient activation of Rap1 by Epac1. We propose that Ran and RanBP2 anchor Epac1 to the nuclear pore, permitting cAMP signals to activate Rap1 at the nuclear envelope.

3.2 INTRODUCTION

For many members of the Ras GTPase superfamily, such as Ras and Rap1, guanine nucleotide exchange factors (GEFs) outnumber the small GTPases that they activate (Ehrhardt et al., 2002; Mitin et al., 2005). The abundance of GEFs permits activation of small GTPases through multiple independent upstream signals. In addition, the localizations of many GEFs can be regulated through specific protein interactions (Bos et al., 2007). This limits the activation of their cognate small GTPases to specific subcellular locations, ensuring more precise spatial control than can be provided by the localization of the small GTPases themselves.

Direct support for the spatial control of Rap1 activation comes from examining the Rap1 exchangers Epac1 and Epac2. Both Epac proteins contain homologous regulatory and catalytic regions. Direct binding of cAMP to each regulatory region triggers a conformational change that allows its respective catalytic region to bind to and activate Rap. The catalytic regions of both Epac1 and Epac2 comprise of a Ras exchanger motif (REM) domain and a CDC25 homology domain that confers GEF activity specifically towards Rap proteins. For Epac2, the REM and CDC25 domains are interrupted by a Ras-association (RA) domain that interacts with activated, GTP-loaded Ras (Ras-GTP) at an affinity similar to those of the classical Ras-GTP effectors such as Raf-1 and B-Raf (Liu et al., 2008). Because the location of Ras and Rap can overlap at the plasma membrane, the recruitment of Epac2 to Ras brings it into proximity with a pool of Rap1 at this locale (Li et al., 2006). This compartmentalization allows Epac2 to activate Rap1 at the PM efficiently in the presence of cAMP.

In contrast, the region between the REM and CDC25 domains in Epac1 contains a putative RA domain for which no binding partner has been identified. Unlike Epac2, Epac1 is predominantly localized to the perinulcear region instead of the PM in multiple cell lines (Dodge-Kafka et al., 2005; Magiera et al., 2004; Qiao et al., 2002; Wang et al., 2006). Recent evidence suggests that Epac1 may function in nuclear processes, such as the nuclear transport of DNA-dependent protein kinase (DNA-PK) (Huston et al., 2008). However, the mechanism for the spatial regulation of Epac1-Rap1 signaling in this subcellular location is unknown. In this study, we identify a novel mechanism underlying the anchored signaling of Epac1 at the nuclear pore via its putative RA domain, and report for the first time the coupling of Rap1 and the nuclear small GTPase Ran at the nuclear envelope (NE).

3.3 MATERIALS AND METHODS

Plasmids.

Human Epac1 was a gift from Johannes Bos, Utrecht University. HA-tagged wild type Ran and RanV19 were gifts from Ian Macara, University of Virginia. Histone2B-mCherry was obtained from Addgene (Cambridge, MA). GFP-Epac1, Epac2, flag-Rap1B and mCherry-RasV12 was described previously (Liu et al., 2008; Wang et al., 2006). Epac1RA2 was constructed by inserting a PCR product for 559-720 aa of Epac2 (corresponding to the Epac2 RA domain) between the sequences for aa 423 and 586 of Epac1, and subcloned into pcDNA3 (Invitrogen, Carlsbad, CA) and pGFP-C1 (Clontech, Mountain View, CA) vectors. GFP-Epac1Δ295 was constructed by subcloning the PCR product for 295-881 aa of Epac1 into pGFP-C1. GFP-Epac1Δ673 was constructed by digestion using existing *Bgl*II and *Pst*I sites in GFP-Epac1Δ295 and ligation of the blunted ends. GFP-Epac1Δ295RA2 was constructed by subcloning the PCR product for the 295-881 aa of Epac1RA2 into pGFP-C1. GFP-RanV19-Epac1RA2 was constructed by in-frame insertion of PCR product of the RanV19 cDNA between *Hind*III and *EcoR*I sites in the GFP-Epac1RA2 vector. All contructs were sequenced and confirmed for the correct insertions.

Antibodies.

Anti-Rap1A/B, anti-Ran, unconjugated and agarose-coupled anti-Flag (M2) were from Sigma-Aldrich (St. Louis, MO). Anti-green fluorescent protein (GFP) antiserum (rabbit) and anti-nuclear pore complex proteins (Mab414) were from Abcam (Cambridge, MA). Anti-Epac1 and anti-Ras (RAS10) were from Upstate Biotechnology. Anti-HA antibody was from Covance (Princeton, NJ). Anti-RanBP2 (N20), anti-Epac1 (H70), anti-FRS2

(M20), and anti-TrkA (763) were from Santa Cruz Biotechnology (Santa Cruz, CA). Anti-RanBP2 (rabbit) from Novus Biologicals (Littleton, CO) and anti-Epac1 (A5) (Santa Cruz) were also used when indicated in the figure legends. Secondary antibodies against mouse, rabbit and goat IgGs were from GE Healthcare.

Chemicals.

8-(4-chloro-phenylthio)-2'-O-methyladenosine-3',5'-cyclic monophosphate (referred to in the text and figures as 2OMe) was purchased from Biolog Life Sciences (Bremen, Germany). 3× Flag peptide, GDP, GTPγS, glutathione peptide, and glutathione-agarose beads were from Sigma-Aldrich (St. Louis, MO).

Cell culture and stable cell lines.

HEK293 cells were cultured in DMEM plus 10% FBS, penicillin-streptomycin, and L-glutamine at 37°C and 5% CO_2. Mel-24 cells were cultured in Eagle Minimum Essential Medium from ATCC (Manassas, VA) plus 10% FBS and penicillin-streptomycin at 37°C and 5% CO_2. Transient transfections were performed with Lipofectamine 2000 (Invitrogen, Carlsbad, CA) according to the manufacturer's instructions. For stable cell lines, HEK293 cells were transfected with flag-Epac1 or pcDNA3 vector and selected with 0.5 mg/ml G418 (Invitrogen) for 4 weeks.

Purification of Epac1-containing complex and mass spectrometry.

Approximately 10^7 HEK293-flag-Epac1 cells or control cells were lysed in lysis buffer (10% glycerol, 1% NP40, 50mM Tris-HCl pH 7.4, 200mM NaCl, 2mM $MgCl_2$, 0.5mM β -glycerolphosphate) supplemented with 1 µM leupeptin, 10 µg/ml soybean trypsin inhibitor, 0.1 µM aprotinin, 1 mM sodium orthovanadate. Clear lysates were incubated

with conjugated anti-Flag (M2) antibodies at 4°C for 4 h. The beads were washed three times in lysis buffer and bound proteins were eluted at room temperature in 0.1 ml of TBS (50 mM Tris-HCl, pH 7.4, 150 mM NaCl) containing 100μg/ml of 3× flag peptides. Eluted proteins were supplemented with 6× lamaeli buffer and resolved on an SDS gradient PAGE gel (5-17%) (Invitrogen) for imperial blue staining (Thermo Scientific, Rockford, IL). Unique bands from the lane for the HEK293-flag-Epac1 cells and the corresponding parts in the control lane were excised and subjected to In-Gel trypsin digestion. Extracted peptides were analyzed using ThermoFinnigan LTQ mass spectrometer. All MS/MS samples were analyzed using Sequest (ThermoFinnigan, San Jose, CA; version 27, rev. 12), which was set up to search a database (C:\Xcalibur\database\UNIPROT\sprot_human_56_2.fasta) assuming the digestion enzyme trypsin. Scaffold (2.02.01, Proteome Software Inc., Portland, OR) was used to validate MS/MS based peptide and protein identifications. Peptide identifications were accepted if they could be established at greater than 90.0% probability as specified by the Peptide Prophet algorithm (Keller et al., 2002). Protein identifications were accepted if they contained at least 2 identified peptides and could be established at greater than 99.0% probability, which were assigned by the Protein Prophet algorithm (Nesvizhskii et al., 2003).

Immunoprecipitation (IP) and western blotting.

Cells in 6cm plates were lysed at 18-24 h after transfection in lysis buffer and equal amounts of clear cell lysate were subjected to IP using antibodies as indicated in the figure legends. For IP of the endogenous proteins, lysates from two confluent 15cm plates were used for each condition. Lysates were incubated with indicated antibodies

overnight, and then incubated for 2 h with protein A beads (Invitrogen) blocked with 1% BSA. For controls, IP was performed with unrelated purified IgG from the same species [anti-TrkA (rabbit IgG) for Epac1 IP (H70, rabbit) and anti-FRS2 (goat IgG) for RanBP2 IP (goat)]. Beads were washed twice in lysis buffer and once in high-salt lysis buffer with NaCl at 300mM. Bound proteins were eluted with 2×Laemmli buffer and detected by immunoblotting with antibodies as indicated in the figure legends.

Protein purification.

GST-Epac1 was expressed and purified using the method described previously for GST-Epac2Δ430 (Liu et al., 2008). pQE-Ran was transformed into M15[pREP4] *E.coli* strain (Qiagen). 10ml overnight culture was used to inoculate 200ml of LB. His-Ran expression was induced by 1mM isopropyl-β-D-thiogalactopyranoside (IPTG) at 37°C for 4 hours after the cell density reached OD600 of 0.6. The cell pellet was resuspended in 20ml lysis buffer (50mM NaH_2PO_4, 300mM NaCl, 10mM imidazole pH8.0) supplemented with phenylmethanesulfonyl fluoride (PMSF) and β-mercaptoethanol and lysed with a French press. The lysate was cleared by centrifugation and the supernatant was incubated with 0.5 ml Ni-NTA for 1 h at 4°C. The beads were washed twice with 15 ml wash buffer (50mM NaH_2PO_4, 300mM NaCl, 20mM imidazole pH8.0). His-Ran was eluted five times with 0.5 ml of elution buffer (50mM NaH_2PO_4, 300mM NaCl, 250mM imidazole pH8.0).

GST pull-down assay.

His-Ran was preloaded with 0.1mM GTPγS or 1mM GDP in 200μl of lysis buffer supplemented with 10mM EDTA at 30°C for 30 min. The reaction was stopped by $MgCl_2$ at 10mM. 0.5ug GST alone or GST-Epac1 was added to increasing amount of

loaded His-Ran and incubated with 20µl of GST agarose beads (50% slurry) for 3 h at 4°C. The beads were washed three times with lysis buffer, boiled in 1×SDS loading dye and subjected to Western Blot.

Rap1 activation assay and quantification.

GTP-bound Rap1 was assayed with the GST-tagged RBD of RalGDS as described previously (Franke et al., 1997). The intensities of the bands from Western blot were quantified with Scion Image (Scion Corp., Frederick, MD). The intensities of Rap1-GTP were normalized to those of total Rap1. All of the experiments were repeated at least three times, and the data from each experiment were expressed as percent of maximum.

Confocal imaging and quantification.

For live-imaging, cells were plated on coverslips coated with poly-D-lysine, transfected on the same day and used for imaging 12-16hr later. The coverslips were clamped into a heated imaging chamber (Warner Instruments, Hamden CT). All imaging experiments were performed with a Yokogawa CSU-10 Nipkow disk confocal scanning unit (Solamere Technology Group, Salt Lake City, UT) mounted on a Nikon TE2000 PFS microscope with continuous focus compensation. A Spectrum 70C Krypton Argon laser (Coherent, Santa Clara, CA) was used for excitation, with laser line selection via an acousto-optic tunable filter (Neos Technologies, Melbourne, FL), paired with fast emission filter switching (Applied Scientific Instrumentation Inc, Eugene, OR). The objectives used were a PlanApo 60×1.45NA or a 100×1.49NA, heated to physiological temperature with appropriate heater bands (Bioptechs, Butler, PA). Device integration was controlled through MetaMorph (Molecular Devices, Downingtown, PA). Timelapse images (500 ms exposures) were captured on an Orca ER CCD camera (Hamamatsu,

Bridgewater, NJ) over the period of time indicated in figure legend. Acquired images were quantified using ImageJ 1.41o (NIH, USA). For the fluorescent intensity of the perinuclear rim, the NE was traced using segmented line of a width of 5 pixels, and the mean gray values along the tracing was recorded (R_0). This measurement took into consideration both the intensities of individual punctum and the frequency of their presence along the NE. The fluorescent intensities of the cytoplasm (C_0) and nucleus (N_0) were also recorded as the mean gray values of representative regions within the two compartments. The gray value from the background was designated as B_0. To quantify the enrichment of Epac1 at the nuclear pore over the cytoplasm, over 50 cells with a wide range of expression levels of GFP-Epac1 were quantified and the absolute rim intensities (R_0-B_0) were plotted against the absolute intensities of the cytoplasm (C_0-B_0). Linear regression was performed for cells with (C_0-B_0) lower than 40 gray values, and the slope ($R= (R_0-B_0) / (C_0-B_0)$) was a constant that reflected the enrichment of GFP-Epac1 at the nuclear pore versus the cytoplasm (Figure 3.2). This parameter (R) was also used to compare the relative enrichment of Epac1 wild type and its mutants at the nuclear pore in Figure 3.4E. Relative distribution of various constructs within the nucleus were quantified using the ratio of $N=(N_0-B_0) / (C_0-B_0)$. For each construct, 30-40 random cells were measured and experiments were repeated 2-4 times using cells of different passages on different days. For the percentage of cells showing enrichment of GFP-RBD_{RalGDS} at the NE (Figure 3.8), cells from at least 30 random fields were scored by person unaware of the transfection conditions, and four experiments were performed and quantified.

Immunofluorescent staining.

MEL-24 cells were grown on poly-D-lysine coated coverslips, fixed in 4% paraformaldehyde for 15 min, and permeablized in 0.2% Triton-X 100 for 10 min. Cells were incubated with 1% BSA in PBS-Tween® (0.1%, USB, Cleveland, OH) buffer for 45 min and then with primary antibodies as indicated for overnight at 4°C. After extensive washing, cells were incubated with indicated secondary antibodies overnight at 4°C. Nuclei were stained with 0.1µg/ml Hoechst for 5 min. Coverslips were mounted with Elvanol (Polyvinyl Alcohol, 88-89%).

RNA interference.

Human Epac1 (RefSeq Number: NM_006105) were targeted using a cocktail of three siRNAs from Ambion Inc. (Austin, TX). The sense sequences were: 5'-CCGAGAUGCCCAAUUCUACtt-3', 5'-GGGAUCUGUCAACGUGGUGtt-3', 5'-GGGCACUUCGUGGUACAUUtt-3'. The scrambled or Epac1 siRNAs were transfected alone using Lipofectamine2000 (Invitrogen) at a final concentration of 100nM in a course of 3-4 days and then cotransfected with indicated plasmids overnight before live imaging.

Statistics.

Prism 3 (GraphPad Software, La Jolla, CA) were used for data plotting and analysis. Unpaired t-tests were performed between groups as indicated, and $p < 0.05$ was regarded as statistically significant.

3.4 RESULTS

3.4.1 Isolation of proteins associated with Epac1.

Using HEK293 cell lines stably transfected with flag-Epac1, or vector alone as a control, we isolated the proteins that associated with Epac1 using affinity purification. Analysis of the complex by mass spectrometry identified five proteins as potential Epac1 binding partners (Table 3.1). Three of these proteins, Ran binding protein 2 (RanBP2 or Nup358), Nucleoporin 205 (Nup205) and 98 (Nup98), are structural components of the nuclear pore complex (NPC). RanBP2 has four Ran binding sites and forms a filamentous structure on the cytoplasmic side of the NPC (Fahrenkrog and Aebi, 2003; Yokoyama et al., 1995). The other two proteins, Importin β-1 and Ran, are well known for their roles in nuclear transport and can also bind to multiple nucleoporins (Rotem et al., 2009) to regulate the assembly and function of the NPC and NE (Moore, 1998). These results strongly suggest the presence of Epac1 within a protein complex at the nuclear pore.

3.4.2 Stable localization of Epac1 to the NPC.

Ran and RanBP2 were the two most represented proteins identified in our analysis after adjusting for their molecular weights. We first examined their ability to interact with Epac1 in HEK293 cells. RanBP2 and Ran were present within the immunoprecipitation (IP) of endogenous Epac1 (Figure 3.1A), and reciprocally, Epac1 and Ran were recovered within the endogenous RanBP2 IP (Figure 3.1B). Interestingly, overexpression of Epac1 increased the amount of Ran associated with RanBP2 (Figure 3.1C), suggesting that Epac1 may stabilize the interaction between Ran and RanBP2. Because RanBP2 preferentially binds to Ran-GTP (Wu et al., 1995; Yokoyama et al., 1995), Epac1 may actually stabilize Ran in its GTP-loaded form. Therefore, we examined whether Ran and

Epac1 interact in a GTP-dependent manner. In a GST pulldown assay *in vitro*, purified GST-Epac1 bound to GTPγS-loaded His-Ran in a dose-dependent manner, while GST-Epac1 interacted with GDP-loaded His-Ran poorly (Figure 3.1D), suggesting a direct role for Ran-GTP in linking Epac1 to RanBP2. To confirm the GTP-dependent binding of Ran to Epac1 *in vivo*, we used RanV19, a constantly GTP-loaded mutant, and RanN24, a constantly GDP-loaded mutant. RanV19 interacts with Epac1 stronger than RanN24, and neither bound to Epac2 (Figure 3.1E).

GFP-Epac1 formed a punctuate rim around the nucleus and colocalized with the staining with Mab414, an antibody recognizing the NPC (Figure 3.2A). In contrast, GFP-Epac2 was distributed diffusely in the cytoplasm and seldom overlapped with the NPC (Figure 3.2B). Importantly, staining of the endogenous Epac1 in melanoma derived Mel-24 cells, which expresses high levels of Epac1 (Baljinnyam et al., 2009), colocalized with Mab414 and overlapped with the pattern seen with GFP-Epac1, although additional staining was seen within the nucleus (Figure 3.2C). Imaging of GFP-Epac1 in living cells significantly improved the quality of acquired images (Figure 3.2D), probably because the NPC and the shape of the nucleus are better preserved under these conditions. We quantified the fluorescent intensity of GFP-Epac1 at the perinuclear rim, and found it to be three-fold of the intensity at the cytoplasm (See Methods and Figure 3.2E).

The perinuclear localization of GFP-Epac1 remained largely unchanged after treatment with the Epac-specific agonist 8-pCPT-2'-O-Me-cAMP (2OMe) (Figure 3.2F). Translocation of GFP-Epac1 from cytoplasm to the PM in response to 2OMe was detected in cells expressing higher levels of GFP-Epac1, consistent with a recent study (Ponsioen et al., 2009).

3.4.3 Role of RA domain in Ran-Epac1 association.

Epac1 and Epac2 are each composed of a regulatory region and a catalytic region depicted in Figure 3.3A. To determine the domains of Epac1 that bind to Ran, we constructed a series of truncations of Epac1 (Figure 3.3A). Deletion of the regulatory region of Epac1 (residues 1-295) did not affect the interaction between Epac1Δ295 and RanV19. Further deletion of residues 296-673, including the putative RA domain of Epac1 (RA1), disrupted the binding between Epac1Δ673 and RanV19, suggesting a potential Ran binding site within this region (Figure 3.3B).

To examine whether Ran interacted with the RA1 domain, we generated a chimera (Epac1RA2) by swapping the RA1 domain for the analogous RA domain from Epac2 (RA2) as shown in Figure 3.3A. Because the overall conformation should be preserved in Epac1RA2, any impaired binding of this mutant could be attributed to the loss of RA1 domain. GFP-Epac1RA2 lost the ability to interact with endogenous Ran (Figure 3.3C), but acquired the ability to bind to RasV12, a constitutively GTP-loaded mutant (Figure 3.3D). However, when expressed alone, the RA1 domain was unable to bind to Ran (Figure 3.3E), suggesting that the regions flanking the RA1 domain were needed to stabilize RA1-Ran binding.

To determine whether the Epac1 RA domain participates in the localization of Epac1, we compared the distribution of GFP-Epac1 and GFP-Epac1RA2. The fluorescent intensity of GFP-Epac1RA2 on the perinuclear rim was significantly reduced compared to GFP-Epac1 (Figures 3.4A, B and E). In addition, Epac1RA2 was excluded from the nucleus while its distribution at the cytoplasm was preserved. Since Ran-GTP is found both at the NPC and within the nucleus, the loss of Ran binding could explain the

reduction of Epac1RA2 at both locations. Interestingly, GFP-Epac1Δ295 exhibited decreased fluorescence at the nuclear rim as well (Figures 3.4C and E), suggesting that the regulatory region also contributes to the localization of Epac1, perhaps by interacting with RanBP2 directly or with other proteins within the NPC. This might account for the residual level of GFP-Epac1RA2 seen at the nuclear pore. Indeed, the mutant lacking both the regulatory region and RA1 (GFP-Epac1Δ295RA2) was neither detected at the nuclear pore, nor detected within the nucleus (Figures 3.4D and E). Collectively, the data show that the RA1 domain targets Epac1 within the nucleus and cooperates with the regulatory region to enrich Epac1 at the NPC.

3.4.4 Ran-Epac1 interaction is crucial for Epac1 mediated Rap1 activation.

The anchoring of Epac1 to the NPC may activate a specific pool of Rap1. Indeed, the cAMP-dependent activation of Rap1 via Epac1 was significantly stronger than that seen with Epac1RA2 (Figure 3.5A). The loss of Rap1 activation by Epac1RA2 was not due to structural defect caused by swapping RA domains *per se*, because Epac1RA2 could be fully activated in the presence of RasV12 (Figure 3.5A). This is comparable to the enhancement of Epac2-dependent Rap1 activation by RasV12 (Liu et al., 2008) and may reflect the ability of RA2 to target Epac1RA2 to the PM. Similar results were seen using Epac1Δ295. This truncation lacks the regulatory region, making it constitutively active. Therefore, although the localization of Epac1Δ295 at the NPC was reduced (Figure 3.4C), it could still activate Rap1 robustly (Figure 3.5B). Like Epac1RA2, Epac1Δ295RA2 was incapable of activating Rap1, which could be rescued following expression of RasV12 (Figure 3.5B). These results suggest that Ran-Epac1 interaction is necessary for efficient Rap1 activation by Epac1.

To test whether the lack of Rap1 activation by Epac1RA2 was due to loss of localization at the NPC, we artificially tethered Epac1RA2 to the NPC by attaching it to RanV19. RanV19 is constitutively loaded with GTP, and has been shown to interact with RanBP2 and localize to the NPC (Lounsbury et al., 1996) (Figure 3.5C). Using this fusion protein depicted in Figure 3.5D (Hutchins et al., 2009) and we can test whether the fused RanV19 is sufficient to restore the localization of Epac1RA2 as well as the downstream Rap1 activation. As expected, GFP-RanV19-Epac1RA2 was highly enriched at the nuclear pore (Figure 3.5C). Importantly, its ability to activate Rap1 was also significantly enhanced compared to Epac1RA2 (Figure 3.5E). These data support a model that localization of Epac1 to the nuclear pore enhances activation of Rap1 by Epac1.

3.4.5 Epac1 activates Rap1 on the nuclear envelope.

Activation of endogenous Rap1 can be directly visualized in cells using a Ras binding domain from RalGDS linked to GFP (hereafter called GFP-RBD_{RalGDS}) (Bivona and Philips, 2005). In cells expressing mCherry-Epac1 and treated with 2OMe, GFP-RBD_{RalGDS} decreased within the cytoplasm and nucleus, while increased at the NE and PM (Figure 3.6A). However, we were unable to see these changes in the absence of transfected Epac1, possibly because the level of endogenous Epac1 and Rap1 were too low to redirect GFP-RBD_{RalGDS} upon 2OMe stimulation (Figure 3.6A and see Appendix 3 for detailed explanation).

Enrichment of GFP-RBD_{RalGDS} at the NE was also seen upon transfection of mCherry-Epac1Δ295 but not mCherry-Epac1Δ295RA2 (Figure 3.6B, ii and iii, left panels). This correlated with the presence of Epac1Δ295 and absence of Epac1Δ295RA2

at the NPC, respectively (Figure 3.6B, ii and iii, middle panels). Together, these results strengthen a role for RA1 in promoting Rap1 activation at the NE. Epac1Δ295RA2 could be redirected to the NPC by the addition of RanV19 at the N-terminus (mCherry-RanV19-Epac1Δ295RA2) (Figure 3.6B, iv, middle panel). Importantly, mCherry-RanV19-Epac1Δ295RA2 restored the pattern of GFP-RBD_{RalGDS} on the NE (Figure 3.6B, iv, left panel). We noted that although Epac1Δ295 is not present at the PM (Ponsioen et al., 2009), it enriched GFP-RBD_{RalGDS} at the PM. This might reflect the trafficking of Rap1 to the PM after its activation (Bivona et al., 2004).

We detected Rap1 on the NE and PM using a GFP-tagged isoform, Rap1B (Figure 3.7A). This pattern is consistent with its localization in COS-1, MDCK and Jurkat T cells (Bivona et al., 2004). GFP-Rap2B, a Rap2 isoform, was not seen on the NE (Figure 3.7A), even though it has a known role in Epac1-dependent nuclear export of DNA-PK (Huston et al., 2008). The C-terminus of Rap2B was more similar to that of H-Ras, which, like Rap2B, was targeted to the PM but not the NE (Figure 3.7A).

Because the GFP-RBD_{RalGDS} reporter does not discriminate between Rap isoforms activation of selected Rap isoforms must be evaluated using GFP-RBD_{RalGDS} only following transfection of each isoform (Bivona and Philips, 2005). Ectopic expression of Rap isoforms may also favor the detection of low levels of GEF activity under basal conditions. Indeed, following transfection, Rap1B and Rap2B appeared to be activated at the NE and PM respectively in the absence of 2OMe (Figure 3.7B). For Rap1B, the enrichment of GFP-RBD_{RalGDS} at the NE was GTP-dependent, as this pattern was reproduced with Rap1B-V12, which was constitutively GTP-loaded, but not by Rap1B-N17, which was constitutively GDP-loaded (Figure 3.7C). Importantly, the signal of

GFP-RBD_{RalGDS} on the NE in the presence of wild type Rap1B was completely abolished by RapGAP (Figure 3.7D), confirming that the distribution of GFP-RBD_{RalGDS} on the NE reflected Rap1B activation.

To ask whether endogenous Epac1 could be responsible for the activation of Rap1B at the NE, we utilized siRNA and reduced the level of Epac1 by 75% (Figure 3.8A). In cells cotransfected with scrambled siRNA, 79% of the cells had enrichment of GFP-RBD_{RalGDS} on the NE in the presence of mCherry-Rap1B, whereas in cells cotransfected with Epac1 siRNA, 41% of the cells with mCherry-Rap1B showed enrichment of GFP-RBD_{RalGDS} on the NE (Figs. 8B and C). The relatively modest reduction might reflect either incomplete depletion of endogenous Epac1 by siRNA or the presence of other Rap exchangers at the NE. However, the data confirm that endogenous Epac1 contributes to the activation of Rap1B at the NE.

3.5 DISCUSSION

The perinuclear localization of Epac1 has been reported previously (Dodge-Kafka et al., 2005; Magiera et al., 2004; Qiao et al., 2002; Wang et al., 2006), but a mechanism for the anchoring of Epac1 to this location has not been established. A detailed understanding of the anchoring mechanism for Epac1 will not only further the microscopic observation made previously, but also provide insight into how Epac1 functions in the cell. Binding of Epac1 to the A-kinase anchoring protein mAKAP has been proposed to localize Epac1 to the perinuclear region in cardiomyocytes (Dodge-Kafka et al., 2005). However, this localization of Epac1 is also seen in cells that do not express mAKAP, so another mechanism must exist in non-cardiac cells. Here, using a proteomic approach, we have identified five potential binding partners that are localized to the nuclear pore complex and expressed in all cells: RanBP2, Nup205, Nup98, Importin β-1 and Ran. Among these proteins, Ran and RanBP2 were the most represented in this screen. We confirmed that endogenous Epac1 could be co-immunoprecipitated with endogenous RanBP2 and Ran. The binding of Epac1 to Ran is GTP-dependent and requires the Ras association (RA1) domain. This is the first characterization of a binding partner for this putative RA1 domain.

RanBP2 has four binding domains for GTP-bound Ran. It is possible that Epac1 binds to Ran-GTP directly and associates with RanBP2 as a consequence of binding to Ran. Two lines of evidence support this model that Ran-GTP binds both Epac1 and RanBP2 in a single complex. One, the expression of Epac1 can increase the level of Ran bound to RanBP2. Two, the optimal localization of Epac1 to the nuclear pore requires the RA1 domain, and this is decreased when this domain is replaced with the RA domain of

Epac2 (Epac1RA2). Because a low level of binding of GFP-Epac1RA2 can be detected at the nuclear pore, it is possible that direct interactions between Epac1 and RanBP2 or other components of the NPC may also participate in this targeting of Epac1 (Figure 3.8D). For example, Importin-β1 was also identified as a binding partner for Epac1. Importin-β1 can bind to multiple nucleoporins including RanBP2, as well as Ran (Clarke and Zhang, 2004; Delphin et al., 1997; Harel and Forbes, 2004; Vetter et al., 1999). Therefore, its association with Epac1 could be indirect. Whether Epac1 is a cargo for Importin-β is not known.

The association of Epac1 with Ran and RanBP2 represents a new mechanism of targeting proteins to the nuclear pore. Ran is efficiently GTP-loaded within the nucleus through action of the Ran exchanger RCC1, which is exclusively nuclear (Nemergut and Macara, 2000). This asymmetry sets up the Ran gradient that drives nuclear trafficking (Macara, 2001). The interaction between Ran-GTP and RanBP2 is known to facilitate the inactivation of Ran by RanGAP, which also binds to RanBP2 (Mahajan et al., 1997). We propose that the stabilization of the association between Ran and RanBP2 by Epac1 reflects the ability of Epac1 to protect Ran-GTP from inactivation by RanGAP. It is not known whether this ability of Epac1 to prolong the association of Ran-GTP with RanBP2 affects Ran-mediated nuclear transport.

The use of GFP-RBD_{RalGDS} as a reporter for Rap activation is well-suited for identifying large pools of Rap-GTP activated by overexpressed GEFs or constitutively active mutants of Rap itself (Bivona and Philips, 2005). This reporter does not discriminate between Rap isoforms, and cotransfection of specific Rap isoforms is required for the examination of isoform-specific activation. Following transfection of

Rap1, we showed that GFP-RalGDS identified a pool of Rap1 at the nuclear envelope that was activated by endogenous Epac1.

It is possible that a portion of the Rap1-GTP that is activated at the nuclear envelope may translocate to other compartments including the PM. Although a recent study showed that Epac1 itself could translocate to the PM upon cAMP stimulation to activate Rap1 and affect cell adhesion, this action requires an intact DEP domain (Ponsioen et al., 2009). The constitutively active truncation of Epac1 used in our study lacks the DEP domain. It is located at the nuclear pore and is incapable of translocating to the PM. Although this mutant predominantly increased the levels of Rap1-GTP detected on the nuclear envelope, it also increased the levels of Rap-GTP detected at the PM. This is consistent with the possibility that Rap1-GTP can translocate to the PM following its activation on the nuclear envelope. Whether this pool of translocated Rap1-GTP behaves similarly to Rap1 directly activated at the PM is not known. In addition, Epac1 was seen within the nucleus and the RA domain of Epac1 was critical for this localization. Ran and RanBP2 have important functions at the chromosome and the mitotic spindle (Chen et al., 2007; Hao and Macara, 2008; Hutchins et al., 2009) and it is possible that a similar complex with Epac1 occurs there as well.

The function of the pool of Rap1 at the nuclear envelope needs further study. Only one previous report linked Rap signaling to the trafficking of nuclear proteins examined the trafficking of DNA-dependent protein kinase (DNA-PK), which requires Rap2, but not Rap1 (Huston et al., 2008). It is possible that Rap1 affects the nuclear/cytoplasmic trafficking of other proteins. Alternatively, Rap1 could activate signaling cascades to affect nuclear transport in general. One established effector of Rap1

is B-Raf, a kinase upstream of the ERK signaling cascade (Kao et al., 2001; Ohtsuka et al., 1996; Stork, 2003). The possibility that Epac1 could activate a localized B-Raf/ERK signaling cascade is particularly attractive since ERK phosphorylation of nucleoporins has recently been shown to regulate Ran-dependent transport (Kosako et al., 2009).

Our study identifies fundamental differences between the RA domains of Epac1 and Epac2. We propose that these RA domains have distinct effects on the ability of Epac1 and Epac2 to activate different pools of Rap1. Epac2 is a *bone fide* Ras effector, acting as a coincidence detector for Ras-dependent signaling and cAMP (Li et al., 2006; Liu et al., 2008). This is because Epac2 requires proper targeting to Ras-GTP via its Ras association domain (RA2) for efficient Rap1 activation. In contrast, Epac1 is not able to bind Ras-GTP and does not require recruitment to Ras to activate Rap1. Instead, Epac1 requires targeting to the nuclear pore for efficient Rap1 activation. In our previous study, we demonstrated the requirement of Ras in the Epac2 dependent activation of Rap1 by introducing a point mutation into its RA domain, which abolished the Ras binding without affecting the catalytic function of Epac2 (Liu et al., 2008). This mutation caused a charge reversal within the RA domain by changing a lysine to glutamate. Epac1 contains a glutamate at this position (Li et al., 2006), explaining the inability of Epac1 to bind to Ras-GTP.

Although we did not identify a specific point mutation in Epac1 able to block Ran binding, we selectively interfered with Ran binding by swapping the RA domain of Epac1 for that of Epac2. This chimera (Epac1RA2) showed a dramatically reduced level of Rap1 activation that was not due to a loss of catalytic function *per se*, as the activity of this chimera could be restored by targeting it to Ras-GTP via the chimeric RA2 domain.

The decreased Rap1 activation induced by Epac1RA2 correlated well with the decreased localization of Epac1RA2 to the nuclear pore, and it could be rescued by redirecting the chimera to the nuclear pore by linking Epac1RA2 to the RanV19. These results and our previous studies of Epac2 suggest that the differential localizations of Epac1 and Epac2 are dictated by their unique RA domains, and are necessary for their ability to activate different pools of Rap1 efficiently in cells.

The ability of one class of small G proteins to signal to other classes of small G proteins promotes crosstalk and integration among signaling pathways (Mitin et al., 2005). The presence of both an RA domain and CDC25 homology domain within a single GEF protein provides one such mechanism. For example, the GEFs Tiam1, Ral-GDS, and PLCε each contain an RA domain that recruits that GEF to a specific activated small G protein, and a CDC25 homology domain that promotes the GTP loading of another small G protein (Mitin et al., 2005). The coupling of Ras to Rap1 by Epac2 (Li et al., 2006; Liu et al., 2008), and the coupling of Ran to Rap1 by Epac1 also fit into this general mode of signaling. These targeting mechanisms highlight the importance of RA domains of diverse GEFs in coupling small G proteins to each other. While many of the previous examples of RA domains have identified the coupling of small G proteins within the Ras family, this study showing the connection between Ran and Rap1 via Epac1 represents the first example of the regulation of a member of the Ras family by the small G protein Ran.

In conclusion, our study has identified a novel role of Ran to anchor Epac1 at the nuclear pore and has characterized NE as a novel intracellular site of Rap1 activation (Figure 3.8D). This anchoring of Epac1 is mediated largely by its RA domain and is

required for the efficient activation of Rap1 by Epac1. Due to this unique localization of Epac1, we propose that Epac1 functions as a cAMP sensor at the nuclear pore, which converts local cAMP elevations into Rap1 activation on the NE. The discovery of Epac1-dependent activation of Rap1 at the NE is likely to reveal a potential role of cAMP and Rap1 in nuclear transport through the nuclear pore and the assembly and functioning of the NE.

3.6 ACKNOWLEDGMENTS

The authors thank Zhiping Wang, Mike Forte, Mihail Iordanov, and Larry David for discussion, John Klimek, Debra McMillen and Srilatha Tavisala for technical assistance, Ian Macara and Johannes Bos for sharing of reagents. This work was funded by NIH NCI grant number CA72971 to Philip Stork, Vertex Scholarship to Chang Liu and training grant NIH-5-T32-CA106195-06A1 to Yanping Li.

Table 3.1

Mass spectrometry analysis of the protein complex in association with Epac1

Identified proteins	MW (kDa)	Number of Assigned Spectra (pcDNA3 cells / flag-Epac1 cells)
RanBP2	358	0/125
Nup205	228	0/5
Nup98	98	0/2
Epac1	104	0/261
Importinβ-1	97	0/20
Ran	24	0/11

MW, molecular weight; kDa, kilodalton. See Methods section for details.

Figure 3.1 Association of Epac1 with Ran and RanBP2.

(A) Co-immunoprecipitation (IP) of endogenous Epac1 with Ran and RanBP2 in HEK293 cells. Cell lysates were subjected to IP using anti-Epac1 (H70), and unrelated IgG from rabbit as a control. Western blotting was performed using anti-RanBP2 (Novus), anti-Epac1 (H70) and anti-Ran antibodies. TCL, total cell lysate.

(B) Co-IP of endogenous RanBP2 with Epac1 and Ran in HEK293 cells. Cell lysates were subjected to IP using RanBP2 antibody (goat) and unrelated IgG from goat as a control. The presence of Ran and Epac1 within the IP was analyzed by western blot using anti-RanBP2 (Novus), anti-Epac1 (A5) and anti-Ran.

(C) Effect of Epac1 overexpression on the association of RanBP2 and Ran. RanBP2 IP was performed as in (B) in the presence (+) or absence (-) of flag-Epac1 (E1), and the presence of Ran, RanBP2 and flag-Epac1 within IP and TCL was determined by western blot. Left panel shows one representative result; right panel shows quantification of three experiments normalized to the level of Ran seen in RanBP2 IP in the absence of transfected Epac1 (mean±SEM, * $p<0.05$).

(D) GTP-dependent interaction between Epac1 and Ran *in vitro*. Increasing amounts of His-Ran loaded with GTPγS or GDP were incubated with GST or GST-Epac1, and detected by western blot using anti-Ran. LE and HE, low and high exposures. GST and GST-Epac1 levels were shown with Coomassie blue.

(E) Association of Ran with Epac1 but not Epac2. HA-RanV19 or HA-RanN24 was coexpressed with flag-tagged Epac1 or Epac2 in HEK293 cells. IP was performed using

anti-HA, and western blotting was performed using anti-flag and anti-HA. Shown data are representative of at least three independent experiments.

Figure 3.1

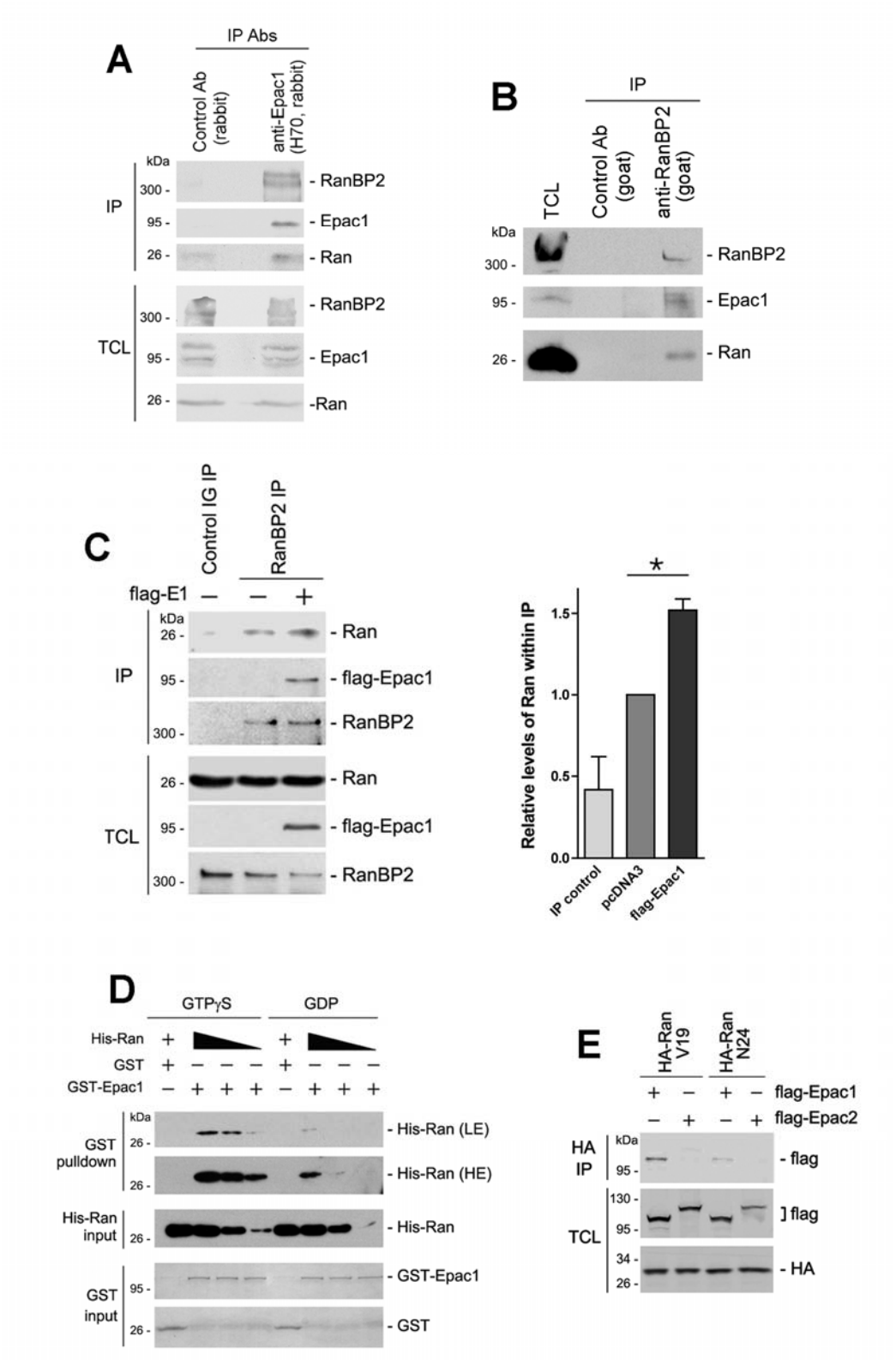
A
IP Abs
Control Ab (rabbit)
anti-Epac1 (H70, rabbit)
kDa
IP
300 -
95 -
26 -
- RanBP2
- Epac1
- Ran
TCL
300 -
95 -
26 -
- RanBP2
- Epac1
-Ran
B
IP
TCL
Control Ab (goat)
anti-RanBP2 (goat)
kDa
300 -
95 -
26 -
- RanBP2
- Epac1
- Ran
C
Control IG IP
RanBP2 IP
flag-E1 – – +
kDa
IP
26 -
95 -
300 -
- Ran
- flag-Epac1
- RanBP2
TCL
26 -
95 -
300 -
- Ran
- flag-Epac1
- RanBP2
*
Relative levels of Ran within IP
1.5
1.0
0.5
0.0
IP control
pcDNA3
flag-Epac1
D
GTPγS
GDP
His-Ran + + + +
GST + – – – + – – –
GST-Epac1 – + + + – + + +
kDa
GST pulldown
26 -
26 -
- His-Ran (LE)
- His-Ran (HE)
His-Ran input
26 -
- His-Ran
GST input
95 -
26 -
- GST-Epac1
- GST
E
HA-Ran V19
HA-Ran N24
+ – + – flag-Epac1
– + – + flag-Epac2
kDa
HA IP
95 -
- flag
TCL
130 -
95 -
] flag
34 -
26 -
- HA

Figure 3.2 Colocalization of Epac1 with the nuclear pore complex (NPC).

(A) GFP-Epac1 colocalizes with the NPC. HEK293 cells were transfected with GFP-Epac1 (left, green) and stained with Mab414 primary and Texas Red secondary antibodies (middle, red) followed by confocal microscopy. Right panel, merged image. Scale bars in A-D and F of this figure represent 10μm.

(B) GFP-Epac2 does not colocalize with the NPC. HEK293 cells were transfected with GFP-Epac2, treated, and presented as in (A).

(C) Colocalization of endogenous Epac1 with the NPC. MEL-24 cells were stained with anti-Epac1 primary antibody and Texas Red-coupled secondary antibody (left panel), and Mab414 primary antibody and FITC-coupled secondary antibody (middle panel). Right panel, merged image.

(D) Localization of GFP-Epac1 expressed in HEK293 cells by confocal live imaging. mCherry-Histone2B was cotransfected to visualize the nuclear chromatin.

(E) Quantification and correlation of the fluorescent intensities of GFP-Epac1 at the perinuclear rim (Y axis) and cytoplasm (X axis) in HEK293 cells over a low range of expression levels (see Methods for detail).

(F) Effect of 2OMe on Epac1 localization. HEK293 cells were transfected with GFP-Epac1, serum starved and treated with 2OMe during confocal live imaging. The two photos on the left show representative localizations of GFP-Epac1 before and after 2OMe treatment. The right panel shows quantification of the relative intensities of GFP-Epac1 at the perinuclear rim over time normalized to the intensities at 0 min. Gray lines, change of intensities in individual cells (n=9). Black line and error bars represent mean±SEM.

Figure 3.2

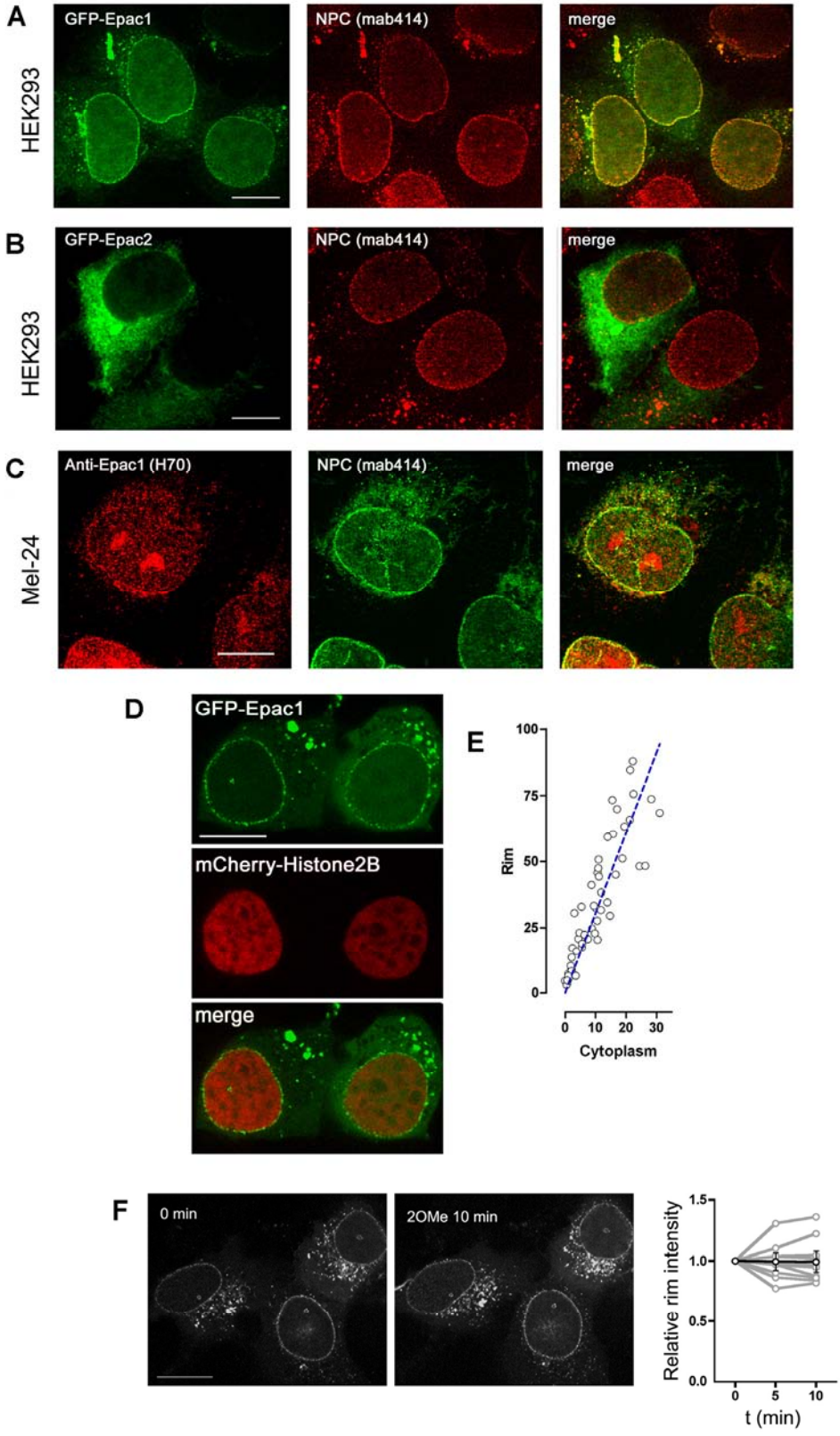
A
GFP-Epac1
NPC (mab414)
merge
HEK293
B
GFP-Epac2
NPC (mab414)
merge
HEK293
C
Anti-Epac1 (H70)
NPC (mab414)
merge
Mel-24
D
GFP-Epac1
mCherry-Histone2B
merge
E
Rim
Cytoplasm
100
75
50
25
0
0
10
20
30
F
0 min
2OMe 10 min
Relative rim intensity
1.5
1.0
0.5
0.0
0
5
10
t (min)

Figure 3.3 Role of RA domain in the association of Ran and Epac1.

(A) Domain structures of Epac1, Epac2 and mutants used in the study. cNBD, cyclic-nucleotide-binding domain; DEP, Dishevelled, Egl-10, Pleckstrin domain; REM, Ras exchange motif; RA, Ras association domain; CDC25-HD, CDC25-homology domain. Epac1 has one and Epac2 has two cNBDs.

(B) Loss of Ran association with Epac1Δ673. HA-RanV19 was coexpressed with GFP, or GFP tagged Epac1 (E1), E1Δ295 or E1Δ673 in HEK293 cells. IP was performed using anti-GFP, and western blot was performed using anti-GFP and anti-HA.

(C) Requirement of the RA domain of Epac1 for Ran-Epac1 association. GFP, GFP-tagged Epac1, and Epac1RA2 (E1RA2) were expressed in HEK293 cells. IP was performed using anti-GFP, and Western blot was performed using anti-Ran and anti-GFP.

(D) Interaction of E1RA2 and RasV12. pcDNA3, flag-Epac1 or E1RA2 were coexpressed with mCherry-RasV12 in HEK293 cells. IP was performed using anti-flag, and proteins detected by western blot using anti-Ras and anti-flag.

(E) Epac1 RA domain (RA1) requires additional sequences to bind RanV19. GFP, GFP-tagged Epac1 (E1) or RA1 domain alone was cotransfected with HA-RanV19 into HEK293 cells followed by IP with anti-GFP, and western blot using anti-HA and anti-GFP.

Figure 3.3

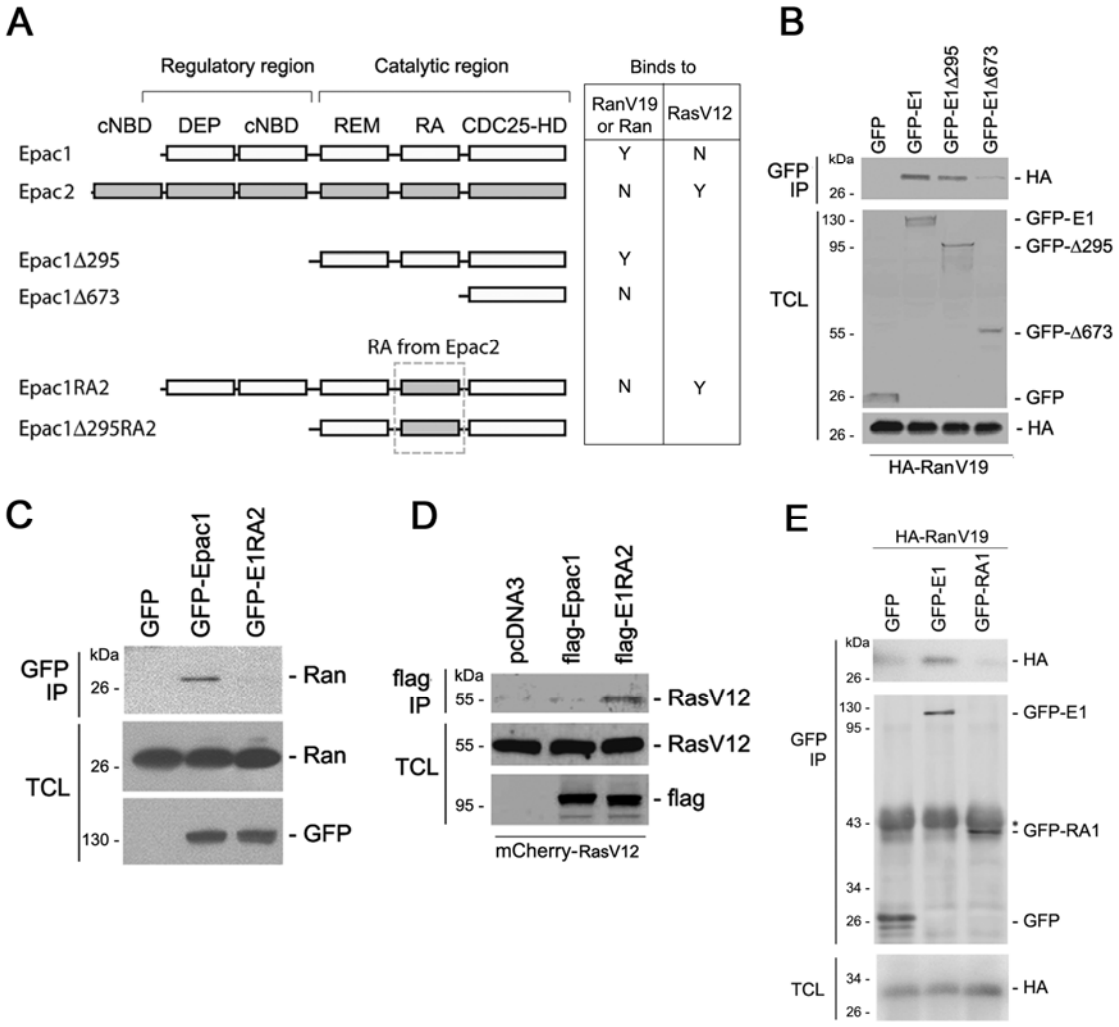
A
Regulatory region
Catalytic region
Binds to
RanV19 or Ran
RasV12
cNBD
DEP
cNBD
REM
RA
CDC25-HD
Epac1
Epac2
Epac1Δ295
Epac1Δ673
RA from Epac2
Epac1RA2
Epac1Δ295RA2
B
GFP
GFP-E1
GFP-E1Δ295
GFP-E1Δ673
GFP IP
kDa
- HA
- GFP-E1
- GFP-Δ295
- GFP-Δ673
TCL
- GFP
HA-RanV19
C
GFP
GFP-Epac1
GFP-E1RA2
GFP IP
- Ran
TCL
- Ran
- GFP
D
pcDNA3
flag-Epac1
flag-E1RA2
flag IP
- RasV12
TCL
- RasV12
- flag
mCherry-RasV12
E
HA-RanV19
GFP
GFP-E1
GFP-RA1
GFP IP
- HA
- GFP-E1
- GFP-RA1
- GFP
TCL
- HA

Figure 3.4 Role of RA1 domain and regulatory region in Epac1 localization.

(A-D) Localization of GFP-tagged Epac1, Epac1RA2, Epac1Δ295 and Epac1Δ295RA2 in HEK293 cells by confocal live imaging. Upper panels show representative distributions of the indicated constructs. Lower panels show the intensity profile across the lines in the photo. Y axis, raw fluorescence intensity; X axis, distance in pixel; dotted line, the levels of fluorescence intensity in the cytoplasm. Scale bar, 10μm.

(E) Quantification of the relative fluorescent intensities of GFP-tagged Epac1 and mutants at the perinuclear rim and within the nucleus (mean±SEM, * p<0.01). AU, artificial units. See Methods for detail.

Figure 3.4

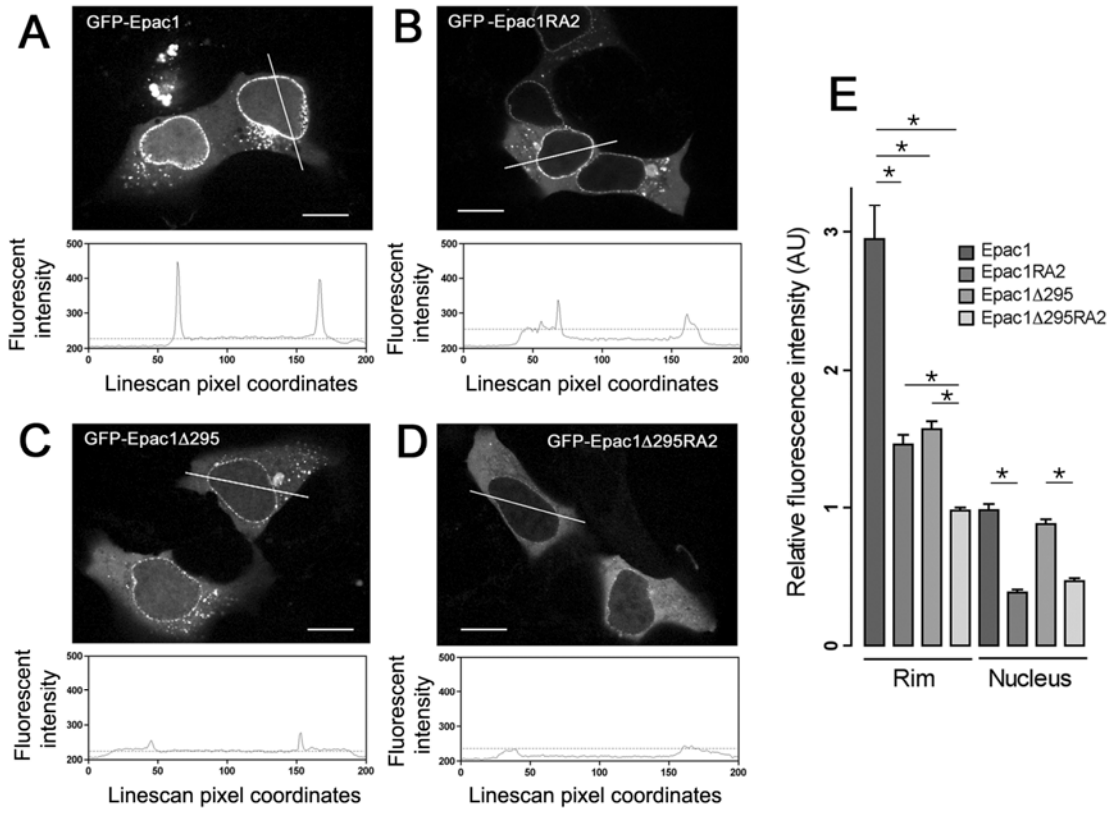
A
GFP-Epac1
B
GFP -Epac1RA2
C
GFP-Epac1Δ295
D
GFP-Epac1Δ295RA2
Fluorescent intensity
Linescan pixel coordinates
E
Relative fluorescence intensity (AU)
Epac1
Epac1RA2
Epac1Δ295
Epac1Δ295RA2
Rim
Nucleus

Figure 3.5 Requirement of the RA1 domain for efficient Rap1 activation via Epac1.

(A) Activation of endogenous Rap1 by Epac1 (E1) and Epac1RA2 (E1RA2). Flag-E1 and flag-E1RA2 were expressed in HEK293 cells in the absence or presence of mCherry-RasV12. Starved cells were treated with 2OMe for 15min or left untreated, and the lysates were assayed for Rap1 activation, as described in Methods. Transfected proteins were blotted with anti-flag and anti-Ras. The lower panel is the quantification of relative Rap1 activation from three independent experiments (mean±SEM, * $p<0.05$); ns, not significant.

(B) GFP-tagged E1Δ295 and E1Δ295RA2 were expressed in HEK293 cells in the absence or presence of mCherry-RasV12. Rap1 activation was assayed and presented as in (A).

(C) Comparison of the localization of mCherry-RanV19, GFP-E1RA2 and GFP-RanV19-E1RA2 in HEK293 cells by confocal live imaging. Representative images are shown in the upper panel. The lower panel is the quantification of relative fluorescence intensities of GFP-E1RA2 (light gray bar) and GFP-RanV19-E1RA2 (dark bar) at the perinuclear rim (Mean±SEM, * $p<0.01$). Scale bars, 10μm.

(D) Schematic of the GFP-RanV19-E1RA2 construct. The domains of Epac1 are listed as in Figure 3.3A. The RA domain of Epac2 (RA2) is shown in gray.

(E) Rap1 activation by GFP-RanV19-Epac1RA2. GFP-tagged Epac1, Epac1RA2 and RanV19-Epac1RA2 were expressed in HEK293 cells and treated with 2OMe for 15min or left untreated. Rap1 activation was assayed and presented as in (A).

Figure 3.5

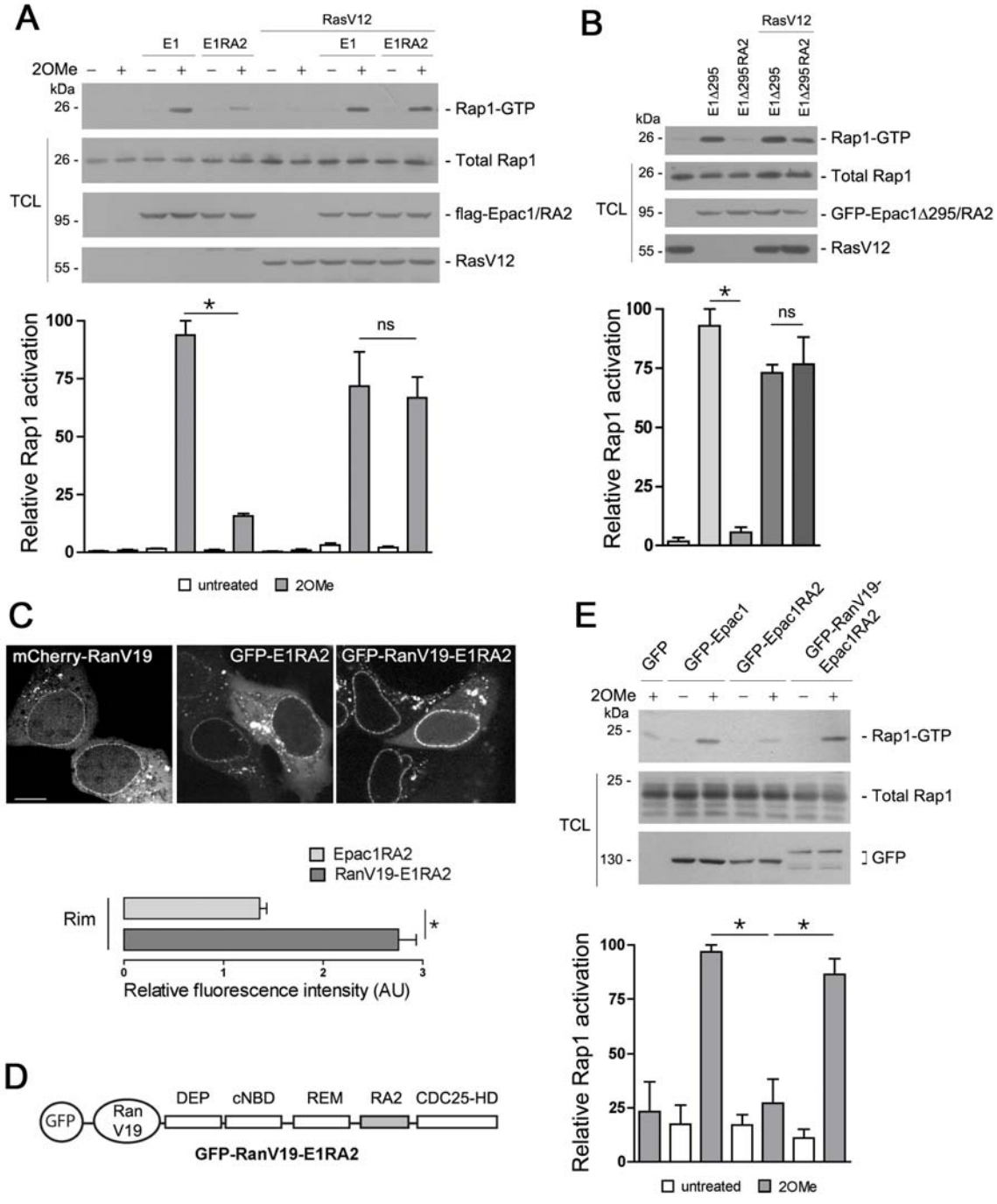
A
RasV12
E1
E1RA2
E1
E1RA2
2OMe
kDa
26 -
- Rap1-GTP
TCL
26 -
- Total Rap1
95 -
- flag-Epac1/RA2
55 -
- RasV12
Relative Rap1 activation
100
75
50
25
0
*
ns
untreated
2OMe
B
RasV12
E1Δ295
E1Δ295RA2
E1Δ295
E1Δ295RA2
kDa
26 -
- Rap1-GTP
TCL
26 -
- Total Rap1
95 -
- GFP-Epac1Δ295/RA2
55 -
- RasV12
Relative Rap1 activation
100
75
50
25
0
*
ns
C
mCherry-RanV19
GFP-E1RA2
GFP-RanV19-E1RA2
Epac1RA2
RanV19-E1RA2
Rim
*
0
1
2
3
Relative fluorescence intensity (AU)
D
GFP
Ran V19
DEP
cNBD
REM
RA2
CDC25-HD
GFP-RanV19-E1RA2
E
GFP
GFP-Epac1
GFP-Epac1RA2
GFP-RanV19-Epac1RA2
2OMe
kDa
25 -
- Rap1-GTP
TCL
25 -
- Total Rap1
130 -
GFP
Relative Rap1 activation
100
75
50
25
0
*
*
untreated
2OMe

Figure 3.6 Activation of endogenous Rap1 at the nuclear envelope (NE).

(A) Dynamic activation of Rap1 by Epac1 at the NE. HEK293 cells were cotransfected with GFP-RBD_{RalGDS} and either mCherry-vector (Vector) or mCherry-Epac1 (Epac1), and treated with 2OMe after serum starvation. Confocal images acquired at indicated time points are shown (representative of 11 cells in each condition from three independent experiments). Arrowheads indicate the NE.

(B) Subcellular localization of Rap1 activation by Epac1 mutants. mCherry (i), mCherry-tagged Epac1Δ295 (ii), Epac1Δ295RA2 (iii), or RanV19- Epac1Δ295RA2 (iv) was cotransfected with GFP-RBD_{RalGDS} into HEK293 cells. Left column, GFP; middle, mCherry; right, merged images. All images presented were from confocal live imaging and are representative of cells examined in two to three independent experiments (n>100). Scale bars, 10μm.

Figure 3.6

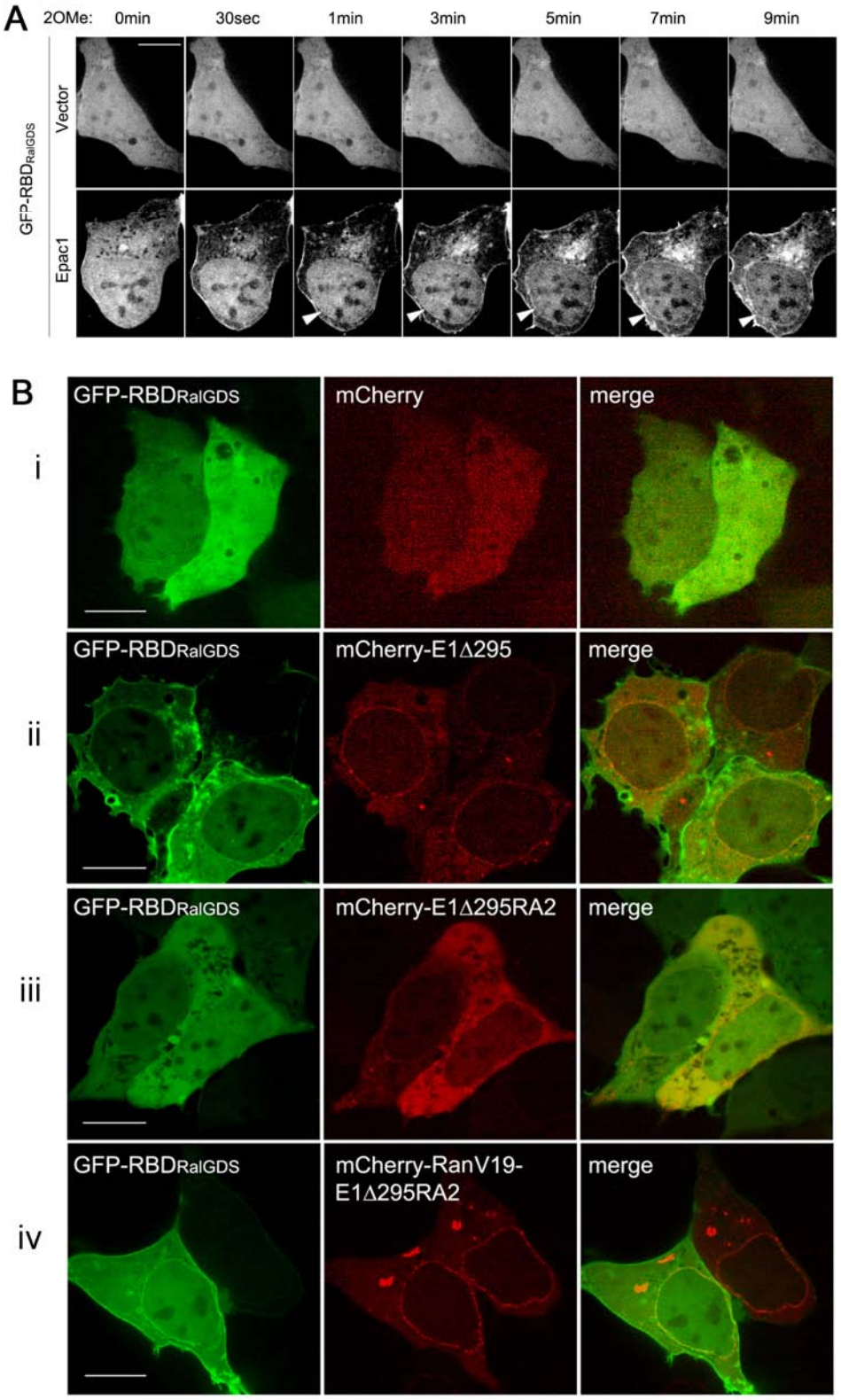
A
2OMe:
0min
30sec
1min
3min
5min
7min
9min
GFP-RBDRalGDS
Vector
Epac1
B
i
GFP-RBDRalGDS
mCherry
merge
ii
GFP-RBDRalGDS
mCherry-E1Δ295
merge
iii
GFP-RBDRalGDS
mCherry-E1Δ295RA2
merge
iv
GFP-RBDRalGDS
mCherry-RanV19-E1Δ295RA2
merge

Figure 3.7 Localization and activation of Rap1B at the NE.

(A) Localization of GFP-tagged Rap1B, Rap2B, and H-Ras expressed in HEK293 cells as indicated. All photos presented were confocal images from unfixed cells. Scale bars, 10μm.

(B) Distribution of GFP-RBD_{RalGDS} in HEK293 cells cotransfected with pcDNA3, flag-Rap1B or flag-Rap2B as indicated.

(C) GTP-dependency of the enrichment of GFP-RBD_{RalGDS} on the NE in HEK293 cells cotransfected with GFP-RBD_{RalGDS} and Rap1B-N17, or Rap1B-V12 as indicated.

(D) Inactivation of Rap1B on the NE by RapGAP. GFP-RBD_{RalGDS} and mCherry-Rap1B were cotransfected into HEK293 cells with pcDNA3 (panels i-iii) or RapGAP (panels iv-vi), as indicated. Panels i and iv, mCherry; panels ii and v, GFP; panels iii and vi, merged images. All the images are representative of cells examined in two to three independent experiments (n>100 cells).

Figure 3.7

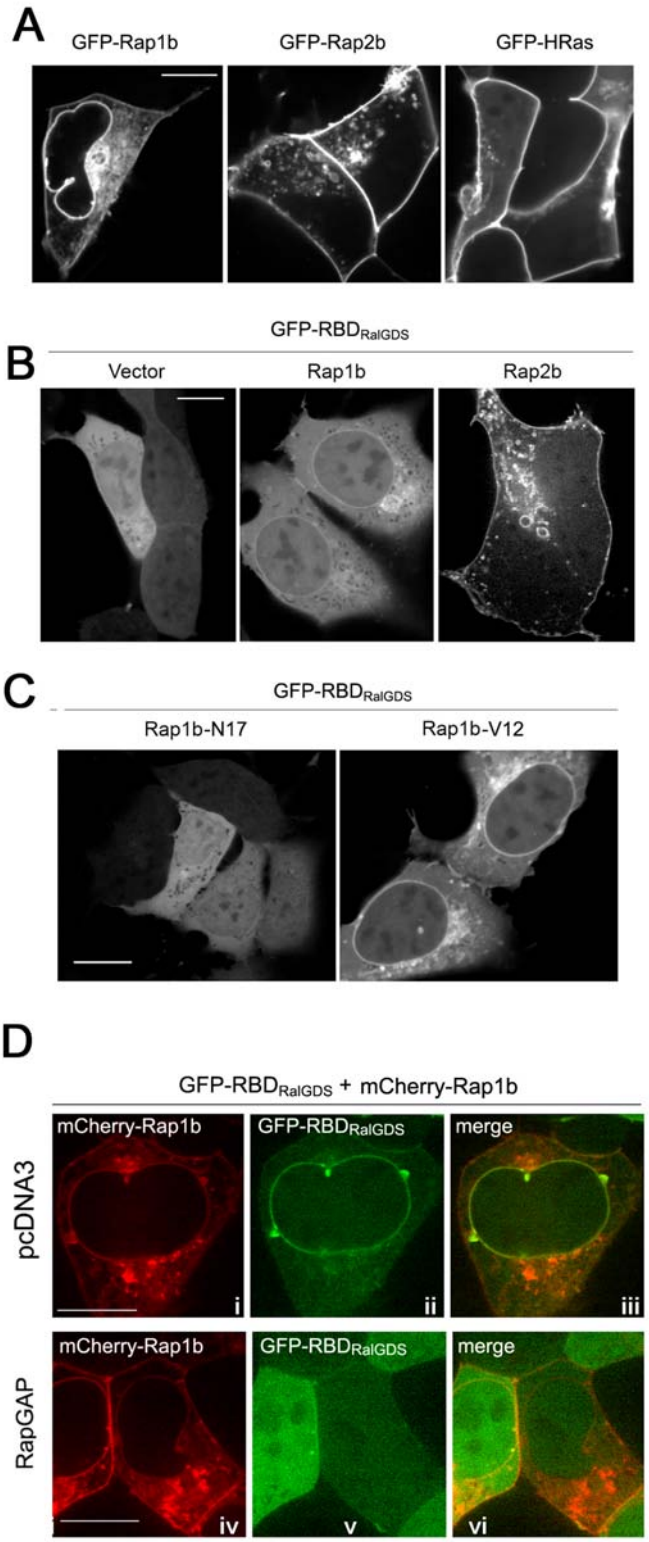
A
GFP-Rap1b
GFP-Rap2b
GFP-HRas
B
GFP-RBD$_{RalGDS}$
Vector
Rap1b
Rap2b
C
GFP-RBD$_{RalGDS}$
Rap1b-N17
Rap1b-V12
D
GFP-RBD$_{RalGDS}$ + mCherry-Rap1b
pcDNA3
RapGAP
mCherry-Rap1b
GFP-RBD$_{RalGDS}$
merge
i
ii
iii
iv
v
vi

Figure 3.8 Attenuation of Rap1 activation at the NE by depletion of endogenous Epac1.

(A) Depletion of Epac1 by siRNA. Left panel, lysates of HEK293 cells transfected with scrambled or Epac1 siRNA were examined by western blot using anti-Epac1 and anti-ERK2 (loading control). Right panel, quantification of three experiments (mean±SEM, * $p<0.05$).

(B) Effect of Epac1 depletion on Rap1 activation at the NE. GFP-RBD_{RalGDS} and mCherry-Rap1B were cotransfected with scrambled or Epac1 siRNA in HEK293 cells. Percentage of cells with enrichment of GFP-RBD_{RalGDS} on the NE were quantified from four independent experiments (mean±SEM, * $p<0.01$).

(C) Representative images from (B) are shown. The top and bottom panels show cells cotransfected with scrambled and Epac1 siRNA, respectively. Left, GFP; middle, mCherry; right, merged images. Scale bars, 10μm.

(D) Model for anchored Epac1 signaling at the NE. The NPC is a large multimeric protein complex shown in cross section spanning the double bilayer of the NE. Epac1 is localized to the NPC through direct interaction between its RA domain and Ran-GTP, which also associates with RanBP2, the major nucleoporin on the cytoplasmic face of the NPC. Epac1 may also make direct contacts with RanBP2 as shown (question mark). The anchored Epac1 allows cAMP to activate local pools of Rap1 that is tethered on the NE.

Figure 3.8

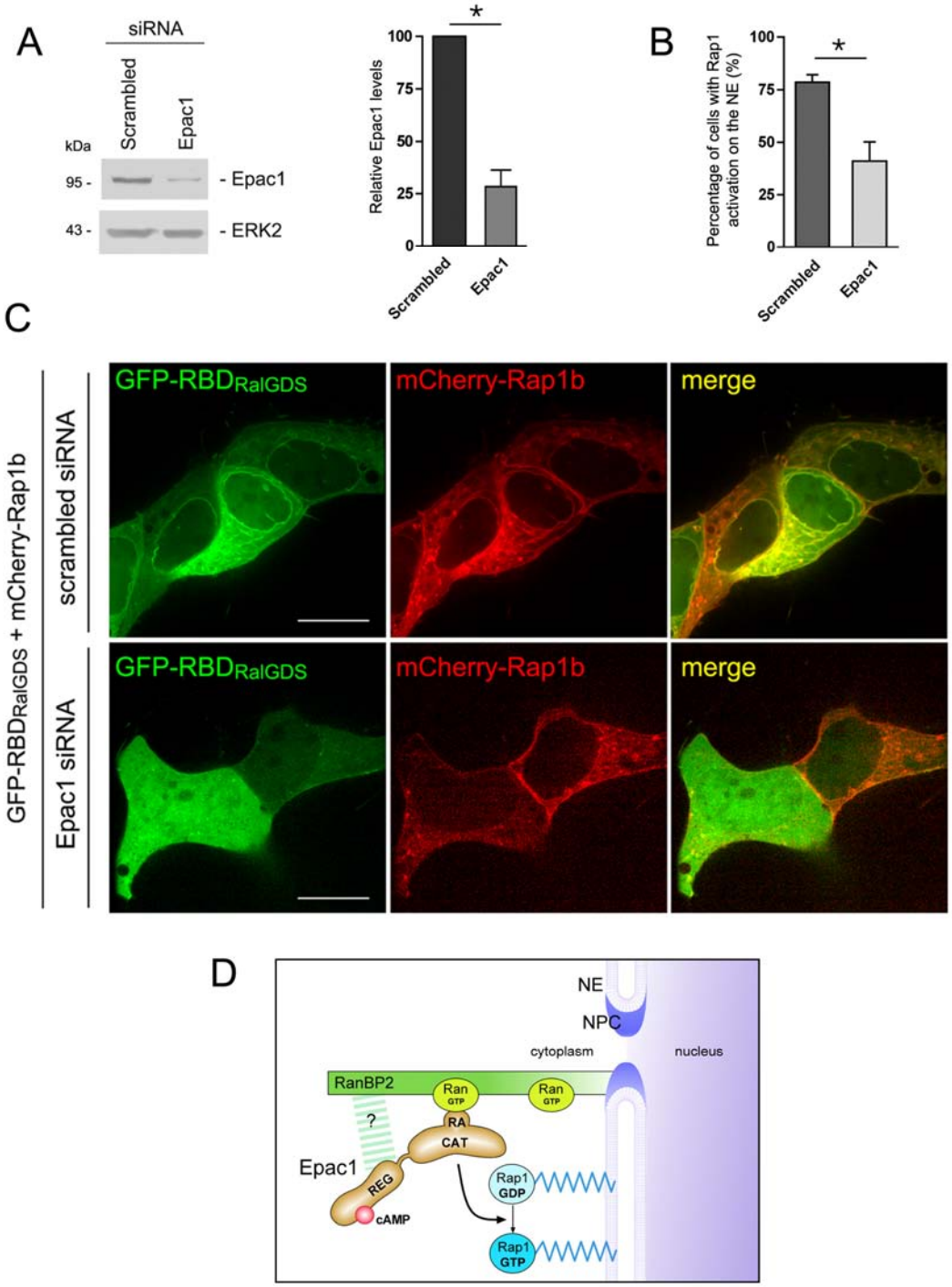
A
siRNA
Scrambled
Epac1
kDa
95 -
- Epac1
43 -
- ERK2
Relative Epac1 levels
100
75
50
25
0
*
Scrambled
Epac1
B
Percentage of cells with Rap1 activation on the NE (%)
100
75
50
25
0
*
Scrambled
Epac1
C
GFP-RBDRalGDS + mCherry-Rap1b
scrambled siRNA
Epac1 siRNA
GFP-RBDRalGDS
mCherry-Rap1b
merge
GFP-RBDRalGDS
mCherry-Rap1b
merge
D
NE
NPC
cytoplasm
nucleus
RanBP2
Ran
GTP
Ran
GTP
?
RA
CAT
Epac1
REG
cAMP
Rap1
GDP
Rap1
GTP

Chapter 4

Summary and Future Directions

4.1 SUMMARY

The discovery of novel targets of cAMP has focused our attention on two homologous exchange factors, Epac1 and Epac2. While both proteins are Rap exchangers directly activated by cAMP, whether they mediate different mode of Rap1 activation to achieve efficiency and specificity in Rap1 signaling was unclear. My thesis work focused on distinct mechanisms for the targeting of Epac1 and Epac2 to different subcellular locations. These mechanisms highlight the importance of the protein interactions mediated by the RA domains of Epac1 and Epac2, which are required for the spatial control of Rap1activation triggered by cAMP. The summary of my thesis work is presented as a schematic in Figure 4.1 and the main points are outlined below.

Epac2, originally regarded as a cAMP sensor, is also a *bona fide* Ras effector (Figure 4.1, box in dotted orange line). It is recruited by Ras-GTP to the PM via its RA domain (RA2), which is required for the efficient activation of Rap1 in the presence of cAMP. This action of Ras can be mimicked by targeting Epac2 to the PM through an engineered CAAX motif that can be lipidified. As a coincidence detector for Ras and cAMP signals, Epac2 activates Rap1 robustly at the PM, which is coupled to ERK activation and promotes neurite outgrowth in PC12 cells. The other roles of Epac2 in the convergent signaling of growth factors and hormones remain to be elucidated.

Epac1 is the first exchange factor found to associate with the NPC (Figure 4.1, box in dotted green line). While the detailed organization of this protein complex might involve multiple components of the NPC including Ran and RanBP2, the direct interaction between Ran and Epac1 via its RA domain (RA1) is crucial. Swapping RA1 for RA2, which abolishes the Ran association, compromises the full enrichment of the

mutant at NPC and the efficient activation of Rap1 on the NE. These defects can be restored by retargeting the mutant to NPC with a fused Ran-GTP. Whether the Rap1 activated on the NE is involved in nuclear transport or other cellular proecesses needs further investigation.

Putting the mechanisms of Epac1 and Epac2 dependent Rap1 signaling into context (Figure 4.1, right half of the schematic; also see Chapter 1), small GTPases can be connected into local cascades and a "global" network via their GEFs. Epac1 and Epac2 play the theme common to many other GEFs summarized in the figure by interacting with an upstream small GTPase (Ran and Ras, respectively) via their RA domains, and activating another downstream small GTPase (Rap1). The unique variation in the case of Epac proteins are: one, both Epac1 and Epac2 needs the second messenger cAMP to overcome their intra-molecular inhibition, and together with the spatial controls via their RA domains, they may be more versatile in integrating different environmental cues; two, while the signaling of most small GTPases were documented on the PM and trafficking vesicles, Epac1-Rap1 signaling at the NE is likely to expand the action of small GTPases to a broader territory.

In conclusion, Epac1 and Epac2 are compartmentalized via specific interaction with Ran and Ras, respectively, and they transduce cAMP signals to activation of Rap1 at different subcellular locations.

4.2 FUTURE DIRECTIONS

The results presented in this thesis supply important links to an emerging network of small GTPases of the Ras superfamily, and they also opened up new questions that are worth further investigation as described below.

4.2.1 Questions related to Epac2

Although Ras-Epac2 interaction can be induced 15 minutes after treatment with EGF, the detailed kinetics of the Ras-Epac2 interaction is not clear. Given that Epac2 enhances the magnitude rather than extending the time course of the ERK phosphorylation, it is possible that Ras-Epac2 interaction is transient and is terminated by either inactivation of Ras or some undetermined negative feedback to Epac2 (e.g. post-translational modifications of the RA domain that abolish its binding to Ras).

As discussed in Chapter 1, Epac2 has been shown to regulate insulin secretion *in vivo*. One physiologically related question regarding the subtle phenotype of the Epac2$^{-/-}$ mice would be whether co-stimulation of Ras can further enhance the cAMP triggered insulin secretion in wild type animals but not the knockout. In a physiological setting, Ras activation could be achieved by stimulation of the receptor tyrosine kinases, and the cAMP can be elevated by action of Glucagon-like peptide 1 (GLP-1) (Lawrence et al., 2008). Considering the strong connection of Epac2-Rap1 signaling to MAPK cascade, it would also be important to determine whether Epac2 play a role in the establishment and maintainence of the population of β cells downstream of environmental cues that stimulate Ras and cAMP.

As Epac2 is abundantly expressed in neuronal cells and serves as a coincidence detector for Ras and cAMP signals, it is reasonable to speculate that it may play a vital role in the remodeling of neuronal circuits as well as learning and memory. Many recent studies identified important roles for Epac2 in the physiology of nervous system. For example, Woolfrey et al. reported that Epac2 induces synapse remodeling and depression and its variants associated with Autism alter the morphology of spines (Woolfrey et al.,

2009). While this important study focused on a novel interaction between Epac2 and neuroligins, it is unknown whether the interaction is direct or regulated by physiological cues. Interestingly, two of the four Autism-related point mutations, V646F and G706R, are located within or immediately close to the RA domain of Epac2. It is important to test whether these mutants are defective in Ras interaction, which might be correlated to their functional defects. In another study, down-regulation of Epac2 expression in the hippocampal CA1 area was shown to impaire fear memory retrieval in a time-limited fashion (when tested 72 h after training) (Ostroveanu et al., 2009). It would be important to carry out neurobehavioral studies in Epac2$^{-/-}$ animals to test definitively the role of Epac2 in advanced brain functions *in vivo*. To address the exact role of Epac2 as a coincidence detector *in vivo* requires more complicated strategies including knock-in of Epac2 mutant (e.g. K684E) incapable of Ras binding as well as Epac2K684E-CAAX on the Epac2 null background.

4.2.2 Questions related to Epac1

The localization of Epac1 predominantly at the NPC rather than the PM raises question about previous models proposing that Epac1 directly activates Rap1 at the PM to stimulate integrin-mediated adhesion. Although the integrin-mediated adhesion could be a cell type dependent phenomenon, the perinuclear enrichment of Epac1 is common among most cell lines examined. However, as shown in Chapter 3, despite the predominant localization of Epac1 at the NPC with little translocation from the cytoplasm to the PM, Epac1 does cause redistribution of GFP-RBD$_{RalGDS}$ to the PM and the NE equally well. Although I envision that Rap1 could be activated at the NE before being transported to the PM, this point was not directly tested and far from being confirmed.

This is partly because there has been no consensus on the identity of the vesicles in which Rap1 resides in the cells. Distribution of GFP-Rap1 can be seen on the secretory pathway including the Golgi network and endoplasmic reticulum; however, GFP-Rap1 containing vesicles were also observed to be trafficking directly between the NE and PM, which falls into the category of non-secretory pathway. These diverse ways of communication between the PM and NE may present considerable difficulties in the choice of inhibitors to block the trafficking of Rap1 in the cell. The presence of a mixed pool of Rap1 and Rap2 at the PM further complicates the matter. Nevertheless, despite the limited understanding of the origin of Rap1-GTP on the PM, abundant evidence is presented in the thesis in support of the activation of Rap1 on the NE by Epac1.

The presence of Epac1 at the NPC suggests that Epac1 could be an integral part of the nuclear transport machinery. One basic question unresolved is how the complex of Epac1, Ran and RanBP2 is organized. Our data suggest that Ran maybe sandwiched between the RA domain of Epac1 and the Ran binding domain of RanBP2, but the possible direct interaction between Epac1 and RanBP2 has not been fully explored. The complex of Epac1, Ran and RanBP2 seems to be very stable and is not significantly affected by overexpression of RanGAP, which in theory can reduce the amount of Ran-GTP in association with RanBP2. In fact, we have preliminary data showing that RanGAP and Epac1 can be co-immunoprecipitated, suggesting that Epac1 and RanGAP can coexist at the NPC and the Epac1-Ran-RanBP2 complex may be insulated from the activity of RanGAP. This idea is not impossible, given that RanBP2 is a very large protein and the four Ran binding sites on RanBP2 may not be “created equal”, with some sites more influenced by RanGAP than others. So, the Ran-Epac1 complex may interact

with RanBP2 at sites far away from where RanGAP binds and remain stable, and further experiments could be designed to test this intriguing hypothesis.

Unlike the interaction between Ras and Epac2, which is dependent on the activation status of Ras and can be induced by extracellular stimuli, the RanBP2-Ran-Epac1 complex is already in place under basal conditions and does not appear to be regulated by any stimulation. However, the NE and NPC are assembled and disassembled during the cell cycle, and the localization of Ran and RanBP2 undergoes dynamic changes too. Thus, it would be important to examine the localization of Epac1 at different stages of the cell cycle and to observe whether knockdown of Epac1 has any effect on the progression of cell cycle.

Another physiological question is the whether Epac1-Rap1 signaling participates in the nuclear transport. So far there was only one report about the novel role of Epac1 and Rap2 in the nuclear transport of any protein. This study identified the Epac1-dependent export of DNA-PK from the nucleus, and knockdown of Rap1 did not affect this process. Given the unique localization of Epac1 and Rap1 at the NPC and NE, respectively, it is possible that Epac1 and Rap1 are involved in the transport of proteins other than DNA-PK. It would be interesting to design an unbiased approach to identify these proteins, and then follow up on the cellular processes that are dependent on these transportations.

4.2.3 Questions related to Rap1 and small GTPases in general

Rap1 is present at multiple membranous compartments in the cell, and these different pools of Rap1 can be differentially activated by Epac1 and Epac2 that are spatially segregated. In addition, the spatial control of Rap1 signaling could also be dynamically regulated by post-translational modifications on itself. As shown in Figure 1.4, both

Rap1A and Rap1B feature C terminal sequences that are rich in positively charged residues and classical PKA sites. The latter may serve as electrostatic switches to trigger the dissociation of Rap1 from the membrane, and we have preliminary data in support of this idea. Because cAMP can simultaneously activate Epac proteins and PKA, it is important to understand how these different levels of spatial controls converge on Rap1 and how they dynamically affect the cellular processes involved.

In terms of the network of small GTPases, probably some basic descriptions of the group behavior of the small GTPases need to be made before other meaningful progresses are possible. For example, with a given stimulus to the cell, we need to know the kinetics of activation and inactivation of multiple small GTPases involved in a network. This is usually labor intensive, and the noise from certain assays sometimes can overwhelm the signals themselves. There has not been report of monitoring the kinetics of more than one endogenous small GTPases *in vivo,* either. Nevertheless, new high-throughput technology in the near future may revolutionize our understanding about the flow of signals among multiple small GTPases in real time and *in vivo*.

Figure 4.1 Summary: Spatial control of Rap1 by Epac proteins and the cascades of small GTPases in different cellular compartments.

Chapter 2 is summrized in the orange-colored box, Chapter 3 in the green-colored box. Pathways in the background are discussed in Chapter 1. See the text in Section 4.1 for details.

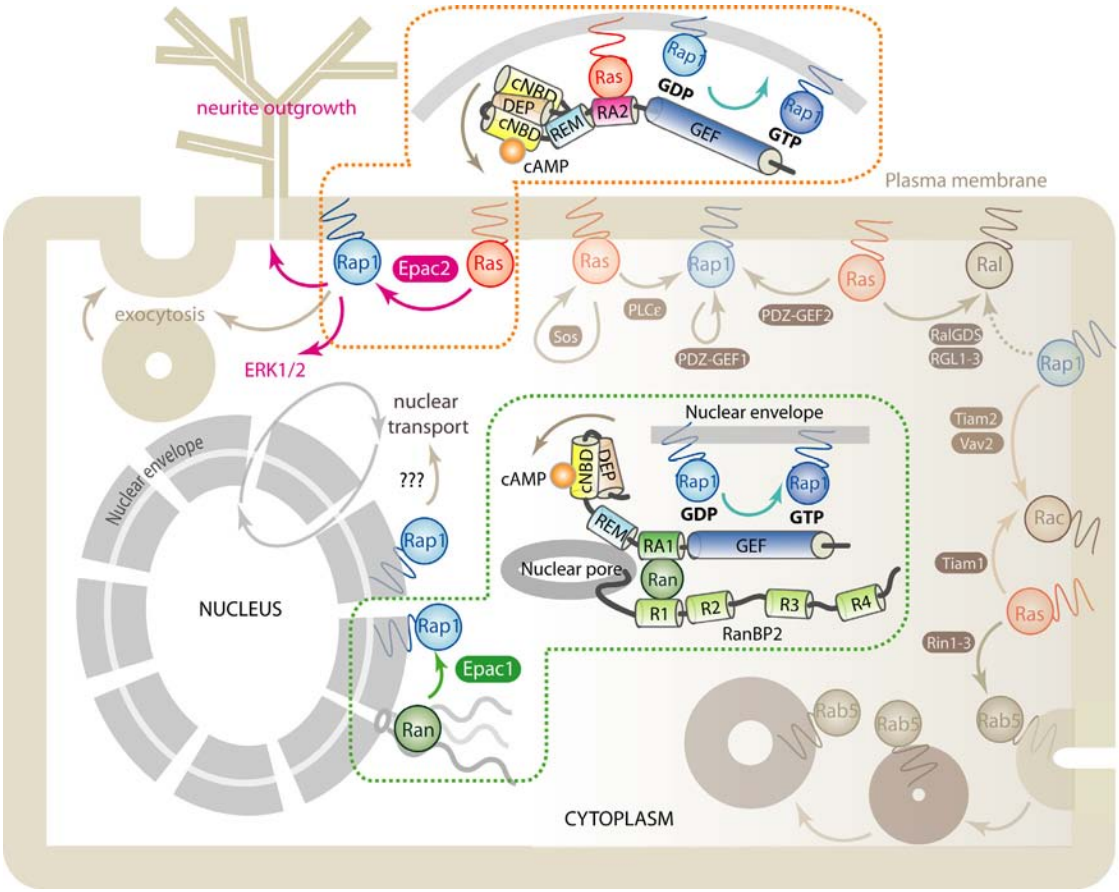

APPENDICES

Appendix 1 Structural modeling

All the structural modeling were performed using the UCSF Chimera package from the Resource for Biocomputing, Visualization, and Informatics at the University of California, San Francisco (Pettersen et al., 2004).

Ras-Epac2 interaction in comparison to the Rap1-C-Raf RBD complex (Figure 2.2B). The goal of this modeling is to visualize the Ras-Epac2 complex and correlate the structure with experimental data. The structure files used in this modeling are obtained from protein data bank (www.pdb.org) and listed in Table A.1.

The structure of Rap1A in complex with CRAF-RBD was used as the template. H-Ras-GTP was first superimposed on Rap1A and then Epac2 RA domain (residue 620-720) was superimposed on CRAF-RBD using the MatchMaker function (Meng et al., 2006), followed by restoration of full length Epac2. The side chains of R89 of CRAF-RBD and K684 of Epac2 were highlighted as sticks.

The two structure pairs appear to be well superimposed (Table A.2, pair 1 and 2). Note that mutations of R89 of CRAF-RBD and K684 of Epac2 disrupted the Ras-CRAF complex (Block et al., 1996) and Ras-Epac2 complex (Figure 2.2C, D), respectively. And here, the side chains of the above two residues occupy the same space at the binding interfaces, supporting the notion that Epac2 and CRAF share the same binding profile towards Ras-GTP (Figure 2.1A, B). Importantly, the regulatory region of Epac2 does not interfere with the Ras-Epac2 interaction, which agrees with our data showing that Ras binds to Epac2 in a cAMP independent manner (Figure 2.1C, D).

The ternary complex of Ras-Epac2-Rap1 (Figure 2.5A). The goal of this modeling is to visualize the Ras-Epac2-Rap1 ternary complex and correlate the structure with experimental data. The structure files used in this modeling are obtained from protein data bank and listed in Table A.1.

The structure of Epac2 in complex with a cAMP analog and Rap1 at the catalytic hairpin was solved recently (Rehmann et al., 2008). The CRAF-RBD was superimposed on the RA domain of Epac2 (PDB code: 3CF6), and the H-Ras-GTP was superimposed on Rap1 (1C1Y chain A) in complex with CRAF-RBD. Using these structure, the spatial relationship between H-Ras-GTP and the Epac2-Rap1 complex was established.

All the structure pairs compared during the modeling are well superimposed. Note that Ras, Rap1 and the RA and CDC25 domains of Epac2 were aligned on a single plane, and we placed the lipid membrane plane parallel to this plane. Importantly, the c-terminal ends of Ras and Rap1 pointed toward the membrane plane at the same time, accommodating the constraints imposed by their c-terminal lipid modifications (side view, see Figure 2.5A).

Table A.1 Structures used in the modeling

Structures	PDB ID	Color	Reference
Epac2	2BYV	RA domain (pink), other domains (green)	(Rehmann et al., 2006)
H-Ras-GTP	2CL7	H-Ras (magenta)	(Klink et al., 2006)
Rap1A/ CRAF-RBD	1C1Y	Rap1 (dark blue), CRAF-RBD (cyan in Figure 2B and hidden in Figure 5A)	(Nassar et al., 1995)
H-Ras/ Sos-1	1BKD	Both chains are hidden in Figure 5A	(Boriack-Sjodin et al., 1998)
Epac2/ Rap1	3CF6	Rap1 (dark blue), Epac2 RA domain (pink), other domains (green)	(Rehmann et al., 2008)

Table A.2 Evaluation of superimpositions of structure pairs in the modeling

Pair	Protein/domain	PDB ID	Chain	N/RMSD (MM-default)
1	Epac2 RA domain	2BYV	E	26/1.188
	CRAF-RBD	1C1Y	C	
2	H-Ras-GTP	2CL7	X	152/0.837
	Rap1A	1C1Y	A	

The evaluation results are of the form N/RMSD, where N is the number of residue pairs matched and RMSD is the corresponding alpha-carbon root-mean-square deviation. MM-default: MatchMaker with default parameters (BLOSUM-62, 30% secondary structure weighting, prior secondary structure calculation, iteration cutoff 2.0 angstroms)

Appendix 2 Computational modeling

Rate of Rap1 activation as a function of the percentage of Epac2 recruited to the membrane (Figure 2.5G). The exchange activity of Epac2 can be briefly expressed by the following 2 reactions.

$$Rap1GDP + Epac2 \xrightarrow{k1} Rap1 \cdot Epac2 + GDP \quad (1)$$

$$Rap1 \cdot Epac2 + GTP \xrightarrow{k2} Rap1GTP + Epac2 \quad (2)$$

The excess of GTP in the cell allows the accumulation of Rap1GTP in the presence of Epac2. The focus of this modeling is not the regulation of Epac2 by cAMP, but the contribution of Ras binding in Epac2 mediated Rap1 activation. Therefore, we started with the condition that Epac2 is already at an open conformation in the presence of adequate amount of cAMP. In this scenario, the rate of the exchange reaction is largely decided by the concentrations of Epac2 and Rap1. Rap1 is normally associated with cellular membranes, and can only interact with Epac2 within the sub-membrane space. We defined the concentration of this pool of Epac2 as $[Epac2]_m$. Therefore, the rate of Rap1 activation will be proportional to $[Rap1]\times[Epac2]_m$. Since the total concentration of Rap1 remains unchanged, we have treated [Rap1] as a constant. Thus, the rate of Rap1 activation will be proportional to $[Epac2]_m$.

We defined [Epac2] as the total Epac2 concentration within the whole cell, *p* as the fraction of Epac2 recruited to the membrane (namely, the percentage of Epac2 in complex with RasGTP), and *A* as the fold difference of the cell volume to the volume of the sub-membrane space. The relationship between membrane associated Epac2 and total Epac2 can be represented as:

$$[Epac2]_m = [Epac2] \times p \times A + [Epac2] \times (1 - p).$$

Therefore, the *Rate of Rap1 activation* $\propto [Epac2] \times p \times A + [Epac2] \times (1 - p)$ (3)

For the simplicity of the model, the role of intracellular membranous structures is not considered and the shape of the cell is constant. In this case, *A* becomes a constant, and the relative rate of Rap1 activation will be a function of only [Epac2] and *p*. For any given cell size, the constant *A* will be maximal if the cell is considered as a sphere, and will increase with the diameter of the sphere. In the general case, the diameter of a cell is approximately 10 μm (Kim et al., 2007) (see also Bionumbers, Roskams and Rodgers, LabRaf). A better estimate of 10 μM is also consistent with the PC12 literature (Das et al., 2004; Greene and Tischler, 1976; Tischler and Greene, 1975). The diameter of a molecule of ~ 100kDa (e.g. Epac2) is approximately 10 nm. Assume the reaction is confined in a thin shell of sub-membrane space with the thickness of 10 nm, the fold enrichment of Epac2, which equals to the fold difference of the cell volume to the volume of the sub-membrane space (*A*), will be 167. *A* could be considerably lower in cultured cells that usually spread out flat and have a much smaller volume/surface ratio.

The modeling takes into consideration only the concentrations of the enzyme before and after relocalization. Two additional approximations have also been made. First, each encounter of Epac2 and Rap1GDP was considered equally productive. However, this may underestimate the rate of Rap1 activation, because structural modeling (Figure 2.5A) suggested that Ras-bound Epac2 may be better oriented to interact with Rap1. This will further accelerate Rap1 activation at the membrane. Second, there may be limits to the maximal level of Rap1 activation. Several factors can contribute to this limit,

including limits to the concentration and diffusion of Rap1 across different membrane microdomains and the differential localization of Rap1GAP within the cell.

The modeling above predicts that membrane recruitment of Epac2 is a very efficient mechanism to regulate the rate of Rap1 activation. At one extreme where $p = 0$, the rate of Rap1 activation becomes 1 (equation 3). If Epac2 were to be completely relocated to the membrane (i.e. $p = 1$), the rate of Rap1 activation is predicted to increase by a factor defined by A (estimated to be 167 in the spherical cell model). A more physiological situation might have the percentage of Epac2 on the membranes increasing from 5% (i.e. $p = 0.05$) to 15% (i.e. $p = 0.15$) (see Figure 2.2E), the rate of Rap1 activation would increase more than 2 fold, which is in agreement with our experimental data (Figure 2.3B, lane 8 and 12). Importantly, these dramatic increases are accomplished only by relocating Epac2 without any change in Epac2 synthesis.

Rate of Rap1 activation in relation to the level of Ras activation and affinity between Epac2 and RasGTP (Figure 2.5H). The percentage of Epac2 recruited to the membrane (p) can be expressed using the dissociation constant (Kd) of Ras-Epac2 binding and the concentration of activated Ras [RasGTP].

$$RasGTP + Epac2 \xleftrightarrow{Kd} RasGTP \cdot Epac2$$

$$Kd = \frac{[RasGTP] \times [Epac2]}{[RasGTP \cdot Epac2]}$$

$$\frac{Kd}{[RasGTP]} = \frac{[Epac2]}{[RasGTP \cdot Epac2]}$$

Note that [Epac2] is the concentration of Epac2 in the whole cell, while [RasGTP·Epac2] and [RasGTP] are concentrations of bound RasGTP·Epac2 complext and free RasGTP in

the sub-membrane space. The concentration of bound RasGTP also represents to that of bound Epac2 in the same space. Other Ras effectors are not considered here. Therefore, *p* (the percentage of Epac2 recruitment) can be calculated from the concentrations of free and bound Epac2 and the factor *A*.

$$\frac{Kd \times A}{[RasGTP]} = \frac{[Epac2] \times A}{[RasGTP \cdot Epac2]}$$

$$\frac{Kd \times A + [RasGTP]}{[RasGTP]} = \frac{[Epac2] \times A + [RasGTP \cdot Epac2]}{[RasGTP \cdot Epac2]}$$

$$\frac{[RasGTP]}{Kd \times A + [RasGTP]} = \frac{[RasGTP \cdot Epac2]}{[Epac2] \times A + [RasGTP \cdot Epac2]} = \frac{[RasGTP \cdot Epac2]}{[Epac2]_{total}} = p$$

Therefore,

$$p = \frac{[RasGTP]}{Kd \times A + [RasGTP]} \quad (4)$$

By coupling (3) and (4), we are able to plot the rate of Rap1 activation against level of Ras activation, and different Kds of Epac2 WT and Epac2-684E towards RasGTP.

How much Epac2 is recruited to the membrane depends on the level of Ras activation and the Kd of Epac2 towards RasGTP. The rate of Rap1 activation is increased when Ras is activated. Importantly, the steepest slope of the plot occurs when the concentration of RasGTP is relatively low, and the plot gradually approaches a plateau as RasGTP continues to increase.

For Epac2 WT and the RA domain mutant (Epac2-684E), the differences in their respective Kds towards RasGTP would dramatically affect how fast the plot reaches plateau, dictating the speed of the recruitment to the membrane in response to Ras

activation. Epac2 WT exhibited a small Kd towards RasGTP and was rapidly enriched on the membrane, and the rate of Rap1 activation also increased swiftly. However, Epac2-684E exhibited a Kd of one magnitude higher, and would be recruited at a much slower rate, resulting in a much slower rate of Rap1 activation.

All the plots were generated with MATLAB 7.0.1

Appendix 3 Proposed mechanism for the visualization of Rap activation using GFP-RBD_{RalGDS} (Figure A.1)

The Ras binding domain (RBD) of RalGDS interacts with Rap1 at high affinity, thus when tagged with GFP, it can serve as a reporter to visualize the level of Rap1-GTP at subcellular resolutions. However, a unifying theory is not available to accommodate different observations under various experimental conditions used in my study (see Chapter 3). One possible mechanism underlying the assay is proposed here so as to integratively explain the imaging data presented with reasonable logic.

(A to B) Rap1 is cycling between its GTP-loaded form and GDP-loaded form. GEF catalyses the release of GDP in exchange for GTP, while GAP catalyses the hydrolysis of GTP. The relative strengths of GEF and GAP dictate the level of Rap1-GTP at a specific subcellular location. If GFP-RBD_{RalGDS} can be recruited to a subcellular structure (e.g. either PM or NE) at a level beyond the background fluorescence, the profile of that particular structure can be perceived under the microscope. This requires that the amount of Rap1-GTP at that location rises above certain threshold to create a perceivable contrast between the GFP-RBD_{RalGDS} enriched at that location and the GFP-RBD_{RalGDS} in the background or cytoplasm. Under basal conditions, not enough Rap1-GTP is present in the cell, thus the distribution of GFP-RBD_{RalGDS} appears to be uniform across the whole cell. The endogenous Rap1 can be robustly activated in the following ways: (1) in the presence of exogenous Epac1 and its ligand, 2OMe; (2) in the presence of constitutively active Epac1Δ295; (3) in the presence of the chimeric protein, RanV19-Epac1Δ295RA2. Under all these conditions with stronger actions of the GEF (symbolized with thicker upper arch in B), we can observe that GFP-RBD_{RalGDS} lights up the NE, reflecting increased level of Rap1-GTP at the location.

(A to C) Then, why is GFP-RBD_{RalGDS} enriched at the NE simply upon expression of exogenous Rap1? This can be possibly explained by a slight imbalance between the strengths of GEF and GAP for Rap1 at the location, with the GEF being stronger. The imbalance is "slight" because, in the absence of overexpressed Rap1, it can not accumulate enough Rap1-GTP to enrich GFP-RBD_{RalGDS} above the background. However, when Rap1 is overexpressed, the increased level of substrates may allow generation of more Rap1-GTP beyond the detection limit, without altering the strengths of GEF or GAP. Interestingly, using FRET-based sensors, Mochzuki et al also observed increased level of Rap1-GTP around the nucleus under basal conditions (Mochizuki et al., 2001).

(C to D) and (C to E) The mechanism underlying the change from (A) to (C) proposed above can be further tested by manipulating the strengths of GEF and GAP in the system. In the presence of overexpressed RapGAP (indicated by thicker lower arch in D), Rap1-GTP will be depleted and Rap1-GDP will accumulate, abolishing the enrichment of GFP-RBD_{RalGDS} at the NE. Similarly, by interfering endogenous Epac1 (indicated by thinner upper arch in E), which might be the major source of the perinuclear GEF activity, Rap1-GDP will build up and the production of Rap1-GTP will decrease, which also abolishes the enrichment of GFP-RBD_{RalGDS} at the NE.

Figure A.1

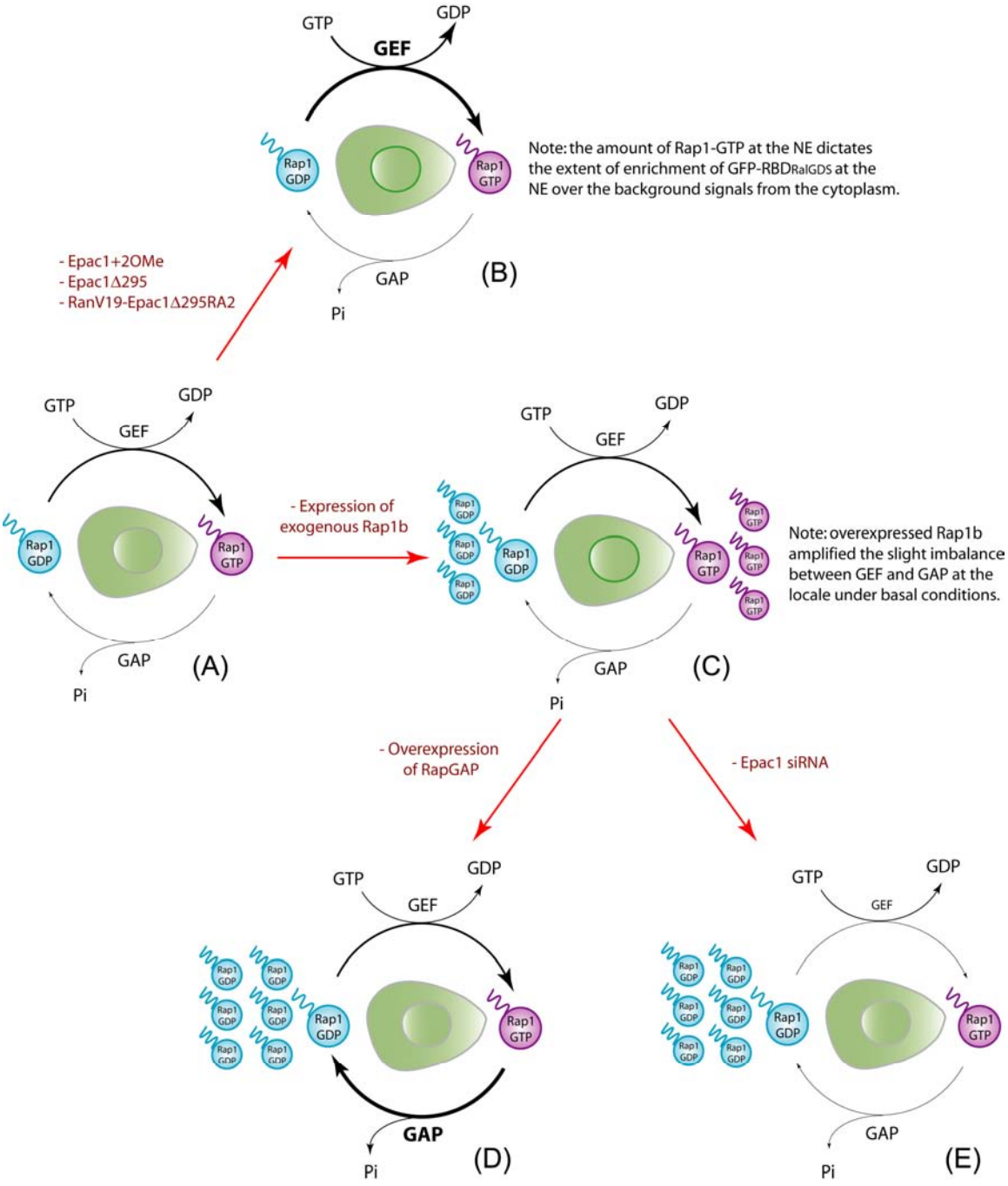
GTP
GDP
GEF
Rap1 GDP
Rap1 GTP
GAP
Pi
(B)
Note: the amount of Rap1-GTP at the NE dictates the extent of enrichment of GFP-RBDRalGDS at the NE over the background signals from the cytoplasm.
- Epac1+2OMe
- Epac1Δ295
- RanV19-Epac1Δ295RA2
(A)
- Expression of exogenous Rap1b
(C)
Note: overexpressed Rap1b amplified the slight imbalance between GEF and GAP at the locale under basal conditions.
- Overexpression of RapGAP
- Epac1 siRNA
(D)
(E)

REFERENCES

Abankwa, D., Hanzal-Bayer, M., Ariotti, N., Plowman, S. J., Gorfe, A. A., Parton, R. G., McCammon, J. A., and Hancock, J. F. (2008). A novel switch region regulates H-ras membrane orientation and signal output. Embo J *27*, 727-735.

An, Y., Shao, Y., Alory, C., Matteson, J., Sakisaka, T., Chen, W., Gibbs, R. A., Wilson, I. A., and Balch, W. E. (2003). Geranylgeranyl switching regulates GDI-Rab GTPase recycling. Structure *11*, 347-357.

Apolloni, A., Prior, I. A., Lindsay, M., Parton, R. G., and Hancock, J. F. (2000). H-ras but not K-ras traffics to the plasma membrane through the exocytic pathway. Mol Cell Biol *20*, 2475-2487.

Armstrong, S. A., Hannah, V. C., Goldstein, J. L., and Brown, M. S. (1995). CAAX geranylgeranyl transferase transfers farnesyl as efficiently as geranylgeranyl to RhoB. J Biol Chem *270*, 7864-7868.

Arthur, W. T., Quilliam, L. A., and Cooper, J. A. (2004). Rap1 promotes cell spreading by localizing Rac guanine nucleotide exchange factors. J Cell Biol *167*, 111-122.

Baljinnyam, E., Iwatsubo, K., Kurotani, R., Wang, X., Ulucan, C., Iwatsubo, M., Lagunoff, D., and Ishikawa, Y. (2009). Epac increases melanoma cell migration by a heparan sulfate-related mechanism. Am J Physiol Cell Physiol *297*, C802-813.

Ballif, B. A., Arnaud, L., Arthur, W. T., Guris, D., Imamoto, A., and Cooper, J. A. (2004). Activation of a Dab1/CrkL/C3G/Rap1 pathway in Reelin-stimulated neurons. Curr Biol *14*, 606-610.

Behnia, R., and Munro, S. (2005). Organelle identity and the signposts for membrane traffic. Nature *438*, 597-604.

Behnia, R., Panic, B., Whyte, J. R., and Munro, S. (2004). Targeting of the Arf-like GTPase Arl3p to the Golgi requires N-terminal acetylation and the membrane protein Sys1p. Nat Cell Biol *6*, 405-413.

Birukova, A. A., Burdette, D., Moldobaeva, N., Xing, J., Fu, P., and Birukov, K. G. (2010). Rac GTPase is a hub for protein kinase A and Epac signaling in endothelial barrier protection by cAMP. Microvasc Res *79*, 128-138.

Birukova, A. A., Zagranichnaya, T., Alekseeva, E., Bokoch, G. M., and Birukov, K. G. (2008). Epac/Rap and PKA are novel mechanisms of ANP-induced Rac-mediated pulmonary endothelial barrier protection. J Cell Physiol *215*, 715-724.

Bivona, T. G., and Philips, M. R. (2005). Analysis of Ras and Rap activation in living cells using fluorescent Ras binding domains. Methods *37*, 138-145.

Bivona, T. G., Quatela, S. E., Bodemann, B. O., Ahearn, I. M., Soskis, M. J., Mor, A., Miura, J., Wiener, H. H., Wright, L., Saba, S. G., *et al.* (2006). PKC regulates a farnesyl-electrostatic switch on K-Ras that promotes its association with Bcl-XL on mitochondria and induces apoptosis. Mol Cell *21*, 481-493.

Bivona, T. G., Wiener, H. H., Ahearn, I. M., Silletti, J., Chiu, V. K., and Philips, M. R. (2004). Rap1 up-regulation and activation on plasma membrane regulates T cell adhesion. J Cell Biol *164*, 461-470.

Block, C., Janknecht, R., Herrmann, C., Nassar, N., and Wittinghofer, A. (1996). Quantitative structure-activity analysis correlating Ras/Raf interaction in vitro to Raf activation in vivo. Nat Struct Biol *3*, 244-251.

Booden, M. A., Baker, T. L., Solski, P. A., Der, C. J., Punke, S. G., and Buss, J. E. (1999). A non-farnesylated Ha-Ras protein can be palmitoylated and trigger potent differentiation and transformation. J Biol Chem *274*, 1423-1431.

Boriack-Sjodin, P. A., Margarit, S. M., Bar-Sagi, D., and Kuriyan, J. (1998). The structural basis of the activation of Ras by Sos. Nature *394*, 337-343.

Bos, J. L. (2005). Linking Rap to cell adhesion. Curr Opin Cell Biol *17*, 123-128.

Bos, J. L., de Rooij, J., and Reedquist, K. A. (2001). Rap1 signalling: adhering to new models. Nat Rev Mol Cell Biol *2*, 369-377.

Bos, J. L., Rehmann, H., and Wittinghofer, A. (2007). GEFs and GAPs: critical elements in the control of small G proteins. Cell *129*, 865-877.

Boykevisch, S., Zhao, C., Sondermann, H., Philippidou, P., Halegoua, S., Kuriyan, J., and Bar-Sagi, D. (2006). Regulation of ras signaling dynamics by Sos-mediated positive feedback. Curr Biol *16*, 2173-2179.

Bunney, T. D., Harris, R., Gandarillas, N. L., Josephs, M. B., Roe, S. M., Sorli, S. C., Paterson, H. F., Rodrigues-Lima, F., Esposito, D., Ponting, C. P., *et al.* (2006). Structural

and mechanistic insights into ras association domains of phospholipase C epsilon. Mol Cell *21*, 495-507.

Cadwallader, K. A., Paterson, H., Macdonald, S. G., and Hancock, J. F. (1994). N-terminally myristoylated Ras proteins require palmitoylation or a polybasic domain for plasma membrane localization. Mol Cell Biol *14*, 4722-4730.

Caloca, M. J., Zugaza, J. L., Vicente-Manzanares, M., Sanchez-Madrid, F., and Bustelo, X. R. (2004). F-actin-dependent translocation of the Rap1 GDP/GTP exchange factor RasGRP2. J Biol Chem *279*, 20435-20446.

Carmona, G., Gottig, S., Orlandi, A., Scheele, J., Bauerle, T., Jugold, M., Kiessling, F., Henschler, R., Zeiher, A. M., Dimmeler, S., and Chavakis, E. (2009). Role of the small GTPase Rap1 for integrin activity regulation in endothelial cells and angiogenesis. Blood *113*, 488-497.

Carney, D. S., Davies, B. A., and Horazdovsky, B. F. (2006). Vps9 domain-containing proteins: activators of Rab5 GTPases from yeast to neurons. Trends Cell Biol *16*, 27-35.

Casanova, J. E. (2007). Regulation of Arf activation: the Sec7 family of guanine nucleotide exchange factors. Traffic *8*, 1476-1485.

Chen, T., Muratore, T. L., Schaner-Tooley, C. E., Shabanowitz, J., Hunt, D. F., and Macara, I. G. (2007). N-terminal alpha-methylation of RCC1 is necessary for stable chromatin association and normal mitosis. Nat Cell Biol *9*, 596-603.

Cherfils, J., Menetrey, J., Mathieu, M., Le Bras, G., Robineau, S., Beraud-Dufour, S., Antonny, B., and Chardin, P. (1998). Structure of the Sec7 domain of the Arf exchange factor ARNO. Nature *392*, 101-105.

Chiu, V. K., Bivona, T., Hach, A., Sajous, J. B., Silletti, J., Wiener, H., Johnson, R. L., Cox, A. D., and Philips, M. R. (2002). Ras signalling on the endoplasmic reticulum and the Golgi. Nat Cell Biol *4*, 343-350.

Choy, E., Chiu, V. K., Silletti, J., Feoktistov, M., Morimoto, T., Michaelson, D., Ivanov, I. E., and Philips, M. R. (1999). Endomembrane trafficking of ras: the CAAX motif targets proteins to the ER and Golgi. Cell *98*, 69-80.

Chrzanowska-Wodnicka, M., Kraus, A. E., Gale, D., White, G. C., 2nd, and Vansluys, J. (2008). Defective angiogenesis, endothelial migration, proliferation, and MAPK signaling in Rap1b-deficient mice. Blood *111*, 2647-2656.

Chrzanowska-Wodnicka, M., Smyth, S. S., Schoenwaelder, S. M., Fischer, T. H., and White, G. C., 2nd (2005). Rap1b is required for normal platelet function and hemostasis in mice. J Clin Invest *115*, 680-687.

Chu, H., Awasthi, A., White, G. C., 2nd, Chrzanowska-Wodnicka, M., and Malarkannan, S. (2008). Rap1b regulates B cell development, homing, and T cell-dependent humoral immunity. J Immunol *181*, 3373-3383.

Clarke, P. R., and Zhang, C. (2004). Spatial and temporal control of nuclear envelope assembly by Ran GTPase. Symp Soc Exp Biol, 193-204.

Clyde-Smith, J., Silins, G., Gartside, M., Grimmond, S., Etheridge, M., Apolloni, A., Hayward, N., and Hancock, J. F. (2000). Characterization of RasGRP2, a plasma membrane-targeted, dual specificity Ras/Rap exchange factor. J Biol Chem *275*, 32260-32267.

Colicelli, J. (2004). Human RAS superfamily proteins and related GTPases. Sci STKE *2004*, RE13.

Crittenden, J. R., Bergmeier, W., Zhang, Y., Piffath, C. L., Liang, Y., Wagner, D. D., Housman, D. E., and Graybiel, A. M. (2004). CalDAG-GEFI integrates signaling for platelet aggregation and thrombus formation. Nat Med *10*, 982-986.

D'Souza-Schorey, C., and Chavrier, P. (2006). ARF proteins: roles in membrane traffic and beyond. Nat Rev Mol Cell Biol *7*, 347-358.

Das, K. P., Freudenrich, T. M., and Mundy, W. R. (2004). Assessment of PC12 cell differentiation and neurite growth: a comparison of morphological and neurochemical measures. Neurotoxicol Teratol *26*, 397-406.

de Rooij, J., Boenink, N. M., van Triest, M., Cool, R. H., Wittinghofer, A., and Bos, J. L. (1999). PDZ-GEF1, a Guanine Nucleotide Exchange Factor Specific for Rap1 and Rap2. J Biol Chem *274*, 38125-38130.

de Rooij, J., Rehmann, H., van Triest, M., Cool, R. H., Wittinghofer, A., and Bos, J. L. (2000). Mechanism of regulation of the Epac family of cAMP-dependent RapGEFs. J Biol Chem *275*, 20829-20836.

de Rooij, J., Zwartkruis, F. J., Verheijen, M. H., Cool, R. H., Nijman, S. M., Wittinghofer, A., and Bos, J. L. (1998). Epac is a Rap1 guanine-nucleotide-exchange factor directly activated by cyclic AMP. Nature *396*, 474-477.

Delphin, C., Guan, T., Melchior, F., and Gerace, L. (1997). RanGTP targets p97 to RanBP2, a filamentous protein localized at the cytoplasmic periphery of the nuclear pore complex. Mol Biol Cell *8*, 2379-2390.

Delprato, A., and Lambright, D. G. (2007). Structural basis for Rab GTPase activation by VPS9 domain exchange factors. Nat Struct Mol Biol *14*, 406-412.

Der, C. J., and Van Dyke, T. (2007). Stopping ras in its tracks. Cell *129*, 855-857.

Dodge-Kafka, K. L., Soughayer, J., Pare, G. C., Carlisle Michel, J. J., Langeberg, L. K., Kapiloff, M. S., and Scott, J. D. (2005). The protein kinase A anchoring protein mAKAP coordinates two integrated cAMP effector pathways. Nature *437*, 574-578.

Dube, N., Kooistra, M. R., Pannekoek, W. J., Vliem, M. J., Oorschot, V., Klumperman, J., Rehmann, H., and Bos, J. L. (2008). The RapGEF PDZ-GEF2 is required for maturation of cell-cell junctions. Cell Signal *20*, 1608-1615.

Duchniewicz, M., Zemojtel, T., Kolanczyk, M., Grossmann, S., Scheele, J. S., and Zwartkruis, F. J. (2006). Rap1A-deficient T and B cells show impaired integrin-mediated cell adhesion. Mol Cell Biol *26*, 643-653.

Dumaz, N., and Marais, R. (2005). Integrating signals between cAMP and the RAS/RAF/MEK/ERK signalling pathways. Based on the anniversary prize of the Gesellschaft fur Biochemie und Molekularbiologie Lecture delivered on 5 July 2003 at the Special FEBS Meeting in Brussels. Febs J *272*, 3491-3504.

Ebinu, J. O., Bottorff, D. A., Chan, E. Y., Stang, S. L., Dunn, R. J., and Stone, J. C. (1998). RasGRP, a Ras guanyl nucleotide- releasing protein with calcium- and diacylglycerol-binding motifs. Science *280*, 1082-1086.

Ehrhardt, A., Ehrhardt, G., Guo, X., and Schrader, J. (2002). Ras and relatives-job sharing and networking keep an old family together. Exp Hematol *30*, 1089.

Evellin, S., Nolte, J., Tysack, K., vom Dorp, F., Thiel, M., Weernink, P. A., Jakobs, K. H., Webb, E. J., Lomasney, J. W., and Schmidt, M. (2002). Stimulation of phospholipase C-epsilon by the M3 muscarinic acetylcholine receptor mediated by cyclic AMP and the GTPase Rap2B

J Biol Chem *277*, 16805-16813.

Fabian, J. R., Vojtek, A. B., Cooper, J. A., and Morrison, D. K. (1994). A single amino acid change in Raf-1 inhibits Ras binding and alters Raf-1 function. Proc Natl Acad Sci U S A *91*, 5982-5986.

Fahrenkrog, B., and Aebi, U. (2003). The nuclear pore complex: nucleocytoplasmic transport and beyond. Nat Rev Mol Cell Biol *4*, 757-766.

Farazi, T. A., Waksman, G., and Gordon, J. I. (2001). The biology and enzymology of protein N-myristoylation. J Biol Chem *276*, 39501-39504.

Ferro, E., Magrini, D., Guazzi, P., Fischer, T. H., Pistolesi, S., Pogni, R., White, G. C., and Trabalzini, L. (2008). G-protein binding features and regulation of the RalGDS family member, RGL2. Biochem J *415*, 145-154.

Fivaz, M., and Meyer, T. (2005). Reversible intracellular translocation of KRas but not HRas in hippocampal neurons regulated by Ca2+/calmodulin. J Cell Biol *170*, 429-441.

Franke, B., Akkerman, J.-W., and Bos, J. L. (1997). Rapid Ca^{2+}-mediated activation of rap1 in human platelets. EMBO J *16*, 252-259.

Freedman, T. S., Sondermann, H., Friedland, G. D., Kortemme, T., Bar-Sagi, D., Marqusee, S., and Kuriyan, J. (2006). A Ras-induced conformational switch in the Ras activator Son of sevenless. Proc Natl Acad Sci U S A *103*, 16692-16697.

Fukuyama, T., Ogita, H., Kawakatsu, T., Inagaki, M., and Takai, Y. (2005). Activation of Rac by cadherin through the c-Src-Rap1-phosphatidylinositol 3-kinase-Vav2 pathway. Oncogene.

Galabova-Kovacs, G., Matzen, D., Piazzolla, D., Meissl, K., Plyushch, T., Chen, A. P., Silva, A., and Baccarini, M. (2006). Essential role of B-Raf in ERK activation during extraembryonic development. Proc Natl Acad Sci U S A *103*, 1325-1330.

Gao, X., Satoh, T., Liao, Y., Song, C., Hu, C. D., Kariya Ki, K., and Kataoka, T. (2001). Identification and characterization of RA-GEF-2, a Rap guanine nucleotide exchange factor that serves as a downstream target of M-Ras. J Biol Chem *276*, 42219-42225.

Ghomashchi, F., Zhang, X., Liu, L., and Gelb, M. H. (1995). Binding of prenylated and polybasic peptides to membranes: affinities and intervesicle exchange. Biochemistry *34*, 11910-11918.

Gloerich, M., and Bos, J. L. (2010). Epac: defining a new mechanism for cAMP action. Annu Rev Pharmacol Toxicol *50*, 355-375.

Goldberg, J. (1998). Structural basis for activation of ARF GTPase: mechanisms of guanine nucleotide exchange and GTP-myristoyl switching. Cell *95*, 237-248.

Goodwin, J. S., Drake, K. R., Rogers, C., Wright, L., Lippincott-Schwartz, J., Philips, M. R., and Kenworthy, A. K. (2005). Depalmitoylated Ras traffics to and from the Golgi complex via a nonvesicular pathway. J Cell Biol *170*, 261-272.

Greene, L. A., and Tischler, A. S. (1976). Establishment of a noradrenergic clonal line of rat adrenal pheochromocytoma cells which respond to nerve growth factor. Proc Natl Acad Sci U S A *73*, 2424-2428.

Guo, Z., Ahmadian, M. R., and Goody, R. S. (2005). Guanine nucleotide exchange factors operate by a simple allosteric competitive mechanism. Biochemistry *44*, 15423-15429.

Gupta, S., Ramjaun, A. R., Haiko, P., Wang, Y., Warne, P. H., Nicke, B., Nye, E., Stamp, G., Alitalo, K., and Downward, J. (2007). Binding of ras to phosphoinositide 3-kinase p110alpha is required for ras-driven tumorigenesis in mice. Cell *129*, 957-968.

Gureasko, J., Galush, W. J., Boykevisch, S., Sondermann, H., Bar-Sagi, D., Groves, J. T., and Kuriyan, J. (2008). Membrane-dependent signal integration by the Ras activator Son of sevenless. Nat Struct Mol Biol *15*, 452-461.

Hall, A. (1990). The cellular functions of small GTP-binding proteins. Science *249*, 635-640.

Hall, A., and Self, A. J. (1986). The effect of Mg2+ on the guanine nucleotide exchange rate of p21N-ras. J Biol Chem *261*, 10963-10965.

Han, L., and Colicelli, J. (1995). A human protein selected for interference with Ras function interacts directly with Ras and competes with Raf1. Mol Cell Biol *15*, 1318-1323.

Han, L., Wong, D., Dhaka, A., Afar, D., White, M., Xie, W., Herschman, H., Witte, O., and Colicelli, J. (1997). Protein binding and signaling properties of RIN1 suggest a unique effector function. Proc Natl Acad Sci U S A *94*, 4954-4959.

Hancock, J. F. (2003). Ras proteins: different signals from different locations. Nat Rev Mol Cell Biol *4*, 373-384.

Hancock, J. F., Magee, A. I., Childs, J. E., and Marshall, C. J. (1989). All ras proteins are polyisoprenylated but only some are palmitoylated. Cell *57*, 1167-1177.

Hancock, J. F., Paterson, H., and Marshall, C. J. (1990). A polybasic domain or palmitoylation is required in addition to the CAAX motif to localize p21ras to the plasma membrane. Cell *63*, 133-139.

Hao, Y., and Macara, I. G. (2008). Regulation of chromatin binding by a conformational switch in the tail of the Ran exchange factor RCC1. J Cell Biol *182*, 827-836.

Harding, A., and Hancock, J. F. (2008). Ras nanoclusters: combining digital and analog signaling. Cell Cycle *7*, 127-134.

Harding, A., Tian, T., Westbury, E., Frische, E., and Hancock, J. F. (2005). Subcellular localization determines MAP kinase signal output. Curr Biol *15*, 869-873.

Harel, A., and Forbes, D. J. (2004). Importin beta: conducting a much larger cellular symphony. Mol Cell *16*, 319-330.

Heo, W. D., Inoue, T., Park, W. S., Kim, M. L., Park, B. O., Wandless, T. J., and Meyer, T. (2006). PI(3,4,5)P3 and PI(4,5)P2 lipids target proteins with polybasic clusters to the plasma membrane. Science *314*, 1458-1461.

Herrmann, C., Horn, G., Spaargaren, M., and Wittinghofer, A. (1996). Differential interaction of the ras family GTP-binding proteins H-Ras, Rap1A, and R-Ras with the putative effector molecules Raf kinase and Ral-guanine nucleotide exchange factor. J Biol Chem *271*, 6794-6800.

Hisata, S., Sakisaka, T., Baba, T., Yamada, T., Aoki, K., Matsuda, M., and Takai, Y. (2007). Rap1-PDZ-GEF1 interacts with a neurotrophin receptor at late endosomes, leading to sustained activation of Rap1 and ERK and neurite outgrowth. J Cell Biol *178*, 843-860.

Hofer, F., Fields, S., Schneider, C., and Martin, G. S. (1994). Activated Ras interacts with the Ral guanine nucleotide dissociation stimulator. Proc Natl Acad Sci U S A *91*, 11089-11093.

Holz, G. G., Kang, G., Harbeck, M., Roe, M. W., and Chepurny, O. G. (2006). Cell physiology of cAMP sensor Epac. J Physiol *577*, 5-15.

Hu, C. D., Kariya, K., Tamada, M., Akasaka, K., Shirouzu, M., Yokoyama, S., and Kataoka, T. (1995). Cysteine-rich region of Raf-1 interacts with activator domain of post-translationally modified Ha-Ras. J Biol Chem *270*, 30274-30277.

Hu, H., Milstein, M., Bliss, J. M., Thai, M., Malhotra, G., Huynh, L. C., and Colicelli, J. (2008). Integration of transforming growth factor beta and RAS signaling silences a RAB5 guanine nucleotide exchange factor and enhances growth factor-directed cell migration. Mol Cell Biol *28*, 1573-1583.

Huang, C. C., You, J. L., Wu, M. Y., and Hsu, K. S. (2004). Rap1-induced p38 mitogen-activated protein kinase activation facilitates AMPA receptor trafficking via the GDI.Rab5 complex. Potential role in (S)-3,5-dihydroxyphenylglycene-induced long term depression. J Biol Chem *279*, 12286-12292.

Huang, L., Hofer, F., Martin, G. S., and Kim, S. H. (1998). Structural basis for the interaction of Ras with RalGDS. Nat Struct Biol *5*, 422-426.

Hunker, C. M., Giambini, H., Galvis, A., Hall, J., Kruk, I., Veisaga, M. L., and Barbieri, M. A. (2006). Rin1 regulates insulin receptor signal transduction pathways. Exp Cell Res *312*, 1106-1118.

Huston, E., Lynch, M. J., Mohamed, A., Collins, D. M., Hill, E. V., MacLeod, R., Krause, E., Baillie, G. S., and Houslay, M. D. (2008). EPAC and PKA allow cAMP dual control over DNA-PK nuclear translocation. Proc Natl Acad Sci U S A *105*, 12791-12796.

Hutchins, J. R., Moore, W. J., and Clarke, P. R. (2009). Dynamic localisation of Ran GTPase during the cell cycle. BMC Cell Biol *10*, 66.

Ichiba, T., Hoshi, Y., Eto, Y., Tajima, N., and Kuraishi, Y. (1999). Characterization of GFR, a novel guanine nucleotide exchange factor for Rap1. FEBS Lett *457*, 85-89.

Impey, S., McCorkle, S. R., Cha-Molstad, H., Dwyer, J. M., Yochum, G. S., Boss, J. M., McWeeney, S., Dunn, J. J., Mandel, G., and Goodman, R. H. (2004). Defining the CREB regulon: a genome-wide analysis of transcription factor regulatory regions. Cell *119*, 1041-1054.

Irie, M., Hata, Y., Takeuchi, M., Ichtchenko, K., Toyoda, A., Hirao, K., Takai, Y., Rosahl, T. W., and Sudhof, T. C. (1997). Binding of neuroligins to PSD-95. Science *277*, 1511-1515.

Je, H. S., Yang, F., Zhou, J., and Lu, B. (2006). Neurotrophin 3 induces structural and functional modification of synapses through distinct molecular mechanisms. J Cell Biol *175*, 1029-1042.

Jin, T. G., Satoh, T., Liao, Y., Song, C., Gao, X., Kariya, K., Hu, C. D., and Kataoka, T. (2001). Role of the CDC25 homology domain of phospholipase Cepsilon in amplification of Rap1-dependent signaling. J Biol Chem *276*, 30301-30307.

Jullien-Flores, V., Dorseuil, O., Romero, F., Letourneur, F., Saragosti, S., Berger, R., Tavitian, A., Gacon, G., and Camonis, J. H. (1995). Bridging Ral GTPase to Rho pathways. RLIP76, a Ral effector with CDC42/Rac GTPase-activating protein activity. J Biol Chem *270*, 22473-22477.

Kao, S., Jaiswal, R. K., Kolch, W., and Landreth, G. E. (2001). Identification of the mechanisms regulating the differential activation of the MAPK cascade by epidermal growth factor and nerve growth factor in PC12 cells. J Biol Chem *276*, 18169-18177.

Kashima, Y., Miki, T., Shibasaki, T., Ozaki, N., Miyazaki, M., Yano, H., and Seino, S. (2001). Critical role of cAMP-GEFII--Rim2 complex in incretin-potentiated insulin secretion. J Biol Chem *276*, 46046-46053.

Kawajiri, A., Itoh, N., Fukata, M., Nakagawa, M., Yamaga, M., Iwamatsu, A., and Kaibuchi, K. (2000). Identification of a novel beta-catenin-interacting protein. Biochem Biophys Res Commun *273*, 712-717.

Kawasaki, H., Springett, G. M., Mochizuki, N., Toki, S., Nakaya, M., Matsuda, M., Housman, D. E., and Graybiel, A. M. (1998a). A family of cAMP-binding proteins that directly activate Rap1. Science *282*, 2275-2279.

Kawasaki, H., Springett, G. M., Toki, S., Canales, J. J., Harlan, P., Blumenstiel, J. P., Chen, E. J., Bany, I. A., Mochizuki, N., Ashbacher, A., *et al.* (1998b). A Rap guanine nucleotide exchange factor enriched highly in the basal ganglia. Proc Natl Acad Sci, USA *95*, 13278-13283.

Kawashima, T., Berthet-Colominas, C., Wulff, M., Cusack, S., and Leberman, R. (1996). The structure of the Escherichia coli EF-Tu.EF-Ts complex at 2.5 A resolution. Nature *379*, 511-518.

Keller, A., Nesvizhskii, A. I., Kolker, E., and Aebersold, R. (2002). Empirical statistical model to estimate the accuracy of peptide identifications made by MS/MS and database search. Anal Chem *74*, 5383-5392.

Kelley, G. G., Reks, S. E., Ondrako, J. M., and Smrcka, A. V. (2001). Phospholipase C(epsilon): a novel Ras effector. EMBO J *20*, 743-754.

Kelley, G. G., Reks, S. E., and Smrcka, A. V. (2004). Hormonal regulation of phospholipase Cepsilon through distinct and overlapping pathways involving G12 and Ras family G-proteins. Biochem J *378*, 129-139.

Kenworthy, A. K. (2007). Nanoclusters digitize Ras signalling. Nat Cell Biol *9*, 875-877.

Khosravi-Far, R., Solski, P. A., Clark, G. J., Kinch, M. S., and Der, C. J. (1995). Activation of Rac1, RhoA, and mitogen-activated protein kinases is required for Ras transformation. Mol Cell Biol *15*, 6443-6453.

Kikuchi, A., Demo, S. D., Ye, Z. H., Chen, Y. W., and Williams, L. T. (1994). ralGDS family members interact with the effector loop of ras p21. Mol Cell Biol *14*, 7483-7491.

Kim, U., Shu, C. W., Dane, K. Y., Daugherty, P. S., Wang, J. Y., and Soh, H. T. (2007). Selection of mammalian cells based on their cell-cycle phase using dielectrophoresis. Proc Natl Acad Sci U S A *104*, 20708-20712.

Kimura, T., Sakisaka, T., Baba, T., Yamada, T., and Takai, Y. (2006). Involvement of the Ras-Ras-activated Rab5 guanine nucleotide exchange factor RIN2-Rab5 pathway in the hepatocyte growth factor-induced endocytosis of E-cadherin. J Biol Chem *281*, 10598-10609.

Kirsch, K. H., Georgescu, M. M., and Hanafusa, H. (1998). Direct binding of p130(Cas) to the guanine nucleotide exchange factor C3G. J Biol Chem *273*, 25673-25679.

Kitayama, H., Sugimoto, Y., Matsuzaki, T., Ikawa, Y., and Noda, M. (1989). A ras-related gene with transformation suppressor activity. Cell *56*, 77-84.

Klink, B. U., Goody, R. S., and Scheidig, A. J. (2006). A Newly designed microspectrofluorometer for kinetic studies on protein crystals in combination with X-Ray diffraction. Biophys J *91*, 981-992.

Knudsen, B. S., Feller, S. M., and Hanafusa, H. (1994). Four proline-rich sequences of the guanine-nucleotide exchange factor C3G bind with unique specificity to the first Src homology 3 domain of Crk. J Biol Chem *269*, 32767.

Kosako, H., Yamaguchi, N., Aranami, C., Ushiyama, M., Kose, S., Imamoto, N., Taniguchi, H., Nishida, E., and Hattori, S. (2009). Phosphoproteomics reveals new ERK MAP kinase targets and links ERK to nucleoporin-mediated nuclear transport. Nat Struct Mol Biol *16*, 1026-1035.

Krapivinsky, G., Krapivinsky, L., Manasian, Y., Ivanov, A., Tyzio, R., Pellegrino, C., Ben-Ari, Y., Clapham, D. E., and Medina, I. (2003). The NMDA receptor is coupled to the ERK pathway by a direct interaction between NR2B and RasGRF1. Neuron *40*, 775-784.

Kuiperij, H. B., de Rooij, J., Rehmann, H., van Triest, M., Wittinghofer, A., Bos, J. L., and Zwartkruis, F. J. (2003). Characterisation of PDZ-GEFs, a family of guanine nucleotide exchange factors specific for Rap1 and Rap2. Biochim Biophys Acta *1593*, 141-149.

Lambert, J. M., Lambert, Q. T., Reuther, G. W., Malliri, A., Siderovski, D. P., Sondek, J., Collard, J. G., and Der, C. J. (2002). Tiam1 mediates Ras activation of Rac by a PI(3)K-independent mechanism. Nat Cell Biol *4*, 621-625.

Larijani, B., and Poccia, D. L. (2009). Nuclear envelope formation: mind the gaps. Annu Rev Biophys *38*, 107-124.

Larsen, C. N., and Wang, H. (2002). The ubiquitin superfamily: members, features, and phylogenies. J Proteome Res *1*, 411-419.

Lawrence, M., Shao, C., Duan, L., McGlynn, K., and Cobb, M. H. (2008). The protein kinases ERK1/2 and their roles in pancreatic beta cells. Acta Physiol (Oxf) *192*, 11-17.

Lein, P. J., Guo, X., Shi, G. X., Moholt-Siebert, M., Bruun, D., and Andres, D. A. (2007). The novel GTPase Rit differentially regulates axonal and dendritic growth. J Neurosci *27*, 4725-4736.

Lerner, E. C., Zhang, T. T., Knowles, D. B., Qian, Y., Hamilton, A. D., and Sebti, S. M. (1997). Inhibition of the prenylation of K-Ras, but not H- or N-Ras, is highly resistant to CAAX peptidomimetics and requires both a farnesyltransferase and a geranylgeranyltransferase I inhibitor in human tumor cell lines. Oncogene *15*, 1283-1288.

Li, W., Knowlton, D., Woodward, W. R., and Habecker, B. A. (2003). Regulation of noradrenergic function by inflammatory cytokines and depolarization. J Neurochem *86*, 774-783.

Li, Y., Asuri, S., Rebhun, J. F., Castro, A. F., Paranavitana, N. C., and Quilliam, L. A. (2006). The RAP1 guanine nucleotide exchange factor Epac2 couples cyclic AMP and Ras signals at the plasma membrane. J Biol Chem *281*, 2506-2514.

Li, Y., Yan, J., De, P., Chang, H. C., Yamauchi, A., Christopherson, K. W., 2nd, Paranavitana, N. C., Peng, X., Kim, C., Munugalavadla, V., *et al.* (2007). Rap1a null mice have altered myeloid cell functions suggesting distinct roles for the closely related Rap1a and 1b proteins. J Immunol *179*, 8322-8331.

Liao, Y., Kariya, K., Hu, C. D., Shibatohge, M., Goshima, M., Okada, T., Watari, Y., Gao, X., Jin, T. G., Yamawaki-Kataoka, Y., and Kataoka, T. (1999). RA-GEF, a novel Rap1A guanine nucleotide exchange factor containing a Ras/Rap1A-associating domain, is conserved between nematode and humans. J Biol Chem *274*, 37815-37820.

Limpert, A. S., Karlo, J. C., and Landreth, G. E. (2007). Nerve growth factor stimulates the concentration of TrkA within lipid rafts and extracellular signal-regulated kinase activation through c-Cbl-associated protein. Mol Cell Biol *27*, 5686-5698.

Linnemann, T., Kiel, C., Herter, P., and Herrmann, C. (2002). The activation of RalGDS can be achieved independently of its Ras binding domain. Implications of an activation mechanism in Ras effector specificity and signal distribution. J Biol Chem *277*, 7831-7837.

Liu, C., Takahashi, M., Li, Y., Song, S., Dillon, T. J., Shinde, U., and Stork, P. J. (2008). Ras is required for the cyclic AMP-dependent activation of Rap1 via Epac2. Mol Cell Biol *28*, 7109-7125.

Liu, Y., Kahn, R. A., and Prestegard, J. H. (2009). Structure and membrane interaction of myristoylated ARF1. Structure *17*, 79-87.

Lonhienne, T. G., Forwood, J. K., Marfori, M., Robin, G., Kobe, B., and Carroll, B. J. (2009). Importin-beta is a GDP-to-GTP exchange factor of Ran: implications for the mechanism of nuclear import. J Biol Chem *284*, 22549-22558.

Lopez, I., Mak, E. C., Ding, J., Hamm, H. E., and Lomasney, J. W. (2001). A novel bifunctional phospholipase c that is regulated by Galpha 12 and stimulates the Ras/mitogen-activated protein kinase pathway. J Biol Chem *276*, 2758-2765.

Lorenzo, P. S., Kung, J. W., Bottorff, D. A., Garfield, S. H., Stone, J. C., and Blumberg, P. M. (2001). Phorbol esters modulate the Ras exchange factor RasGRP3. Cancer Res *61*, 943-949.

Lounsbury, K. M., Richards, S. A., Carey, K. L., and Macara, I. G. (1996). Mutations within the Ran/TC4 GTPase. Effects on regulatory factor interactions and subcellular localization. J Biol Chem *271*, 32834-32841.

Macara, I. G. (2001). Transport into and out of the nucleus. Microbiol Mol Biol Rev *65*, 570-594, table of contents.

Magiera, M. M., Gupta, M., Rundell, C. J., Satish, N., Ernens, I., and Yarwood, S. J. (2004). Exchange protein directly activated by cAMP (EPAC) interacts with the light chain (LC) 2 of MAP1A. Biochem J *382*, 803-810.

Mahajan, R., Delphin, C., Guan, T., Gerace, L., and Melchior, F. (1997). A small ubiquitin-related polypeptide involved in targeting RanGAP1 to nuclear pore complex protein RanBP2. Cell *88*, 97-107.

Maillet, M., Robert, S. J., Cacquevel, M., Gastineau, M., Vivien, D., Bertoglio, J., Zugaza, J. L., Fischmeister, R., and Lezoualc'h, F. (2003). Crosstalk between Rap1 and Rac regulates secretion of sAPPalpha. Nat Cell Biol *5*, 633-639.

Malliri, A., van der Kammen, R. A., Clark, K., van der Valk, M., Michiels, F., and Collard, J. G. (2002). Mice deficient in the Rac activator Tiam1 are resistant to Ras-induced skin tumours. Nature *417*, 867-871.

Marchler-Bauer, A., Anderson, J. B., Chitsaz, F., Derbyshire, M. K., DeWeese-Scott, C., Fong, J. H., Geer, L. Y., Geer, R. C., Gonzales, N. R., Gwadz, M., *et al.* (2009). CDD: specific functional annotation with the Conserved Domain Database. Nucleic Acids Res *37*, D205-210.

Margarit, S. M., Sondermann, H., Hall, B. E., Nagar, B., Hoelz, A., Pirruccello, M., Bar-Sagi, D., and Kuriyan, J. (2003). Structural evidence for feedback activation by Ras.GTP of the Ras-specific nucleotide exchange factor SOS. Cell *112*, 685-695.

Maurer-Stroh, S., Eisenhaber, B., and Eisenhaber, F. (2002). N-terminal N-myristoylation of proteins: prediction of substrate proteins from amino acid sequence. J Mol Biol *317*, 541-557.

McFall, A., Ulku, A., Lambert, Q. T., Kusa, A., Rogers-Graham, K., and Der, C. J. (2001). Oncogenic Ras blocks anoikis by activation of a novel effector pathway independent of phosphatidylinositol 3-kinase. Mol Cell Biol *21*, 5488-5499.

McIlroy, B. K., Walters, J. D., Blackshear, P. J., and Johnson, J. D. (1991). Phosphorylation-dependent binding of a synthetic MARCKS peptide to calmodulin. J Biol Chem *266*, 4959-4964.

McLaughlin, S., and Murray, D. (2005). Plasma membrane phosphoinositide organization by protein electrostatics. Nature *438*, 605-611.

Meng, E. C., Pettersen, E. F., Couch, G. S., Huang, C. C., and Ferrin, T. E. (2006). Tools for integrated sequence-structure analysis with UCSF Chimera. BMC Bioinformatics *7*, 339.

Michaelson, D., Silletti, J., Murphy, G., D'Eustachio, P., Rush, M., and Philips, M. R. (2001). Differential localization of Rho GTPases in live cells: regulation by hypervariable regions and RhoGDI binding. J Cell Biol *152*, 111-126.

Mitin, N., Rossman, K. L., and Der, C. J. (2005). Signaling interplay in Ras superfamily function. Curr Biol *15*, R563-574.

Mochizuki, N., Yamashita, S., Kurokawa, K., Ohba, Y., Nagai, T., Miyawaki, A., and Matsuda, M. (2001). Spatio-temporal images of growth-factor-induced activation of Ras and Rap1. Nature *411*, 1065-1068.

Moore, M. S. (1998). Ran and nuclear transport. J Biol Chem *273*, 22857-22860.

Mossessova, E., Gulbis, J. M., and Goldberg, J. (1998). Structure of the guanine nucleotide exchange factor Sec7 domain of human arno and analysis of the interaction with ARF GTPase. Cell *92*, 415-423.

Mott, H. R., Carpenter, J. W., Zhong, S., Ghosh, S., Bell, R. M., and Campbell, S. L. (1996). The solution structure of the Raf-1 cysteine-rich domain: a novel ras and phospholipid binding site. Proc Natl Acad Sci U S A *93*, 8312-8317.

Nancy, V., Wolthuis, R. M., de Tand, M. F., Janoueix-Lerosey, I., Bos, J. L., and de Gunzburg, J. (1999). Identification and characterization of potential effector molecules of the Ras-related GTPase Rap2. J Biol Chem *274*, 8737-8745.

Nassar, N., Horn, G., Herrmann, C., Block, C., Janknecht, R., and Wittinghofer, A. (1996). Ras/Rap effector specificity determined by charge reversal. Nature Structural Biology *3*, 723-729.

Nassar, N., Horn, G., Herrmann, C., Scherer, A., McCormick, F., and Wittinghofer, A. (1995). The 2.2 a crystal structure of the Ras-binding domain of the serine/threonine kinase cRaf1 in complex with Rap1A and a GTP analogue. Nature *375*, 554-560.

Nemergut, M. E., and Macara, I. G. (2000). Nuclear import of the ran exchange factor, RCC1, is mediated by at least two distinct mechanisms. J Cell Biol *149*, 835-850.

Nemergut, M. E., Mizzen, C. A., Stukenberg, T., Allis, C. D., and Macara, I. G. (2001). Chromatin docking and exchange activity enhancement of RCC1 by histones H2A and H2B. Science *292*, 1540-1543.

Nesvizhskii, A. I., Keller, A., Kolker, E., and Aebersold, R. (2003). A statistical model for identifying proteins by tandem mass spectrometry. Anal Chem *75*, 4646-4658.

Neves, S. R., Ram, P. T., and Iyengar, R. (2002). G protein pathways. Science *296*, 1636-1639.

Niimura, M., Miki, T., Shibasaki, T., Fujimoto, W., Iwanaga, T., and Seino, S. (2009). Critical role of the N-terminal cyclic AMP-binding domain of Epac2 in its subcellular localization and function. J Cell Physiol *219*, 652-658.

Nimnual, A. S., Yatsula, B. A., and Bar-Sagi, D. (1998). Coupling of Ras and Rac guanosine triphosphatases through the Ras exchanger Sos. Science *279*, 560-563.

Obara, Y., Labudda, K., Dillon, T. J., and Stork, P. J. (2004). PKA phosphorylation of Src mediates Rap1 activation in NGF and cAMP signaling in PC12 cells. J Cell Sci *117*, 6085-6094.

Ohashi, Y., Tachibana, K., Kamiguchi, K., Fujita, H., and Morimoto, C. (1998). T cell receptor-mediated tyrosine phosphorylation of Cas-L, a 105-kDa Crk-associated substrate-related protein, and its association of Crk and C3G. J Biol Chem *273*, 6446-6451.

Ohba, Y., Ikuta, K., Ogura, A., Matsuda, J., Mochizuki, N., Nagashima, K., Kurokawa, K., Mayer, B. J., Maki, K., Miyazaki, J., and Matsuda, M. (2001). Requirement for C3G-dependent Rap1 activation for cell adhesion and embryogenesis. Embo J *20*, 3333-3341.

Ohba, Y., Mochizuki, N., Yamashita, S., Chan, A. M., Schrader, J. W., Hattori, S., Nagashima, K., and Matsuda, M. (2000). Regulatory proteins of R-Ras, TC21/R-Ras2, and M-Ras/R-Ras3. J Biol Chem *275*, 20020-20026.

Ohtsuka, T., Hata, Y., Ide, N., Yasuda, T., Inoue, E., Inoue, T., Mizoguchi, A., and Takai, Y. (1999). nRap GEP: a novel neural GDP/GTP exchange protein for rap1 small G protein that interacts with synaptic scaffolding molecule (S-SCAM). Biochem Biophys Res Commun *265*, 38-44.

Ohtsuka, T., Shimizu, K., Yamamori, B., Kuroda, S., and Takai, Y. (1996). Activation of brain B-Raf protein kinase by Rap1B small GTP-binding protein. J Biol Chem *271*, 1258-1261.

Okada, T., Hu, C. D., Jin, T. G., Kariya, K., Yamawaki-Kataoka, Y., and Kataoka, T. (1999). The strength of interaction at the Raf cysteine-rich domain is a critical determinant of response of Raf to Ras family small GTPases. Mol Cell Biol *19*, 6057-6064.

Ostroveanu, A., van der Zee, E. A., Eisel, U. L., Schmidt, M., and Nijholt, I. M. (2009). Exchange protein activated by cyclic AMP 2 (Epac2) plays a specific and time-limited role in memory retrieval. Hippocampus.

Ozaki, N., Shibasaki, T., Kashima, Y., Miki, T., Takahashi, K., Ueno, H., Sunaga, Y., Yano, H., Matsuura, Y., Iwanaga, T., *et al.* (2000). cAMP-GEFII is a direct target of cAMP in regulated exocytosis. Nat Cell Biol *2*, 805-811.

Parton, R. G., and Hancock, J. F. (2004). Lipid rafts and plasma membrane microorganization: insights from Ras. Trends Cell Biol *14*, 141-147.

Pasqualato, S., Renault, L., and Cherfils, J. (2002). Arf, Arl, Arp and Sar proteins: a family of GTP-binding proteins with a structural device for 'front-back' communication. EMBO Rep *3*, 1035-1041.

Peitzsch, R. M., and McLaughlin, S. (1993). Binding of acylated peptides and fatty acids to phospholipid vesicles: pertinence to myristoylated proteins. Biochemistry *32*, 10436-10443.

Pereira-Leal, J. B., and Seabra, M. C. (2001). Evolution of the Rab family of small GTP-binding proteins. J Mol Biol *313*, 889-901.

Peterson, S. N., Trabalzini, L., Brtva, T. R., Fischer, T., Altschuler, D. L., Martelli, P., Lapetina, E. G., Der, C. J., and White, G. C., 2nd (1996). Identification of a novel RalGDS-related protein as a candidate effector for Ras and Rap1. J Biol Chem *271*, 29903-29908.

Pettersen, E. F., Goddard, T. D., Huang, C. C., Couch, G. S., Greenblatt, D. M., Meng, E. C., and Ferrin, T. E. (2004). UCSF Chimera: a visualization system for exploratory research and analysis. Journal of Computational Chemistry *25*, 1605-1612.

Pfeffer, S., and Aivazian, D. (2004). Targeting Rab GTPases to distinct membrane compartments. Nat Rev Mol Cell Biol *5*, 886-896.

Ponsioen, B., Gloerich, M., Ritsma, L., Rehmann, H., Bos, J. L., and Jalink, K. (2009). Direct spatial control of Epac1 by cyclic AMP. Mol Cell Biol *29*, 2521-2531.

Prior, I. A., Harding, A., Yan, J., Sluimer, J., Parton, R. G., and Hancock, J. F. (2001). GTP-dependent segregation of H-ras from lipid rafts is required for biological activity. Nat Cell Biol *3*, 368-375.

Prior, I. A., Muncke, C., Parton, R. G., and Hancock, J. F. (2003). Direct visualization of Ras proteins in spatially distinct cell surface microdomains. J Cell Biol *160*, 165-170.

Qiao, J., Mei, F. C., Popov, V. L., Vergara, L. A., and Cheng, X. (2002). Cell cycle-dependent subcellular localization of exchange factor directly activated by cAMP. J Biol Chem *277*, 26581-26586.

Qiu, R. G., Chen, J., Kirn, D., McCormick, F., and Symons, M. (1995). An essential role for Rac in Ras transformation. Nature *374*, 457-459.

Rebhun, J. F., Castro, A. F., and Quilliam, L. A. (2000). Identification of guanine nucleotide exchange factors for the Rap1 GTPase: regulation of MR-GEF by M-Ras-GTP interaction. J Biol Chem *275*, 34901-34908.

Rehmann, H. (2006). Characterization of the activation of the Rap-specific exchange factor Epac by cyclic nucleotides. Methods Enzymol *407*, 159-173.

Rehmann, H., Arias-Palomo, E., Hadders, M. A., Schwede, F., Llorca, O., and Bos, J. L. (2008). Structure of Epac2 in complex with a cyclic AMP analogue and RAP1B. Nature.

Rehmann, H., Das, J., Knipscheer, P., Wittinghofer, A., and Bos, J. L. (2006). Structure of the cyclic-AMP-responsive exchange factor Epac2 in its auto-inhibited state. Nature *439*, 625-628.

Rehmann, H., Prakash, B., Wolf, E., Rueppel, A., De Rooij, J., Bos, J. L., and Wittinghofer, A. (2003a). Structure and regulation of the cAMP-binding domains of Epac2. Nat Struct Biol *10*, 26-32.

Rehmann, H., Rueppel, A., Bos, J. L., and Wittinghofer, A. (2003b). Communication between the regulatory and the catalytic region of the cAMP-responsive guanine nucleotide exchange factor Epac. J Biol Chem *278*, 23508-23514.

Renault, L., Kuhlmann, J., Henkel, A., and Wittinghofer, A. (2001). Structural basis for guanine nucleotide exchange on Ran by the regulator of chromosome condensation (RCC1). Cell *105*, 245-255.

Renault, L., Nassar, N., Vetter, I., Becker, J., Klebe, C., Roth, M., and Wittinghofer, A. (1998). The 1.7 A crystal structure of the regulator of chromosome condensation (RCC1) reveals a seven-bladed propeller. Nature *392*, 97-101.

Rensland, H., John, J., Linke, R., Simon, I., Schlichting, I., Wittinghofer, A., and Goody, R. S. (1995). Substrate and product structural requirements for binding of nucleotides to H-ras p21: the mechanism of discrimination between guanosine and adenosine nucleotides. Biochemistry *34*, 593-599.

Repasky, G. A., Chenette, E. J., and Der, C. J. (2004). Renewing the conspiracy theory debate: does Raf function alone to mediate Ras oncogenesis? Trends Cell Biol *14*, 639-647.

Resh, M. D. (2006a). Palmitoylation of ligands, receptors, and intracellular signaling molecules. Sci STKE *2006*, re14.

Resh, M. D. (2006b). Trafficking and signaling by fatty-acylated and prenylated proteins. Nat Chem Biol *2*, 584-590.

Riccio, A., Pierchala, B. A., Ciarallo, C. L., and Ginty, D. D. (1997). An NGF-TrkA-mediated retrograde signal to transcription factor CREB in sympathetic neurons. Science *277*, 1097-1100.

Robert, C. H., Cherfils, J., Mouawad, L., and Perahia, D. (2004). Integrating three views of Arf1 activation dynamics. J Mol Biol *337*, 969-983.

Rocks, O., Peyker, A., Kahms, M., Verveer, P. J., Koerner, C., Lumbierres, M., Kuhlmann, J., Waldmann, H., Wittinghofer, A., and Bastiaens, P. I. (2005). An acylation cycle regulates localization and activity of palmitoylated Ras isoforms. Science *307*, 1746-1752.

Rodriguez-Viciana, P., Sabatier, C., and McCormick, F. (2004). Signaling specificity by Ras family GTPases is determined by the full spectrum of effectors they regulate. Mol Cell Biol *24*, 4943-4954.

Rossman, K. L., Der, C. J., and Sondek, J. (2005). GEF means go: turning on RHO GTPases with guanine nucleotide-exchange factors. Nat Rev Mol Cell Biol *6*, 167-180.

Rotem, A., Gruber, R., Shorer, H., Shaulov, L., Klein, E., and Harel, A. (2009). Importin beta regulates the seeding of chromatin with initiation sites for nuclear pore assembly. Mol Biol Cell *20*, 4031-4042.

Rowell, C. A., Kowalczyk, J. J., Lewis, M. D., and Garcia, A. M. (1997). Direct demonstration of geranylgeranylation and farnesylation of Ki-Ras in vivo. J Biol Chem *272*, 14093-14097.

Roy, M. O., Leventis, R., and Silvius, J. R. (2000). Mutational and biochemical analysis of plasma membrane targeting mediated by the farnesylated, polybasic carboxy terminus of K-ras4B. Biochemistry *39*, 8298-8307.

Rudolph, J. L., Shi, G. X., Erdogan, E., Fields, A. P., and Andres, D. A. (2007). Rit mutants confirm role of MEK/ERK signaling in neuronal differentiation and reveal novel Par6 interaction. Biochim Biophys Acta.

Sakkab, D., Lewitzky, M., Posern, G., Schaeper, U., Sachs, M., Birchmeier, W., and Feller, S. M. (2000). Signaling of hepatocyte growth factor/scatter factor (HGF) to the small GTPase Rap1 via the large docking protein Gab1 and the adapter protein CRKL. J Biol Chem *275*, 10772-10778.

Saraste, M., Sibbald, P. R., and Wittinghofer, A. (1990). The P-loop--a common motif in ATP- and GTP-binding proteins. Trends Biochem Sci *15*, 430-434.

Sasagawa, S., Ozaki, Y., Fujita, K., and Kuroda, S. (2005). Prediction and validation of the distinct dynamics of transient and sustained ERK activation. Nat Cell Biol *7*, 365-373.

Sawada, Y., Nakamura, K., Doi, K., Takeda, K., Tobiume, K., Saitoh, M., Morita, K., Komuro, I. I., De Vos, K., Sheetz, M., and Ichijo, H. (2001). Rap1 is involved in cell

stretching modulation of p38 but not ERK or JNK MAP kinase. J Cell Sci *114*, 1221-1227.

Schmidt, M., Evellin, S., Weernink, P. A., von Dorp, F., Rehmann, H., Lomasney, J. W., and Jakobs, K. H. (2001). A new phospholipase-C-calcium signalling pathway mediated by cyclic AMP and a Rap GTPase. Nat Cell Biol *3*, 1020-1024.

Schmitt, J. M., and Stork, P. J. S. (2002). PKA Phosphorylation of Src Mediates cAMP's Inhibition of Cell Growth via Rap1. Mol Cell *9*, 85-94.

Schulze, H., Dose, M., Korpal, M., Meyer, I., Italiano, J. E., Jr., and Shivdasani, R. A. (2008). RanBP10 is a cytoplasmic guanine nucleotide exchange factor that modulates noncentrosomal microtubules. J Biol Chem *283*, 14109-14119.

Scita, G., Nordstrom, J., Carbone, R., Tenca, P., Giardina, G., Gutkind, S., Bjarnegard, M., Betsholtz, C., and Di Fiore, P. P. (1999). EPS8 and E3B1 transduce signals from Ras to Rac. Nature *401*, 290-293.

Scita, G., Tenca, P., Frittoli, E., Tocchetti, A., Innocenti, M., Giardina, G., and Di Fiore, P. P. (2000). Signaling from Ras to Rac and beyond: not just a matter of GEFs. Embo J *19*, 2393-2398.

Seabra, M. C., and Wasmeier, C. (2004). Controlling the location and activation of Rab GTPases. Curr Opin Cell Biol *16*, 451-457.

Sebti, S. M. (2005). Protein farnesylation: implications for normal physiology, malignant transformation, and cancer therapy. Cancer Cell *7*, 297-300.

Setty, S. R., Strochlic, T. I., Tong, A. H., Boone, C., and Burd, C. G. (2004). Golgi targeting of ARF-like GTPase Arl3p requires its Nalpha-acetylation and the integral membrane protein Sys1p. Nat Cell Biol *6*, 414-419.

Severson, E. A., Lee, W. Y., Capaldo, C. T., Nusrat, A., and Parkos, C. A. (2009). Junctional adhesion molecule A interacts with Afadin and PDZ-GEF2 to activate Rap1A, regulate beta1 integrin levels, and enhance cell migration. Mol Biol Cell *20*, 1916-1925.

Shahinian, S., and Silvius, J. R. (1995). Doubly-lipid-modified protein sequence motifs exhibit long-lived anchorage to lipid bilayer membranes. Biochemistry *34*, 3813-3822.

Shi, G. X., Rehmann, H., and Andres, D. A. (2006). A novel cyclic AMP-dependent Epac-Rit signaling pathway contributes to PACAP38-mediated neuronal differentiation. Mol Cell Biol *26*, 9136-9147.

Shibasaki, T., Takahashi, H., Miki, T., Sunaga, Y., Matsumura, K., Yamanaka, M., Zhang, C., Tamamoto, A., Satoh, T., Miyazaki, J., and Seino, S. (2007). Essential role of Epac2/Rap1 signaling in regulation of insulin granule dynamics by cAMP. Proc Natl Acad Sci U S A *104*, 19333-19338.

Shirouzu, M., Morinaka, K., Koyama, S., Hu, C. D., Hori-Tamura, N., Okada, T., Kariya, K., Kataoka, T., Kikuchi, A., and Yokoyama, S. (1998). Interactions of the amino acid residue at position 31 of the c-Ha-Ras protein with Raf-1 and RalGDS. J Biol Chem *273*, 7737-7742.

Silvius, J. R., and l'Heureux, F. (1994). Fluorimetric evaluation of the affinities of isoprenylated peptides for lipid bilayers. Biochemistry *33*, 3014-3022.

Simonsen, A., Wurmser, A. E., Emr, S. D., and Stenmark, H. (2001). The role of phosphoinositides in membrane transport. Curr Opin Cell Biol *13*, 485-492.

Smit, L., van der Horst, G., and Borst, J. (1996). Sos, Vav, and C3G participate in B cell receptor-induced signaling pathways and differentially associate with Shc-Grb2, Crk, and Crk-L adaptors. J Biol Chem *271*, 8564-8569.

Soisson, S. M., Nimnual, A. S., Uy, M., Bar-Sagi, D., and Kuriyan, J. (1998). Crystal structure of the Dbl and pleckstrin homology domains from the human Son of sevenless protein. Cell *95*, 259-268.

Sondermann, H., Soisson, S. M., Boykevisch, S., Yang, S. S., Bar-Sagi, D., and Kuriyan, J. (2004). Structural analysis of autoinhibition in the Ras activator Son of sevenless. Cell *119*, 393-405.

Song, C., Hu, C. D., Masago, M., Kariyai, K., Yamawaki-Kataoka, Y., Shibatohge, M., Wu, D., Satoh, T., and Kataoka, T. (2001). Regulation of a novel human phospholipase C, PLCepsilon, through membrane targeting by Ras. J Biol Chem *276*, 2752-2757.

Song, C., Satoh, T., Edamatsu, H., Wu, D., Tadano, M., Gao, X., and Kataoka, T. (2002). Differential roles of Ras and Rap1 in growth factor-dependent activation of phospholipase Cepsilon. Oncogene *21*, 8105-8113.

Spaargaren, M., and Bischoff, J. R. (1994). Identification of the guanine nucleotide dissociation stimulator for Ral as a putative effector molecule of R-ras, H-ras, K-ras, and Rap. Proc Natl Acad Sci U S A *91*, 12609-12613.

Springett, G. M., Kawasaki, H., and Spriggs, D. R. (2004). Non-kinase second-messenger signaling: new pathways with new promise. Bioessays *26*, 730-738.

Stork, P. J. (2005). Directing NGF's actions: it's a Rap. Nat Cell Biol *7*, 338-339.

Stork, P. J. S. (2003). Does Rap1 deserve a bad Rap? Trends Biochem Sci *28*, 267-275.

Stork, P. J. S., and Schmitt, J. M. (2002). Crosstalk between cAMP and MAP kinase signaling in the regulation of cell proliferation. Trends Cell Biol *12*, 258-266.

Takahashi, M., Rikitake, Y., Nagamatsu, Y., Hara, T., Ikeda, W., Hirata, K., and Takai, Y. (2008). Sequential activation of Rap1 and Rac1 small G proteins by PDGF locally at leading edges of NIH3T3 cells. Genes Cells *13*, 549-569.

Tall, G. G., Barbieri, M. A., Stahl, P. D., and Horazdovsky, B. F. (2001). Ras-activated endocytosis is mediated by the Rab5 guanine nucleotide exchange activity of RIN1. Dev Cell *1*, 73-82.

Tanaka, S., Morishita, T., Hashimoto, Y., Hattori, S., Nakamura, S., Shibuya, M., Matuoka, K., Takenawa, T., Kurata, T., Nagashima, K., and Matsuda, M. (1994). C3G, a guanine nucleotide-releasing protein expressed ubiguitously, binds to the Src homology 3 domains of CRK and GRB2/ASH proteins. Proc Natl Acad Sci, USA *91*, 3443-3447.

ten Klooster, J. P., and Hordijk, P. L. (2007). Targeting and localized signalling by small GTPases. Biol Cell *99*, 1-12.

Teruel, M. N., and Meyer, T. (2000). Translocation and reversible localization of signaling proteins: a dynamic future for signal transduction. Cell *103*, 181-184.

Thissen, J. A., Gross, J. M., Subramanian, K., Meyer, T., and Casey, P. J. (1997). Prenylation-dependent association of Ki-Ras with microtubules. Evidence for a role in subcellular trafficking. J Biol Chem *272*, 30362-30370.

Tian, T., Harding, A., Inder, K., Plowman, S., Parton, R. G., and Hancock, J. F. (2007). Plasma membrane nanoswitches generate high-fidelity Ras signal transduction. Nat Cell Biol *9*, 905-914.

Tian, X., Rusanescu, G., Hou, W., Schaffhausen, B., and Feig, L. A. (2002). PDK1 mediates growth factor-induced Ral-GEF activation by a kinase-independent mechanism. Embo J *21*, 1327-1338.

Tischler, A. S., and Greene, L. A. (1975). Nerve growth factor-induced process formation by cultured rat pheochromocytoma cells. Nature *258*, 341-342.

Tognon, C. E., Kirk, H. E., Passmore, L. A., Whitehead, I. P., Der, C. J., and Kay, R. J. (1998). Regulation of RasGRP via a phorbol ester-responsive C1 domain. Mol Cell Biol *18*, 6995-7008.

Uemura, N., and Griffin, J. D. (1999). The adapter protein Crkl links Cbl to C3G after integrin ligation and enhances cell migration. J Biol Chem *274*, 37525-37532.

Urano, T., Emkey, R., and Feig, L. A. (1996). Ral-GTPases mediate a distinct downstream signaling pathway from Ras that facilitates cellular transformation. EMBO J *15*, 810-816.

van de Wetering, M., Oving, I., Muncan, V., Pon Fong, M. T., Brantjes, H., van Leenen, D., Holstege, F. C., Brummelkamp, T. R., Agami, R., and Clevers, H. (2003). Specific inhibition of gene expression using a stably integrated, inducible small-interfering-RNA vector. EMBO Rep *4*, 609-615.

Vetter, I. R., Arndt, A., Kutay, U., Gorlich, D., and Wittinghofer, A. (1999). Structural view of the Ran-Importin beta interaction at 2.3 A resolution. Cell *97*, 635-646.

Vetter, I. R., and Wittinghofer, A. (2001). The guanine nucleotide-binding switch in three dimensions. Science *294*, 1299-1304.

vom Dorp, F., Sari, A. Y., Sanders, H., Keiper, M., Oude Weernink, P. A., Jakobs, K. H., and Schmidt, M. (2004). Inhibition of phospholipase C-epsilon by Gi-coupled receptors. Cell Signal *16*, 921-928.

Voss, A. K., Gruss, P., and Thomas, T. (2003). The guanine nucleotide exchange factor C3G is necessary for the formation of focal adhesions and vascular maturation. Development *130*, 355-367.

Vossler, M. R., Yao, H., York, R. D., Pan, M. G., Rim, C. S., and Stork, P. J. S. (1997). cAMP activates MAP kinase and Elk-1 through a B-Raf- and Rap1-dependent pathway. Cell *89*, 73-82.

Waltereit, R., and Weller, M. (2003). Signaling from cAMP/PKA to MAPK and synaptic plasticity. Mol Neurobiol *27*, 99-106.

Wang, Y., Waldron, R. T., Dhaka, A., Patel, A., Riley, M. M., Rozengurt, E., and Colicelli, J. (2002). The RAS effector RIN1 directly competes with RAF and is regulated by 14-3-3 proteins. Mol Cell Biol *22*, 916-926.

Wang, Z., Dillon, T. J., Pokala, V., Mishra, S., Labudda, K., Hunter, B., and Stork, P. J. (2006). Rap1-mediated activation of extracellular signal-regulated kinases by cyclic AMP is dependent on the mode of Rap1 activation. Mol Cell Biol *26*, 2130-2145.

Wei, P., Satoh, T., Edamatsu, H., Aiba, A., Setsu, T., Terashima, T., Kitazawa, S., Nakao, K., Yoshikawa, Y., Tamada, M., and Kataoka, T. (2007). Defective vascular morphogenesis and mid-gestation embryonic death in mice lacking RA-GEF-1. Biochem Biophys Res Commun *363*, 106-112.

Wennerberg, K., Rossman, K. L., and Der, C. J. (2005). The Ras superfamily at a glance. J Cell Sci *118*, 843-846.

White, M. A., Nicolette, C., Minden, A., Polverino, A., Van Aelst, L., Karin, M., and Wigler, M. H. (1995). Multiple Ras functions can contribute to mammalian cell transformation. Cell *80*, 533-541.

Williams, J. G., Drugan, J. K., Yi, G. S., Clark, G. J., Der, C. J., and Campbell, S. L. (2000). Elucidation of binding determinants and functional consequences of Ras/Raf-cysteine-rich domain interactions. J Biol Chem *275*, 22172-22179.

Wohlgemuth, S., Kiel, C., Kramer, A., Serrano, L., Wittinghofer, F., and Herrmann, C. (2005). Recognizing and defining true Ras binding domains I: biochemical analysis. J Mol Biol *348*, 741-758.

Wojnowski, L., Zimmer, A. M., Beck, T. W., Hahn, H., Bernal, R., Rapp, U. R., and Zimmer, A. (1997). Endothelial apoptosis in Braf-deficient mice. Nat Genet *16*, 293-297.

Wolthuis, R. M., Bauer, B., van't Veer, L. J., de Vries-Smits, A. M., Cool, R. H., Spaargaren, M., Wittinghofer, A., Burgering, B. M., and Bos, J. L. (1996). RalGDS-like factor (Rlf) is a novel Ras and Rap 1A-associating protein. Oncogene *13*, 353-362.

Woolfrey, K. M., Srivastava, D. P., Photowala, H., Yamashita, M., Barbolina, M. V., Cahill, M. E., Xie, Z., Jones, K. A., Quilliam, L. A., Prakriya, M., and Penzes, P. (2009).

Epac2 induces synapse remodeling and depression and its disease-associated forms alter spines. Nat Neurosci *12*, 1275-1284.

Worthylake, D. K., Rossman, K. L., and Sondek, J. (2000). Crystal structure of Rac1 in complex with the guanine nucleotide exchange region of Tiam1. Nature *408*, 682-688.

Wu, C., Lai, C. F., and Mobley, W. C. (2001). Nerve growth factor activates persistent Rap1 signaling in endosomes. J Neurosci *21*, 5406-5416.

Wu, J., Matunis, M. J., Kraemer, D., Blobel, G., and Coutavas, E. (1995). Nup358, a cytoplasmically exposed nucleoporin with peptide repeats, Ran-GTP binding sites, zinc fingers, a cyclophilin A homologous domain, and a leucine-rich region. J Biol Chem *270*, 14209-14213.

Xu, J., Shi, S., Matsumoto, N., Noda, M., and Kitayama, H. (2007). Identification of Rgl3 as a potential binding partner for Rap-family small G-proteins and profilin II. Cell Signal *19*, 1575-1582.

Yamauchi, J., Miyamoto, Y., Tanoue, A., Shooter, E. M., and Chan, J. R. (2005). Ras activation of a Rac1 exchange factor, Tiam1, mediates neurotrophin-3-induced schwann cell migration. Proc Natl Acad Sci U S A *102*, 14889-14894.

Yan, J., Li, F., Ingram, D. A., and Quilliam, L. A. (2008). Rap1a is a key regulator of fibroblast growth factor 2-induced angiogenesis and together with Rap1b controls human endothelial cell functions. Mol Cell Biol *28*, 5803-5810.

Yokote, K., Hellman, U., Ekman, S., Saito, Y., Ronnstrand, L., Saito, Y., Heldin, C. H., and Mori, S. (1998). Identification of Tyr-762 in the platelet-derived growth factor alpha-receptor as the binding site for Crk proteins. Oncogene *16*, 1229-1239.

Yokoyama, N., Hayashi, N., Seki, T., Pante, N., Ohba, T., Nishii, K., Kuma, K., Hayashida, T., Miyata, T., Aebi, U., and et al. (1995). A giant nucleopore protein that binds Ran/TC4. Nature *376*, 184-188.

York, R. D., Yao, H., Dillon, T., Ellig, C. L., Eckert, S. P., McCleskey, E. W., and Stork, P. J. S. (1998). Rap1 mediates sustained MAP kinase activation induced by nerve growth factor. Nature *392*, 622-625.

Yoshikawa, Y., Satoh, T., Tamura, T., Wei, P., Bilasy, S. E., Edamatsu, H., Aiba, A., Katagiri, K., Kinashi, T., Nakao, K., and Kataoka, T. (2007). The M-Ras-RA-GEF-2-

Rap1 pathway mediates tumor necrosis factor-alpha dependent regulation of integrin activation in splenocytes. Mol Biol Cell *18*, 2949-2959.

Zacharias, D. A., Violin, J. D., Newton, A. C., and Tsien, R. Y. (2002). Partitioning of lipid-modified monomeric GFPs into membrane microdomains of live cells. Science *296*, 913-916.

Zaldua, N., Gastineau, M., Hoshino, M., Lezoualc'h, F., and Zugaza, J. L. (2007). Epac signaling pathway involves STEF, a guanine nucleotide exchange factor for Rac, to regulate APP processing. FEBS Lett *581*, 5814-5818.

Zerial, M., and McBride, H. (2001). Rab proteins as membrane organizers. Nat Rev Mol Cell Biol *2*, 107-117.

Zhang, C. L., Katoh, M., Shibasaki, T., Minami, K., Sunaga, Y., Takahashi, H., Yokoi, N., Iwasaki, M., Miki, T., and Seino, S. (2009). The cAMP sensor Epac2 is a direct target of antidiabetic sulfonylurea drugs. Science *325*, 607-610.

Zhang, X., Odom, D. T., Koo, S. H., Conkright, M. D., Canettieri, G., Best, J., Chen, H., Jenner, R., Herbolsheimer, E., Jacobsen, E., *et al.* (2005). Genome-wide analysis of cAMP-response element binding protein occupancy, phosphorylation, and target gene activation in human tissues. Proc Natl Acad Sci U S A *102*, 4459-4464.

Zwartkruis, F. J., Wolthuis, R. M., Nabben, N. M., Franke, B., and Bos, J. L. (1998). Extracellular signal-regulated activation of Rap1 fails to interfere in Ras effector signalling. EMBO J *17*, 5905-5912.

CHANG LIU

1011 Curry Street Apt. 7
Portland OR, 97139
Chang6@gmail.com
Phone: 503-709-1055

EDUCATION

Vollum Institute, Oregon Health & Science University (OHSU) — Portland, OR
Ph.D. candidate in Cell and Developmental Biology — September 2004 – June 2010

Peking Union Medical College (PUMC) and West China University of Medical Sciences (WCUMS), — Beijing & Chengdu, China
M.D., Eight-year program in Clinical Medicine — September 1996 - July 2004

RESEARCH EXPERIENCE

Stork lab, Vollum Institute, OHSU — Portland, OR
Graduate student. Thesis advisor: Philip Stork, M.D. — August 2005 – Present

Thesis project entitled "Spatial Regulation of Rap1 signaling by cAMP" includes the following parts: (1) The regulation of Rap1 signaling by PKA mediated phosphorylation; (2) The molecular mechanism of the perinuclear localization of Epac1; (3) Necessity of Ras for Epac2 mediated Rap1 activation.

Chen Lab, Vollum Institute/Ullman Lab, Department of Biochemistry, OHSU — Portland, OR
Rotation student. Advisor: Wenbiao Chen, Ph.D. and Buddy Ullman, Ph.D. — September 2004 – June 2005

Projects: (1) Separation of GFP-tag from its downstream protein by ubiquitin mediated cleavage in cell culture and zebrafish; (2) Role of endocytosis on the processing and stability of Delta receptor in Notch signaling; (3) Screening the genomic library of Leishmania Donovani and cloning of three genes (ADSS, GMPS and ASL) involved in its purine salvage pathway.

Key Laboratory of the Ministry of Health, Division of Endocrinology, PUMC — Beijing, China
Research assistant. Thesis advisor: Zhengpei Zeng, M.D. — October 2003 – June 2004

Thesis project in the medical school: Expression profile of angiotensin II receptor subtypes in normal human adrenal gland and pheochromocytoma tissues, and its clinical and pathological correlation.

CLINICAL EXPERIENCE

Department of Pathology, OHSU — Portland, OR
Elective rotation. Supervisor: David Sauer, M.D. — July 2009 – August 2009

Cardiovascular Division, OHSU — Portland, OR
Elective rotation. Supervisor: Joseph Weiss, M.D., Ph.D. — March 2009 – July 2009

Peking Union Medical College Hospital / West China Hospital — Beijing / Chengdu, China
Clerkship. Supervisor: Chao Ni, M.D. and Xuehong Wan, M.D. — April 2001 - October 2003

ECFMG CERTIFICATE October 9, 2009

SELECTED PUBLICATIONS

- **Liu C**, Takahashi M, Li Y, Song S, Dillon TJ, Shinde U, Stork PJ. Ras is required for the cAMP-dependent activation of Rap1 via Epac2. Mol Cell Biol. 2008 Dec;28(23):7109-25.
- Zeng ZP, Liu GQ, Li HZ, Fan XR, Liu DM, Tong AL, Zheng X, **Liu C**. The effects of urotensin-II on proliferation of pheochromocytoma cells and mRNA expression of urotensin-II and its receptor in pheochromocytoma tissues. Ann N Y Acad Sci. 2006 Aug;1073:284-9.

Liu C, Takahashi M, Li Y, Dillon TJ, Kaech S, Stork PJ. Interaction of Ran and Epac1 promotes Rap1 activation at the nuclear envelope. Mol Cell Biol. (submitted)

ORAL/POSTER PRESENTATIONS

- **Liu C**, Stork PJ. The molecular mechanism of perinuclear localization of Epac1. *2009 Annual OHSU Student Research Forum, Portland, OR. (Oral presentation)*
- **Liu C**, Takahashi M, Li Y, Song S, Dillon TJ, Shinde U, Stork PJ. Epac2 is a novel Ras effector and contributes to Rap1-dependent ERK activation. *2008 Annual American Society for Cell Biology (ASCB) Meeting, San Francisco, CA. (Poster presentation)*
- Stork PJ, **Liu C**. Ras activates Rap1 via Epac2. *2006 International Meeting on Anchored cAMP Signaling Pathways, Portland, OR. (Oral presentation)*
- **Liu C**, Zeng Z. mRNA expression of Angiotensin II receptor subtypes in normal human adrenal and pheochromocytoma tissues. *2004 Third International Huaxia Congress of Endocrinology, Shanghai, China. (Oral presentation)*

HONORS/AWARDS

2009 Best Paper Award, Program in Molecular and Cellular Biosciences, OHSU

2009 Vertex Scholar, Vertex Pharmaceutical & OHSU

2008 Predoctoral Travel Stipend, American Society for Mass Spectrometry

2008 Predoctoral Travel Award, American Society for Cell Biology

2008 Best Poster Award, Program in Molecular and Cellular Biosciences, OHSU

1997, 1998 & 2000 Medical Scholarship, The Ministry of Health, China

1997 & 1998 Academic Excellence Scholarship, WCUMS, China

HOBBIES

Brush calligraphy and seal art; painting and illustration; hiking and swimming.